



University
of Glasgow

<https://theses.gla.ac.uk/>

Theses Digitisation:

<https://www.gla.ac.uk/myglasgow/research/enlighten/theses/digitisation/>

This is a digitised version of the original print thesis.

Copyright and moral rights for this work are retained by the author

A copy can be downloaded for personal non-commercial research or study, without prior permission or charge

This work cannot be reproduced or quoted extensively from without first obtaining permission in writing from the author

The content must not be changed in any way or sold commercially in any format or medium without the formal permission of the author

When referring to this work, full bibliographic details including the author, title, awarding institution and date of the thesis must be given

Enlighten: Theses

<https://theses.gla.ac.uk/>
research-enlighten@glasgow.ac.uk

STRUCTURAL DAMAGE TO THE RABBIT RETINA AND
CHOROID FROM LIGHT EXPOSURE

BY

NICOL M. McKECHNIE, B.Sc.

THESIS SUBMITTED IN ONE VOLUME FOR THE DEGREE OF DOCTOR
OF PHILOSOPHY IN THE FACULTY OF MEDICINE, UNIVERSITY OF
GLASGOW.

JULY, 1981

TENNENT INSTITUTE OF OPHTHALMOLOGY,
GLASGOW UNIVERSITY AND WESTERN INFIRMARY,
GLASGOW, G11 6NT.

ProQuest Number: 10644181

All rights reserved

INFORMATION TO ALL USERS

The quality of this reproduction is dependent upon the quality of the copy submitted.

In the unlikely event that the author did not send a complete manuscript and there are missing pages, these will be noted. Also, if material had to be removed, a note will indicate the deletion.



ProQuest 10644181

Published by ProQuest LLC (2017). Copyright of the Dissertation is held by the Author.

All rights reserved.

This work is protected against unauthorized copying under Title 17, United States Code
Microform Edition © ProQuest LLC.

ProQuest LLC.
789 East Eisenhower Parkway
P.O. Box 1346
Ann Arbor, MI 48106 – 1346

GLASGOW
UNIVERSITY
LIBRARY

Thesis
6532
Copy 2

LIST OF CONTENTS	I
LIST OF ILLUSTRATIONS	V
ACKNOWLEDGEMENTS	XIII
SUMMARY	XVI

LIST OF CONTENTS

LIST OF CONTENTS

	Page
Chapter 1 INTRODUCTION	1
1.1 Introduction	2
1.2 The Structure of the Eye	4
1.3 The Structure and Function of the Retina and Choroid	5
1.3.1 The Retina	5
1.3.2 The Choroid	8
1.4 Background to the Present Study	9
1.5 Aims of Project	18
Chapter 2 MATERIALS AND METHODS	19
2.1 Animals	20
2.2 Light Sources and Fibre Optics	20
2.3 Methods Employed in the Non-Survival Light Damage Experiments	22
2.4 Methods Employed in the Survival Light Damage Experiments	22
2.5 Tissue Preparation for Light and Electron Microscopy	24
2.6 Microscopy	25
2.6.1 Light Microscopy	25
2.6.2 Electron Microscopy	25
Chapter 3 THE APPEARANCE OF THE NORMAL RABBIT RETINA AND CHOROID BY LIGHT AND ELECTRON MICROSCOPY	26
3.1 Introduction	27
3.2 Light Microscopy	27
3.2.1 The Retina	27
3.2.2 The Choroid	31
3.3 Electron Microscopy of the Retina	33
3.3.1 The Retinal Pigment Epithelium	33
3.3.2 The Receptor Cells	36
3.3.3 The Muller Cell	39
3.3.4 The Cells of the Inner Retina	41
3.3.5 The Ganglion Cells and Nerve Fibre Layer	42
3.4 Electron Microscopy of the Choroid	44
3.4.1 Bruch's Membrane	44
3.4.2 The Choriocapillaris	45
3.4.3 The Cells and Blood Vessels of the Stroma	46
3.4.4 The Suprachoroidea	49
Chapter 4 THE IMMEDIATE EFFECTS ON THE STRUCTURE OF THE RETINA AND CHOROID OF EXPOSURE TO LIGHT FOR ONE HOUR	50
4.1 Introduction	51
4.2 Light Damage: Its Immediate Effects as Assessed by Light Microscopy	52
4.2.1 Group 6	52
4.2.2 Group 5	52
4.2.3 Group 4	53
4.2.4 Group 3	53
4.2.5 Group 2	54
4.2.6 Group 1	55

4.3	Light Damage: Its Immediate Effects as Assessed by Electron Microscopy	56
4.3.1	Group 6	56
4.3.2	Group 5	56
4.3.3	Group 4	57
4.3.4	Group 3	58
4.3.5	Group 2	59
4.3.6	Group 1	61
4.4	Light Damage: Its Immediate Effects as Assessed by Quantification of the Changes in the Cellular Components of the Outer Nuclear Layer	64
4.4.1	Introduction	64
4.4.2	Results	66
4.5	Discussion	69
Chapter 5	RECOVERY OF THE RABBIT RETINA AND CHOROID FOLLOWING LIGHT DAMAGE	84
5.1	Introduction	85
5.2	Recovery of the Rabbit Retina and Choroid Following Light Damage: Light Microscopy; Low Intensity Group.	85
5.2.1	Group 2. 6 Hours Recovery	86
5.2.2	Group 2. 24 Hours Recovery	87
5.2.3	Group 2. 48 Hours Recovery	88
5.2.4	Group 2. 4 Days Recovery	89
5.2.5	Group 2. 1 Week Recovery	90
5.2.6	Group 2. 2 Weeks Recovery	90
5.2.7	Group 2. 4 Weeks Recovery	92
5.3	Recovery of the Rabbit Retina and Choroid Following Light Damage: Light Microscopy; High Intensity Group.	93
5.3.1	Group 1. 6 Hours Recovery	93
5.3.2	Group 1. 24 Hours Recovery	95
5.3.3	Group 1. 48 Hours Recovery	96
5.3.4	Group 1. 4 Days Recovery	98
5.3.5	Group 1. 1, 2 and 4 Weeks Recovery	100
5.4	Recovery of the Rabbit Retina and Choroid Following Light Damage: Electron Microscopy; Low Intensity Group	102
5.4.1	Group 2. 6 Hours Recovery	102
5.4.2	Group 2. 24 Hours Recovery	103
5.4.3	Group 2. 48 Hours Recovery	104
5.4.4	Group 2. 4 Days Recovery	104
5.4.5	Group 2. 1 Week Recovery	105
5.4.6	Group 2. 2 Weeks Recovery	105
5.4.7	Group 2. 4 Weeks Recovery	108
5.5	Recovery of the Rabbit Retina and Choroid Following Light Damage: Electron Microscopy; High Intensity Group	109
5.5.1	Group 1. 6 Hours Recovery	109
5.5.2	Group 1. 24 Hours Recovery	111
5.5.3	Group 1. 48 Hours Recovery	113
5.5.4	Group 1. 4 Days Recovery	117
5.5.5	Group 1. 1,2 and 4 Weeks Recovery	120
5.6	Discussion	126

Chapter 6	FINAL DISCUSSION	144
6.1	Findings in relation to aims	145
6.2	Possible Modifications of Experimental Design	151
6.3	Other Possible Experimental Techniques	152
6.4	Future Lines of Investigation	153
	APPENDICES	155
	Appendix 1	155
	Appendix 2	158
	Appendix 3	172
	Appendix 4	189
	REFERENCES	191

LIST OF ILLUSTRATIONS

LIST OF ILLUSTRATIONS

CHAPTER 1

- Fig. 1.1 Diagram of a Rabbit Eye.
Fig. 1.2 Electron Micrograph of the Rabbit Retina.
Fig. 1.3 Diagram of the Retina.

CHAPTER 2

- Fig. 2.1 Diagram of Light Sources and Fibre Optics.
Fig. 2.2 Photograph of Light Source 1.
Fig. 2.3 Photograph of Light Source 2.
Fig. 2.4 Table of Light Intensities.
Fig. 2.5 Diagram of Block Labeling System.
Fig. 2.6 Tissue Processing Protocol.

CHAPTER 3

- Fig. 3.1 Light Micrograph: Retina and Choroid (Visual Streak).
Fig. 3.2 Light Micrograph: Outer Retina (Visual Streak).
Fig. 3.3 Light Micrograph: Inner Retina (Visual Streak).
Fig. 3.4 Light Micrograph: Inner Retina (Visual Streak).
Fig. 3.5 Light Micrograph: Retina and Choroid (Periphery).
Fig. 3.6 Light Micrograph: Retina and Choroid (Medullated Fibre Region).
Fig. 3.7 Light Micrograph: Retina and Choroid (Visual Streak/Medullated Fibres).
Fig. 3.8 Light Micrograph: Nerve Fibre Bundle.
Fig. 3.9 Light Micrograph: Choriocapillaris
Fig. 3.10 Light Micrograph: Choroidal Stroma.
Fig. 3.11 Light Micrograph: Choroidal Inflammatory Cells.
Fig. 3.12 Light Micrograph: Choroidal Arteriole.
Fig. 3.13 Light Micrograph: Suprachoroidea
Fig. 3.14 Light Micrograph: Ciliary Nerve.
Fig. 3.14 Electron Micrograph: Retinal Pigment Epithelium.
Fig. 3.16 Electron Micrograph: Bruch's Membrane.
Fig. 3.17 Electron Micrograph: Basal Infoldings.
Fig. 3.18 Electron Micrograph: Pigment Epithelium.
Fig. 3.19 Electron Micrograph: R.P.E. Junctional Complex.
Fig. 3.20 Electron Micrograph: R.P.E. Junctional Complex
Fig. 3.21 Electron Micrograph: Retinal Pigment Epithelium.
Fig. 3.22 Electron Micrograph: R.P.E. Basal Cytoplasm.
Fig. 3.23 Electron Micrograph: Retina.
Fig. 3.24 Electron Micrograph: Rod Outer Segment.
Fig. 3.25 Electron Micrograph: Proximal Region of Rod Outer segment.
Fig. 3.26 Electron Micrograph: Rod Connecting Cilium.
Fig. 3.27 Electron Micrograph: Rod Inner Segment.
Fig. 3.28 Electron Micrograph: Outer Region of the Outer Nuclear Layer.
Fig. 3.29 Electron Micrograph: Outer Plexiform Layer.
Fig. 3.30 Electron Micrograph: Muller Cell Micro Villi.
Fig. 3.31 Electron Micrograph: Outer Plexiform Layer.
Fig. 3.32 Electron Micrograph: Inner Nuclear Layer.
Fig. 3.33 Electron Micrograph: Inner Retina.
Fig. 3.34 Electron Micrograph: Inner Limiting Membrane.
Fig. 3.35 Electron Micrograph: Amacrine Cell.
Fig. 3.36 Electron Micrograph: Inner Nuclear Layer.

Fig. 3.37	Electron Micrograph:	Ganglion Cell.
Fig. 3.38	Electron Micrograph:	Nerve Fibre Bundle.
Fig. 3.39	Electron Micrograph:	Nerve Fibre Bundles.
Fig. 3.40	Electron Micrograph:	Retinal Blood Vessel.
Fig. 3.41	Electron Micrograph:	Oligodendrocyte.
Fig. 3.42	Electron Micrograph:	Endothelial Cell Junction.
Fig. 3.43	Electron Micrograph:	Bruch's Membrane.
Fig. 3.44	Electron Micrograph:	Bruch's Membrane.
Fig. 3.45	Electron Micrograph:	Choriocapillaris.
Fig. 3.46	Electron Micrograph:	Choriocapillaris (Fenestrations).
Fig. 3.47	Electron Micrograph:	Bruch's Membrane.
Fig. 3.48	Electron Micrograph:	Choriocapillaris and Choroidal Stroma.
Fig. 3.49	Electron Micrograph:	Choroidal Arteriole.
Fig. 3.50	Electron Micrograph:	Choroidal Fibroblast.
Fig. 3.51	Electron Micrograph:	Choroidal Melanocyte.
Fig. 3.52	Electron Micrograph:	Choroidal Intravascular Inflammatory Cells.
Fig. 3.53	Electron Micrograph:	Choroidal Extravascular Inflammatory Cells.
Fig. 3.54	Electron Micrographs:	Inflammatory Cells.
Fig. 3.55	Electron Micrograph	Choroidal Macrophage.
Fig. 3.56	Electron Micrograph:	Ciliary Nerve (In Choroid).

CHAPTER 4

Fig. 4.1	Light Micrograph:	Retina and Choroid: Light Intensity 4.
Fig. 4.2	Light Micrograph:	Retina and Choroid: Light Intensity 4.
Fig. 4.3	Light Micrograph:	Retinal Fold: Light Intensity 3.
Fig. 4.4	Light Micrograph:	Outer Retina: Light Intensity 3.
Fig. 4.5	Light Micrograph:	Retina and Choroid: Light Intensity 3.
Fig. 4.6	Light Micrograph:	Retina and Choroid: Light Intensity 3.
Fig. 4.7	Light Micrograph:	Inflammatory Cell: Light Intensity 3.
Fig. 4.8	Light Micrograph:	Outer Retina: Light Intensity 3.
Fig. 4.9	Light Micrograph:	Inner Retina: Light Intensity 2.
Fig. 4.10	Light Micrograph:	Choroid: Light Intensity 2.
Fig. 4.11	Light Micrograph:	Choroid: Light Intensity 2.
Fig. 4.12	Light Micrograph:	Neural Retina: Light Intensity 2.
Fig. 4.13	Light Micrograph:	Pigment Epithelium: Light Intensity 2.
Fig. 4.14	Light Micrograph:	Outer Nuclear Layer: Light Intensity 2.
Fig. 4.15	Light Micrograph:	Inner Retina: Light Intensity 1.
Fig. 4.16	Light Micrograph:	Inner Retina: Light Intensity 1.
Fig. 4.17	Light Micrograph:	Choroid: Light Intensity 1.
Fig. 4.18	Electron Micrograph:	Pigment Epithelium: Light Intensity 5.
Fig. 4.19	Electron Micrograph:	Retina: Light Intensity 4.

Fig. 4.20	Electron Micrograph:	Disrupted RPE Cell: Light Intensity 4.
Fig. 4.21	Electron Micrograph:	Outer Retina: Light Intensity 3.
Fig. 4.22	Electron Micrograph:	Pigment Epithelium: Light Intensity 3.
Fig. 4.23	Electron Micrograph:	Pigment Epithelium: Light Intensity 3.
Fig. 4.24	Electron Micrograph:	Inner Retina: Light Intensity 3.
Fig. 4.25	Electron Micrograph:	Outer Retina and Choroid: Light Intensity 3.
Fig. 4.26	Electron Micrograph:	Pigment Epithelium: Light Intensity 2.
Fig. 4.27	Electron Micrograph:	Neural Retina: Light Intensity 2.
Fig. 4.28	Electron Micrograph:	Outer Plexiform Layer: Light Intensity 2.
Fig. 4.29	Electron Micrograph:	Outer Plexiform Layer: Light Intensity 2.
Fig. 4.30	Electron Micrograph:	Ganglion Cell: Light Intensity 2.
Fig. 4.31	Electron Micrograph:	Choriocapillaris: Light Intensity 1.
Fig. 4.32	Electron Micrograph:	Pigment Epithelium and Choroid: Light Intensity 1.
Fig. 4.33	Electron Micrograph:	Outer Retina: Light Intensity 1.
Fig. 4.34	Electron Micrograph:	RPE Apical Surface: Light Intensity 1.
Fig. 4.35	Electron Micrograph:	Receptor Cell Debris: Light Intensity 1.
Fig. 4.36	Electron Micrograph:	Inner Nuclear Layer: Light Intensity 1.
Fig. 4.37	Electron Micrograph:	Inner Retina: Light Intensity 1.
Fig. 4.38	Electron Micrograph:	Muller Cell Cytoplasm: Light Intensity 1.
Fig. 4.39	Electron Micrograph:	Choroid: Light Intensity 1.
Fig. 4.40	Table of Qualitative Findings.	
Fig. 4.41	Electron Micrograph showing the Area Defined as the Outer Nuclear Layer.	
Fig. 4.42	Control Results of Point Counting.	
Fig. 4.43	Graph of Animal Results (All Features) Plotted Against Light Intensity.	
Fig. 4.44	Animal F Ratios (Receptor Cell Nuclei) Plotted Against Light Intensity.	
Fig. 4.45	Animal F Ratios (Receptor Cell Cytoplasm) Plotted Against Light Intensity.	
Fig. 4.46	Animal F Ratios (Muller Cell Cytoplasm) Plotted Against Light Intensity.	
Fig. 4.47	Graph of Group Results (All Features) Plotted Against Light Intensity.	
Fig. 4.48	Group F Ratios (All Features) Plotted Against Light Intensity.	

CHAPTER 5

- Figs. 5.1 to 5.4 Diagrams of Retinal Lesions.
- Fig. 5.5 Light Micrograph: Retina
Group 2, 6 Hours Recovery.
- Fig. 5.6 Light Micrograph: Outer retina and Choroid
Group 2, 6 Hours Recovery.
- Fig. 5.7 Light Micrograph: Outer retina and Choroid
Group 2, 24 Hours Recovery.
- Fig. 5.8 Light Micrograph: Retina and Choroid
Group 2, 24 Hours Recovery.
- Fig. 5.9 Light Micrograph: Outer Retina and Choroid
Group 2, 48 Hours Recovery.
- Fig. 5.10 Light Micrograph: Retina and Choroid
Group 2, 4 Days Recovery.
- Fig. 5.11 Light Micrograph: Outer Retina and Choroid
Group 2, 4 Days Recovery.
- Fig. 5.12 Light Micrograph: Retina and Choroid
Group 2, 1 Week Recovery.
- Fig. 5.13 Light Micrograph: Retina and Choroid
Group 2, 2 Weeks Recovery.
- Fig. 5.14 Light Micrograph: Retina and Choroid
Group 2, 2 Weeks Recovery.
- Fig. 5.15 Light Micrograph: Retina and Choroid
Group 2, 2 Weeks Recovery.
- Fig. 5.16 Light Micrograph: Retina and Choroid
Group 2, 2 Weeks Recovery.
- Fig. 5.17 Light Micrograph: Retina and Choroid
Group 2, 4 Weeks Recovery.
- Fig. 5.18 Light Micrograph: Retina and Choroid
Group 2, 4 Weeks Recovery.
- Fig. 5.19 Light Micrograph: Neural Retina
Group 2, 4 Weeks Recovery.
- Fig. 5.20 Light Micrograph: Pigment Epithelium and Choroid
Group 2, 4 Weeks Recovery.
- Fig. 5.21 Light Micrograph: Retina and Choroid
Group 1, 6 Hours Recovery.
- Fig. 5.22 Light Micrograph: Retina and Choroid
Group 1, 6 Hours Recovery.
- Fig. 5.23 Light Micrograph: Retina
Group 1, 24 Hours Recovery.
- Fig. 5.24 Light Micrograph: Retina
Group 1, 24 Hours Recovery
- Fig. 5.25 Light Micrograph: Retina and Choroid
Group 1, 48 Hours Recovery.
- Fig. 5.26 Light Micrograph: Retina and Choroid
Group 1, 48 Hours Recovery.
- Fig. 5.27 Light Micrograph: Retina and Choroid
Group 1, 48 Hours Recovery.
- Fig. 5.28 Light Micrograph: Outer Retina and Choroid
Group 1, 4 Days Recovery.
- Fig. 5.29 Light Micrograph: Outer Retina and Choroid
Group 1, 4 Days Recovery.
- Fig. 5.30 Light Micrograph: Retina and Choroid
Group 1, 4 Days Recovery.
- Fig. 5.31 Light Micrograph: Retina and Choroid
Group 1, 4 Days Recovery.
- Fig. 5.32 Light Micrograph: Retina and Choroid
Group 1, 2 Weeks Recovery.

- Fig. 5.33 Light Micrograph: Retina and Choroid
Group 1, 4 Weeks Recovery.
- Fig. 5.34 Light Micrograph: Retina and Choroid
Group 1, 4 Weeks Recovery.
- Fig. 5.35 Light Micrograph: Retina
Group 1, 1 Week Recovery.
- Fig. 5.36 Light Micrograph: Retina
Group 1, 4 Weeks Recovery.
- Fig. 5.37 Light Micrograph: Retina and Choroid
Group 1 4 Weeks Recovery.
- Fig. 5.38 Electron Micrograph: Outer Retina and Choroid
Group 2, 6 Hours Recovery.
- Fig. 5.39 Electron Micrograph: Outer Retina
Group 2, 6 Hours Recovery.
- Fig. 5.40 Electron Micrograph: Outer Nuclear Layer
Group 2, 6 Hours Recovery.
- Fig. 5.41 Electron Micrograph: Outer Retina
Group 2, 24 Hours Recovery.
- Fig. 5.42 Electron Micrograph: Outer Retina and Choroid
Group 2, 48 Hours Recovery.
- Fig. 5.43 Electron Micrograph: Macrophage
Group 2, 48 Hours Recovery.
- Fig. 5.44 Electron Micrograph: Bruch's Membrane
Group 2, 48 Hours Recovery.
- Fig. 5.45 Electron Micrographs: Pigment epithelium
Group 2, 4 Days Recovery.
- Fig. 5.46 Electron Micrograph: Pigment epithelium
Group 2, 4 Days Recovery.
- Fig. 5.47 Electron Micrograph: Pigment epithelium
Group 2, 4 Days Recovery.
- Fig. 5.48 Electron Micrograph: Outer Retina and Choriocapillaris
Group 2, 1 Week Recovery.
- Fig. 5.49 Electron Micrograph: Outer Retina and Choroid
Group 2, 2 Weeks Recovery.
- Fig. 5.50 Electron Micrograph: Pigment Epithelium and Bruch's Membrane
Group 2, 2 Weeks Recovery.
- Fig. 5.51 Electron Micrograph: Outer Retina and Choroid
Group 2, 2 Weeks Recovery.
- Fig. 5.52 Electron Micrograph: Pigment Epithelium
Group 2, 2 Weeks Recovery.
- Fig. 5.53 Electron Micrograph: Neural Retina
Group 2, 2 Weeks Recovery.
- Fig. 5.54 Electron Micrograph: Choroid
Group 2, 4 Weeks Recovery.
- Fig. 5.55 Electron Micrograph: Outer Retina
Group 2, 4 Weeks Recovery.
- Fig. 5.56 Electron Micrograph: Neural Retina
Group 2, 4 Weeks Recovery.
- Fig. 5.57 Electron Micrograph: Pigment Epithelium and Choroid
Group 2, 4 Weeks Recovery.
- Fig. 5.58 Electron Micrograph: Outer Retina and Choroid
Group 1, 6 Hours Recovery.
- Fig. 5.59 Electron Micrograph: Pigment Epithelium
Group 1, 6 Hours Recovery.
- Fig. 5.60 Electron Micrograph: Neural Retina
Group 1, 6 Hours Recovery.
- Fig. 5.61 Electron Micrograph: Pigment Epithelium
Group 1, 6 Hours Recovery.

Fig. 5.62	Electron Micrograph:	Outer Retina and Choriocapillaris Group 1, 24 Hours Recovery.
Fig. 5.63	Electron Micrograph:	Neural Retina Group 1, 24 Hours Recovery.
Fig. 5.64	Electron Micrograph:	Pigment Epithelium and Chorio- capillaris Group 1, 24 Hours Recovery.
Fig. 5.65	Electron Micrograph:	Pigment Epithelium and Bruch's Membrane Group 1, 24 Hours Recovery.
Fig. 5.66	Electron Micrograph:	Pigment Epithelium Group 1, 24 Hours Recovery.
Fig. 5.67	Electron Micrograph:	Muller Cell Microvilli Group 1, 24 Hours Recovery.
Fig. 5.68	Electron Micrograph:	Choriocapillaris Group 1, 24 Hours Recovery.
Fig. 5.69	Electron Micrograph:	Outer Retina and Choroid Group 1, 48 Hours Recovery.
Fig. 5.70	Electron Micrograph:	Neural Retina Group 1, 48 Hours Recovery.
Fig. 5.71	Electron Micrograph:	Retina (Outer Limiting Membrane) Group 1, 48 Hours Recovery.
Fig. 5.72	Electron Micrograph:	Pigment Epithelium and Choroid Group 1, 48 Hours Recovery.
Fig. 5.73	Electron Micrograph:	Choroidal Vessel Group 1, 48 Hours Recovery.
Fig. 5.74	Electron Micrograph:	Neural Retina Group 1, 48 Hours Recovery.
Fig. 5.75	Electron Micrograph:	Pigment Epithelium and Choroid Group 1, 48 Hours Recovery.
Fig. 5.76	Electron Micrograph:	Outer Retina Group 1, 48 Hours Recovery.
Fig. 5.77	Electron Micrograph:	Outer Retina Group 1, 48 Hours Recovery.
Fig. 5.78	Electron Micrograph:	Outer Nuclear Layer Group 1, 48 Hours Recovery.
Fig. 5.79	Electron Micrograph:	Outer Retina and Choroid Group 1, 48 Hours Recovery.
Fig. 5.80	Electron Micrograph:	Pigment Epithelium Group 1, 48 Hours Recovery.
Fig. 5.81	Electron Micrograph:	Outer Retina and Choroid Group 1, 4 Days Recovery
Fig. 5.82	Electron Micrograph:	Outer Retina and Choroid Group 1, 4 Days Recovery.
Fig. 5.83	Electron Micrograph:	Outer Retina and Choroid Group 1, 4 Days Recovery.
Fig. 5.84	Electron Micrograph:	Pigment Epithelial Processes Group 1, 4 Days Recovery.
Fig. 5.85	Electron Micrograph:	Outer Retina Group 1, 4 Days Recovery.
Fig. 5.86	Electron Micrograph:	Photoreceptors Group 1, 4 Days Recovery
Fig. 5.87	Electron Micrograph:	Outer Retina Choroid Group 1, 4 Days Recovery
Fig. 5.88	Electron Micrograph:	Outer Retina and choroid Group 1, 4 Days Recovery
Fig. 5.89	Electron Micrograph:	Mononuclear cell Group 1, 4 Days Recovery
Fig. 5.90	Electron Micrograph:	Outer Retina Group 1, 4 Days Recovery
Fig. 5.91	Electron Micrograph:	Retina and Choroid Group 1, 2 Weeks Recovery

- Fig. 5.92 Electron Micrographs: Bruch's Membrane and Muller
Cell Cytoplasm
Group 1, 1 Week Recovery
- Fig. 5.93 Electron Micrograph: Retina and choroid
Group 1, 4 Weeks Recovery
- Fig. 5.94 Electron Micrograph: Outer Retina and Choroid
Group 1, 4 Weeks Recovery
- Fig. 5.95 Electron Micrograph: Retina and Choroid
Group 1, 4 Weeks Recovery
- Fig. 5.96 Electron Micrographs: Receptor Cell Outer Segments
Group 1, 4 Days and 4 Weeks Recovery
- Fig. 5.97 Electron Micrographs: Outer Retina and Choroid
Group 1, 1 Week Recovery
- Fig. 5.98 Electron Micrographs: Suspected Pigment Epithelial
Proliferation
Group 1, 1 Week Recovery
- Fig. 5.99 Electron Micrographs: Outer Retina and Choroid
Group 1, 4 Weeks Recovery
- Fig. 5.100 Electron Micrographs: Suspected Pigment Epithelial Proliferation
Group 1, 4 Weeks Recovery
- Fig. 5.101 Table of Findings in Each Block. Group 2 (Lower Intensity)
- Fig. 5.102 Table of Findings in Each Block. Group 1 (Higher Intensity)
- Fig. 5.103 Table showing retinal illumination levels associated with
various light sources

CHAPTER 6

- Fig. 6.1 Table of light intensities and their Maximum Permissible
Exposure Times.
- Fig. 6.2 Graphic representation of the qualitative results of
Chapter 4.

ACKNOWLEDGEMENTS

This investigation was partly supported by the Medical Research Council (Grant No. G971/366/6), and partly by the Wellcome Trust (Grant No. 9543/1.5). Their generous help is acknowledged.

The experimental procedures reported in this thesis were carried out in the Tennent Institute of Ophthalmology, Glasgow. I am grateful to Professor W.S. Foulds for providing these facilities. I also wish to thank Professor W.S. Foulds and Professor W.R. Lee for their valuable help and guidance throughout this study. I am extremely grateful to Dr. H. Moseley, Department of Clinical Physics and Bio-Engineering, Glasgow, and Dr. D. Allan, Tennent Institute of Ophthalmology, Glasgow, for their assistance in the measurement of light intensities and associated parameters. I would also like to thank Mr. R. Taylor for his assistance with the manuscript and Mrs. J. Milliken for typing the manuscript.

The work reported in this thesis is entirely the work of the author, except for the mathematics in Appendix 2 which is the work of Dr. D. Allan.

Material from this thesis has been published and presented at conferences as shown below

- 1) Some Aspects of Radiant Energy Damage to the Retina
(In conjunction with W.S. Foulds)
Proc. VI Annual Meeting of the European Club for
Ophthalmic Fine Structure. Paris, 1978.
Albrecht v. Graefes Arch. klin. exp. Ophthal. 208,
109-124 (1978).
- 2) Recovery of the Rabbit Retina After Light Damage
(In conjunction with W.S. Foulds)
Proc. German Ophthalmological Society
Wundheilug des Auges und ihre Komplikationen
- 3) Recovery of the Rabbit Retina After Light Damage
(Preliminary observations)
(In conjunction with W.S. Foulds)
Proc. VII Annual Meeting of the European Club for
Ophthalmic Fine Structure, Ystad, 1972.
Albrecht v. Graefes. Arch. klin. exp. Ophthal. 212,
271-283 (1980).

4) Qualitative Observations on the Variation of Light
Induced Damage to the Rabbit Retina.
(In conjunction with W.S. Foulds)
Proc. VIII Annual Meeting of the European Club for
Ophthalmic Fine Structure. West Berlin 1980.
Albrecht von Graefes Arch. Klin. Ophthalmol. 215:
305-325 (1981).

SUMMARY

This thesis reports the findings of an investigation into the effects of various intensities of white light on the morphology of the rabbit retina and choroid as studied by light and electron microscopy. The exposure period was one hour in all the experimental procedures. The light levels employed ranged from an estimated retinal illumination of 20.4mWcm^{-2} to 84.4mWcm^{-2} . These levels of illumination are similar to those experienced by human retinæ during procedures such as indirect ophthalmoscopy (Calkins and Hochheimer, 1980).

The experimental procedures were divided into two categories:-

1) An investigation into the appearance of the retina and choroid immediately after exposure to various intensities of white light. Alterations in retinal and choroidal structure were assessed by both light and electron microscopy. In addition, it was attempted to quantify changes in the cellular components of the outer nuclear layer by a random point counting system.

2) An investigation, by light and electron microscopy, into the morphology of the retina and choroid at various times after a damaging light exposure with special consideration of the fate of the cellular debris produced by light damage.

To assess the immediate effects of light exposure, the eyes of nineteen adult Dutch rabbits were subjected to one of six light intensities. The estimated retinal illumination levels were 84.4, 38.6, 32.8, 28.9, 23.2 and 20.4mWcm^{-2} . Following exposure to the two lowest light intensities the retinal and choroidal tissues appeared normal. At slightly higher levels of retinal illumination (28.9mWcm^{-2} to 38.6mWcm^{-2}) there were disturbances of the receptor cells' outer segments as well as slight

distension of the pigment epithelium's smooth endoplasmic reticulum and mitochondria. Cone receptor cells were slightly more susceptible to damage than rod receptor cells. With higher light intensity both the degree and variability of damage increased markedly. At the retinal illumination level of 38.6mWcm^{-2} the morphology of the receptor cells and pigment epithelial cells was highly variable. These cells could appear swollen with both their cytoplasmic organelles and their nuclei being swollen, also, conversely, they could be shrunken, their cytoplasm becoming densely stained and their nuclei pyknotic. The choroid, at these light intensities, was usually normal in appearance but occasionally there did appear to be a slight inflammatory response in the vessels of the choriocapillaris. This response was usually confined to the appearance of degranulating platelets and a few polymorphonuclear leucocytes and monocytes. Very occasionally the vessels of the choroid were filled with impacted red cells. These regions of choroidal abnormality were usually associated with the regions of most extreme retinal damage.

At the highest level of illumination (84.4mWcm^{-2}) damage to the inner retina was variable in appearance. Damage to the receptor cells and pigment epithelial cells was present and often very severe. As was seen in animals exposed to lower light intensities, regions of severe retinal damage were associated with areas of choroidal abnormality.

The quantification of the cellular components of the outer nuclear layer yielded disappointing results. The results of the point counting system did seem to reflect the appearance of individual tissue blocks. However, the variation within retinae (block to block) and between animals was so great that there

could be no meaningful correlations. The variation in damage, determined by F ratios, was greater in animals exposed to the higher light intensities. These F ratios did show a positive correlation with light intensity for some of the features assessed.

The two highest light intensities employed were chosen in order to assess the recovery processes: exposure to these light intensities was known to result in considerable damage to the outer retina. Twenty eight Dutch rabbits were used. After exposure to one of the two light intensities (estimated retinal illuminations 38.6mWcm^{-2} and 84.4mWcm^{-2}) the rabbits were allowed to recover for period of 6 hours, 24 hours, 48 hours 4 days, 1 week, 2 weeks or 4 weeks.

Exposure to the Lower Intensity

Six and twenty four hours after exposure to the lower intensity there was distension of the pigment epithelium and disturbances of the receptor cell outer segments. Twenty four hours after exposure pyknotic receptor cell nuclei were present. After forty eight hours of recovery the pigment epithelium was greatly reduced in thickness and very densely stained. At this time macrophages were seen among the cell debris in the sub-retinal space. Mononuclear cells were common within the choriocapillaris and the extravascular tissues of the choroid. After four days recovery macrophages were plentiful within the subretinal space. One to four weeks after the photic insult the morphology of the retina was returning to normal appearance. Regions of damaged retina were still present, however. These areas were usually associated with disturbances of the choriocapillaris.

Exposure to the Higher Intensity

Six hours after exposure to the higher intensity the receptor cells were severely damaged and many of the receptor

cell nuclei were pyknotic. The pigment epithelium had lost much of its normal cellular architecture. There was also evidence of slight damage to the inner retina. Twenty four hours after exposure mononuclear cells were present in the choriocapillaris and macrophages were present within the subretinal space. There was also evidence of further degeneration within the inner retina. Forty eight hours after exposure both macrophages and Müller cells appeared to be active in the phagocytosis of receptor cell material. In some areas the Müller cell's cytoplasm was expanding into the outer nuclear layer filling the spaces produced by the degenerating receptor cells. Four days after exposure macrophages were still plentiful in the subretinal space. Mononuclear cells were present within the choriocapillaris and occasionally within Bruch's membrane. In some areas Müller cell cytoplasm was in direct contact with Bruch's membrane: the outer retina being lost. One to four weeks after the exposure a few large macrophages were still present within the retina, although the majority of the cellular debris had been removed. Surviving receptor cells had regenerated their outer segments. These outer-segments were often of abnormal appearance. Where there had been complete destruction of the receptor cells and pigment epithelium the retina was composed primarily of Müller cells, although other cell types could be identified. In less severely damaged regions abnormalities of the pigment epithelium, possibly reactionary hyperplasia, were encountered. Thickenings of Bruch's membrane and loss of the choriocapillaris were often associated with areas of severe retinal damage or pigment epithelial abnormality.

These findings and their implications are discussed.

STRUCTURAL DAMAGE TO THE RABBIT RETINA AND
CHOROID FROM LIGHT EXPOSURE

CHAPTER 1

INTRODUCTION

The vertebrate eye is a remarkably complex sense organ. The optical properties of the eye produce a projection of the visual field on the retina. The retina contains, in man, about 100 million receptor cells, which are connected in a complicated fashion to about a million fibres in the optic nerve: when light falls upon the retina the receptor cells are excited and this excitation eventually leads to the production of electrical activity, in the form of action potentials, in the optic nerve fibres.

The light sensitivity of the eye is due to the existence in the photoreceptor cells of a visual pigment, whose function is to absorb light and in so doing, to initiate the chain of events leading to excitation of the optic nerve fibres. The photochemical reaction initiated by the absorption of light bleaches the pigment, which has to be regenerated before it regains its photosensitivity.

The range of sensitivity of the eye is enormous: the brightest light in which we can see is about 10^{10} times the intensity of the dimmest. There are several mechanisms which enable this wide range to be perceived, which constitute the phenomena of visual adaptation. Dark adaptation is the increase in sensitivity which occurs in surroundings of dim illumination, and light adaptation is the reverse of this.

Visible light consists of a very limited region of the electromagnetic spectrum. The visible spectrum, the range of electromagnetic radiation that can pass through the eye and cause a photochemical change in the visual pigments covers the wavelengths from about 400nm (violet) to about 700nm (red) longer wavelengths out to about 1,300nm are transmitted by the ocular media but as they are not absorbed by the visual pigments they are not perceived.

Light is emitted and absorbed in discrete packets known as quanta or photons. In a photochemical reaction, one molecule of pigment absorbs one quantum of light. The energy of quantum varies with the wavelength and is given by $E = hv$, where v is the frequency (the velocity of light divided by the wavelength) and h is Planck's constant, 6.63×10^{-34} Js. Thus quanta for blue light is more energetic than red.

1.2 The Structure of the Eye

The photoreceptor cells of the eye, and the nerve cells which they innervate form a thin layer, the retina, which coats the inner surface of the eye. The rest of the eye consists of accessory structures concerned directly or indirectly, with assisting the retina in the perception of the visual field.

The gross structure of the vertebrate eye is shown in Fig. 1.1. The outer coat of the eye, the sclera is protective in function and also, maintains the shape of the globe. The cornea is the transparent region of the sclera and in most vertebrates is responsible for the greater part of the refraction of light needed to produce an image on the retina. Inside the sclera is a vascular layer, the choroid, which is usually pigmented.

The interior of the eye contains the lens, the aqueous humour in the anterior chamber and the vitreous humour which fills the cavity behind the lens. The curved surface of the cornea acts as a lens, so that a parallel beam of light entering a lensless human eye is brought to a focus at about 31.2mm behind the front face of the cornea. Since the length of the eye is about 24.4mm, the cornea, aqueous and vitreous alone cannot produce a sharp image on the retina. The required

extra focussing power is provided by the lens which is of a higher refractive index than the aqueous and vitreous humours. The power of the lens can be increased by contraction of the ciliary muscles; this process accommodation, allows images of near objects to be focused on the retina.

In front of the lens is a diaphragm, the iris, whose aperture (the pupil) can be varied by contraction of the iris muscles. Thus the activity of the iris can, over a limited range, regulate the amount of light entering the eye. The pupil is in fact controlled reflexly by light intensity.

The direction in which the eye looks is controlled by the six extraocular muscles.

1.3 The Structure and Function of the Retina and Choroid

1.3.1 The Retina

The neural structure of the retina is much more complex than that of most other peripheral sense organs. The developmental reason for this is that it is formed by an outgrowth of the brain in the embryo. The photoreceptors have probably evolved from flagellated cells forming the ependymal lining of the cavities of the brain. This accounts for their position on the external side of the mature retina, so that light must pass through the rest of the retina before reaching them.

The structure of the retina is shown in Fig. 1.2. From light microscopy studies the retina has been described as consisting of eleven layers, although these layers do not accurately describe the cellular relationships within the retina. These layers are (1) The retinal pigment epithelium, (2) The outer

segments, (3) The inner segments, (4) The external limiting membrane, (5) The outer nuclear layer, (6) The outer plexiform layer, (7) The inner nuclear layer, (8) The inner plexiform layer, (9) The ganglion cell layer, (10) The nerve fibre layer and (11) The internal limiting membrane.

The photoreceptor cells are of two types, described, from their shapes, as rods and cones. They synapse with small interneurons, the bipolar cells, which themselves synapse with the ganglion cells. The axons of the ganglion cells form the optic nerve, and carry visual information from the retina to the brain. In addition to this sequential system, there are two lateral systems of neurons: the horizontal cells, which form interconnections between the receptor cells, and the amacrine cells, which synapse with each other, with the ganglion cells, and with the proximal ends of the bipolars. Filling the spaces between these various neurons are the Müller cells.

The relationships of the various cell types to the retinal layers are as follows: The pigment epithelium cells form a continuous monolayer of cells external to the neural retina and forms layer (1) of the retina. The receptor cells, both rods and cones, extend over several retinal layers. The photoreceptive elements of the receptor cells are the outer segments. Internal to the outer segments are the inner segments, which can be regarded as specialised energy supplying regions of the receptor cells. Separating the receptor cell nuclei, in the outer nuclear layer, from the inner and outer segments is the outer limiting membrane. Electron microscopic studies have revealed that the external limiting membrane is not a true membrane but a regular array of cell junctions between the receptor cells and the fine distal processes of the Müller cells. The outer plexiform layer contains the

dendrites and synapses of the rods and cones, the bipolars and the horizontal cells. The inner nuclear layer contains the nuclei of the bipolars, horizontal cells and Müller cells. The inner plexiform layer contains the synapses and dendritic processes of the bipolar cells, amacrine cells and ganglion cells. The ganglion cell layer contains the nuclei and cell bodies of the ganglion cells, their axons forming the nerve fibre layer. Finally, the inner limiting membrane is formed by the basement membrane of the Müller cells and vitreous collagen fibres. These inter relations are summarised diagrammatically in Fig. 1.3.

The structure of rods and cones is shown roughly in Fig. 1.3. The outer segment, which contains the visual pigment, consists of a stack of membranous discs in rods or possibly infoldings of the cell membrane in cones. The outer segment is connected to the inner segment, which contains numerous mitochondria, by a thin neck whose structure is very like that of a cilium. Inner to the inner segment is the cell body which contains the nucleus. The inner portion of the receptor cell extends into the outer plexiform layer where the receptor cell synapse is located.

It has become apparent that the rods and cones have different functions. The rods are used for vision in conditions of low light intensity and are not involved in colour vision. The cones are used at higher light intensities, and for colour vision. In the primate retina, at least, visual acuity is higher for cone vision than for rod vision. This comprises the basis of the duplicity theory, which was first proposed by Schultz in 1866. It is well known that, in very low light intensities, the fovea is practically blind, and vision depends upon the extrafoveal regions of the retina; colour vision is absent under

those conditions. Schultz pointed out that these features correlate with the distribution of the two types of photoreceptor cells.

There are no rods in the fovea. He went on to examine the retinae of a variety of different vertebrates, and showed that nocturnal animals tend to have a great preponderance of rods, and diurnal animals have a corresponding preponderance of cones. The rabbit, being crepuscular, has both rods and cones, although rods predominate constituting about 92% of the rabbit photoreceptors (Hughes, 1971).

Some information about the functional state of the retina can be derived from the electroretinogram (E.R.G.). The ERG is a mass electrical response of the retina recorded with external electrodes, one placed on the cornea and the other at some indifferent point on the body. An enormous amount of work has been done on this response since its discovery in 1865 by Holmgren (Einthoven and Jolly, 1908, Granit, 1947, 1962. Brown, 1968). The ERG has been used to assess the effects of various noxious stimuli on the function of the retina, including light damage (Noel, 1965; Noel, Walker, Kang and Berman, 1966; Gorn and Kuwabara, 1967; Lawwill, 1973).

1.3.2 The Choroid

The choroid, lying between the neural retina and the sclera, is a thin, vascular, pigmented tissue. Because of its great vascularity, the choroid has some of the properties of an erectile tissue. The choroidal capillaries, the choroicapillaris, form a very unusual pattern, being arranged in a single layer immediately adjacent to the neural retina; this arrangement enables the capillary layer to provide nutrition to the outer retina. In the majority of mammalian species the retina is nourished

by separate retinal and choroidal circulations. The retinal vessels supply the inner retina including the ganglion cell and inner nuclear layers. The arterial vessels of the retinal circulation are derived from the central retinal artery which in many animals arises as a branch of the ophthalmic artery. However, the rabbit all but lacks a retinal circulation, the entire nutritional requirements of the retina being met by the choroidal circulation. Under these conditions the choroidal circulation is of extreme importance for the maintenance of structure and function of the neural retina. The choroidal stroma contains a considerable number of melanocytes, these cells contain the pigment, melanin, which is responsible for the dusky brown appearance of the choroidal tissues. This pigmentation, in addition to the pigment present within the retinal pigment epithelium acts in much the same way as the antihalation layer of a photographic film in reducing the back scattering of light which would otherwise degrade the quality of the image formed on the retina.

In addition to meeting some or all the nutritional requirements of the retina, the choroidal vessels supply blood to and receive blood from the anterior portion of the eye. The nerves that supply the anterior part of the eye also pass through the choroid into the ciliary body. The choroid itself has an extensive nerve supply, which is possibly important in the regulation of the choroidal blood supply.

1.4 Background to the Present Study

In general, the aim of this thesis is to examine by light and electron microscopy the morphology of the rabbit

retina following exposure to moderate intensity, moderate duration illumination such as encountered in some diagnostic and therapeutic procedures.

Eye damage from light exposure has been recognised since early recorded history. Plato in his "Phaedo" reports cases of eclipse blindness. Galileo is known to have injured his eyes by observing the sun through his telescope (Walker, 1916). More recently, in 1916, solar eclipse burns on the retinae of observers were described by Verhoff and Bell.

During World War II military plane spotters were purported to have received eye damage from viewing the sun through high power binoculars (Flynn, 1942).

Some of the first modern, quantitative work measuring the amount of light required to produce retinal lesions was done in the later 1940s by Meyer-Schwickerath (Meyer-Schwickerath 1969) while working with the Carl Zeiss Optical Company.

This work led to the development of the retinal photocoagulator, a device which used xenon arclamps to produce light which was sufficiently intense to produce retinal lesions. These lesions were used as "welds" to tack down detached retinae.

During the early 1950s Ham and others began investigating the possibility of retinal burns occurring as a consequence of observation of atomic explosions (Buettner and Rose, 1953; Byrnes, Brown, Rose and Cibis, 1955; Rose, Brown, Byrnes and Cibis, 1956; Byrnes, Brown, Rose and Cibis, 1956; Ham, Weisinger, Schmidt, Williams, Ruffin, Schaffer and Guerry, 1958). Sources of light for these studies were somewhat scarce, and flash burns from atomic detonations were not considered to be a public health problem.

Since the development of the first operational laser (Maiman, 1960) there has been considerable research aimed at determining the effects of lasers on the eye. Lasers can be divided into two groups depending on the nature of their output.

- 1) Continuous wave (CW) or quasi-CW (a number of short pulses per second).

- 2) Pulsed lasers which may be worked "normal mode" with a pulse length around 1ms, or Q-switched, producing a giant pulse with a very short duration of between 10 and 300ns.

The effects of pulsed lasers are beyond the scope of this thesis, as the extremely short pulse durations give rise to a variety of non-linear effects such as steam and melanin granule explosions with associated shock waves often producing massive mechanical damage to the retina. Electric field effects, electrostrictive stresses and radiation pressure effects may all occur in very high energy short duration pulses.

However, the thermal and associated mechanical effects produced by pulses of high energy and short duration are so destructive to the retina that they need not be considered in any discussion of near threshold light damage (Mellerio, 1967; Makous and Gould, 1968; Marshall and Mellerio, 1968; Leibovitz, Peacock and Friedman, 1969; Marshall, 1970; Marshall and Mellerio, 1970; Van Pelt, Payne and Peterson, 1973; Ham, Mueller, Goldman, Newman, Holland and Kuwabara, 1974; Goldman, Ham and Mueller, 1975).

The effects of CW lasers are far more predictable in terms of the retinal damage they are likely to produce. Although parameters such as wavelength, area of retinal illumination, pigmentation, pulse duration and retinal illuminance

have to be taken into consideration as well as the possibility of photochemical effects in long duration, low energy exposures (Campbell, Rittler, Noyori, Swope and Koester, 1966; L'Esperance and Kelly, 1969; Rosan, Flocks, Vassiliadis, Rose, Peabody and Hammend, 1969; Bresnick, Frisch, Powel, Landers, Holst and Dallas, 1970. Ham, Geeraetes, Mueller, Williams, Clarke and Cleavy, 1970; Frisch, Beatrice and Holsen, 1971; Marshall, Fankhauser, Lotman and Roulier, 1971; Powel, Bresnick, Yanoff, Frisch and Chester, 1971; Adams, Beatrice and Bedell, 1972; Sliney and Freasier, 1973; Apple, Goldberg and Wyhinny, 1973; Cavonius, Elgin and Robbins, 1974; Marshall, Hamilton and Bird, 1975; Ham, Mueller and Sliney, 1976; Lerche, Beeger and Russow, 1978).

Photocoagulation of the retina has become common in the treatment of proliferative diabetic retinopathy and other conditions which can lead to retinal detachment and blindness. Photocoagulation of the retina can be achieved with both CW lasers and xenon arc photocoagulators, lesions of this nature are usually thermal in origin; (Geeraets, Williams, Chan, Ham, Guery and Schmidt, 1962) coagulation of the retinal proteins being produced by heat transfer from the retinal component which has absorbed the incident light, usually the melanin of the pigment epithelium and choroid or occasionally blood in the retinal vessels. The retinal lesions with which this thesis is concerned are those which cannot be explained on the basis of thermal coagulation or protein denaturation. However, CW lasers have been used in low intensity long exposure experiments. Lawwill (1973), and Lawwill, Crockett and Currier (1977a, 1977b) employed the argon laser at low

levels of continuous illumination for 4 hours to produce retinal damage in rabbits and monkeys. The results of these studies are comparable to those of this study, although Lawwill placed less emphasis on structural damage as revealed by light and electron microscopy and more on functional damage as demonstrated by electrophysiology. Lawwill has also suggested that light damage might be mediated by the visual pigment as light of 514.4nm (argon laser), which is quite close to the peak absorption of rhodopsin, about 500nm, is up to 5 times more effective in producing retinal damage than white light of the same intensity. However, it has been shown by Ham, Mueller, and Sliney (1976) and Ham, Ruffolo, Mueller, Clarke and Moon (1978) that the retina's sensitivity to damage increases markedly at short wavelengths. The threshold for damage produced by light of around 450nm being more than 2 orders of magnitude lower than that for light of 600-700nm. Anderson, Coyle and O'Steen (1972) have also reported increased sensitivity to damage from blue light. The mechanisms underlying this increased sensitivity to damage at the shorter wavelengths are, as yet, unknown but it probably involves photochemical reactions mediated other than by the visual pigments (Ham, Mueller and Sliney, 1976).

There have been a considerable number of studies on the effects of retinal illumination produced by instruments such as the indirect ophthalmoscope, (Friedman and Kuwabara, 1968; Tso, Wallow, Powell and Zimmerman, 1972; Tso, Fine and Zimmerman, 1972; Tso, 1973) intra ocular light sources such as are used in vitrectomy, (Pavel, Machamer and Aumagr, 1974; Fuller, Machamer and Knighton, 1978) and even slit lamps and operating microscopes (Hochheimer, D'Anna and Calkins, 1977).

Exposure of monkey retinae to all of these sources for periods ranging from 15 to 60 minutes have been shown to result in detectable lesions of the retina. However, with light sources such as the indirect ophthalmoscope the area of illumination in the monkey eye is about half that in the human eye with a corresponding increase in the intensity of retinal illumination, therefore it has been argued that human retinae are probably safe from damage (Pomerantzeff, Govignon and Schepens, 1969).

Concern about environmental light levels has been expressed by Cogan (1968) who noted that interior light levels might reach 10,000ft-c, equivalent to sunlight out-of-doors. In the experiments of Noel, Walker, Kang and Berman (1966), Gorn and Kuwabara (1967), Grignolo, Orzalesi, Castellazzo and Vittone (1969), continuous exposure of albino rats to light of about 700-1000ft-c resulted in irreversible damage to the retina, usually in the form of photoreceptor damage and loss and pigment epithelial disturbances. However, albino rats appear to be highly sensitive to retinal damage resulting from continuous exposure to light.

More recently in an editorial Dobson (1976) expressed concern about phototherapy. It has become common in many neonatal intensive-care units to use phototherapy to lower the bilirubin level in low-birth-weight infants who suffer from hyperbilirubinaemia. The light levels employed are in the order of 300-500ft-c. Exposure durations range from a few hours to 6 or more days of continuous or intermittent (e.g. 6 hours on, 2 hours off) exposure. Experiments using piglets, whose retinae are similar to those of newborn infants, showed extensive retinal damage after as little as 12 hours

exposure to light in a commercially produced phototherapy unit. (Sisson, Glauser, Glauser, Tasman and Kuwabara, 1970).

Additionally, the short wavelengths of light which are the most effective in producing retinal damage are also the wavelengths that are the most efficient in lowering bilirubin levels. In follow up studies on infants receiving phototherapy, with their eyes occluded, no evidence of retinal damage has been detected. (Kalina and Forrest, 1971; Dobsen, Cowett and Riggs, 1975).

In relation to the inability to detect retinal damage in infants who had received phototherapy, it is interesting to note that Anderson and O'Steen (1972) reported black-white and pattern discrimination in rats in which the photoreceptors had disappeared following light damage. To explain this anomalous finding they postulated that some retinal element other than the photoreceptor was capable of detecting light. However, in 1976 Cicerone and LaVail independently described surviving photoreceptors in the light damaged rat retina.

From their synaptic organisation and nuclear chromatin distribution these cells appeared to be cones. La Vail (1976a) suggested that these surviving cone cells may have been responsible for the black-white and pattern discrimination observed in light damaged rats by Anderson and O'Steen (1972). These observations would suggest that there is considerable redundancy within the retina and that many photoreceptors would have to be lost before any great impairment of visual function would result. It has been suggested by Kuwabara and Okisaka (1976) that the retina may have an overabundance of photo-

receptors to compensate for their gradual loss due to ageing or damage. It is possible that exposure to light, even within physiological limits, results in a slow loss of photoreceptors which is not readily detected by ophthalmoscopy or electrophysiological investigation. Subtle alterations of, and damage to, the photoreceptors are probably only apparent at the levels of resolution afforded by light microscopy of thin plastic sections or by electron microscopy.

The damage produced by moderate intensity light is usually restricted to the outer retina, i.e. the retinal pigment epithelium and the photoreceptors. However, Radnot, Jabbagg, Heszeiger and Lovas (1969) reported ultrastructural changes in the Müller cells and horizontal cells, in human retina.

Fifkova, (1972 and 1973) has reported thinning of the outer nuclear layer and outer plexiform layer in rats following light exposure.

Damage to the photoreceptors is first apparent within the outer segment. This manifests itself as a breakdown in the ordered nature of the membraneous discs of the outer segments. These discs take on appearances variously described as whorls or vesicles (Friedman and Kuwabara, 1968). At about the same time as damage to the outer segments becomes apparent, changes in the ultrastructure of the pigment epithelium are encountered. These changes are less obvious than those in the receptor cell outer segment and are initially restricted to distension of cell organelles such as: the nucleus the mitochondria and the smooth endoplasmic reticulum.

Increased severity of damage results in increased outer segment disturbances and usually involvement of the receptor cell inner segment (mitochondrial swelling) and cell body

(nuclear pyknosis, swelling or shrinkage of receptor cell cytoplasm). Receptor cell nuclear pyknosis is thought, ultimately, to lead to cell death and complete degeneration of the receptor cell. Light damaged outer segments have been shown to be capable of complete regeneration, provided the receptor cell body and the retinal pigment epithelium are undamaged (Wyse, 1980). Severe damage to the receptor cells can result in complete receptor cell loss accompanied by fusion of the apical surface of the retinal pigment epithelium with the Müller cells of the retina (Kuwabara and Gorn, 1968). In some instances, presumably when damage to the outer retina is very severe, complete loss of receptor cells and retinal pigment epithelium has been observed. In these instances, Müller cells form an adhesion with Bruchs membrane, the outer retina being completely absent (Hanson, 1970a). In instances of severe receptor cell damage and/or pigment epithelial damage, phagocytic cells have been observed among the receptor cell outer segment debris. These cells appear to be particularly active phagocytes, and there has been much speculation as to their origins (Gloor, 1969; Hansson, 1970a; O'Steen and Lytle, 1971; Tso, 1973; O'Steen and Karciglu, 1974). During recovery from light damage hyperplasia and hyper-pigmentation of the retinal pigment epithelium have been observed (Ts'o, Fine and Zimmerman, 1972; Tso, 1973).

- 1) To investigate by light and electron microscopy the fine structural changes in the rabbit retina resulting from moderate intensity, moderate duration (1 hour) exposures to white light.
- 2) To determine the threshold for light damage.
- 3) To investigate qualitatively and quantitatively damage to individual retinal components resulting from various degrees of supra-threshold light exposure.
- 4) To investigate any possible effect of light on the structure of the choroid and to assess the role of choroidal damage in producing secondary retinal changes.
- 5) To study the repair processes following light damage.

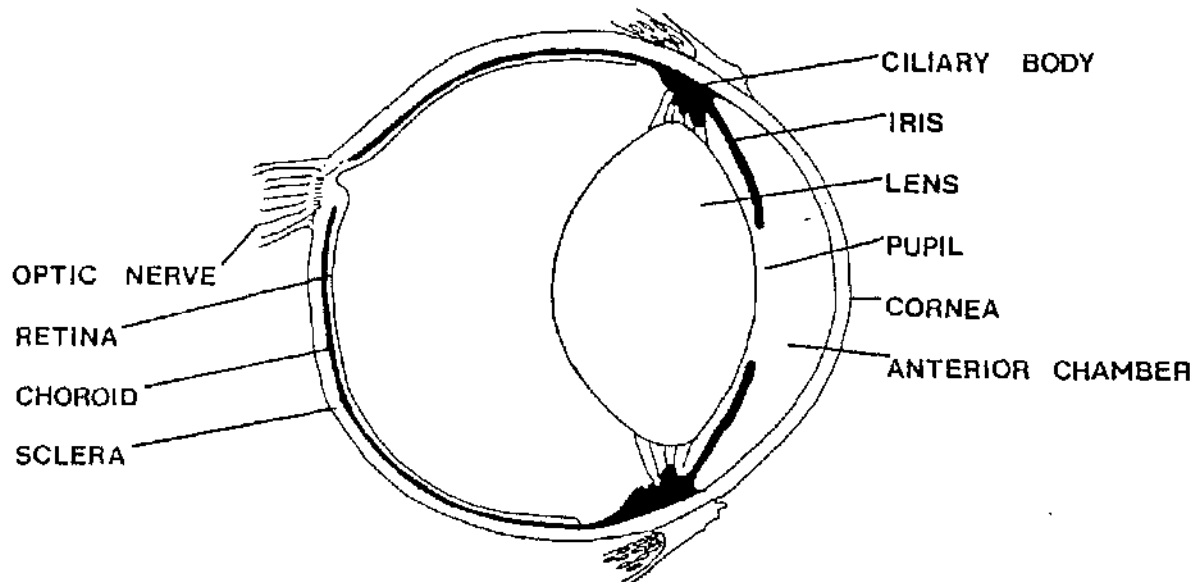


Fig. 1.1. Vertical section of a vertebrate eye, in this case rabbit, showing the relations of the major anatomical features.

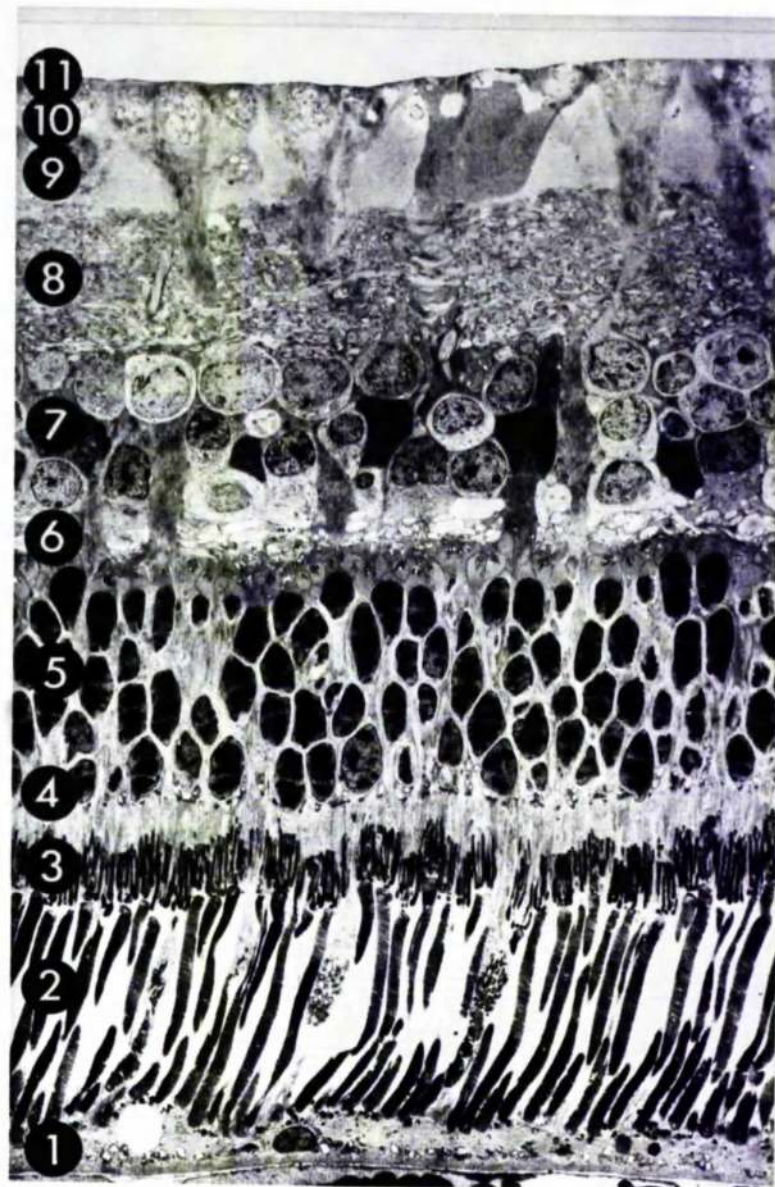


Fig. 1.2. Electron micrograph of the retina. Shown are the eleven layers described from light microscopic studies.

1. The retinal pigment epithelium, 2. The outer segments, 3. The inner segments, 4. The external limiting membrane, 5. The outer nuclear layer, 6. The outer plexiform layer, 7. The inner nuclear layer, 8. The inner plexiform layer, 9. The ganglion cell layer, 10. The nerve fibre layer, 11. The internal limiting membrane.

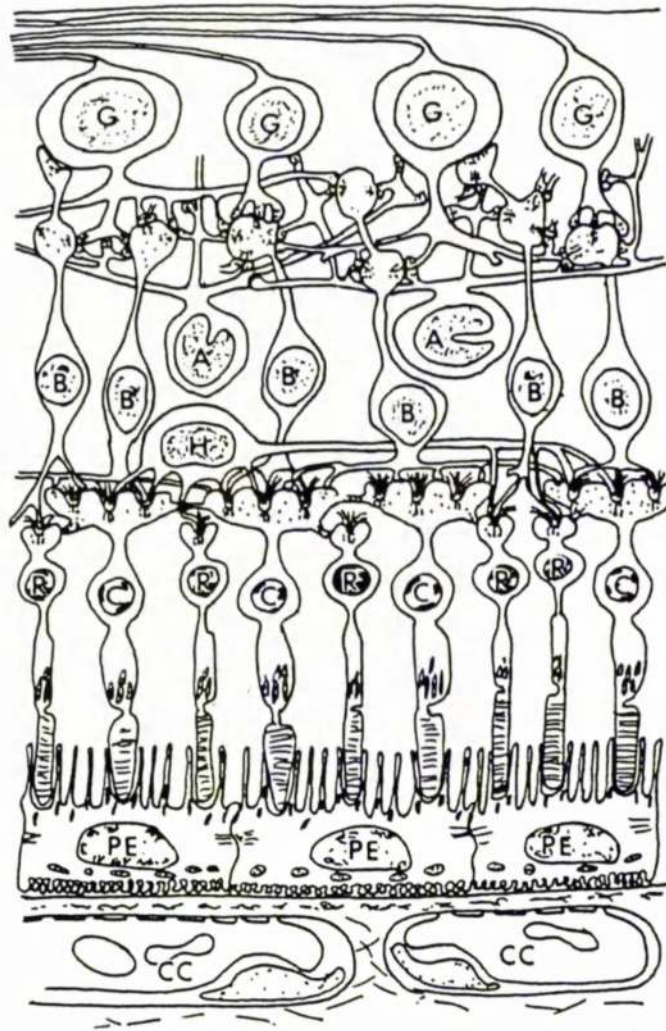


Fig. 1.3. Diagrammatic representation of interrelationships of cells in the retina. P E: pigment epithelium; R: rod cell; C: cone cell; H: horizontal cell; A: amacrine cell; B: bipolar cell; G: ganglion cell; CC: choriocapillaris. (From Dowling and Boycott, 1966 slightly modified).

CHAPTER 2

MATERIALS AND METHODS

The retinal and choroidal tissues examined were obtained from a total of 47 adult male Dutch rabbits weighing between 1.3 and 2.3kg. with a mean weight of 1.83kg. and a standard deviation of ± 0.26 kg. (see Appendix 1 for fuller details). In addition, a small number of normal eyes were obtained at the end of experiments conducted by others within the department.

On all occasions light was delivered to the experimental eye through a specifically designed fibre optic light guide (Appendix 2 for specifications). The light input for the fibre optics was from either one, or both of two light sources. This was possible due to the optical arrangement of the fibre optic guide (Fig. 2.1).

Source 1 was a commercially available unit, marketed as a light source for fibre optic systems. It contained a mains transformer giving a range of voltage outputs to 21.5 volts. The light source was a pre-focused 150 watt projector lamp, Atlas A1/184 (Fig. 2.2). Due to the design, the lamp's brightness could only be adjusted by reducing the lamp's supply voltage. Unfortunately, this also reduced the colour temperature of the lamp. Consequently this was considered as an unacceptable method of producing various intensities of light output from the fibre optic light guide. This source was only used, with the lamp driven at its maximum, with Source 2 to obtain the highest intensity employed in these investigations (Appendix 2 for further specifications).

Source 2 was specially constructed (Fig. 2.3). It contained a mains transformer giving an output of 24 volts.

The light source was a 24 volt, 250 watt projector lamp (Atlas A1/235). The optical arrangement (Fig. 2.3) included an iris diaphragm, which allowed continuous variation of the light entering the fibre optic light guide, without affecting the colour temperature of the lamp. (Appendix 2 for further specifications)

Only when the highest possible light intensity was desired were both light sources used together (Fig. 2.1). All other light intensities were obtained from Source 2. The output of this source could be reduced, by use of the iris diaphragm, until the desired output was obtained.

The lower outputs of Source 2 were measured as a percentage of the full output of the source. This was achieved by measuring the light intensity in the centre of the beam at the end of the light guide with a photodiode light meter (Appendix 2 for specifications). The voltage output of the photodiode light meter was displayed on an oscilloscope. (Linearity of the light meter was checked using a range of Kodak neutral density filters. It was found to be accurate within the limits of the filters.) The iris diaphragm of Source 2 was then adjusted until the required percentage of the output of the source was obtained.

Measurements of the light intensities employed in this investigation were conducted at the Department of Clinical Physics and Bio-engineering, West Graham Street, Glasgow. These measurements were then used to calculate the light levels in mWcm^{-2} within the beam emitted by the fibre optics and incident upon the retinae of the experimental animals (Fig. 2.4). (See Appendix 2 for raw data and method of estimating retinal illumination.)

Damage Experiments

The animals were anaesthetised with 40% urethane (ethyl carbamate made up in distilled water) injected over 10-15 minutes via the marginal ear vein until the corneal reflex had disappeared. The dose of anaesthetic was dependant on body weight: the amount given varying between 4 to 6ml. per kilogram body weight. The pupil of the experimental eye was maximally dilated with topically instilled 1.0% cyclopentolate and 10% phenylephrine. The animal was placed on its side and covered with a felt blanket. This covering was found sufficient to maintain the animal at its normal body temperature (36-38°C). The lids of the experimental eye were retracted with a speculum. The distal end of the fibre optic guide was positioned centrally, 2mm. from the cornea. This produced an area of illumination approximately 14mm. in diameter (See Appendix 2 for calculations of area of retinal illumination). The animals were exposed to one of six intensities (see Fig. 2.4 and Appendix 1). At the end of the various exposures the rabbits were killed with an overdose of urethane and the eyes removed and fixed. (Tissue preparation is described in Section 2.5.) Retinal and choroidal tissues were then taken for histological investigation.

Damage Experiments

The animals used were anaesthetised with Sagatal (6% sodium pentobarbitol). As intravenous administration was required throughout the course of the experiment a 23 gauge needle was left in position in the marginal ear vein. To prevent blood coagulation and allow finer adjustment of the level of anaesthesia

the Sagatal was diluted with saline and heparin. Two slightly different doses were used. Firstly, 2ml. of Sagatal and 1ml. of heparin (1,000 units) were made up to 10ml. by the addition of 7ml. of saline (0.9% w/v). Secondly, 3ml. of Sagatal and 1ml. of heparin (1,000 units) were made up to 10ml. by the addition of 6ml. of saline (0.9% w/v). The dose was dependant on body weight: the amount given in the first case being about 4ml. per kg. of body weight and in the second case 3ml. per kg. of body weight.

The pupils of the experimental eyes were maximally dilated with 1.0% cyclopentolate and 10% phenylephrine. Topical anaesthetic, (1.0% amethocaine hydrochloride) was given approximately 10 minutes before insertion of the speculum. The animals were exposed to one or other of the highest light intensities (Fig. 2.4, intensities 1 and 2). After the one hour light exposure the animals were placed in a dark environment to recover from the anaesthetic. Once the animals were active they were returned to the animal house and left to recover for periods of 6 hours, 24 hours, 48 hours, 4 days, 1 week, 2 weeks or 4 weeks (see Appendix 1). During the recovery period the animals were maintained under normal laboratory conditions of artificial illumination from 7.30am to 17.30pm.

At the end of the appropriate recovery period the animals were killed with an overdose of anaesthetic, the eyes removed, and retinal and choroidal tissues taken for histological investigation.

Immediately after removal the eyes were bisected in the equatorial plane and the vitreous removed. The posterior halves were immersed in 3% glutaraldehyde buffered with 0.2M sodium cacodylate (pH 7.2-7.4) at room temperature for a minimum of 4 hours. Before processing, areas of retinal and choroidal tissue were taken from selected regions. Sixteen blocks were taken from each experimental eye (Fig. 2.5). In all cases 4 blocks were taken from each control eye. The blocks were selected from anywhere within an area which corresponded to the area from which tissue was selected in the experimental eye. The pieces of tissue were dissected out in buffered sucrose (0.2M sodium cacodylate in 1% sucrose solution). The tissue pieces were washed at least 3 times in this solution prior to secondary fixation with buffered osmium tetroxide (0.2M sodium cacodylate) for 1 hour. After osmication the tissue was again washed in buffered 1% sucrose. This was followed by dehydration through a graded series of alcohols. From 100% alcohol the tissue was passed through increasing concentrations of Spurr's resin (Spurr, 1969). The embedded tissue was cured for 18 hours at 60°C (Fig. 2.6).

Selected plastic embedded tissue blocks were trimmed to size with razor blades under a low power microscope. After trimming, sections for both light and electron microscopy were cut with an L.K.B. Ultratome III.

2.6.1

Light Microscopy

1 to 2 μ m sections were cut with glass knives. The sections were transferred to glass slides and gently dried on a hotplate. The sections were stained, while hot, with toluidine blue (1% toluidine blue plus an equal volume of 2.5% sodium carbonate) for 5 to 10 seconds. The stained sections were then differentiated in distilled water and 70% methyl alcohol. The dried sections were then fitted with coverslips and mounted in Harleco's synthetic resin.

Sections were examined with a Leitz Orthoplan microscope. Suitable sections were then photographed, either on Kodak Kodachrome 25 or Kodak Panatomic X.

2.6.2

Electron Microscopy

Following light microscopy blocks of interest were retrimmed and cut with glass knives. Sections 70-80nm in thickness (Silver-gold in appearance by reflected light) after stretching with chloroform, were collected on copper grids of 100 or 150 mesh size. These were double stained with lead citrate (Reynolds, 1963) and uranyl acetate.

The sections were examined with a Philips EM.301 electron microscope. Suitable sections were photographed at a variety of magnifications on Kodak electron imaging film.

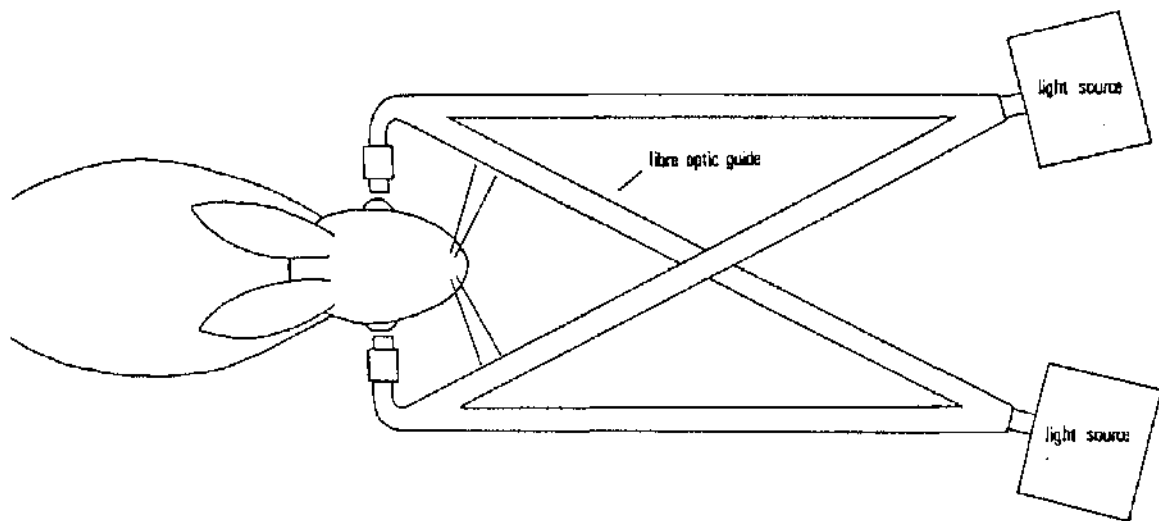


Figure 2.1

Diagrammatic representation of the arrangement of the light sources and fibre optics.

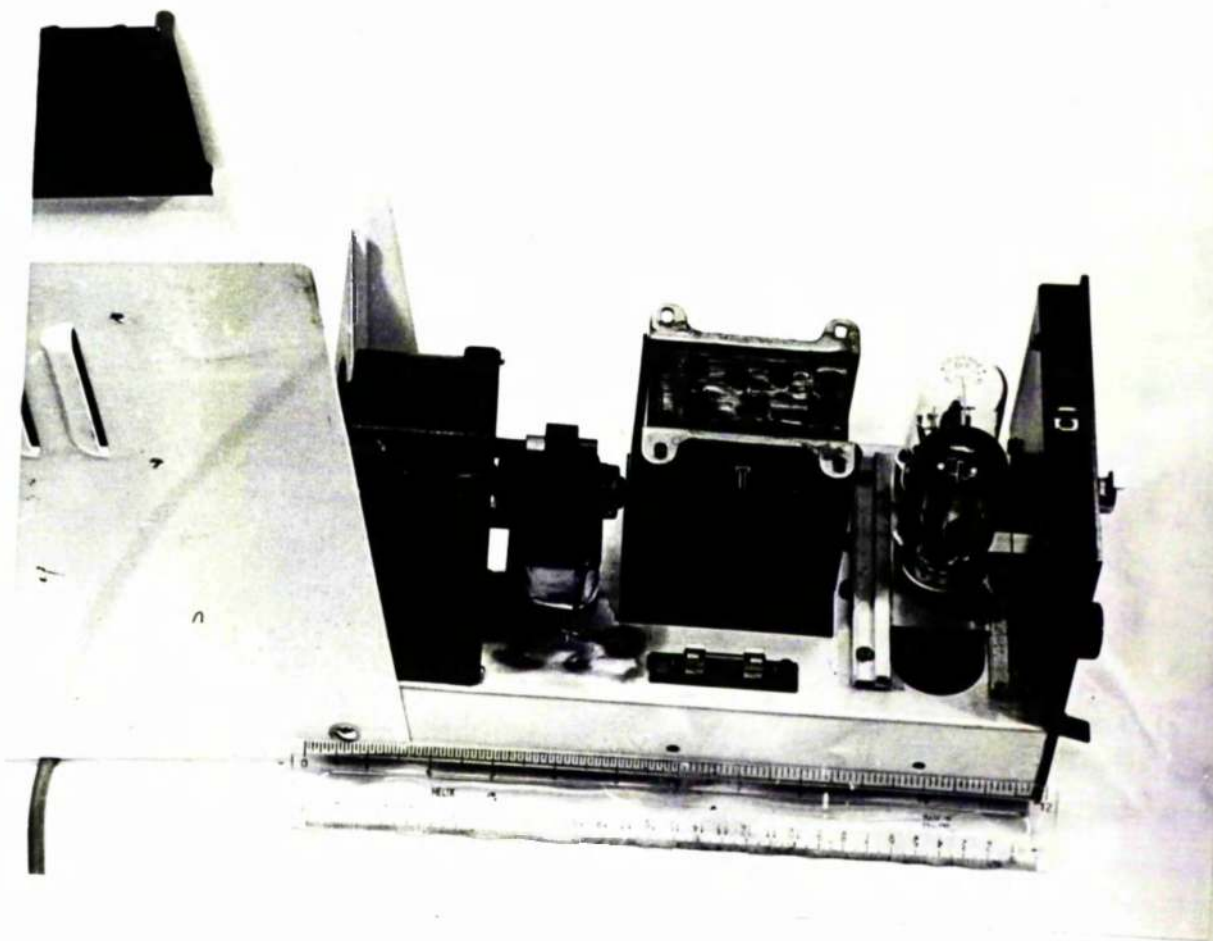


Figure 2.2

Photograph showing the internal arrangement of light Source 1. T: transformer; L: lamp with internal reflector.

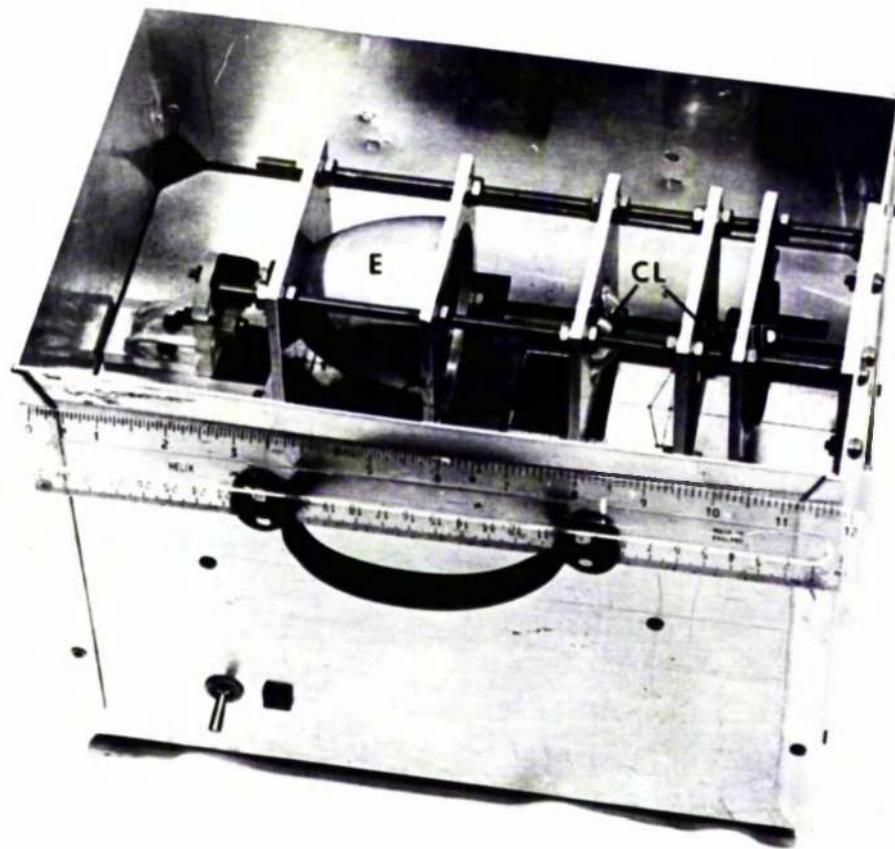


Figure 2.3

Photograph showing the internal arrangement of light Source 2. E: elipsoidal reflector; CL: condensing lenses; ID: iris diaphragm.

LIGHT INTENSITIES

GROUP	SOURCES		INTENSITY AT VARIOUS DISTANCES ¹			ESTIMATED RETINAL ILLUMINATION	
	1	2	50cm	15cm	2.5cm	A*	B*
1	ON	100% ON	0.91mWcm ⁻²	10.08mWcm ⁻²	363mWcm ⁻²	84.4mWcm ⁻²	168.4mWcm ⁻²
2	OFF	100% ON	0.41mWcm ⁻²	4.61mWcm ⁻²	166mWcm ⁻²	38.6mWcm ⁻²	77.2mWcm ⁻²
3	OFF	85% ON	0.34mWcm ⁻²	3.92mWcm ⁻²	140mWcm ⁻²	32.8mWcm ⁻²	65.6mWcm ⁻²
4	OFF	75% ON	0.31mWcm ⁻²	3.46mWcm ⁻²	116mWcm ⁻²	28.9mWcm ⁻²	57.9mWcm ⁻²
5	OFF	60% ON	0.25mWcm ⁻²	2.77mWcm ⁻²	100mWcm ⁻²	23.2mWcm ⁻²	46.3mWcm ⁻²
6	OFF	53% ON	0.22mWcm ⁻²	2.44mWcm ⁻²	80mWcm ⁻²	20.4mWcm ⁻²	40.9mWcm ⁻²

1) ASSUMING INVERSE SQUARE LAW APPLIES

A* ASSUMING AREA OF RETINAL ILLUMINATION
TO BE AS ESTIMATED

B* ASSUMING AREA OF RETINAL ILLUMINATION
TO BE 1/2 OF THAT ESTIMATED

Figure 2.4

Table giving measurements of the light intensities employed and estimates of actual retinal illumination levels.

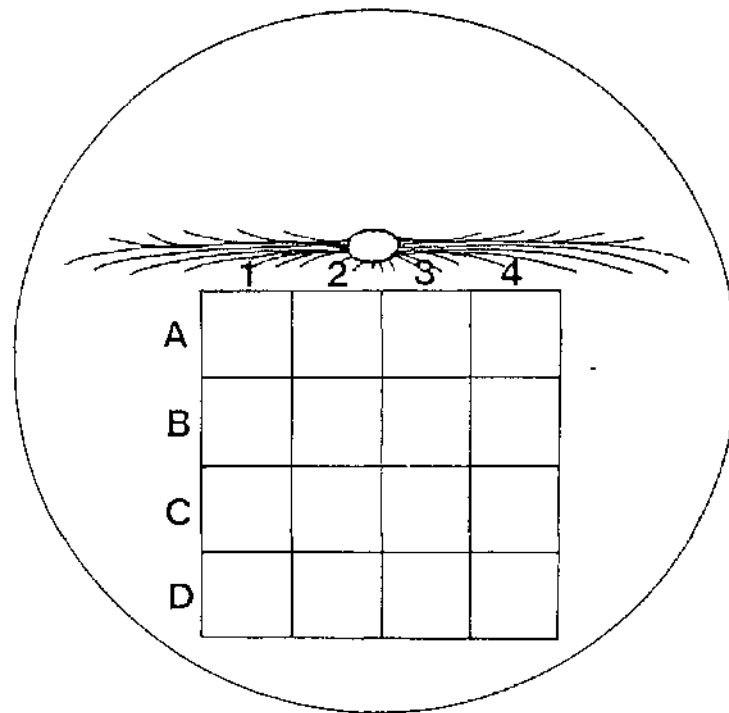


Figure 2.5

Diagram showing the grid used to identify tissue blocks.

TISSUE PREPARATION

- 1) IMMERSION FIX 3% GLUTERALDEHYDE IN CACODYLATE BUFFER (MINIMUM 24 HOURS).
- 2) TISSUE DISECTION. 3 WASHES CACODYLATE BUFFER.
- 3) SECONDARY FIXATION 1% OSMIUM TETROXIDE IN CACODYLATE BUFFER (1 HOUR).
- 4) 3 WASHES OVER 15MIN. IN CACODYLATE BUFFER.
- 5) DEHYDRATE THROUGH GRADED SERIES OF ALCOHOLS 10,30,60 AND 90%, PLUS 4 CHANGES OF 100% OVER 1 HOUR.
- 6) IMPREGNATE THROUGH GRADED SERIES OF ALCOHOL / SPURRS RESIN MIXTURES 50%, 75%, 100% RESIN. BLOCKED OUT INTO FRESH RESIN.
- 7) CURE FOR 20 HOURS AT 60°C.

FIXATIVE

0.2M NA CACODYLATE 33ML.
25% GLUTERALDEHYDE 12ML.
DISTILLED H₂O 55ML.
1.0M CALCIUM CHLORIDE 0.9ML *

BUFFER

0.2M NA CACODYLATE 33ML.
8% SUCROSE 12.6ML.
DISTILLED H₂O 54.5ML.

* FREQUENTLY OMITTED DUE TO TENDENCY TO FORM PRECIPITATE.

Figure 2.6

Table giving the tissue processing protocol.

CHAPTER 3

THE APPEARANCE OF NORMAL RABBIT RETINA AND CHOROID BY LIGHT AND ELECTRON MICROSCOPY

The purpose of this chapter is to describe the morphology of the rabbit retina and choroid in sufficient detail to allow comparisons to be made between the normal condition and the abnormal conditions described in later chapters.

The structure of the retinae of a very large variety of vertebrate species, including the rabbit, is well documented. Therefore detailed descriptions given in this chapter will be limited to those cell types of particular interest, i.e. the retinal pigment epithelium, the receptor cells, and the Müller cells. The other cells of the retina will be described but in less detail.

The choroid was of particular interest as it was thought to be the source of the exogenous macrophages, observed in the experimental tissue, either directly or from its blood supply. It is therefore necessary to give a description of its normal morphology and the various cell types which were encountered in this tissue.

A general description of the appearance of the retina and choroid by light microscopy will be given and a more detailed description of the cell types of particular interest by electron microscopy.

The rabbit is a crepuscular animal and this is reflected in the structure of the retina. The retina is devoid of a fovea and is rod dominated, although cone cells are present.

Histologically, the retina can be divided into three regions: the visual streak (approximately row B or C in Fig. 2.5), the periphery (row D and below in Fig. 2.5), and the region of the medullated fibres (row A and above in Fig. 2.5).

The visual streak (Fig. 3.1). This region is the thickest and most highly developed. It was characterised by well developed receptor cell outer segments, a thick outer nuclear layer, a thick inner nuclear layer, and an almost continuous single layer of ganglion cells. The high ratio of receptor cells to ganglion cells implies considerable summation of visual information within the retina. The characteristically thick inner and outer plexiform layers, typical of nocturnal animals, probably provide the structural basis, with their many synapses, for the summation of visual information.

The following description of the retinal layers can generally be applied to all three regions of the retina. The outer retina included the retinal pigment epithelium and the receptor cells (Fig. 3.2). The pigment epithelium consisted of a monolayer of cells extending all directions from the optic nerve head to the ora serrata. The cells of the retinal pigment epithelium were usually mono or binucleate, with conspicuous melanin granules in their apical cytoplasm. Inner to the retinal pigment epithelium were the receptor cells. These appeared to be of two distinct morphological types. By far the most numerous were rod cells. These cells had long slender outer segments and short inner segments. The other cell type, the cones, had longer inner segments than the rods and consequently shorter outer segments. The inner segments of both the rods and cones were clearly separated from the outer nuclear layer

by the outer limiting membrane, which appeared by light microscopy as a discontinuous, intensely staining line. Inner to the outer limiting membrane were the receptor cell nuclei. These appeared to be of two types, distinguishable by size and chromatin pattern. The larger, less frequently observed nuclei, had a diffuse chromatin pattern, were frequently found adjacent to the outer limiting membrane, and belonged to the cone cells (Fig. 3.2). The small nuclei were more numerous, possessed a more pronounced chromatin pattern, and belonged to the rod cells (Fig. 3.2).

The receptor cell synapses formed the outer margin of the outer plexiform layer (Fig. 3.3) and were of two types. The rod synapses were small and spherical while the cone synapses were larger and often triangular in outline with the apices of the triangles pointing toward the pigment epithelium. The inner regions of the outer plexiform layer were formed by numerous processes from cells lying in the inner nuclear layer.

The inner nuclear layer (Fig. 3.3) contained the cell bodies of the horizontal cells, the bipolar cells and the amacrine cells. The remainder of the inner nuclear layer was occupied by Müller cell cytoplasm. The nuclei of the Müller cells were also found in the inner nuclear layer. They were situated centrally in the layer, were angular in outline, lacked a nucleolus, and stained more evenly than the other nuclei of the layer. Horizontal cells were found on the outer side of the inner nuclear layer. Their nuclei were large, pale staining, and often surrounded by very poorly staining cytoplasm. The amacrine cells were found on the inner side of the inner nuclear layer. Their nuclei often showed an indented profile and the occasional nucleolus.

lus. The bipolar cells, like the Müller cells, had their nuclei centrally situated in the inner nuclear layer. Their nuclei were less angular than those of the Müller cells and could be frequently identified by the presence of a prominent nucleolus.

Inner to the inner nuclear layer was the inner plexiform layer (Fig. 3.4). This layer was composed of processes from the amacrine cells, bipolar cells, Müller cells, and ganglion cells. The ganglion cells (Fig. 3.4) lay inner to the inner plexiform layer and, in the region of the visual streak, formed an almost continuous row of cells. The nuclei and cytoplasm of the ganglion cells were similar in their staining characteristics, although some nuclei showed a prominent nucleolus.

Inner to the ganglion cell layer was the nerve fibre layer (Fig. 3.4). All around the cell bodies of the ganglion cells and their axons, which formed the nerve fibre layer, extended Müller cell cytoplasm. The innermost aspect of the retina was marked by the termination of the Müller cell cytoplasm at the inner limiting membrane (Fig. 3.4).

The peripheral retina (Fig. 3.5). This region of the retina was thinner and less well developed than the retina in the region of the visual streak. The receptor cells of the periphery had shorter segments than those of the visual streak. The thickness of the outer nuclear layer was reduced compared to the visual streak. This indicated a lower receptor cell density. The outer plexiform layer was also noticeably thinner. In the inner nuclear layer the number of nuclei appeared to be reduced, as did the number of ganglion cells, which did not form a continuous layer. Inner to the reduced ganglion cell layer was the nerve fibre layer, which was represented by small scattered bundles of unmyelinated nerves.

The region of the medullated fibres (Fig. 3.6). The retina in the region of these fibres was similar in organisation to the peripheral retina apart from the large bundles of myelinated nerve fibres which were present above the retina. Close to the optic nerve head the nerve bundles were large and the retina further reduced in thickness. Further from the nerve head, in the direction of the visual streak, the nerve bundles were reduced in thickness and the retina became increasingly similar in organisation to the visual streak (Fig. 3.7).

Among the myelinated nerve fibres glial cells were frequently found. These appeared to be of two types. The more numerous type had an oval, pale staining nucleus and were thought to be astrocytes. The less common type had a more intensely staining nucleus and were thought to be oligodendrocytes (Fig. 3.8).

In association with the myelinated nerve fibre bundles were found the retinal blood vessels (Fig. 3.8). Retinal vessels only occurred in the region of the medullated fibres and were generally extra-retinal. Occasionally, blood vessels were found within the nerve fibre bundles but they never penetrated to the retina beneath.

3.2.2 The Choroid

The rabbit retina being avascular, apart from the vessels of the medullated fibre region, must obtain its nutritive supply from the choroidal vasculature.

The inner surface of the choroid was firmly attached to Bruch's membrane. It was at its thickest and most pigmented posteriorly in the region of the visual streak. The choroid gradually became thinner towards the ora ciliaris, where it merged with

the ciliary body. However, as only the posterior regions of the choroid are of importance in later chapters, the description given of the normal choroid will be limited to the posterior region.

The choroid, as seen by light microscopy, can be divided into three morphologically identifiable regions: the choriocapillaris, the stroma, and the suprachoroidea.

The choriocapillaris (Fig. 3.9a and b). The capillaries of the choroid formed a single layer of highly anastomosed vessels directly below Bruch's membrane. The capillary lumen was unusually large and often flattened in the plane of Bruch's membrane. The appearance of the capillaries was highly variable and was found to depend greatly on the orientation of section.

In some sections they often appeared ovoid and regularly arranged (Fig. 3.9a). In other sections this organisation was lost and they appeared as long tubular structures (Fig. 3.9b). The choroidal capillaries were supplied by larger arterial vessels, lying scleral to the choriocapillaris, which were in turn supplied by the posterior ciliary arteries. Venous drainage of the choriocapillaris was through the venules of the choroid into the vortex veins. The arterioles and venules, with associated connective tissue, formed the stroma of the choroid.

The stroma (Fig. 3.10). The thickness of the stroma was found to be highly variable. This may be due, in part, to varying degrees of collapse of the choroidal arterioles and venules during enucleation. The extravascular tissues appeared as a loose network of various cell types. The most numerous cell types were fibroblasts and melanocytes. Frequently macrophages, mast cells, plasma cells and lymphocytes were observed.

They often formed "nests" near or between the larger vessels of the stroma, although they could be frequently identified in isolation (Fig. 3.11). The fibroblasts and melanocytes became more numerous in the outer two thirds of the stroma. Occasionally, in favourable sections, the smooth muscle cells surrounding the choroidal arterioles could be identified (Fig. 3.12).

Suprachoroidea (Fig. 3.13). The suprachoroidea appeared to be the transitional zone between the choroid and sclera. It was formed by lamellae of fibroblasts and melanocytes. Occasionally large nerves were encountered in this region (Fig. 3.14).

3.3 Electron Microscopy of the Retina

The description of the ultrastructure of the retina will be concerned, primarily, with the retinal pigment epithelium, the receptor cells and the Müller cells. The other cell types of the retina will be described but in less detail. The ultrastructure of the various cell types varied little with location. Therefore, a general description which applies to all locations studied will be given.

3.3.1 The Retinal Pigment Epithelium

The retinal pigment epithelium formed a single layer of cells which were rectangular in vertical section (Fig. 3.15). The cells showed membrane specialisation on their apical, basal and lateral surfaces.

The basal surfaces of the cells were in intimate contact with Bruch's membrane. The basement membrane of the pigment epithelium formed one of the five recognisable layers of

Bruch's membrane (Fig. 3.16). The basal membrane of the pigment epithelium was highly convoluted and formed a recognisable region of the cell, the basal infoldings (Fig. 3.16). Their convoluted nature could be appreciated more readily in horizontal section (Fig. 3.17). Numerous mitochondria were found adjacent to the basal infoldings. These specialisations are characteristic of cells involved in fluid transport (Pease, 1956; Bernstein, 1961; Bernstein and Hollenberg, 1965).

The apical surface of the pigment epithelium was composed of numerous finger-like or ridge-like processes which either ensheathed the distal portion of the receptor cell outer segments or extended into the interphotoreceptor space. Melanin granules were frequently observed within these processes and in the apical cytoplasm (Fig. 3.18). The intimate association between the apical surface of the pigment epithelium and the photoreceptor outer segments (Spitznas and Hogan, 1970) is probably related to the phagocytosis of receptor cell outer segment material which occurs during the renewal of the receptor cell outer segment (Dowling and Gibbons, 1962; Bairati and Orzalesi, 1963; young, 1965; Young, 1967; Young, 1969; Young and Bok, 1969; Young, 1971; Hogan, Wood and Steinberg, 1974; Young, 1976; Anderson, Fisher and Steinberg, 1978). Phagosomes of receptor cell outer segment material were frequently encountered within the cytoplasm of the pigment epithelium (Fig. 3.19).

The lateral cell membrane of the pigment epithelium was generally smooth and was characterised by a terminal bar or apical junctional complex. These apical junctional complexes were described for a variety of vertebrate species by Hudspeth and Yee (1973) and appeared to differ from those of other epithelia such as were described by Farquhar and Palade

(1963), who described the elements of the junctional complex as: a zonula occludens (tight junctions), zonula adhaerens (intermediary junction) and a macula adhaerens (desmosome) succeeding each other in the order given in an apical to basal direction. The pigment epithelial junctional complex as described by Hudspeth and Yee (1973) appeared to comprise, apically a gap junction, basally a zonula adhaerens, and a zonula occludens between and overlapping the other two junctions (Fig. 3.20).

The zonulae occludentes are thought, by the obliteration of the intercellular space, to be responsible for the barrier to diffusion of macro molecules formed by the pigment epithelium (Noel, 1963; Peyman, Spitznas and Straatsma, 1971a&b Peyman and Bok, 1972; Raviola, 1977) and for the high trans-epithelial resistance (the R. membrane) (Cohen, 1965). The gap junction of the apical complex is thought to mediate electrical coupling between adjacent pigment epithelial cells (Revel, Yee and Hudspeth, 1971; Hudspeth and Yee, 1973).

The cytoplasm of the pigment epithelium contained large amounts of smooth endoplasmic reticulum, which was evenly distributed throughout the cytoplasm of the cell (Fig. 3.21). Rough endoplasmic reticulum was limited in amount and was usually found in the apical cytoplasm near to the nucleus (Figs. 3.15 and 3.21). Free ribosomes and small membrane-bound vesicles occurred throughout the cytoplasm. The small membrane-bound vesicles may be involved in trans-epithelial transport (Fig. 3.22). The Golgi complex was well developed and, like the rough endoplasmic reticulum, was normally found close to the nucleus. The nuclei of the pigment epithelial cells were typically ovoid, long axes parallel to Bruch's membrane, they were basally situated in the cell (Fig. 3.15).

Binucleate cells were frequently encountered. According to the study of Tso and Friedman (1967) 85 per cent of rabbit pigment epithelial cells are binucleate.

A particularly prominent feature of the rabbit pigment epithelium was the presence of large lipid droplets. These were often sufficiently large to distort the apical surface of the cell (Fig. 3.21). These lipid droplets may be important in the storage of Vitamin A or its compounds (Young and Bok, 1970).

From these observations it is apparent that the pigment epithelium is responsible for the integrity of the blood retinal barrier, the control of, and exchange of, metabolites between the retina and choroidal blood supply, and the maintenance of the photoreceptor outer segment environment.

3.3.2 The Receptor Cell

The receptor cells were long slender cells which extended from the apical surface of the pigment epithelium to the outer plexiform layer of the retina.

The receptor cells appeared to be of two types, which correspond to the Type I and Type II receptors described by Sjostrand and Nilsson (1964). Morphologically, the Type I receptor was a typical rod (Fig. 3.23). There has been some controversy over the existence of cones in the rabbit retina. Although Sjostrand and Nilsson (1964) described a Type II receptor, they denied the existence of cones. Hughes (1971) clarified the problem by identifying the Type II receptor as an atypical cone. More recently Bunt (1978) has shown that the mechanism of replacement of outer segment membranes in the Type II receptor was similar to the replacement of cone outer segment material in other vertebrates (as shown by Young and Droz (1969); Young (1978) and Anderson,

Fisher and Steinberg (1978).) Apart from the outer segment the Type II receptors of the rabbit retina are morphologically similar to the cone cells of other vertebrates. Subsequently these cells will be referred to as cones.

Structurally, both rod and cone cells can be divided into distinct morphological regions: 1) The outer segment, 2) The inner segment, which can be further divided into elipsoid and myoid regions, 3) The cell somata, 4) The synaptic region, 5) The inner and outer receptor fibres, which connect the inner segment to the cell body and the cell body to the synaptic region respectively.

The outer segments of both rods and cones appeared to be formed by a highly ordered stack of membrane discs lying at right angles to the long axis of the outer segment. These discs were enclosed within the plasma membrane (Fig. 3.24). The rod outer segments were longer than those of the cones and consequently contained more discs. Within the membranes of the discs the photopigments are thought to be distributed (Denton, 1959; Wald, Brown and Gibbons, 1962). From other studies it has been suggested that the discs of the cone outer segment are continuous with the plasma membrane (Laties, Bok and Liebman, 1976). However, the discs of the rod outer segment appeared to be separate from the plasma membrane apart from the first few discs at the proximal end of the outer segment (Fig. 3.25). The distal ends of the photoreceptors were enveloped by the apical processes of the pigment epithelium. This ensheathing of the receptor cell outer segment was more marked for cone outer segments (Fig. 3.18). The outer segments of both rods and cones were connected to the inner segment by a narrow neck of cytoplasm supported by fibrils

extending from a basal body within the elipsoid of the inner segment (Fig. 3.26). Some of these fibrils extended the length of the outer segment. Fibrils also extended from the basal body through the elipsoid region of the cell and terminated in the myoid region.

The elipsoid region of both rods and cones contained numerous mitochondria (Fig. 3.23) whose long axes lay parallel to the length of the receptor cell. The myoid region of both rods and cones contained cisternae of rough and smooth endoplasmic reticulum, free ribosomes and neurotubules, in addition to well developed Golgi complexes (Fig. 3.27).

The cell bodies of the receptor cells were connected to the myoid region of the receptor cell by the outer receptor fibres. These fibres were of varying lengths, depending on the position of the cell body. As the cone cell nuclei were invariably adjacent to the external limiting membrane they virtually lacked outer receptor fibres. The more prominent outer receptor fibres contained a few small mitochondria, tubules of smooth endoplasmic reticulum, free ribosomes and many neurotubules (Fig. 3.28). The nuclei of the cone cells, and consequently the cell bodies, were larger than those of their rod counterparts. The rod and cone nuclei also differed noticeably in chromatin staining (Fig. 3.28). The inner receptor fibres connected the synaptic region to the body of the cell. Those of cone cells were generally thicker than those of the rods. The fibres contained many neurotubules, occasional mitochondria, a few vesicles and occasional free ribosomes.

The inner receptor fibres terminated at the receptor

synapses. The receptor synapses of both rods and cones lay at the scleral aspect of the outer plexiform layer. The synaptic region of cones differed structurally from that of the rods. The rod synaptic regions, termed spherules, were oval and contained a single ribbon synapse. The inner surface of the spherule was invaginated and contained processes from cells of the inner nuclear layer. In comparison, the cones synaptic region termed pedicles, were larger. The inner surface of the pedicle was flattened and possessed several invaginations, each associated with a ribbon synapse and processes from cells of the inner nuclear layer (Fig. 3.29). It was thought that the deeper lateral elements within the synaptic invagination were horizontal cell processes, while the central elements were bipolar cell dendrites. This general arrangement holds for both rod and cone synapses (Stell, 1965; Dowling and Boycott, 1966; Stell, 1967; Kolb, 1970; Dowling, 1970). The cone pedicle also synapsed with cells of the inner nuclear layer on its flattened surface, these were not associated with any invagination of the cell membrane (Fig. 3.29).

The receptor cells showed a distinct structural segmentation, each segment exhibiting a very different morphology. This segmental pleomorphism was probably a direct result of the extreme specialisation of function within each segment of the receptor cells.

3.3.3 The Müller Cell

The Müller cells were the major non-neural component of the retina. Their cytoplasm extended from the outer limiting membrane to the inner limiting membrane (Fig. 3.23).

External to the outer limiting membrane the Müller cells extend villous processes into the interphotoreceptor space. These processes surround the inner segments of the receptor cells (Fig. 3.30). Mitochondria were present within the Müller cells' cytoplasm inner to the villi, and suggested possible involvement of the cells in fluid transport.

The external limiting membrane was composed of zonulae adherentes between the Müller cells and the receptor cells. From tracer studies it has been concluded that these junctions offer little resistance to the passage of molecules, either from the outer retina inward, or from inner retina outward (Peyman, Spitznas and Straatsma, 1971 a and b).

The cytoplasm of the Müller cells continued inwardly, from the outer limiting membrane, packing the spaces between the receptor cells and ramifying into, and filling, the spaces between the neural elements of the outer plexiform layer (Fig. 3.31).

The nuclei of the Müller cells were found in the inner nuclear layer. They were angular, more evenly and more intensely stained than the other nuclei of the layer. Occasionally, some cisternae of rough endoplasmic reticulum, scattered tubules of smooth endoplasmic reticulum, and Golgi complexes were found in the region of the nucleus (Fig. 3.32).

The considerable quantities of glycogen reported to be present in the Müller cell (Kuwabara and Cogan, 1961; Magalhaes and Coimbra, 1972 and Johnson, 1977) were not observed in this study, probably as a consequence of the methods of fixation and dehydration (alcohol) employed.

From the inner nuclear layer the Müller cells' cytoplasm extended inward through the inner plexiform layer as a vertical column of cytoplasm sending off radial processes

which filled the intercellular spaces between the neural elements comprising the inner plexiform layer (Fig. 3.33).

Once clear of the inner plexiform layer the Müller cells' cytoplasm extended laterally and inwardly, totally enveloping the ganglion cells and their axons which formed the nerve fibre layer. The inner limiting membrane, the innermost aspect of the retina, was formed by the basement membrane of the Müller cells and vitreous fibres (Fig. 3.34).

3.3.4 The Neural Cells of the Inner Retina

Three neural cell types had their somata within the inner nuclear layer: the horizontal cells, the bipolar cells and the amacrine cells.

The horizontal cell somata were found along the outer margin of the inner nuclear layer. Their large, pale staining nuclei were often surrounded by considerable quantities of cytoplasm, which contained mitochondria, ribosomes and numerous Golgi complexes (Fig. 3.33 and 3.35). Pale staining processes, seen in favourable sections to originate from horizontal cells, spread laterally through the outer plexiform layer for considerable distances. It has been suggested that horizontal cells mediate lateral interactions within the outer plexiform layer (Polyak, 1941; Dowling and Boycott, 1966).

The bipolar cell somata lay in the outer half of the inner nuclear layer. The bipolar cells lining the outer margin of the inner nuclear layer had a greater amount of cytoplasm than those deeper in the layer (Figs. 3.33 and 3.36). The bipolar cells' cytoplasm contained many mitochondria, scattered cisternae of rough endoplasmic reticulum, neurotubules, fibrils and small Golgi complexes. The synapses

of the bipolar cells were present in both the outer plexiform and inner plexiform layers. They could be identified in the inner plexiform layer by their characteristic ribbon synapses (Raviola and Raviola, 1967).

The amacrine cell somata lay along the inner surface of the inner nuclear layer. The nuclei were usually large, pale staining, and often showed an invagination of the nuclear envelope. The moderate amount of cytoplasm which surrounded the nucleus contained plentiful endoplasmic reticulum, and scattered mitochondria and Golgi complexes (Fig. 3.33 and 3.36).

The processes of the bipolar cells, amacrine cells, and the dendrites of the ganglion cells, along with the supportive elements of the Müller cells, formed the inner plexiform layer (Fig. 3.33).

3.3.5 The Ganglion Cells and the Nerve Fibre Layer

The ganglion cells had large pale, uniformly staining nuclei, which often contained a nucleolus. Their cytoplasm contained large amounts of rough endoplasmic reticulum and free ribosomes. Scattered throughout the cytoplasm were neurotubules, smooth endoplasmic reticulum and occasional lysosome-like bodies. The Golgi complexes were frequently well developed. The mitochondria of the ganglion cells were usually poorly preserved and appeared as small rounded structures containing a few cisternae within an electron lucent matrix (Fig. 3.37). The ganglion cells' axons, which formed the nerve fibre layer, contained many neurotubules and neurofilaments, some free ribosomes and occasional mitochondria.

The morphology of the nerve fibre layer varied considerably with position. In the periphery and in the visual streak,

the axons forming the nerve layer were unmyelinated (Fig. 3.38). As the axons approached the optic nerve head they became myelinated. It was these myelinated fibres that gave the medullated fibres their characteristic appearance. Although unmyelinated nerves were still present (Fig. 3.39).

Glial cells were common among the nerve fibres. They appeared to be of two types, astrocytes and oligodendrocytes. The astrocytes had large round nuclei which were usually centrally placed in the cytoplasm. Their cytoplasm contained the usual variety of cell organelles as well as fine fibrils which were more pronounced in the cell processes (Figs. 3.39 and 3.40). The astrocyte processes frequently extended to the retinal/vitreous interface and, in some areas, provided the basement membrane forming the inner limiting membrane (Fig. 3.40). Occasionally, the processes of the astrocytes extended through the inner limiting membrane and enveloped the overlying vessels (Figs. 3.39 and 3.40).

The oligodendrocytes had small and irregular, eccentrically situated nuclei. Their cytoplasm was intensely staining and contained profiles of rough endoplasmic reticulum, neurotubules, and a few mitochondria (Fig. 3.41). The processes of the oligodendrocytes were smaller and more intensely stained than those of the astrocytes. Like the astrocyte processes they contained numerous neurotubules. From their morphology it would appear that the astrocytes and oligodendrocytes have a supportive and nutritive role in the nerve fibre bundles much as the Müller cell does in the retina.

The blood supply of the medullated fibre region did not constitute a true retinal supply as the vessels were

never seen to penetrate into the retina proper. This observation was in agreement with the findings of Tripathi and Ashton (1971). The vessels were generally free within the vitreous or surrounded by astrocytic processes (Figs. 3.39 and 3.40). Where the nerve fibre bundles were extremely thick (near the optic nerve head) the vessels penetrated among the nerve fibres, although they never penetrated as far as the underlying retina.

The endothelium of the retinal vessels were thought to possess tight junctions, as plasma protein staining could be observed within the vessels, but never external to them. Electron microscopy of the junctions was inconclusive in detecting tight junctions, probably as a result of the staining methods employed. ("En bloc" staining with uranyl acetate may have been more appropriate) (Fig. 3.42).

3.4 Electron Microscopy of the Choroid

A general description of the choroid has already been given by light microscopy. Therefore the description of the electron microscopy of the choroid will be limited to those structures or cell types which are of particular interest in later chapters.

The electron microscopy of the normal choroid will be described under the following headings: Bruch's membrane; the choriocapillaries; and The cells and blood vessels of the stroma and the suprachoroidea.

3.4.1 Bruch's Membrane

Bruch's membrane could be regarded as the division between the retina and the choroid. However, by electron microscopy, it can be seen that both the pigment epithelium and the endothelial cells of the choriocapillaries contribute

to its structure (Fig. 3.15). In accordance with Nakaizumi (1964), Bruch's membrane could be divided into five layers (Fig. 3.43).

- 1) The basement membrane of the pigment epithelium
- 2) The inner collagenous layer
- 3) The elastic layer
- 4) The outer collagenous layer
- 5) The basement membrane of the endothelial cells of the choriocapillaris.

The elastic layer was not particularly prominent when sectioned vertically. In tangential section, however, it was more prominent (Fig. 3.44). As layer 5 of Bruch's membrane was formed by the basement membrane of the endothelial cells of the choriocapillaris it was absent in the intercapillary zones (Fig. 3.15).

3.4.2 The Choriocapillaris

The choriocapillaris was formed by a single layer of highly anastomosed capillaries directly adjacent to Bruch's membrane. The capillary endothelial cells were enclosed by a basement membrane, the inner aspect of which formed layer 5 of Bruch's membrane. The endothelial cells showed some structural specialisation. Adjacent to Bruch's membrane their cytoplasm was extremely thin and showed numerous fenestrations (Figs. 3.15, 3.16 and 3.45). The lateral walls and the outer walls of the capillaries were usually thicker, showed fewer or lacked fenestrations, and contained the majority of the cell's organelles including the nucleus. The nuclei were irregular in outline and had prominent marginal heterochromatin. The cytoplasm contained a few mitochondria, smooth endoplasmic reticulum, and occasional

Golgi complexes (Fig. 3.45).

Endothelial to endothelial cell junctions were common. There did not appear to be any membrane fusion at these junctions (Fig. 3.43), and it was thought unlikely that these junctions offered any significant resistance to diffusion.

The fenestrations of the choriocapillaris were unusual in that they possessed a diaphragm (Fig. 3.46). The function of this diaphragm was unclear, as from tracer studies the endothelium has been found to offer little or no resistance, to diffusion (Peyman, Spitznas and Straatsma, 1971b; Peyman and Bok, 1972).

3.4.3 The Cells and Blood Vessels of the Stroma

The extravascular tissue of the stroma was comprised of a loose network of collagen fibres in which were found fibroblasts, melanocytes, and a mixed assemblage of inflammatory cells. Between the capillaries of the choriocapillaris it could be seen that the collagen fibres of the stroma were continuous with those of the outer collagenous layer of Bruch's membrane (Fig. 3.47).

The vascular tissue of the stroma was comprised of, in the inner regions, small venules and arterioles (Fig. 3.48). The arterioles were surrounded by smooth muscle cells. Unmyelinated nerves were often found in close association with the smooth muscle cells but synaptic contacts were not observed (Fig. 3.49).

The extravascular cells of the stroma were divided into two groups: 1) The fibroblasts and melanocytes. 2) A mixed assemblage of inflammatory cells.

The fibroblasts of the choroid were usually orientated with their long axes parallel to Bruch's membrane. However,

in the region of the choroidal vessels they tended to follow the contours of the vessel walls. The cells had elongated bodies which contacted most of the choroidal structures as well as other fibroblasts and melanocytes. Their cytoplasm contained profiles of rough endoplasmic reticulum, free ribosomes, mitochondria, and occasional Golgi complexes. The nuclei of the cells were moderately large and elongated. They showed a diffuse heterochromatin pattern with fine nuclear margination (Fig. 3.50).

The choroidal melanocytes, like the fibroblasts, were usually orientated with their long axes parallel to Bruch's membrane. In the vicinity of choroidal vessels, however, they tended to follow the contours of the vessels. Melanocytes became far more numerous, and more elongated, as the suprachoroidea was approached.

Ultrastructurally, their most conspicuous characteristic was the large number of melanosomes, which were scattered throughout the cytoplasm. The melanosomes of the melanocytes were more irregular in outline than those of the pigment epithelium. The remainder of the cytoplasmic inclusions were unremarkable. There were a few profiles of rough endoplasmic reticulum, occasional mitochondria and Golgi complex. Their nuclei were elongated, with their long axes parallel to Bruch's membrane.

The nuclei usually showed a diffuse chromatin pattern with a slight margination (Fig. 3.51).

Inflammatory cells were commonly seen in blood vessels and in the extravascular tissues of the choroid. Intra-vascular inflammatory cells were occasionally seen in fortuitous sections. These included monocytes, lymphocytes, and a variety of polymorphonuclear leucocytes (Fig. 3.52).

The extravascular inflammatory cells were usually encountered in the stroma in isolation or, infrequently, in "nests" between the larger vessels of the stroma (Fig. 3.53). The cell types identified in the extra vascular tissues were mast cells, plasma cells, lymphocytes, monocytes and macrophages.

Mast cells occurred infrequently, and usually singly, throughout the stroma. These cells were characterised by numerous cytoplasmic inclusions of varying electron lucency. This appearance differed from other descriptions of mast cells in which the cytoplasmic inclusions are of extreme electron density (Hogan, Alvarado and Weddel, 1971). It was thought likely that the electron lucency of the granules was due to leaching of their contents during processing for electron microscopy. The nuclei of the mast cells were often irregular in shape and showed pronounced heterochromatin staining. Mitochondria, Golgi complexes, and sparse endoplasmic reticulum occurred throughout the cytoplasm. Villous cytoplasmic processes were frequently observed extending into the media surrounding the cell (Fig. 3.54a).

Characteristically, the plasma cells contained extensive rough endoplasmic reticulum, and occasional mitochondria. The nuclei, although tending to be round, often showed irregularities of outline and showed marked marginal heterochromatin staining. The cell surface occasionally showed a few small villi (Fig. 3.54b).

The choroidal lymphocytes were of typical appearance, having little cytoplasm in relation to the size of the nucleus. Their cytoplasm contained scant profiles of rough endoplasmic reticulum, few mitochondria, and plentiful free ribosomes. The nuclei were usually round with very dense marginal heter-

ochromatin (Fig. 3.54c).

The macrophages of the choroid varied considerably in morphology, presumably reflecting their differentiation from monocyte to mature macrophage. It was often extremely difficult to distinguish between lymphocytes and monocytes. However, the monocytes were usually larger. Their nuclei were often invaginated and they possessed slightly more cytoplasm than the lymphocytes. The monocyte cytoplasm often contained small intensely stained bodies, 0.1-1.6 μ m. in diameter, in addition to the normal range of organelles (Fig. 3.54d).

The appearance of the macrophages of the choroid was highly variable. In addition to the normal range of cell organelles they frequently contained primary and secondary lysosomes. Occasionally the choroidal macrophages contained melanosomes, presumably derived from the choroidal melanocytes (Fig. 3.55).

3.4.4

The Suprachoroidea

The suprachoroidea can be regarded as the transition zone between the choroid and the sclera. Its cells were of two types: melanocytes and fibroblasts. The melanocytes and fibroblasts of this region were essentially similar to those of the choroidal stroma. However, the cells of the suprachoroidea were more elongated in profile than those of the stroma. A feature of this region was the presence of large nerves (presumably ciliary nerves) which contained both myelinated and unmyelinated axons (Fig. 3.56).

The junction between the suprachoroidea and the sclera was never observed as the sclera was always dissected off prior to processing for electron microscopy.

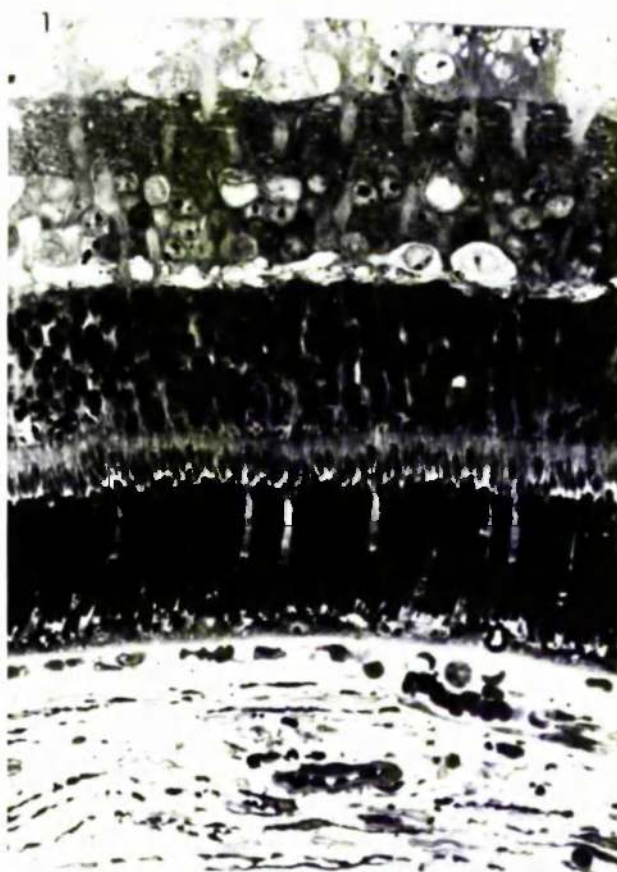


Figure 3.1.

Light micrograph of the retina in the region of the visual streak (x 400).

Figure 3.2.

Light micrograph of the outer retina in the region of the visual streak. C C: choriocapillaris; P E: pigment epithelium; Arrow heads: cone inner segments and cone cell nuclei (x 1000).

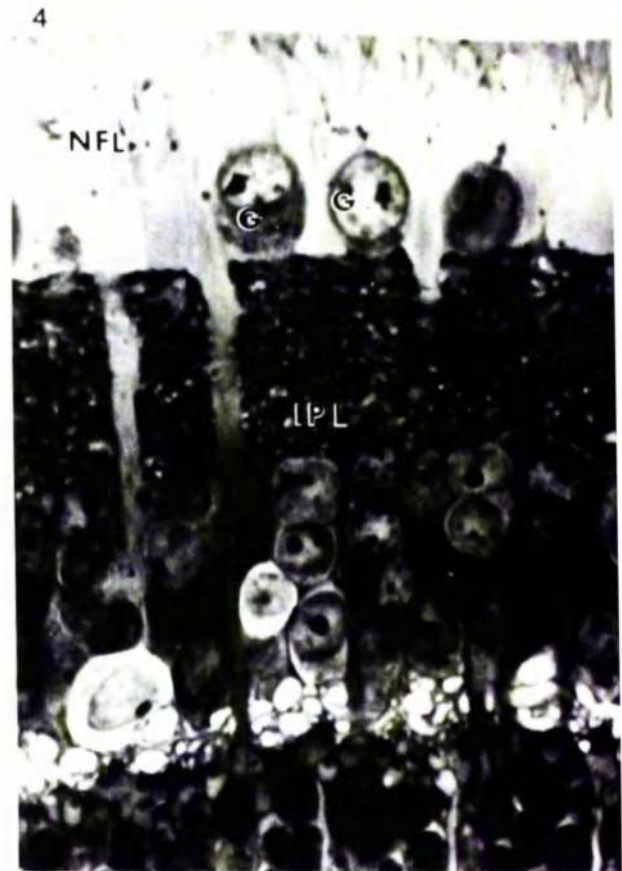
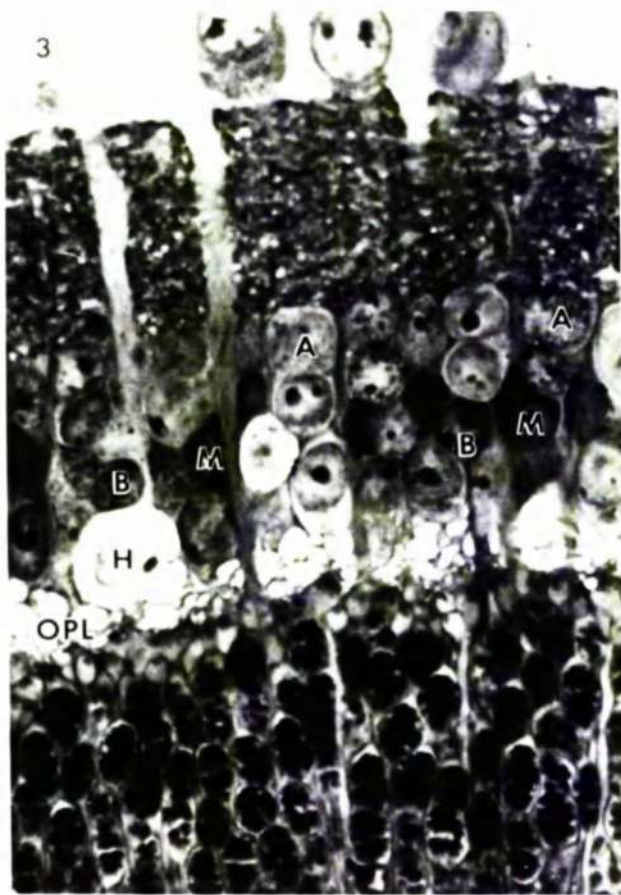


Figure 3.3.

Light micrograph of the inner retina in the region of the visual streak. OPL: outer plexiform layer; H: horizontal cell; B: bipolar cell; A: amacrine cell; M: Müller cell (x 1000).

Figure 3.4

Light micrograph of the inner retina in the region of the visual streak. I P L: inner plexiform layer; G : ganglion cell; N F L: nerve fibre layer (x 1000).

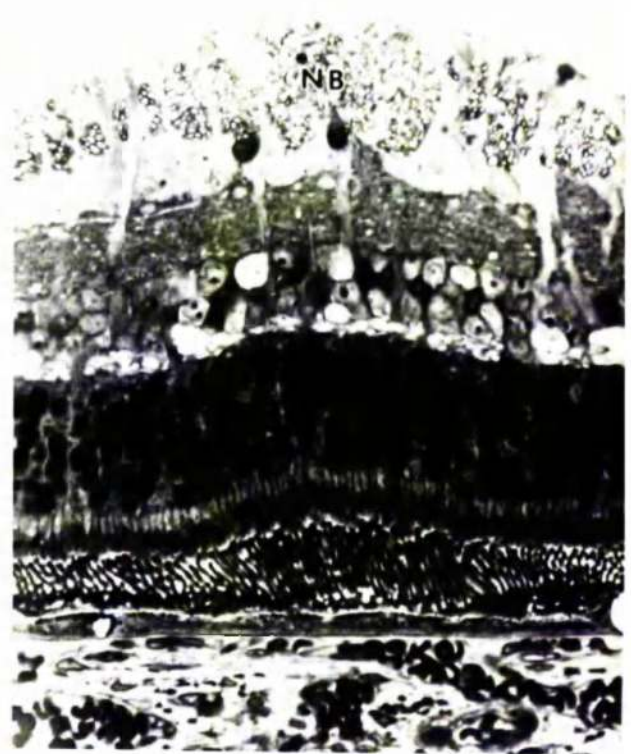
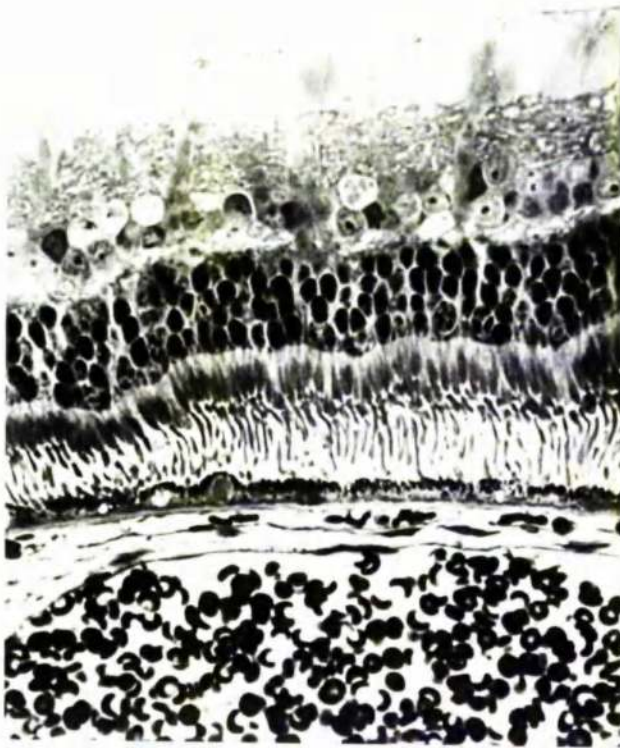


Figure 3.5

Light micrograph of the peripheral retina (x 400).

Figure 3.6

Light micrograph of the retina in the region of the medullated fibres. N B: nerve bundles (x 400).

7

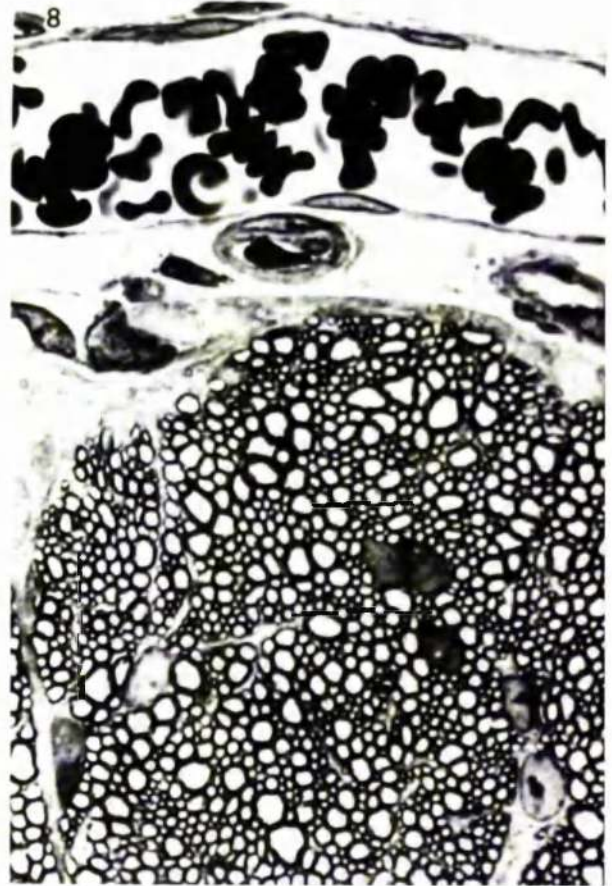
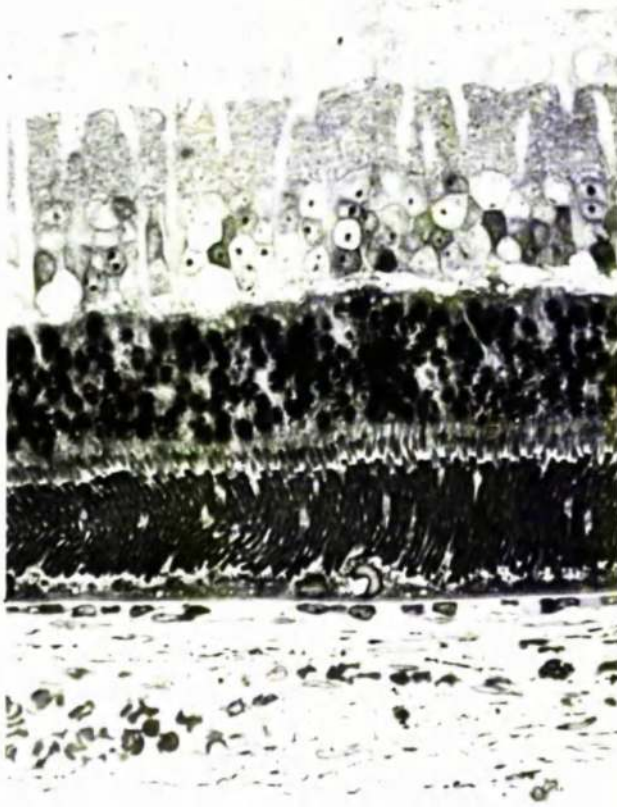


Figure 3.7

Light micrograph showing a region of retina between the visual streak and the medallated fibres (x 400).

Figure 3.8

Light micrograph of a myelinated nerve fibre bundle and associated blood vessels (x 1000).



Figure 3.9a and b

Light micrographs showing the highly variable appearance of the choriocapillaris and choroidal vessels. C C: choriocapillaris (both $\times 1000$).

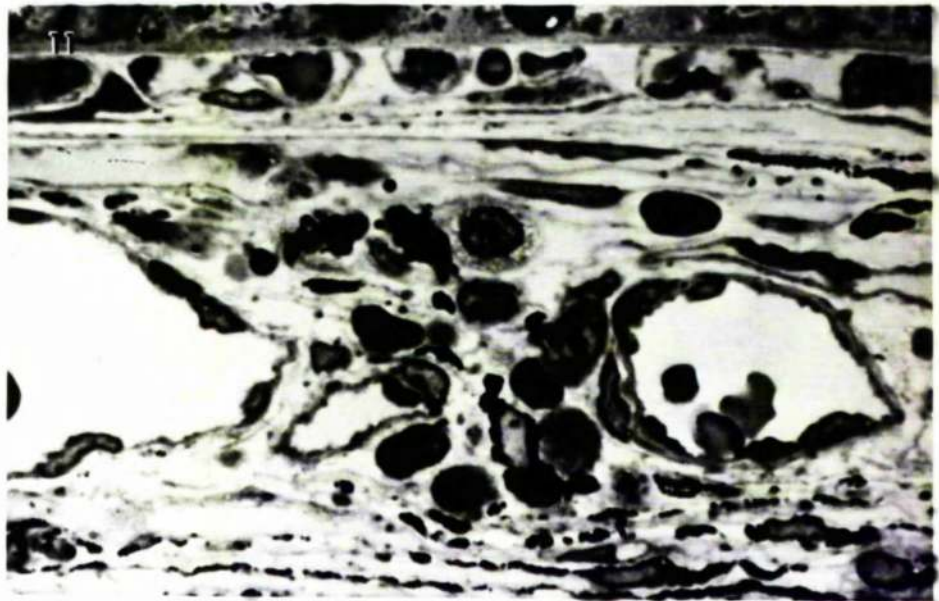


Figure 3.10

Light micrograph of the choroidal stroma. Me: melanocytes; F: fibroblasts (x 1000).

Figure 3.11

Light micrograph of the choroid showing "nests" of inflammatory cells occasionally seen between the larger vessels of the choroidal stroma (x 1000).

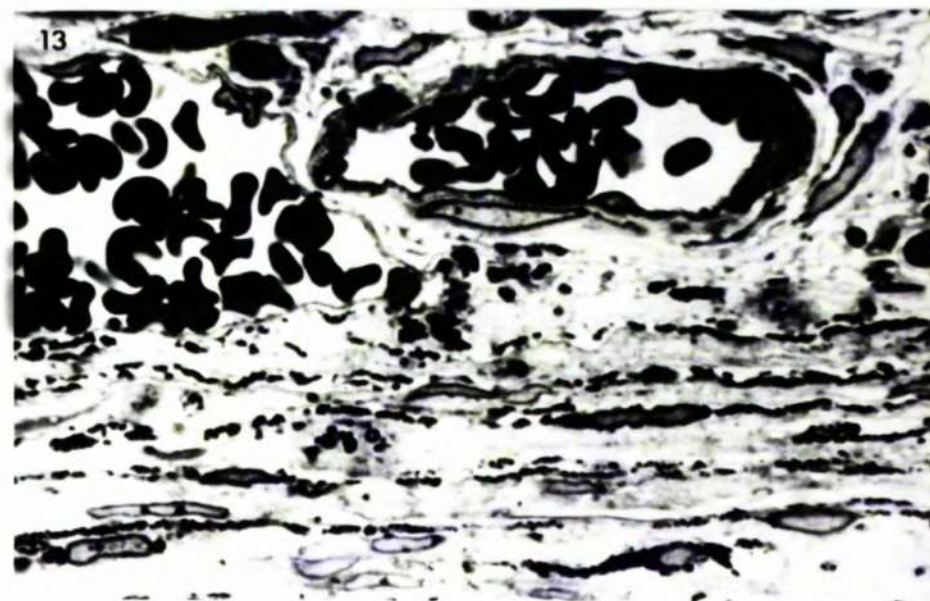
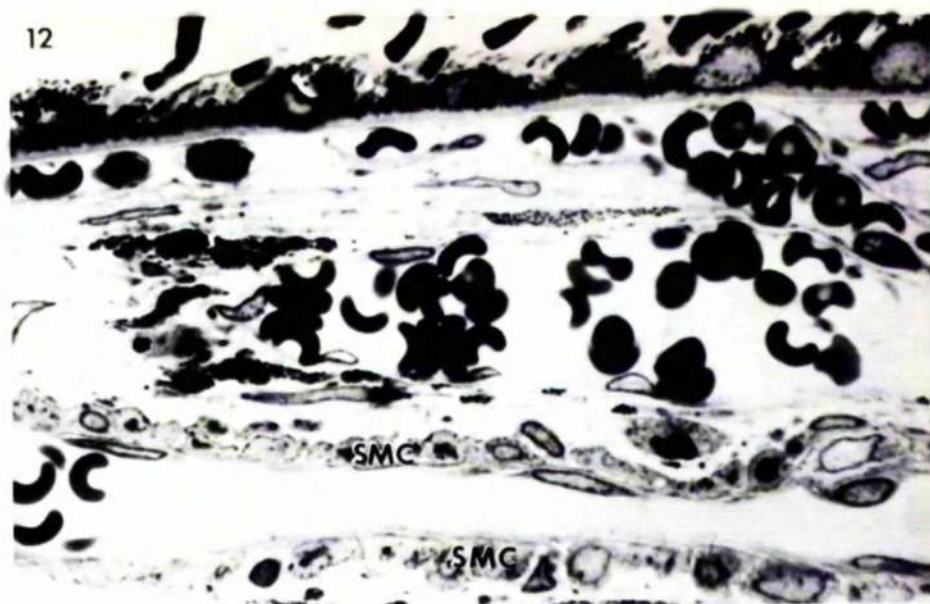


Figure 3.12

Light micrograph of a choroidal arteriole showing the organisation of the encircling smooth muscle cells. S M C: smooth muscle cells (x 1000).

Figure 3.13

Light micrograph showing the lamellar arrangement of fibroblasts and melanocytes in the suprachoroidea (x 1000).

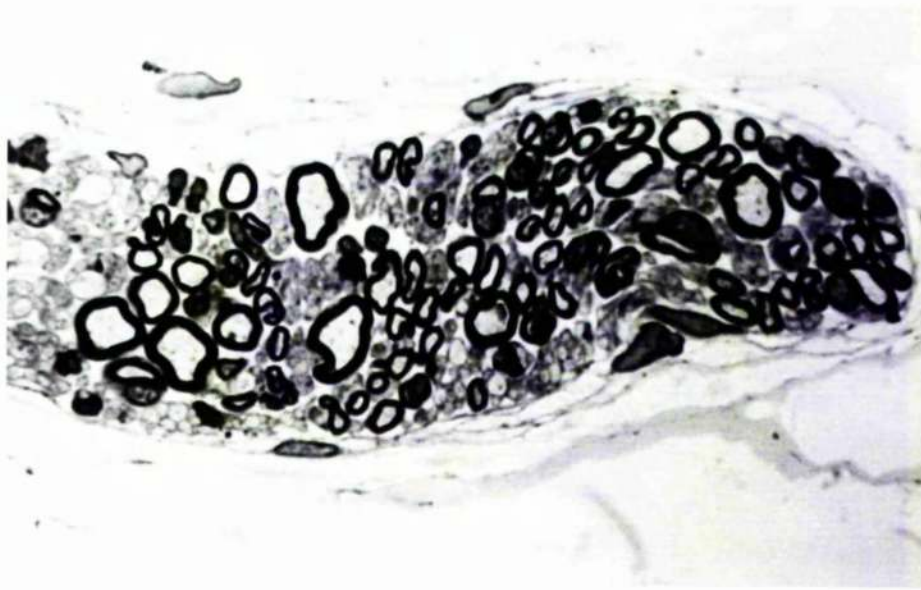


Figure 3.14

Light micrograph showing a portion of one of the large ciliary nerves occasionally encountered in the suprachoroidea.
($\times 1000$)

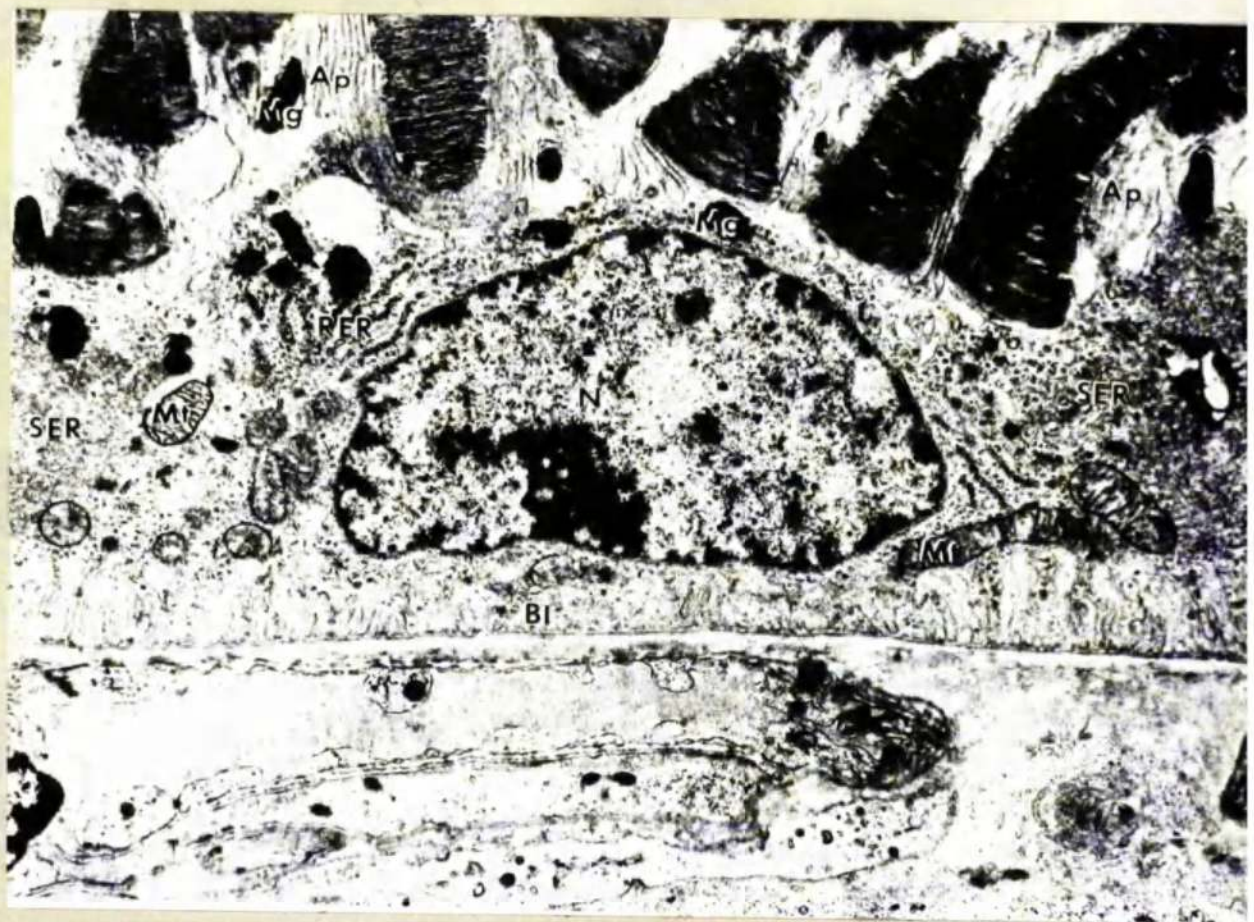


Figure 3.15

Electron micrograph of a normal pigment epithelial cell. N: nucleus, Mt: mitochondrion; S E R: smooth endoplasmic reticulum; R E R: rough endoplasmic reticulum; B I: basal infoldings; Mg: melanin granule; A p: apical processes (x 9,500).

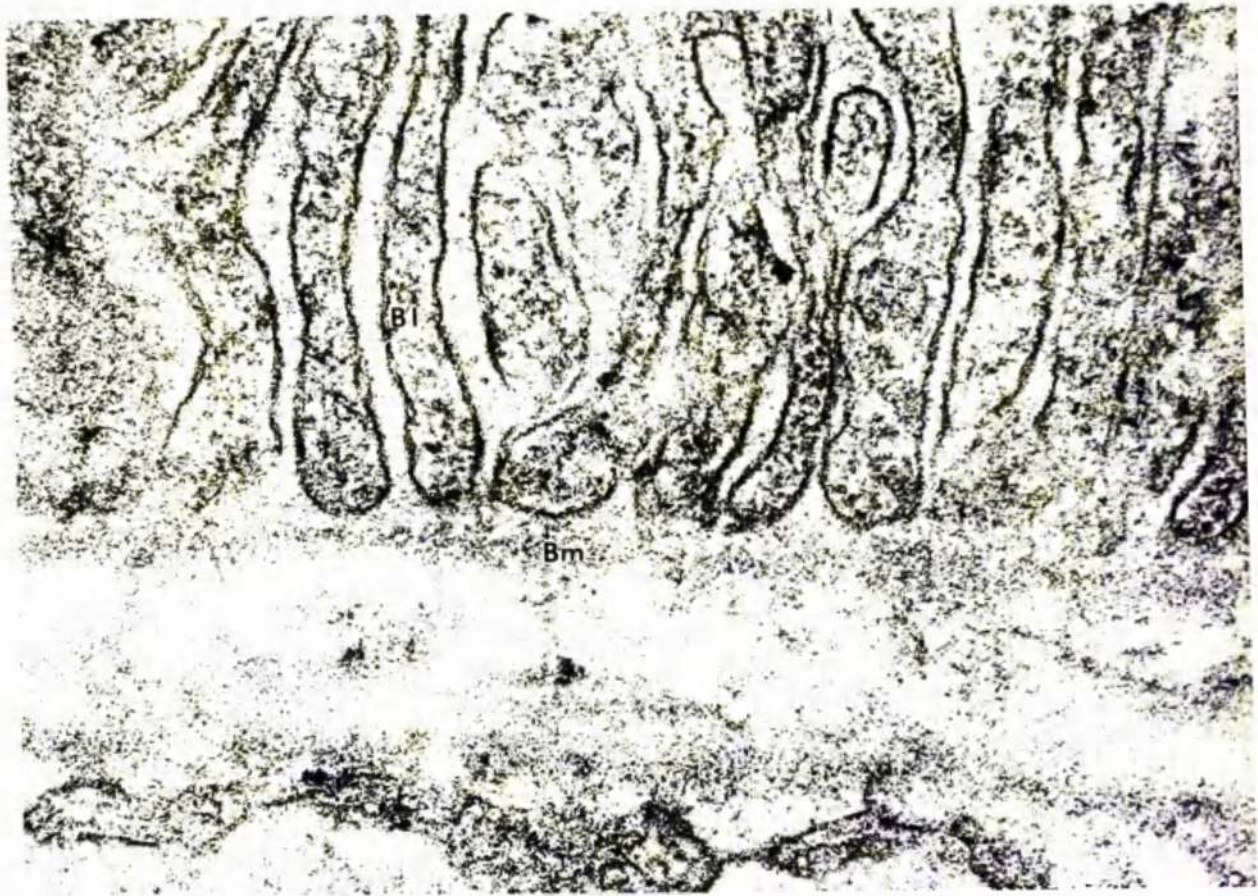


Figure 3.16

High power electron micrograph of the basal infoldings and Bruch's membrane. BI: basal infoldings; Bm: basement membrane of the pigment epithelium (x 117,000).



Figure 3.17

Electron micrograph showing a horizontal section through the basal infoldings of the pigment epithelium to show their highly convoluted nature (x 31,000).



Figure 3.18

Electron micrograph showing the intimate association between the apical processes of the pigment epithelium and the distal ends of the photoreceptors C O S: cone outer segment; R O S: rod outer segment; Ap: Apical processes (x 9,200).

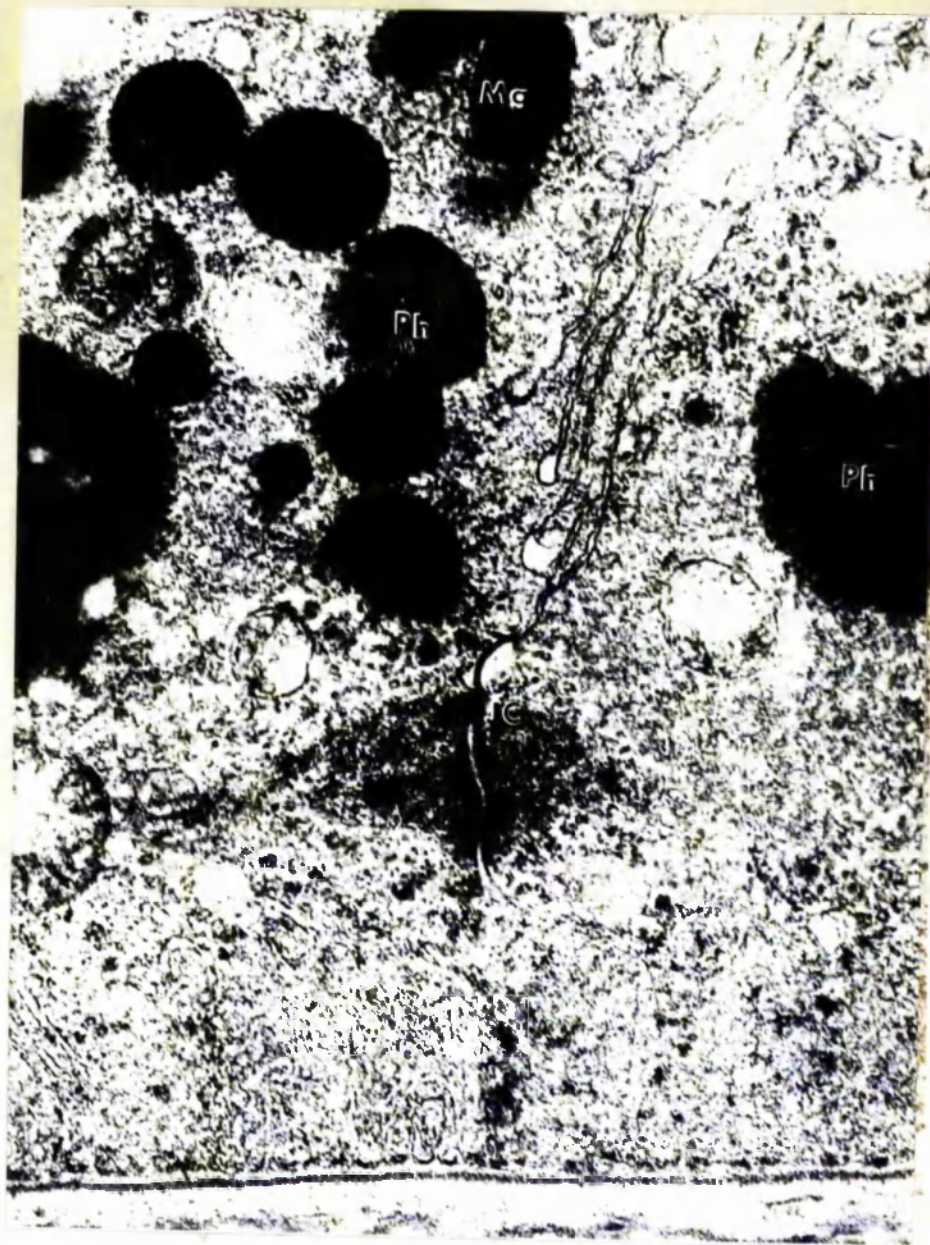


Figure 3.19

Electron micrograph of the junctional complex of the pigment epithelium. The adjacent cytoplasm contains melanin granules and phagosomes of receptor cell outer segment material
[C: junctional complex; Mg: melanin granule; Ph: phagosome
(x 32,000).

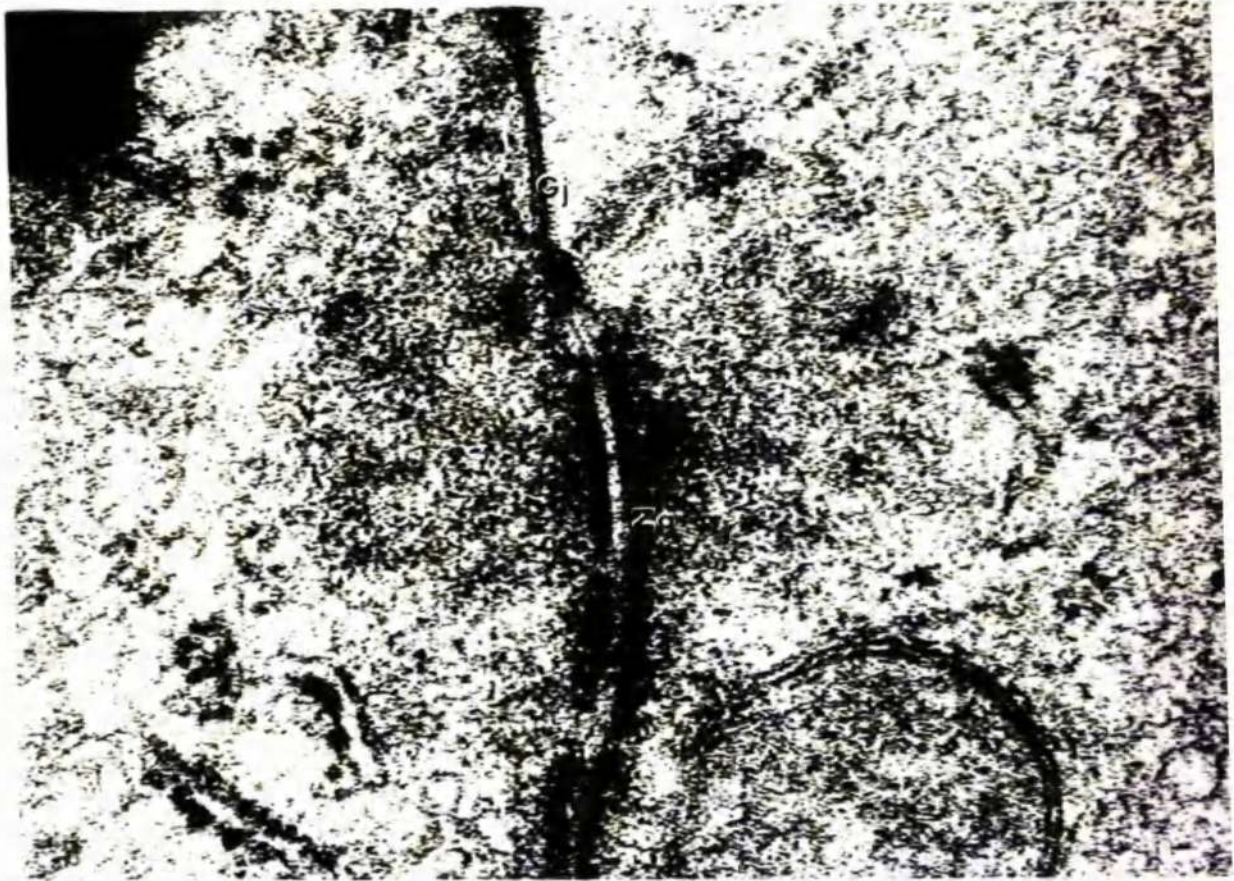


Figure 3.20

High magnification electron micrograph of pigment epithelium junctional complex. The gap junction and the zonula adhaerens are apparent but zonula occludens is not resolved, probably because of staining technique. Gj: gap junction; Za: zonula adhaerens (x 111,000).

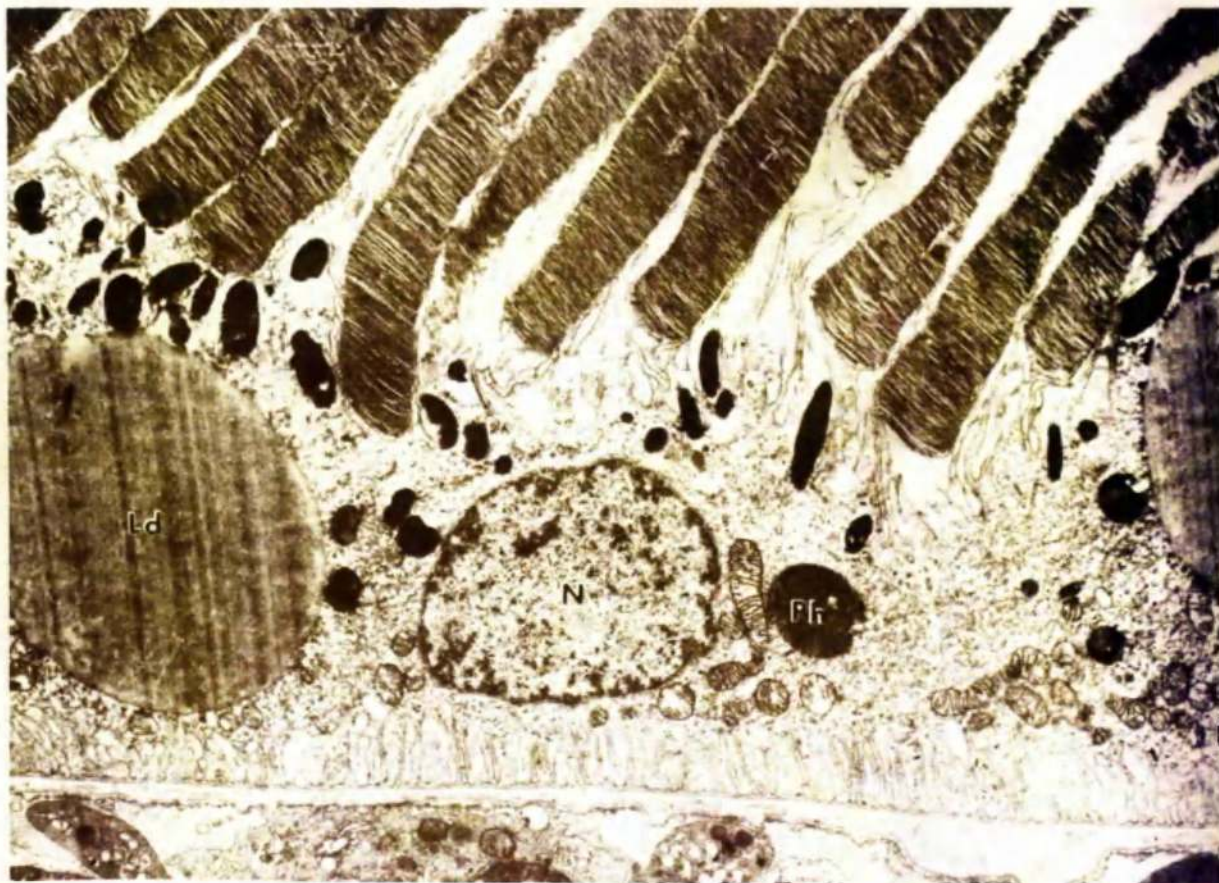


Figure 3.21

Electron micrograph of the pigment epithelium showing plentiful smooth endoplasmic reticulum and the large lipid droplets which are characteristic of the pigment epithelium.

N: nucleus; Ld: lipid droplet; Ph: phagosome (x 7,600).

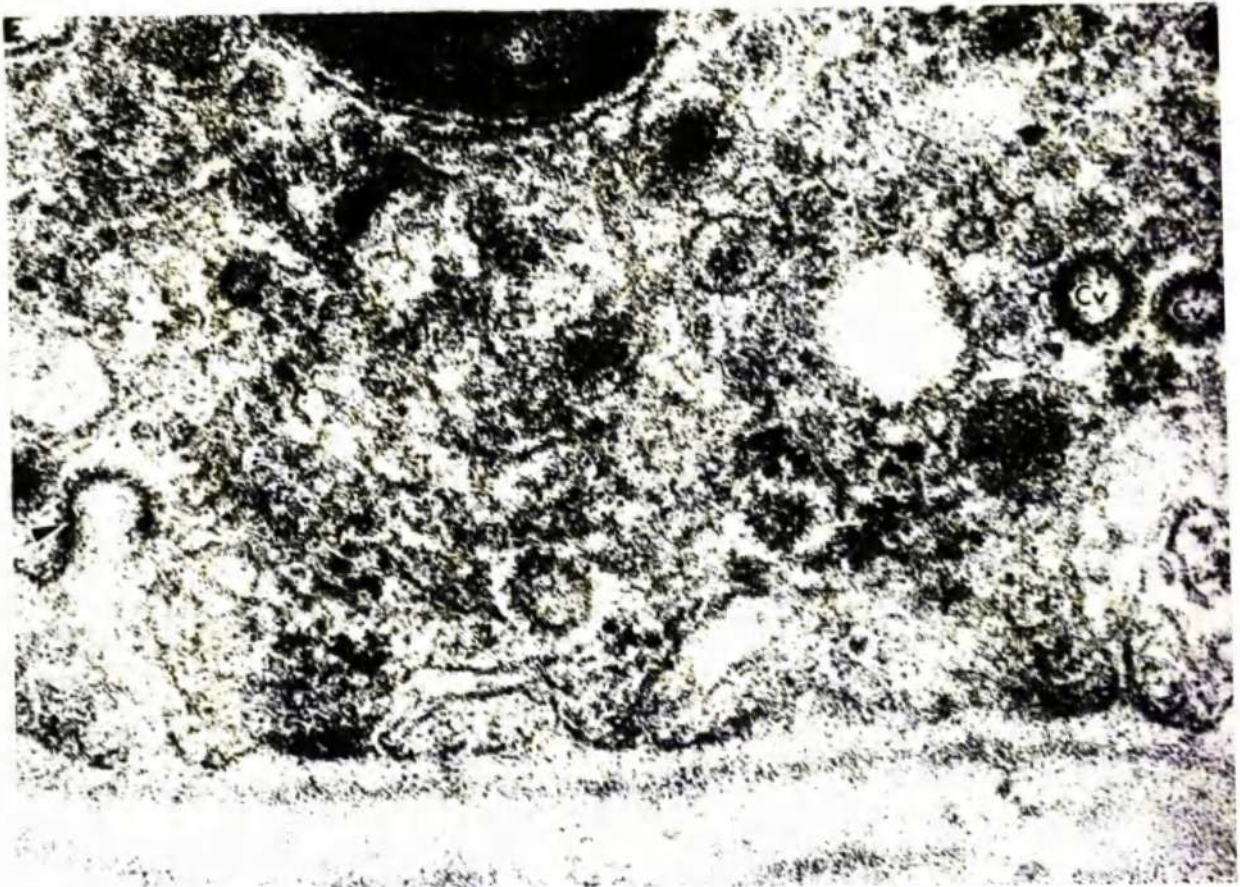


Figure 3.22

High power electron micrograph of the basal cytoplasm of the pigment epithelium showing coated vesicles within the cytoplasm and another developing from, or fusing with, the basal membrane. Cv: coated vesicle; Arrow: coated vesicle in association with cell membrane (x 130,000).

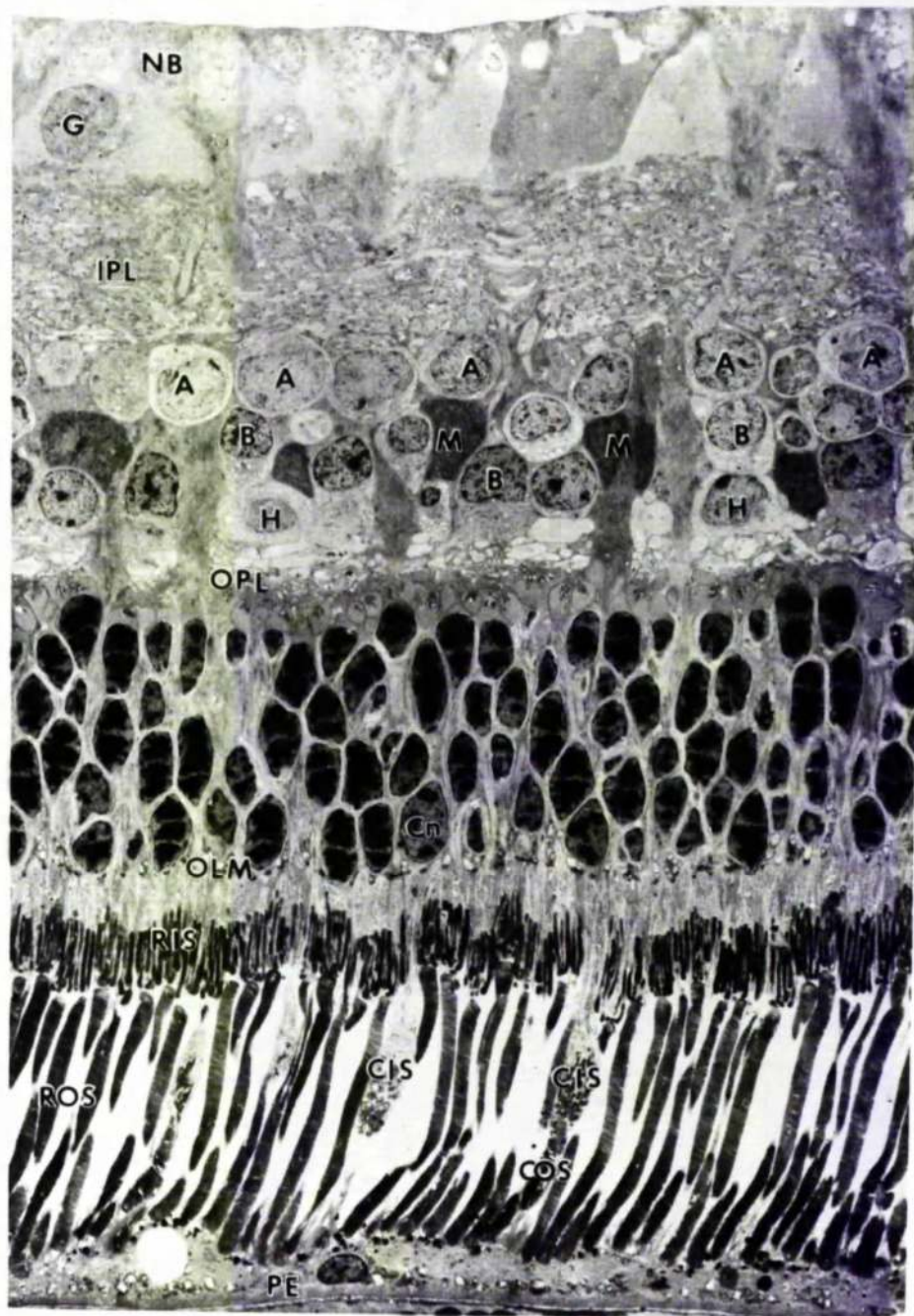


Figure 3.23

Low magnification electron micrograph of the neural retina. PE: pigment epithelium; ROS: rod outer segments; COS: cone outer segment; RIS: rod inner segment; CIS: cone inner segment; OLM: outer limiting membrane; Cn: cone nucleus; OPL: outer plexiform layer; H: horizontal cell; B: bipolar cell; A: amacrine cell; M: Müller cell; IPL: inner plexiform layer; G : ganglion cell; NB: nerve bundle (x 1,200).



Figure 3.24

Electron micrograph showing the ordered nature of the discs within the rod outer segment. (x 5,400).



Figure 3.25

Electron micrograph of the proximal region of a rod outer segment showing that the first few discs are open to the inter photoreceptor space.

Arrows: openings; Cc: connecting cilium; Mt: mitochondrion (x 53,000).

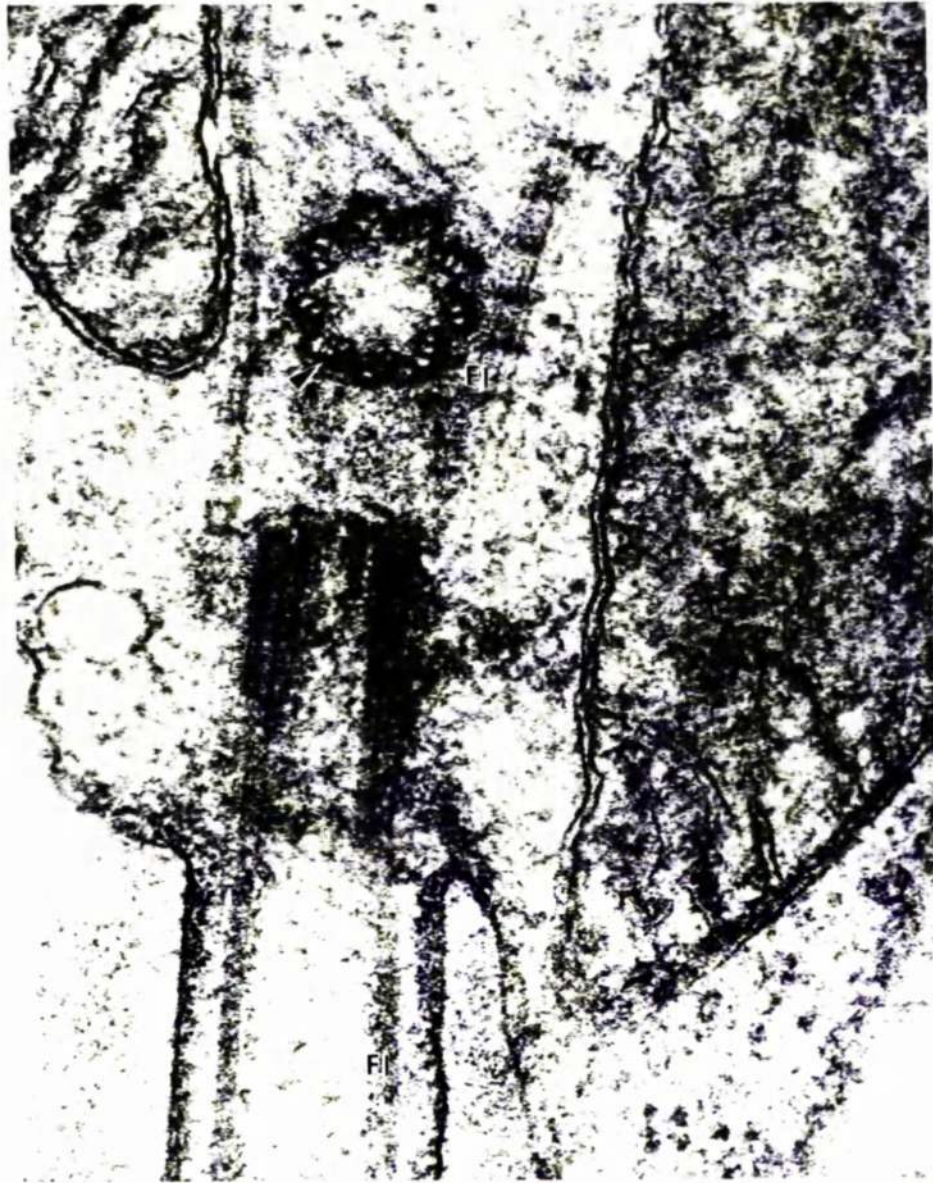


Figure 3.26

Electron micrograph of a rod connecting cilium and basal body. Fibrils can be seen extending into both the inner and outer segments.

Arrow: one of nine sets of triplets forming basal body;
Fl: fibrils (x 120,000).

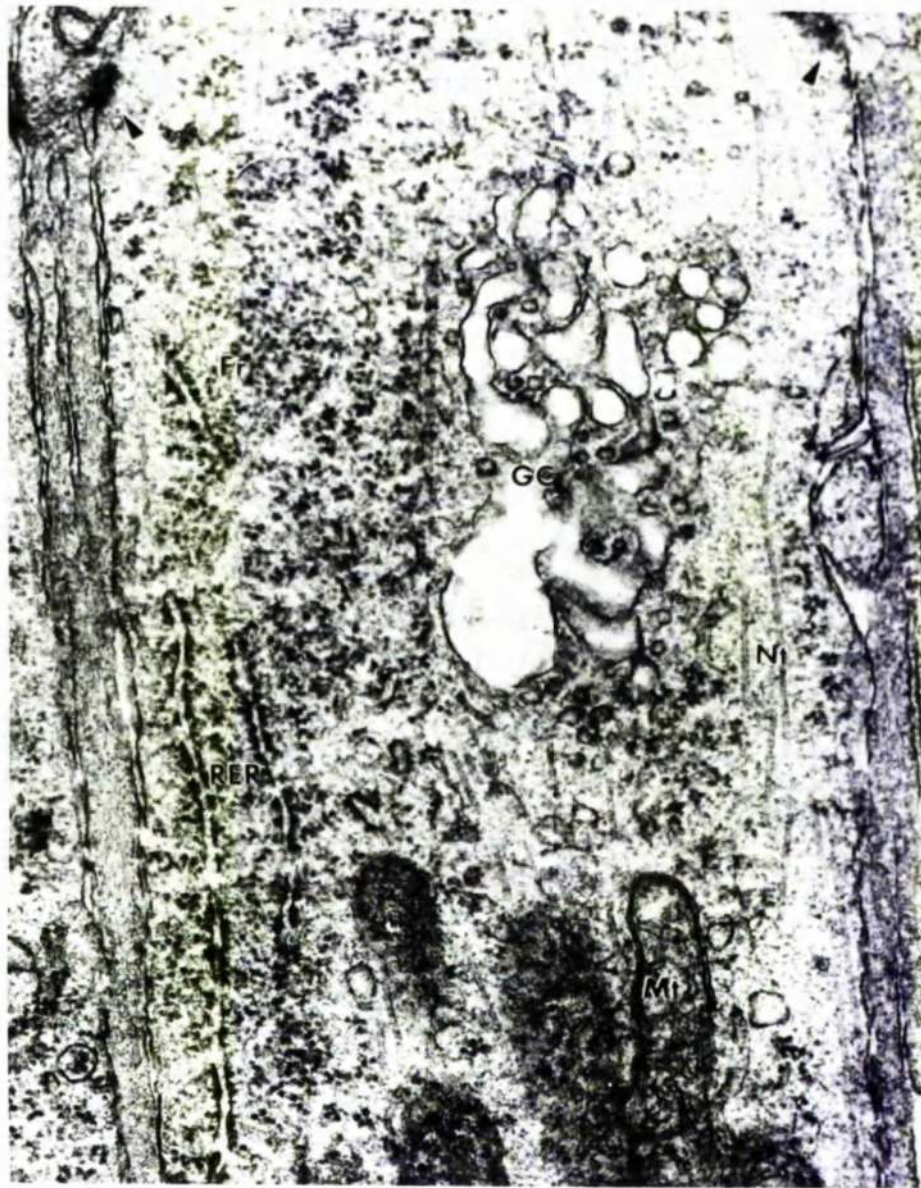


Figure 3.27

Electron micrograph of the inner segment of a rod.
 Mt: mitochondrion; R E R: rough endoplasmic reticulum;
 Fr: free ribosomes; Nt: neurotubules; G C: Golgi complex;
 Arrows: outer limiting membrane (x 42,000).

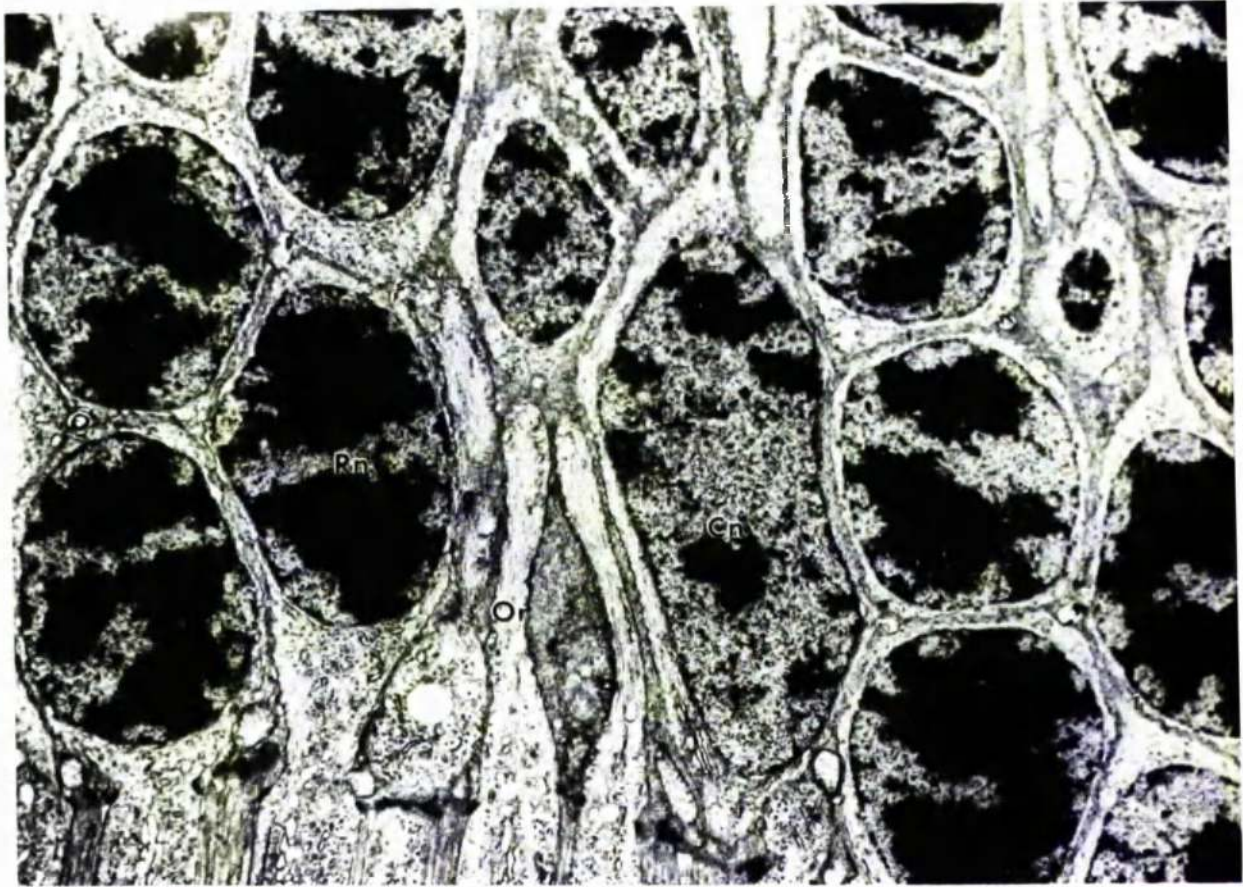


Figure 3.28

Electron micrograph of the outer region of the outer nuclear layer. Or: outer receptor fibre; Cn: cone nucleus; Rn: rod nucleus (x 6,500).

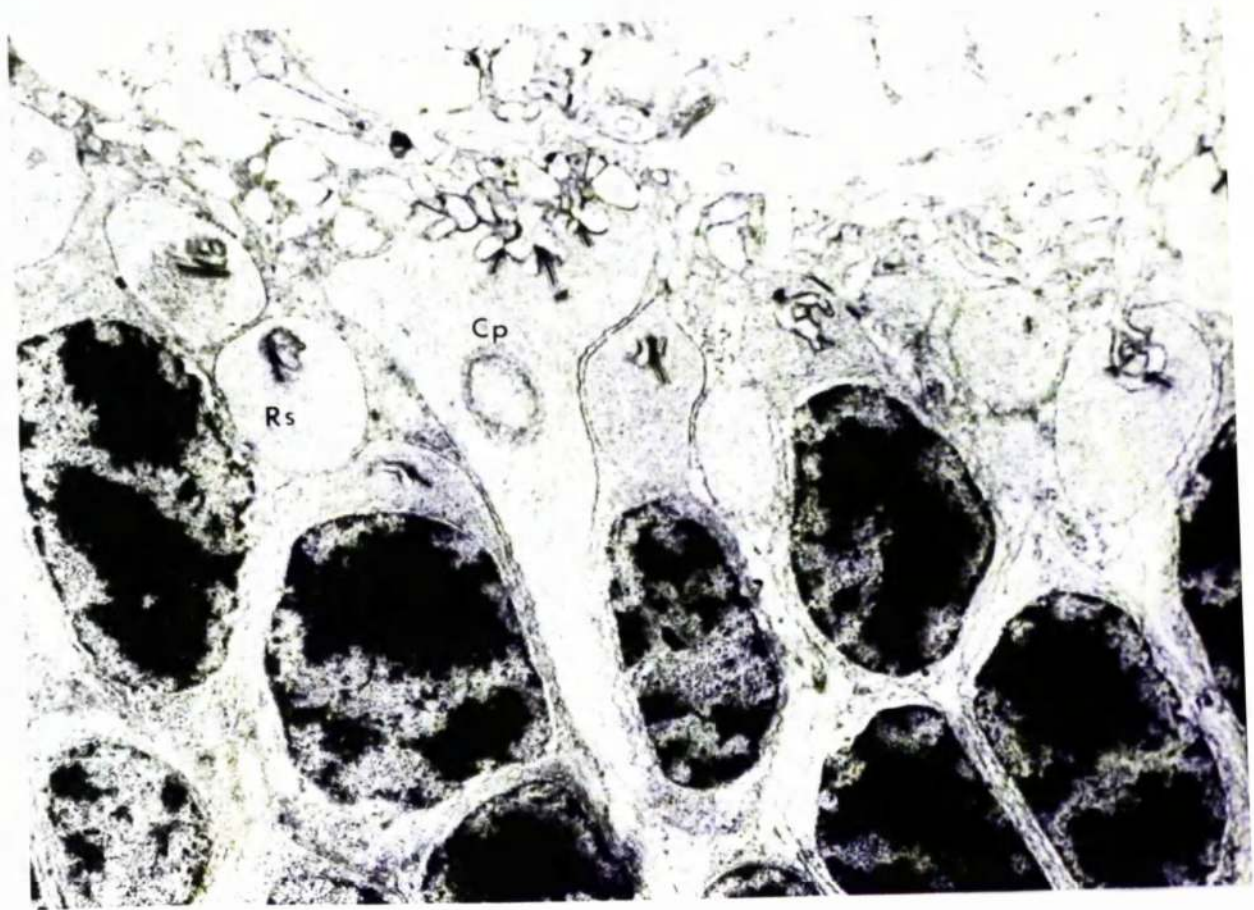


Figure 3.29

Electron micrograph of the outer plexiform layer. Rs: rod spherule; Cp: cone pedicle (x 6,500).



Figure 3.30

Electron micrograph showing the fine villous Müller cell processes extending beyond the outer limiting membrane. Mp: Müller cell processes; Cn: cone nucleus; R I S: rod inner segment (x 21,000).



Figure 3.31

Electron micrograph of outer plexiform layer showing extensive Müller cell cytoplasm between the neural elements. Rn. rod nucleus Rs. rod spherule Mc. Müller cell cytoplasm; Mn: Müller cell nucleus ($\times 8,600$).

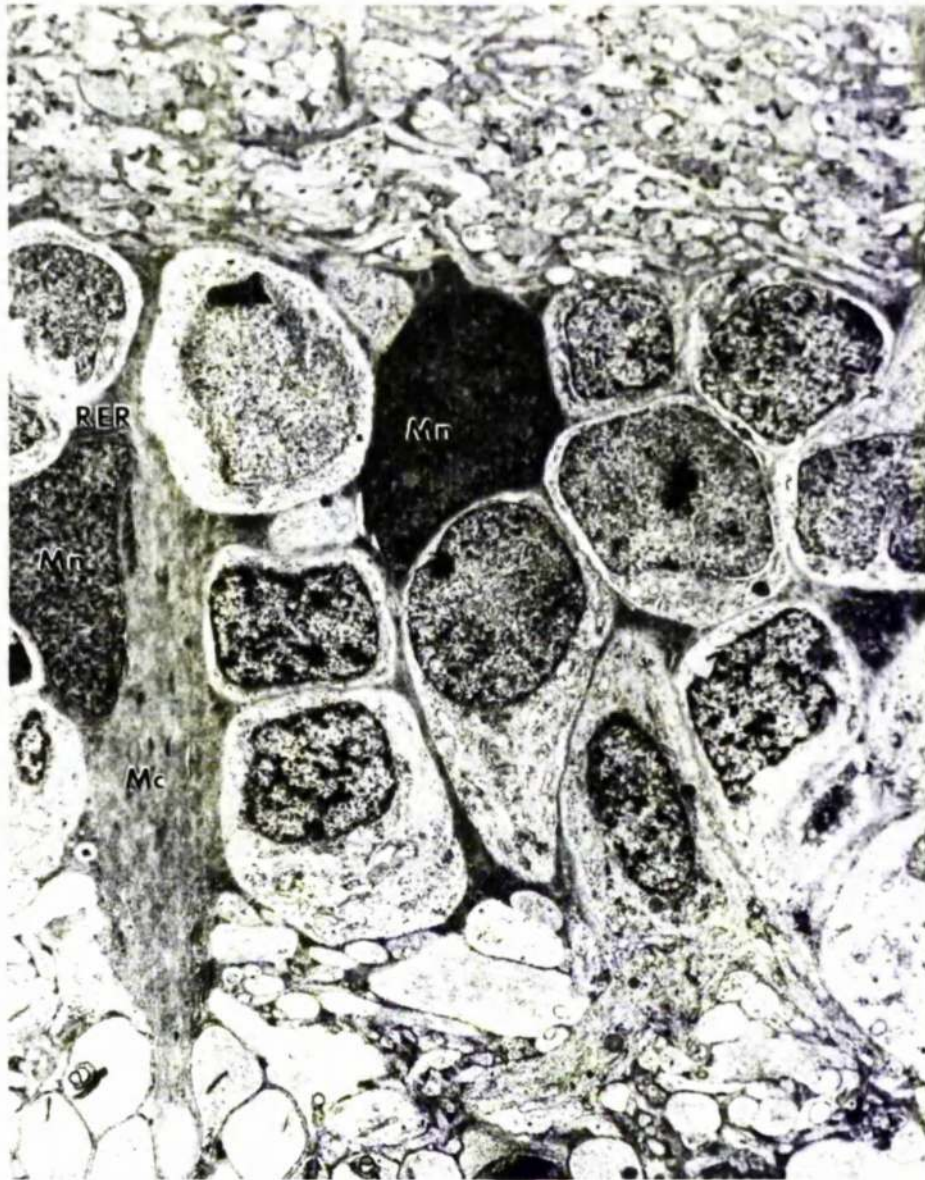


Figure 3.32

Electron micrograph of inner nuclear layer showing position of Müller cell nuclei and cytoplasm. Mn: Müller cell nucleus, Mc: Müller cell cytoplasm; RER: rough endoplasmic reticulum ($\times 3,600$).



Figure 3.33

Low power electron micrograph of inner retina showing a vertical column of Müller cell cytoplasm rising through the inner plexiform layer. Mc: Müller cell cytoplasm; Mn: Müller cell nucleus; G : ganglion cell; NB: nerve bundles (x 2,100).

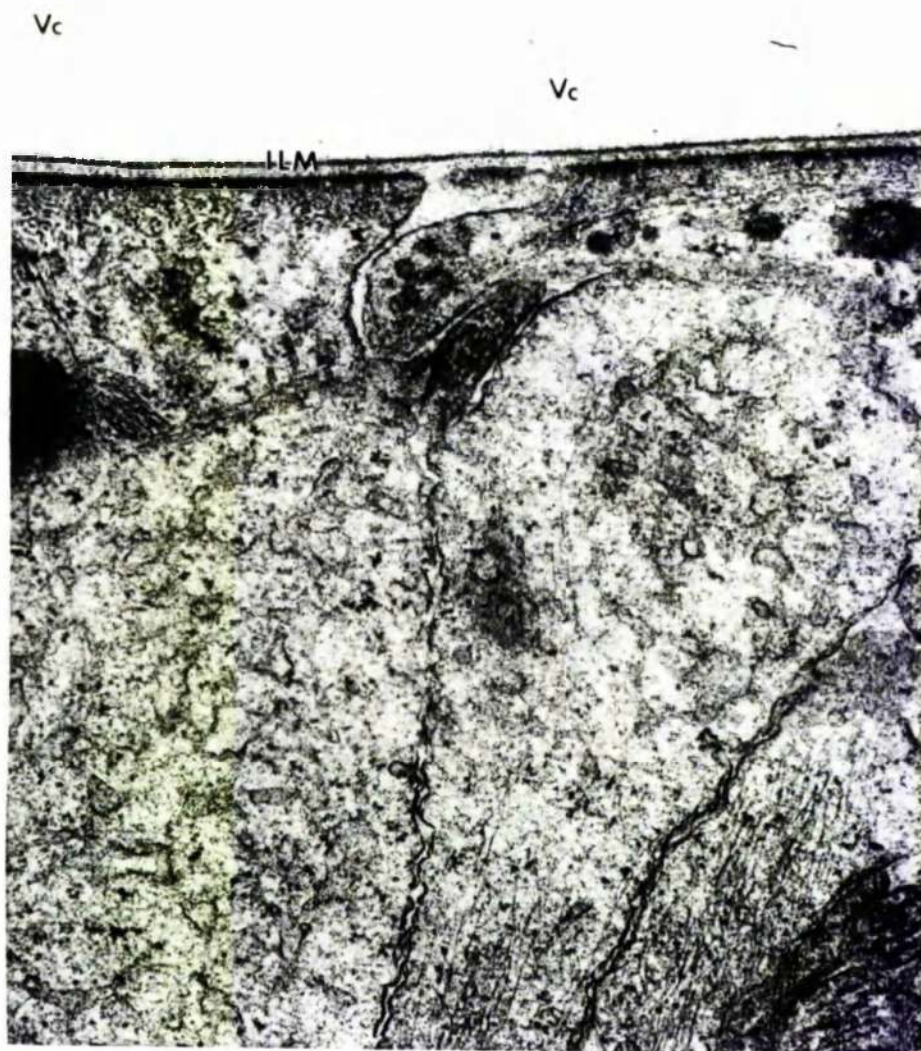


Figure 3.34

Electron micrograph of the inner limiting membrane.
Mc: Müller cell cytoplasm; Vc: vitreous collagen; I L M:
inner limiting membrane (x 3,800).

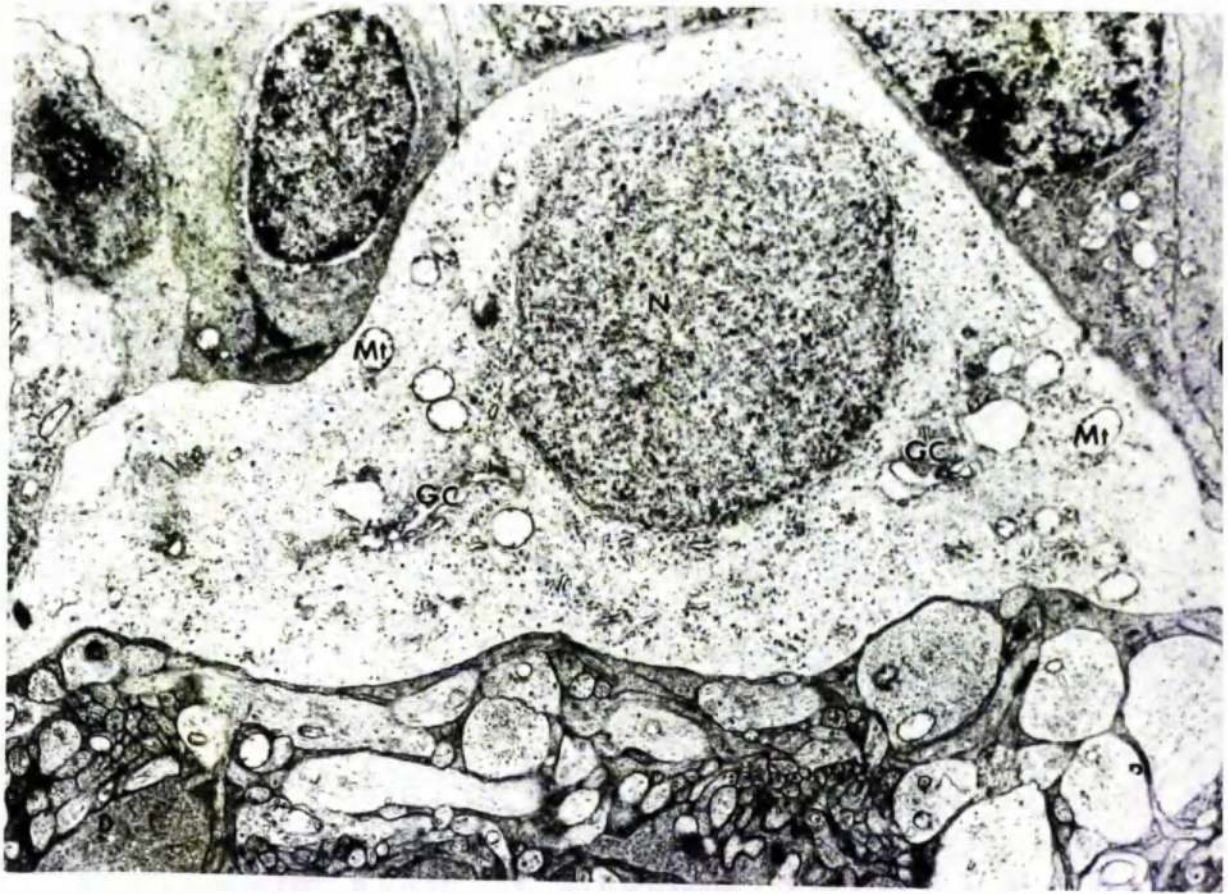


Figure 3.35

Electron micrograph of a horizontal cell. N: nucleus;
Mt: mitochondrion; G C: Golgi complex (x 6,500).



Figure 3.36

Electron micrograph of inner region of inner nuclear layer. Bn: bipolar cell nucleus; An: amacrine cell nucleus; Ba: bipolar cell axon; Mc: Müller cell cytoplasm (x 6,500).



Figure 3.37

Electron micrograph of ganglion cell. N: nucleus;
 R E R: rough endoplasmic reticulum; Mt: mitochondria;
 G C: Golgi complex; Mc: Müller cell cytoplasm (x 8,600)

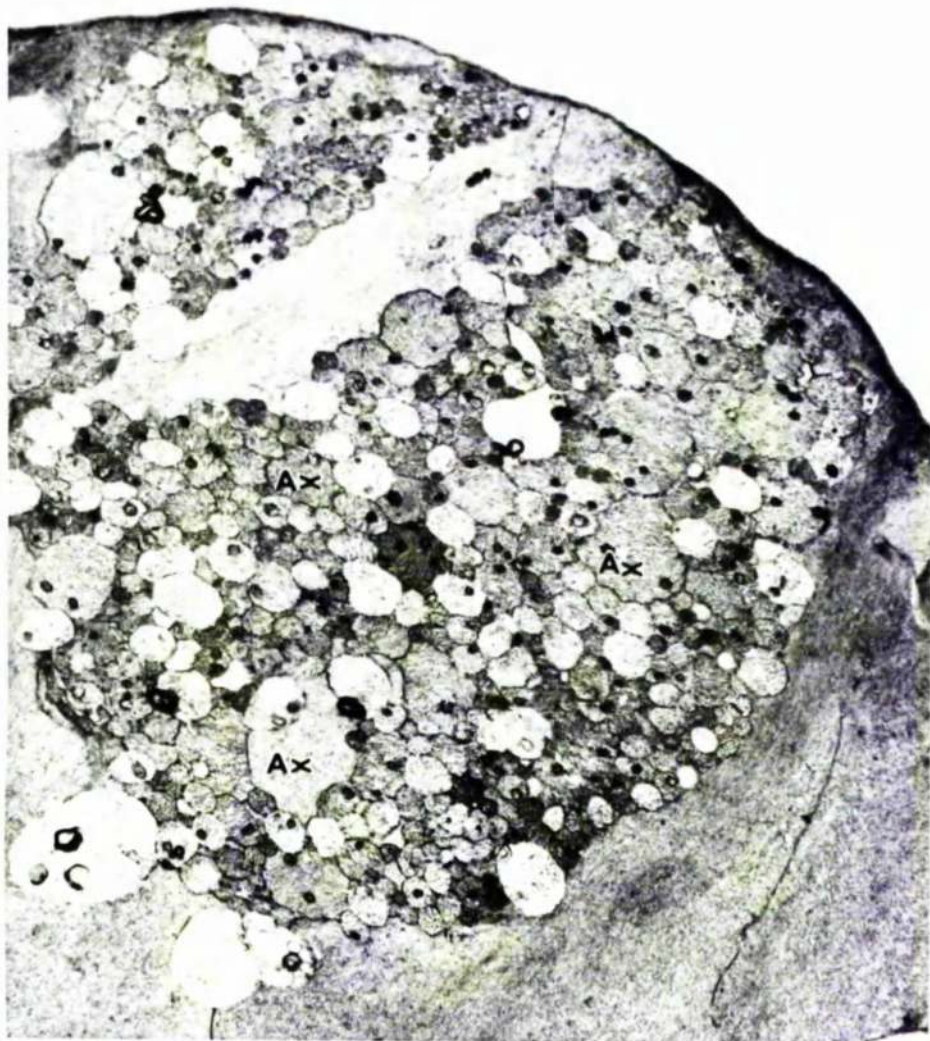


Figure 3.38

Electron micrograph of nerve fibre bundle in a region remote from the optic nerve. The axons are all unmyelinated. Ax: axon (x 6,500).



Figure 3.39

Electron micrograph of the nerve bundles in a region close to the optic nerve. Many of the axons are myelinated.

G : ganglion cell; As: astrocyte; Arrow: Astrocyte cytoplasm extending beyond inner limiting membrane to contact blood vessel; Rc: red cell (x 1,800).

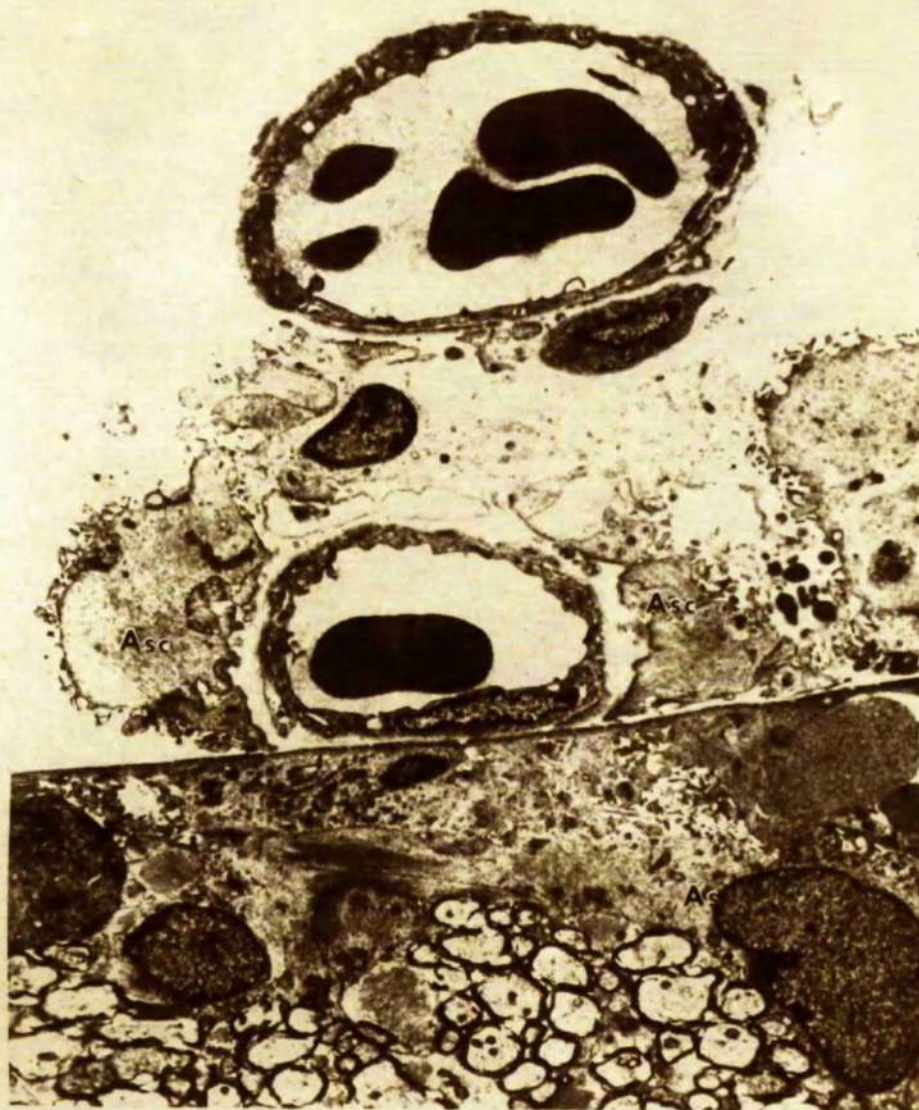


Figure 3.40

Electron micrograph of the blood vessels present in conjunction with the myelinated nerves of the nerve fibre layer. As: astrocyte; Asc: astrocyte cytoplasm in association with the blood vessels overlying the myelinated nerves (x 4,200).

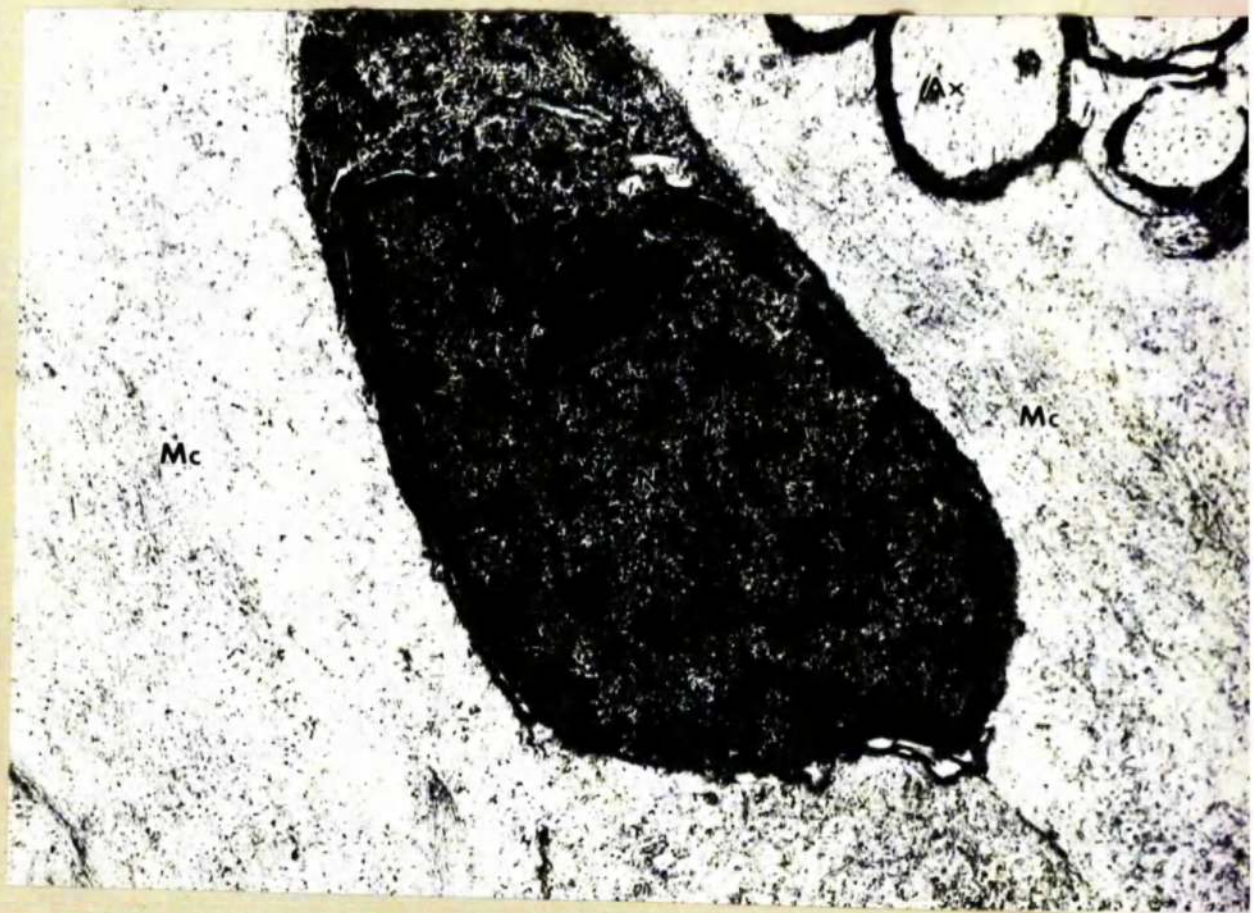


Figure 3.41

Electron micrograph of an oligodendrocyte showing the characteristically intense staining of both nucleus and cytoplasm. Ax: axon; N: nucleus; Mc: Müller cell cytoplasm; (x 14,000).



Figure 3.42

Electron micrograph of a junction in the endothelium of the epi-retinal vessels. Due to staining technique tight junctions were not apparent (x 139,000).

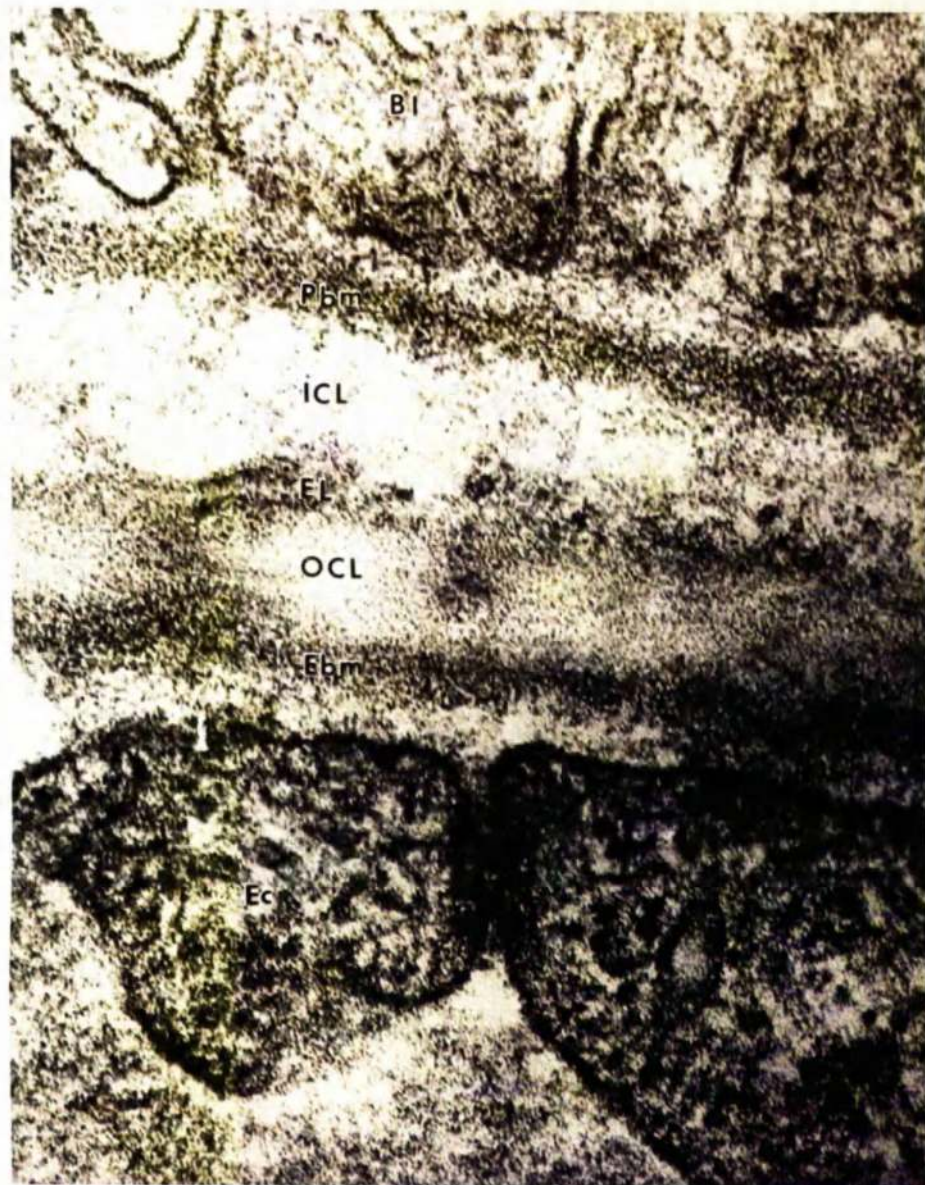


Figure 3.43

High power electron micrograph of Bruch's membrane.

B l: basal infoldings; P b m: pigment epithelium basement membrane; I C L: inner collagenous layer; E L: elastic layer; O C L: outer collagenous layer; E b m: endothelial basement membrane; E c: endothelial cell cytoplasm ($\times 176,000$).



Figure 3.44

Electron micrograph showing tangential section of Bruch's membrane. BI: pigment epithelium basal infoldings; Pbm: pigment epithelium basement membrane; ICL: inner collagenous layer; EL: elastic layer; OCL: outer collagenous layer; Ebm: Endothelial basement membrane; Ec: endothelial cytoplasm showing numerous fenestrations; CC: choriocapillaris ($\times 18,000$).

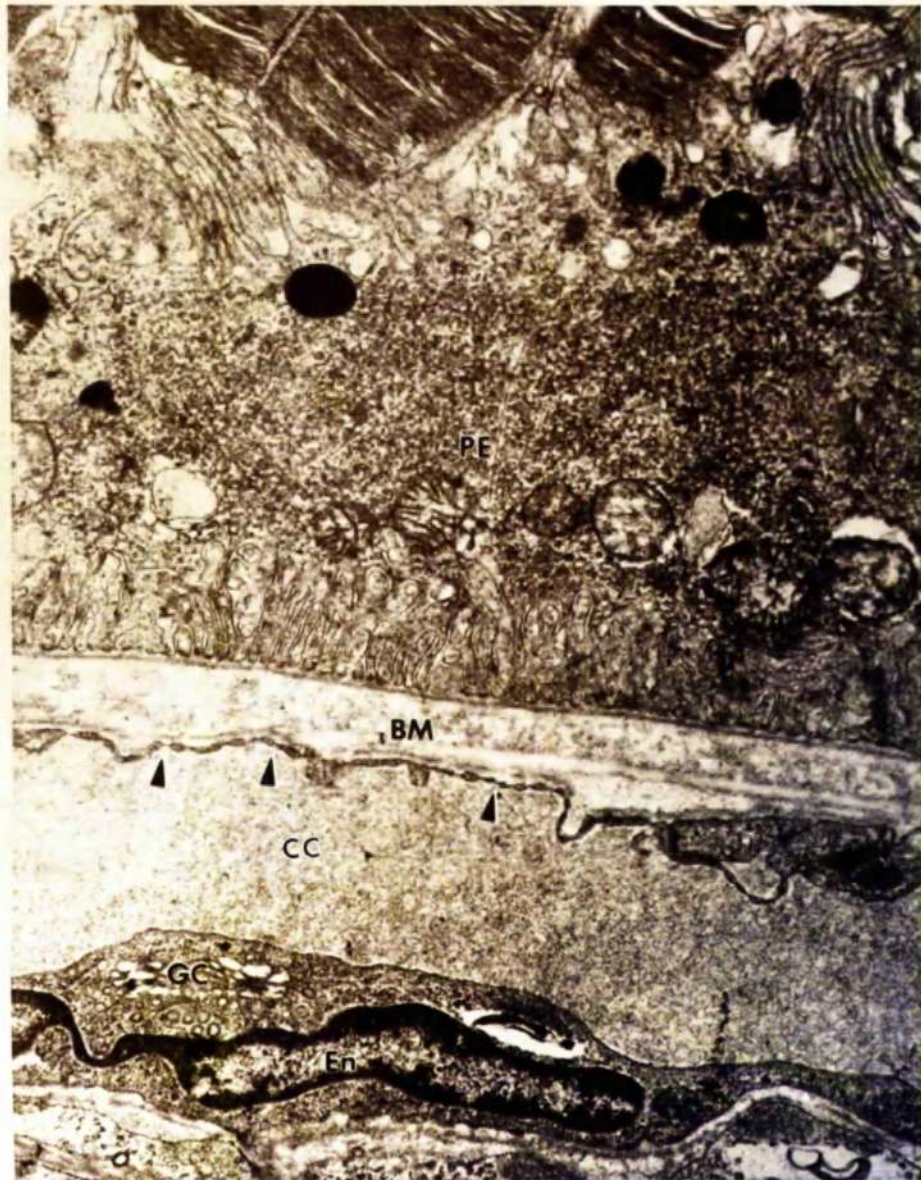


Figure 3.45

Electron micrograph showing the pigment epithelium and choriocapillaris. P E: pigment epithelium; B M: Bruch's membrane; C C: choriocapillaris; E n: endothelial cell nucleus; G C: Golgi complex; Arrows: capillary fenestrations (x 17,000).

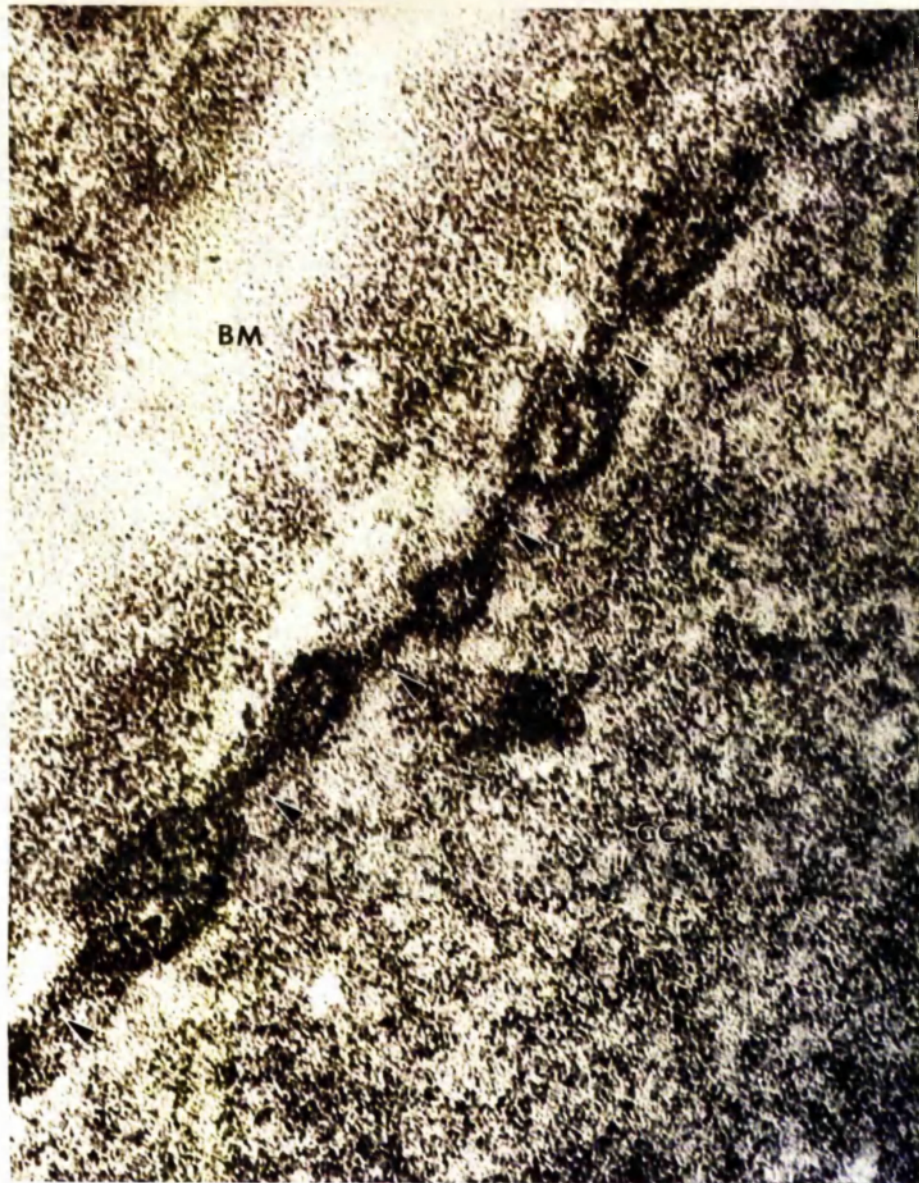


Figure 3.46

High power electron micrograph of endothelial cell fenestrations. The fenestrations appear to have a membrane diaphragm. B M: Bruchs membrane; Arrows: fenestrations; C C: choriocapillaris (x 210,000).



Figure 3.47

Electron micrograph of Bruch's membrane in a region between two capillaries of the choriocapillaris. In such regions layer 5 of Bruch's membrane, the basement membrane of the choriocapillaris, is absent. The outer collagenous layer of Bruch's is continuous with the extravascular tissues of the stromal region of the choroid. CC: choriocapillaris; BM: Bruch's membrane; Arrows: endothelial cell basement membrane (x 18,000).

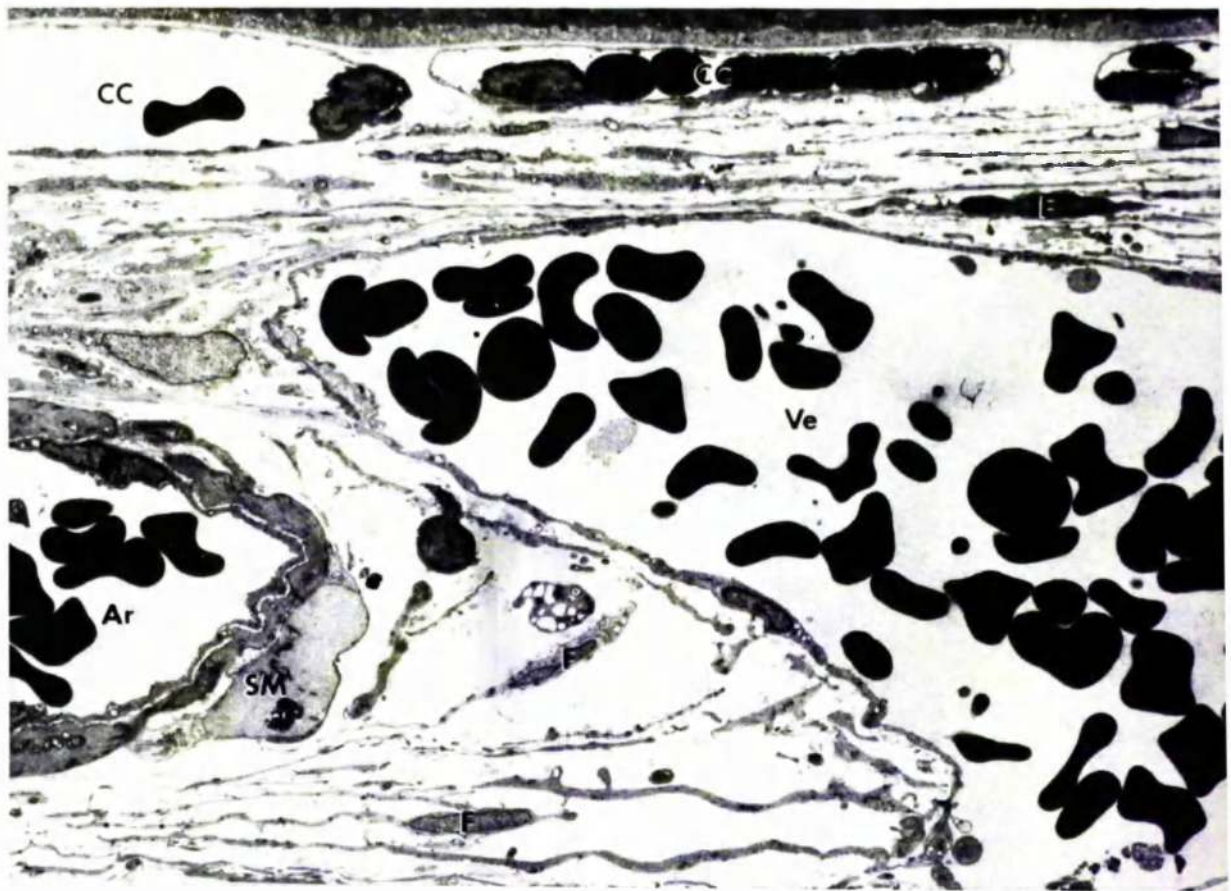


Figure 3.48

Electron micrograph of the choriocapillaris and stroma of the choroid. C C: choriocapillaris; Ar: Arteriole; Ve: venule; S M: smooth muscle; F: fibroblast ($\times 2,400$).

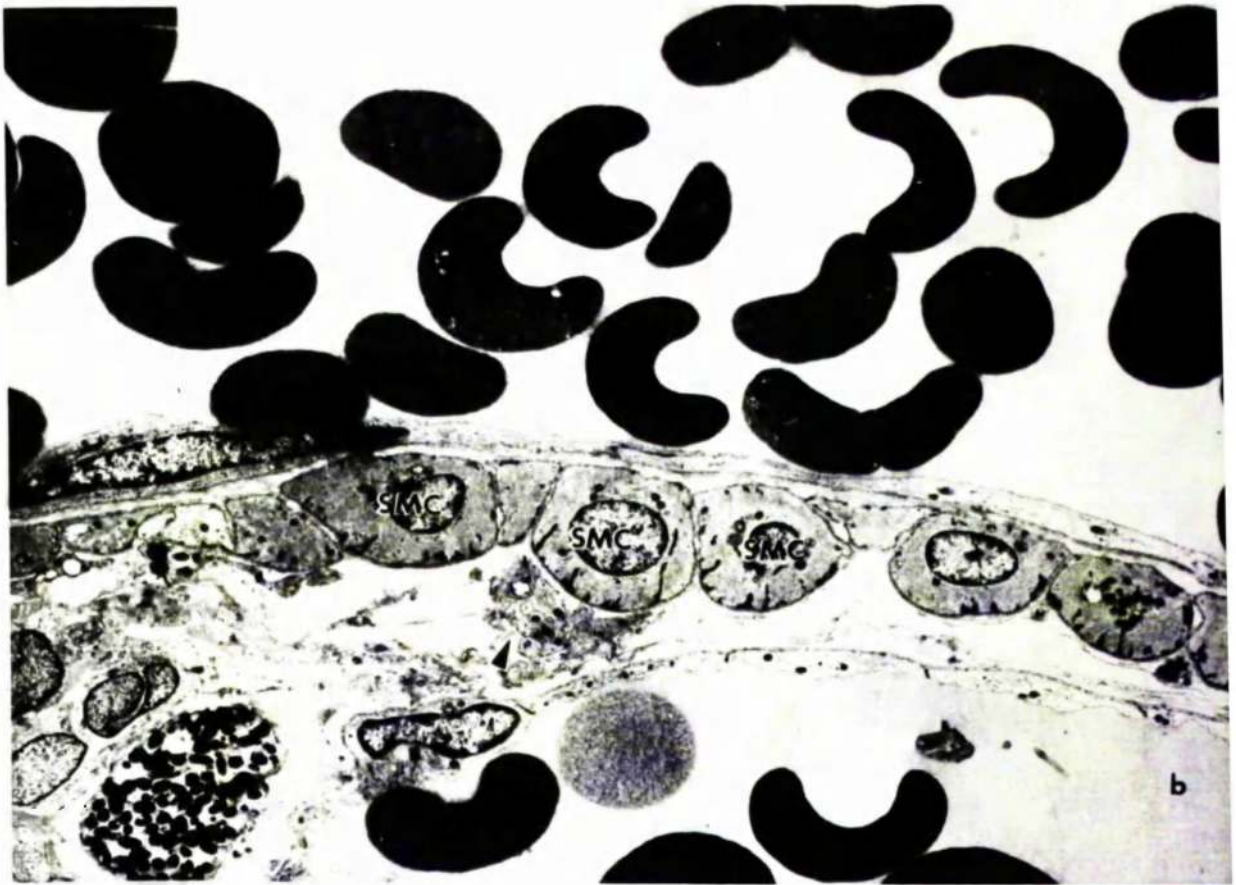


Figure 3.49

Electron micrograph of a choroidal arteriole showing encircling smooth muscle cells and associated unmyelinated nerves. S M C: smooth muscle cell; arrow : unmyelinated nerve bundle (x39,000).

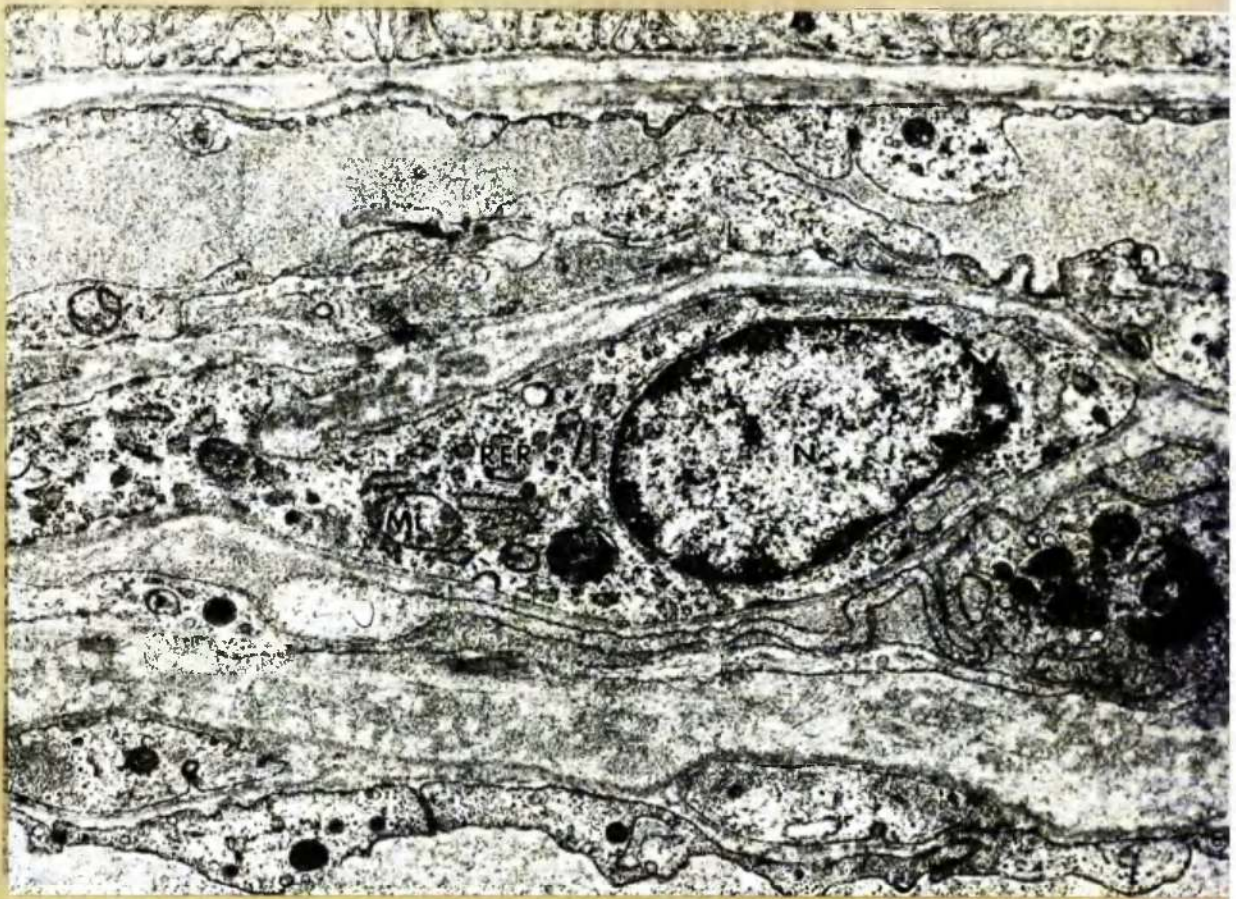


Figure 3.50

Electron micrograph of a choroidal fibroblast.

N: nucleus; Mt: mitochondrion; RER: rough endoplasmic reticulum (x 18,000).

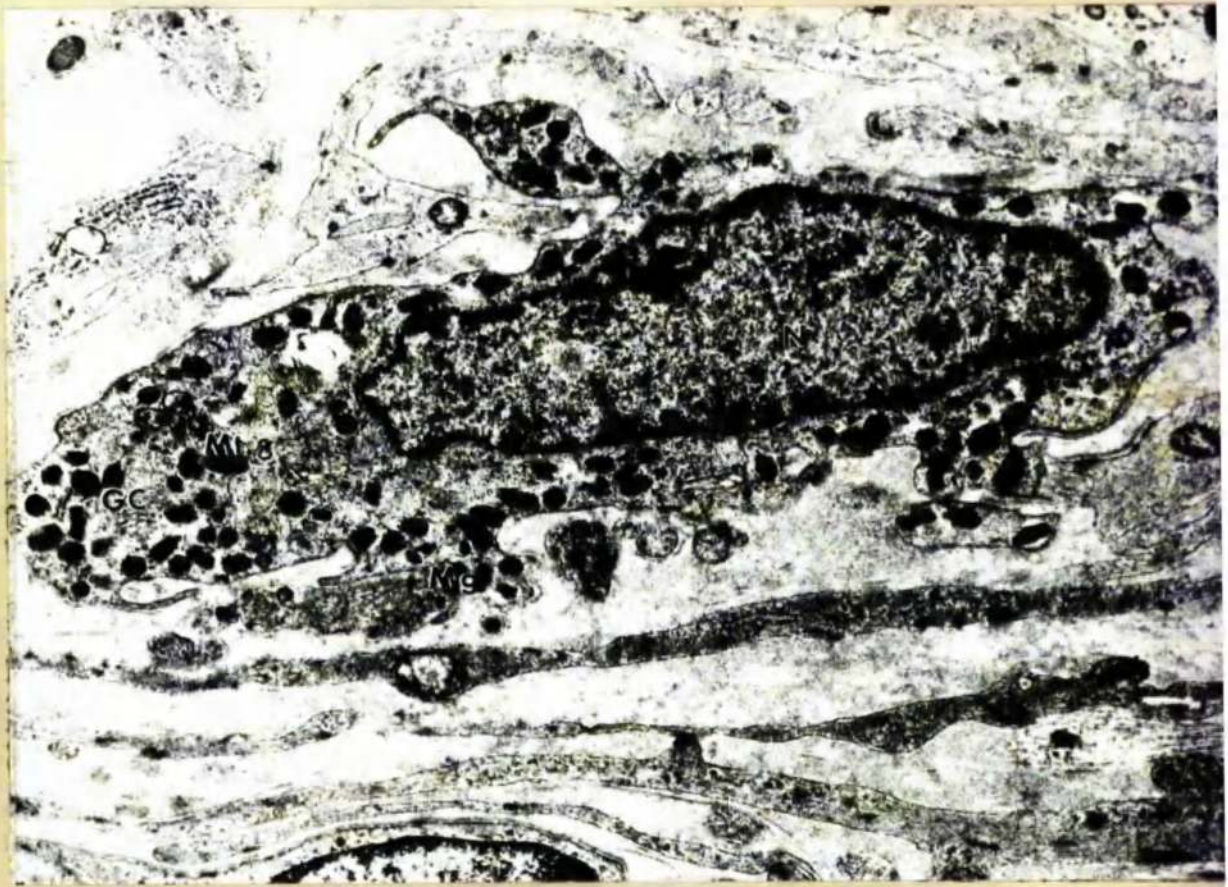


Figure 3.51

Electron micrograph of a choroidal melanocyte. N. nucleus.
GC: Golgi complex; Mt: mitochondrion; Mg: melanin granule.
(x 11,000).

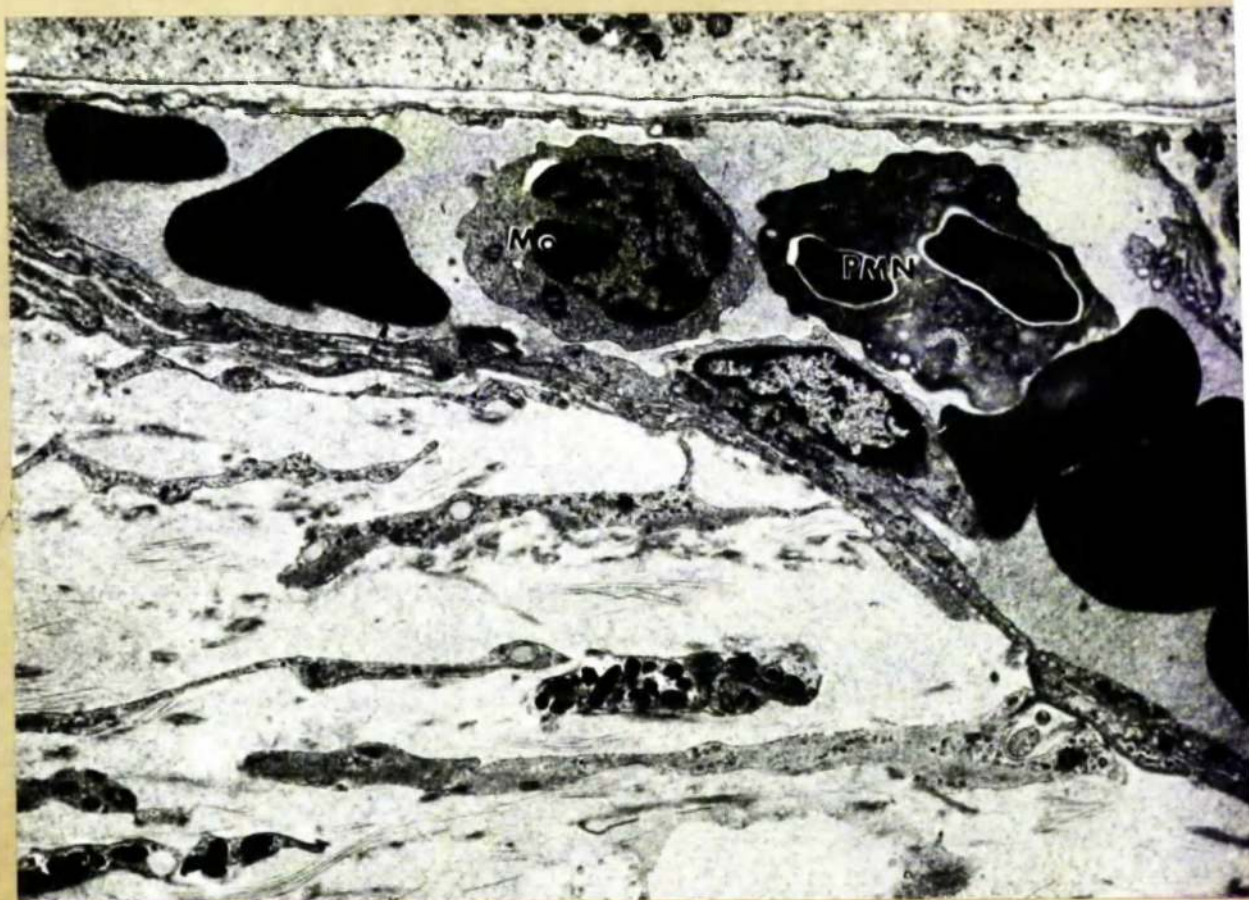


Figure 3.52

Electron micrograph showing the presence of intravascular inflammatory cells which were occasionally seen in the vessels of the choroid. Mo: monocyte; PMN: Polymorphonuclear leucocyte (x 5,300).



Figure 3.53

Low power electron micrograph showing a "nest" of inflammatory cells within the stroma of the choroid. P C: plasma cell; M o: monocyte; M a: Macrophage; (x 2,400).

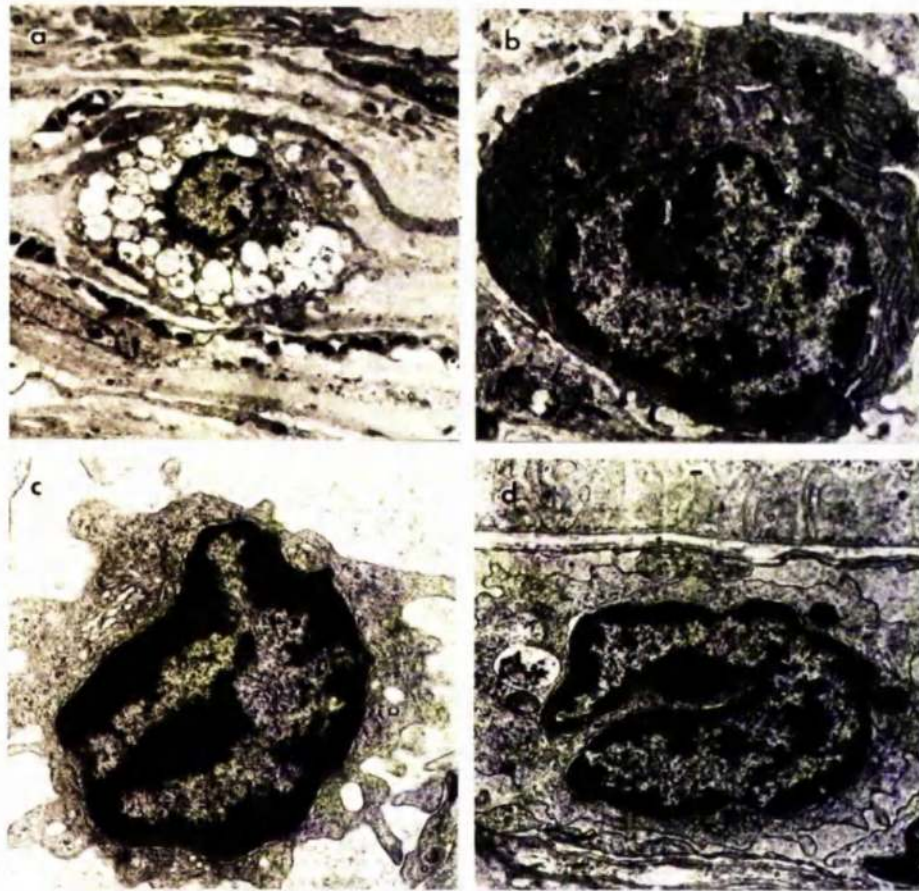


Figure 3.54

Electron micrographs illustrating some of the inflammatory cells of the choroid. a) mast cell (x 3,400). b) plasma cell (x 9,100). c) lymphocyte (x 12,000). d) monocyte (x 10,000).

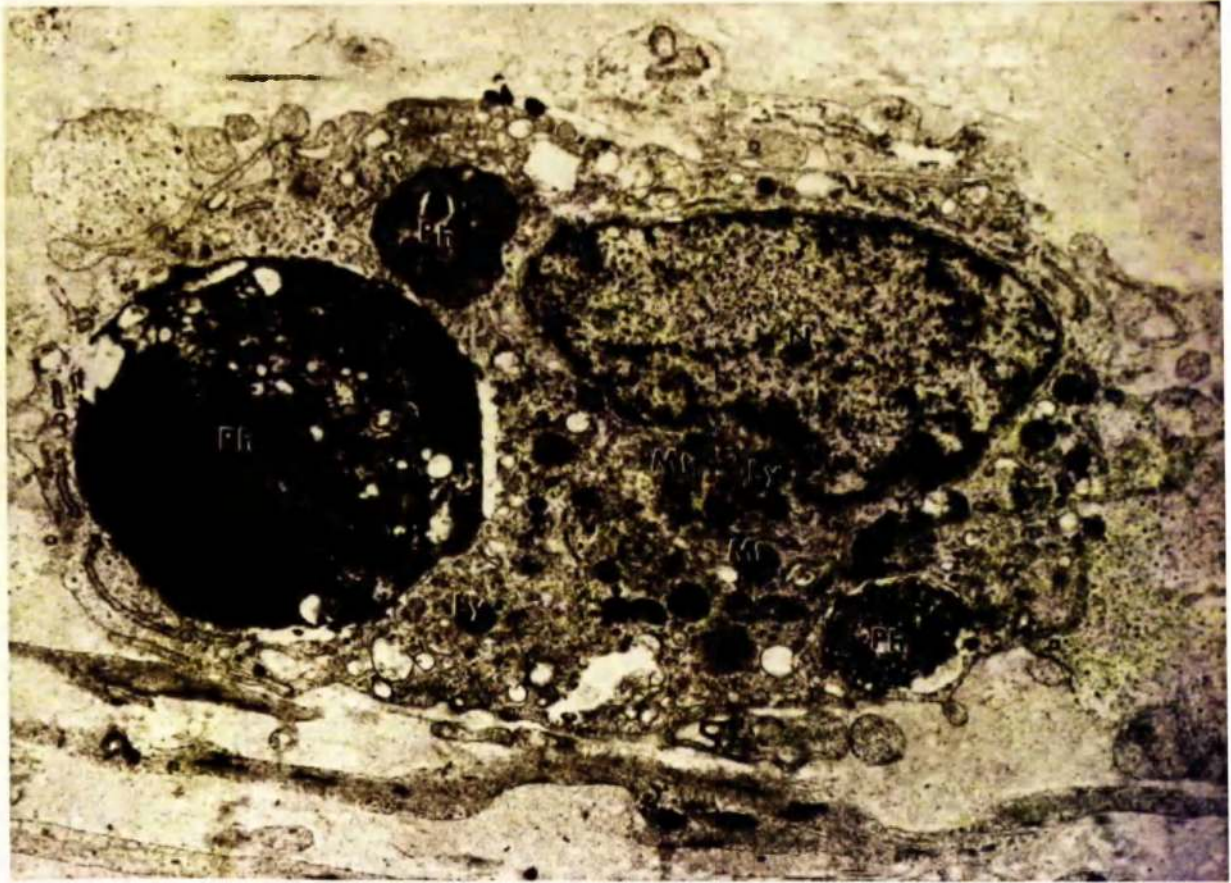


Figure 3.55

Electron micrograph showing the appearance of a mature macrophage in the choroidal stroma. N: nucleus; M.t: mitochondrion; L y: lysosomes; P h: phagosomes or secondary lysosomes (x9,200).



Figure 3.56

Electron micrograph showing a portion of a ciliary nerve. These were occasionally encountered in the suprachoroidea. Ax: axons; MAx: myelinated axon; Sn: Schwann cell nucleus (x3,600).

CHAPTER 4

THE IMMEDIATE EFFECTS ON THE STRUCTURE OF THE RETINA
AND CHOROID OF EXPOSURE TO LIGHT FOR ONE HOUR.

This chapter describes the structural changes in the retina and choroid after exposure of the rabbit eye to various intensities of light for one hour.

The materials and methods employed are described in Chapter 2. Details of the animals employed are given in Appendix 1. Nineteen animals were exposed to one of six intensities for one hour. Immediately after exposure the animals were killed and the retinal and choroidal tissues examined by light and electron microscopy. The observations made will be described under two headings. These are:-

1. Light damage: its immediate effects as described by light and electron microscopy.

2. Light damage: its immediate effects as quantified by an assessment of the changes in the cellular components of the outer nuclear layer.

As the receptor cells and the pigment epithelium appeared to be the primary sites of damage, these are therefore described in detail. The Müller cells, all but resistant to the damaging effects of light, played an important role in the recovery or repair of the retina following photic injury and are therefore described in this, and the following chapter.

The patency of the choroidal circulation appears to be related to the degree of damage suffered by the retina. The choroid is therefore described in this chapter.

4.2 Light Damage: Its immediate Effects as Assessed by Light Microscopy

An initial observation, and problem, was the extreme variation in the pattern of damage in the experimental eyes. The pattern of damage did not appear to be strictly related to the area of illumination as would be expected. Therefore, in the description of the effects of illumination on the experimental eye, attention will be given to the "worst case" observed within any particular group. However, it must be borne in mind that, although increasing intensity of illumination does induce more severe damage to the retina and choroid, each experimental group exhibited changes in structure ranging from normal to the "worst case" observed in any particular group.

The effects of one hour exposures as observed by light microscopy will be described for each of the six intensities of illumination, starting with the lowest intensity.

4.2.1 Group 6 (1 animal) Estimated Retinal Illumination: 20.4mWcm⁻²

On gross examination the entire retina of the experimental eye appeared flat and attached. By light microscopy no differences were detectable between the experimental eye and control tissue, in either the retina or choroid.

4.2.2 Group 5 (2 animals) Estimated Retinal Illumination: 23.2mWcm⁻²

On gross examination the retinae of the experimental eyes appeared flat and attached. No structural changes were observed in either the retinal or choroidal tissues examined by light microscopy.

4.2.3 Group 4 (4 animals) Estimated Retinal Illumination:
 28.9mWcm^{-2}

On gross examination, the retinae of the experimental eyes appeared flat and attached. By light microscopy the pigment epithelium occasionally appeared to be slightly distended. This distension was associated with paler staining of the cytoplasm and rounding of the cells' nuclei. The receptor cells in these areas showed slightly disturbed inner and outer segments. This was often accompanied by slight oedema of the receptor cells' cytoplasm (Fig. 4.1). Rarely, focal disruptions of the pigment epithelium were seen (Fig. 4.2). Disturbances of the inner retina or the choroid were never observed within this experimental group.

4.2.4 Group 3 (4 animals) Estimated Retinal Illumination:
 32.8mWcm^{-2}

On gross examination the retinae of the experimental eyes showed small irregular folds, although the retinae did not appear to be detached.

By light microscopy some of the retinal folds were highly conspicuous (Fig. 4.3). In addition to the slight structural changes observed in the lower intensity group more extensive oedema of the pigment epithelium was seen (Fig. 4.4). There were also regions of atypical pigment distribution within the pigment epithelium (Fig. 4.5). The receptor cells frequently showed disturbed inner and outer segments. This was associated with oedema of the receptor cells' cytoplasm and of the receptor cells' synaptic regions in the outer plexiform layer (Fig. 4.6). Disturbances to the inner layers of the retina, apart from the nerve fibre layer, (Fig. 4.6) were not observed within this experimental group. The choroid of one animal within this group did show marked inflammatory cell invasion (Figs. 4.6 and 4.7) but it was uncertain whether this was directly attributable to the photic insult or to some other agency.

4.2.5 Group 2 (4 animals) Estimated Retinal Illumination:
38.6mWcm⁻²

On gross examination the retinae within this group showed folding and some areas of whitish discolouration, which were thought to be the highly oedematous areas seen later by light microscopy.

This group, in addition to the structural changes exhibited by tissues exposed to the lower intensities, showed more severe damage to the pigment epithelium and receptor cells. In some areas of the tissue examined the pigment epithelial nuclei were pyknotic. Cells containing such nuclei frequently showed a decrease in cell volume and an increase in their intensity of cytoplasmic staining (Fig. 4.8). Receptor cells in such areas were highly disturbed. The organised appearance of the inner and outer segments was lost, being replaced by a disorganised layer of vesicular cell debris (Fig. 4.8). Cells of the outer nuclear layer were oedematous, and pyknotic nuclei were seen. Oedema of the receptor cells' synaptic regions was also evident in the outer plexiform layer. Oedematous horizontal, bipolar and amacrine cells were present within the inner nuclear layer. The Müller cells, rather than appearing oedematous, showed a slight increase in the intensity of their staining (Fig. 4.9). The ganglion cells appeared to be of normal morphology; slight oedema was observed in both the inner plexiform layer and the nerve fibre layer. The Müller cell cytoplasm of the inner retina was also disturbed and showed considerable variation in its density of staining (Fig. 4.9).

Within the choroidal vessels platelet aggregation and large areas of impacted red cells were frequently observed (Fig. 4.10 and 11). These areas of platelet aggregation and red cell impaction were almost always associated with the more severely damaged regions of retina.

4.2.6 Group 1 (4 animals) Estimated Retinal Illumination:
84.4mWcm⁻²

On gross examination the retina of the experimental eyes showed numerous small folds. Large areas of retina were slightly discoloured and appeared to be detached.

By light microscopy this group was characterised by severe damage to the pigment epithelium and receptor cells. Pigment epithelial cell debris was frequently found among the plentiful outer segment debris (Fig. 4.12). In other areas the pigment epithelial cell debris had remained in more intimate association with severely damaged, but still recognisable, pigment epithelial cells (Fig. 4.13). The presence of pigment epithelial cell debris in association with outer segment material (Fig. 4.12) may have been due to artifactual separation through the damaged pigment epithelial cells.

The receptor cells' outer segments were highly disorganised and appeared as vesicular structures (Figs. 4.12 and 4.13). The inner segments were swollen and contained numerous translucent vesicles, presumably distended mitochondria (Fig. 4.14). Much of the receptor cells' cytoplasm, including the synaptic region was highly oedematous and many of the nuclei of the outer nuclear layer were pyknotic (Fig. 4.14).

Horizontal, bipolar and amacrine cells were frequently oedematous, as were some of the cell processes within the inner plexiform layer. The ganglion cells, and their axons in the nerve fibre layer, were frequently swollen and oedematous (Fig. 4.15). As in the previous group, some variation in the intensity of the staining of Müller cell cytoplasm was also apparent (Fig. 4.15).

A rare finding within this group, and some experimental eyes from other groups, was the appearance of macrophage-like cells on the inner limiting membrane of the retina. The finding of these cells did not appear to be related to the presence of damaged retinal tissues (Figs. 4.1 and 4.16).

As in Group 2, areas of severely damaged retina were associated with platelet aggregation and red cell impaction within the choriocapillaris, and in some of the deeper vessels of the choroid (Fig. 4.17).

4.3 Light Damage: Its Immediate Effects as Assessed by Electron Microscopy

This section describes the immediate effects of light damage as observed by electron microscopy. As in the previous section the descriptions will be concerned with the "worst case" in any experimental group. The groups will be described in order of increasing light intensity.

4.3.1 Group 6 (1 animal) Estimated Retinal Illumination: 20.4mWcm^{-2}

By light microscopy there was no detectable difference between the experimental tissue of this group and normal tissue. Similarly, by electron microscopy, the retinal and choroidal tissues appeared normal.

4.3.2 Group 5 (2 animals) Estimated Retinal Illumination: 23.2mWcm^{-2}

No departure from normal was observed in any of the retinal tissues examined in this group. However, in the choroid of one animal (LD52) a few platelets and inflammatory cells were observed within the choriocapillaris (Fig. 4.18). In all other respects the tissues appeared normal.

4.3.3 Group 4 (4 animals) Estimated Retinal Illumination: 32.8mWcm⁻²

Definite abnormalities of retinal structure were first detected within this group. The retinal pigment epithelial cells showed rounding of their nuclei, and mitochondrial distension. The basal infoldings, lipid droplets, junctional complexes, melanin granules and apical villi were all of normal appearance (Fig. 4.19). On rare occasions complete disruption of individual pigment epithelial cells was seen. This finding was unusual in that the neighbouring pigment epithelial cells were of normal morphology (Fig. 4.20).

The receptor cell outer segments showed slight irregularities in their disc stacking (Fig. 4.19). Cone cell outer segments appeared to be more susceptible to damage than rod outer segments. The cone outer segments often showed marked vesiculation while neighbouring rod outer segments were only slightly disturbed. This was also true of the cone inner segments which appeared to be more severely damaged than their rod cell equivalents (Fig. 4.19). The cone inner segments were swollen and contained distended mitochondria.

The cells of the inner layers of the retina were all of normal appearance.

The choroid was of normal appearance, although intravascular inflammatory cells and platelets may have been more common in the choriocapillaris than would have been expected.

4.3.4 Group 3 (4 animals) Estimated Retinal Illumination: 32.8m Wcm⁻²

Structural damage to the retina was far more extensive in this group than in the groups described. As in the lower intensity group (group 4), the pigment epithelium showed rounding of its nuclei and distension of its mitochondria (Figs. 4.21 and 4.22). Distension of the pigment epithelial smooth endoplasmic reticulum, not seen in the previous group, was present within this group (Fig. 4.22). This type of damage was probably the equivalent of the oedematous pigment epithelium seen by light microscopy. The pigment epithelium of one animal (LD3.2) showed other variations of damage. One variation, noted by light microscopy, was atypical pigment granule distribution. The cytoplasm of these cells contained numerous phagosomes and large electron-lucent vesicles. Their apical surfaces were displaced into the interphotoreceptor space. This apical region of the pigment epithelial cells contained much of the cells' melanin and gave rise to the unusual appearance seen by light microscopy (Fig. 4.5 light micrograph and 4.23a electron micrograph). In other regions within the retina of this animal pigment epithelial cells contained pyknotic nuclei, showed alterations of their basal infoldings, and showed marked cytoplasmic densification (Fig. 4.23.b).

The receptor cell outer segments were often disturbed, appearing twisted and ruptured (Fig. 4.21). Cone cell outer segments, as in the previous group, appeared to be more susceptible than their rod cell counterparts (Fig. 4.21). The receptor cell inner segment mitochondria appeared distended, but not ruptured. Again, the inner segments of cones appeared to be more severely damaged than their rod counterparts. The cytoplasm of the cone inner segments was often noticeably more lightly stained, and

the distension of the mitochondria appeared to be slightly greater than in the rods (Fig. 4.21). The receptor cell nuclei were often rounded and surrounded by a halo of electron-lucent cytoplasm. This swelling of receptor cell cytoplasm was also present in the rod spherules. However, the cone pedicles and cell bodies often appeared less oedematous than the rod cell spherules and cell bodies (Fig. 4.21).

Müller cells and the cells of the inner layers of the retina were all of normal appearance, although in one animal, again LD3.2, what appeared to be pyknotic Müller cell nuclei were observed. This was a rare finding but was thought to be of interest because of its demonstration of the ramifications of Müller cell cytoplasm throughout the retina. (Fig. 4.24).

In three of the four animals in this group the choroid appeared to be normal. However, as shown by light microscopy, the choroid of one animal (LD 3.2) appeared to contain numerous inflammatory cells. This was confirmed by electron microscopy (Fig. 4.25). These regions of inflammatory cell infiltrate were usually associated with the more severely damaged regions of retina. Macrophages, polymorphs and plasma cells were all evident. It was unclear whether these cells were present in response to the damaged retinal tissues, which seemed unlikely due to the short duration of the insult, or to some pre-existing condition.

4.3.5 Group 2 (4 animals) Estimated Retinal Illumination: 38.6mWcm⁻²

Within this group damage was observed, to some extent, in all layers of the retina. The damaged pigment epithelium showed two different appearances: it either appeared swollen with electron lucent cytoplasm, or shrunken with electron-dense cytoplasm (Fig. 4.26). The nuclei of the swollen cells were rounded, the mito-

chondria were either slightly swollen or small and electron dense. The swollen appearance, by light microscopy, was presumably due to distension of the cells abundant smooth endoplasmic reticulum. The remainder of the identifiable cell organelles, the melanin granules, lipid droplets and junctional complexes, were all of normal appearance (Fig. 4.26a). Within the densely stained pigment epithelium there was a marked loss of cell volume while the nuclei were shrunken and very densely stained. Mitochondria, although identifiable within the cytoplasm, were poorly preserved. The apical processes were lost and the melanin granules dispersed throughout the apical cytoplasm of the cell. The large lipid droplets, characteristic of the rabbit retina, were still present but, due to the shrunken nature of the cells, they appeared disproportionately large. Junctional complexes could not be identified, presumably due to their lack of contrast against the intensely stained cytoplasm (Fig. 4.26b).

The receptor cells were severely damaged (Fig. 4.27).

The outer segments were highly disordered and showed extensive loss of structural organisation. Within the outer retina it was no longer possible to discriminate between cone and rod outer segments. However, cone cell inner segments were identifiable amongst the outer segment debris. They appeared as intensely stained pear shaped structures containing distended mitochondria (Fig. 4.27). Many of the receptor cell nuclei were surrounded by a halo of electron-lucent cytoplasm. Occasionally pyknotic nuclei were present in the outer nuclear layer (Fig. 4.27). The rod cell spherules appeared swollen and electron-lucent in contrast to cone pedicles which often retained their normal morphology (Fig. 4.28).

The Müller cell cytoplasm within the inner nuclear layer retained its normal morphology, although, some of the Müller cells were more intensely stained than normal (Fig. 4.27). The other cells of this layer, horizontal cells, bipolar cells and amacrine cells, frequently had swollen electron-lucent cytoplasm and distended mitochondria (Fig. 4.27). Many of the processes of the inner plexiform layer were swollen and electron-lucent as were some of the ganglion cells (Figs. 4.27 and 4.29). The Müller cell cytoplasm of the innermost regions was of variable electron density but of normal morphology (Fig. 4.29).

As in the preceding groups, regions of extensively damaged retina were associated with the presence of platelets and inflammatory cells in the choriocapillaris (Fig. 4.30). The remainder of the choroid appeared normal.

4.3.6 Group 1 (4 animals) Estimated Retinal Illumination:
84.4mWcm⁻²

In this group the greatest damage to the retinal and choroidal tissues of experimental eyes was observed. As in the previous group, the pigment epithelium either appeared distended and electron-lucent, or shrunken and electron-dense. The electron-dense cells were similar in morphology to those described in Group 2 (see Fig. 4.26b). However, the electron-lucent regions differed considerably from those described in the previous section (4.3.5). The pigment epithelial basal infoldings, although present and often still in apposition to Bruch's membrane, were highly altered (Figs. 4.31 and 4.32). The nuclei were still evident but they were rounded and had an atypical chromatin pattern (Fig. 4.31). Mitochondria were highly atypical and were thought to be represented by the small vesicular structures present within the cytoplasm (Fig. 4.31). The most

prominent features were extremely large vesicular structures which greatly distended the pigment epithelial cells. These structures were filled with a flocculate material, resembling the plasma of the choroidal blood vessels in its staining characteristics (Figs. 4.31 and 4.32).

Of the remaining pigment epithelial cell inclusions and organelles only the lipid droplets could be identified in the basal portion of these severely distended cells (Fig. 4.32), and the melanin granules in what remained intact of the apical surface of the cells. The apical surfaces of the pigment epithelial cells formed a layer which was comprised of small vesicular structures, melanin granules, and swollen finger-like structures which interdigitated with the damaged photoreceptor outer segments (Fig. 4.33).

The receptor cell outer segments were distended and highly vesiculated, often having the appearance of membrane-filled bags (Fig. 4.34). Damaged rod and cone cell outer segments were indistinguishable. Within the inner segments it was no longer possible to distinguish between myoid and elipsoid regions. The inner segments appeared as sack-like structures filled with distended mitochondria (Figs. 4.34 and 35).

The majority of the receptor cells nuclei were surrounded by a halo of electron-lucent cytoplasm (Fig. 4.35) although some pyknotic nuclei were also present in the outer nuclear layer (Fig. 4.35). The synaptic region of both rods and cones were swollen in this group, unlike those in the previous group (Fig. 4.35).

Horizontal, bipolar, and amacrine cells were highly oedematous, as were their cell processes in both the outer plexiform layer (especially horizontal cell processes) and the inner plexiform layer (Fig. 4.36). The cell organelles of these severely swollen cells were often aggregated in the vicinity of the nucleus.

The ganglion cells, and their axons in the nerve fibre layer, appeared swollen and electron-lucent. The ganglion cells often showed aggregation of their organelles within their cytoplasm similar to that seen in the horizontal, bipolar, and amacrine cells in the inner nuclear layer (Fig. 4.37).

The majority of the Muller cell cytoplasm was of unusual appearance. In addition to the variation in electron-density, similar to that seen in the previous group, the cells contained numerous electron-lucent vesicles, which were possibly distended tubules of smooth endoplasmic reticulum, and numerous electron-dense granules (Figs. 4.37 and 38) of unknown origin.

As in the preceding groups, severely damaged regions of retina were associated with the presence of platelets and inflammatory cells in the choriocapillaris and deeper vessels of the choroid (Figs. 4.31 and 32).

Many of the endothelial cells of the choriocapillaris and the deeper blood vessels had swollen electron-lucent cytoplasm and swollen organelles. They also showed blebbing of their cytoplasm into the lumen of the blood vessels (Figs. 4.31 and 39). The deeper choroidal structures were of normal appearance apart from fibroblasts in the vicinity of the choriocapillaris. These cells often showed distension of their cytoplasm and cytoplasmic organelles. Their nuclei apart from slight crenellation, were of normal appearance (Fig. 4.39).

A summary of the results of this section are shown in Fig. 4.40, which gives a qualitative assessment of the damage seen in Groups 1 to 6.

4.4 Light Damage: Its Immediate Effects as Assessed by Quantification of the Changes in the Cellular Components of the Nuclear Layer.

4.4.1 Introduction

The aim of the quantification described in this section was to obtain a repeatable method of assessing the changes in retinal structure observed by electron microscopy. The material and methods employed were described in Chapter 2, Section 3. For clarity, however, a brief description will be given here.

The tissue used in this investigation was the same as that used in the preceding section. The tissue selection was described in Chapter 2, Section 5.

As an aid to quantification, a readily identifiable area of retina had to be selected. For this investigation the outer nuclear layer was chosen; the photoreceptors are among the first cells of the retina to show structural changes following exposure to excessive illumination. Additionally, the outer nuclear layer was readily identifiable in all sections of retina, regardless of the degree of damage suffered by the tissue. The outer nuclear layer was defined as the area between the outer limiting membrane and the innermost aspect of the receptor cell synapses (Fig. 4.41). The receptor cell spherules and pedicles were included as they often exhibited structural changes paralleled by the appearance of damage in the outer nuclear layer.

The features assessed in the outer nuclear layer were as follows:

- a) Pyknotic receptor cell nuclei
- b) Receptor cell nuclei
- c) Receptor cell cytoplasm

d) Müller cell cytoplasm

Four blocks were examined from each experimental eye and one from each control eye. Two, 100 mesh grid, squares were photographed from sections from each block. From these 100 mesh size fields, two discrete areas were printed and used for quantification. Thus sixteen prints were examined for each experimental eye and four for each control eye.

For analysis, a grid of 100 random points (derived from random number tables) on a 6" x 4" (152.5mm x 102.0mm) acetate sheet with a minimum point separation of 0.1in. (2.54mm) was placed over the 6" x 4" photomicrographs. Points which fell on features of interest in the outer nuclear layer were counted and expressed as a percentage of the total number of points landing on the outer nuclear layer. The area of each 6" x 4" print corresponded to $5,880\mu\text{m}^2$.

To test the reproducibility of the method a set of prints from one animal were recounted after a time period of 5 months.

The differences in the results were expressed as a percentage of the original result for each block counted (4 prints). These were summed for the 5 blocks re-analysed. The differences in the results are as follows:

Receptor Cell Nuclei $11\% \pm 5\%$

Receptor Cell Cytoplasm $8\% \pm 6\%$

Müller Cell Cytoplasm $34\% \pm 14\%$

The large error in the Müller cell cytoplasm counts was probably related to the low number of counts obtained for Müller cell cytoplasm. Inter-observer errors were not calculated.

For complete numerical data see Appendix 3.

Control Results

The results for the 19 control eyes, are presented as histograms (Fig. 4.42) showing means and standard deviations. The standard deviations arise from the fact that four micrographs were analysed for each block of tissue. The features analysed were receptor cell nuclei, receptor cell cytoplasm, and Müller cell cytoplasm. Results for pyknotic receptor cell nuclei were not obtained as such features did occur in any of the control tissues examined. In addition, the results for each feature counted were combined for all 19 control eyes to give a pooled control result for each feature (Fig. 4.42). These pooled control results were used in the subsequent statistical analysis of the experimental results.

Experimental Results

The results for receptor cell nuclei, receptor cell cytoplasm, and Müller cell cytoplasm were calculated for each individual block (4 prints) and presented as histograms showing means and standard deviations. The individual block results (4 blocks per animal) for receptor cell nuclei, receptor cell cytoplasm, and Müller cell cytoplasm were then t tested against the pooled control results. The levels of significance obtained are given with the raw data in Appendix 3. Results which differed significantly from the control values were more common in animals which had been exposed to the higher light intensities. This trend was not particularly marked. The results of the block counts

for pyknotic receptor cell nuclei are shown in Appendix 3. Unfortunately, their distribution, within individual eyes and between experimental groups, did not in any way appear to be related to the light intensity to which the animal, or group of animals, had been exposed.

The aim of this analysis was to correlate changes within the outer nuclear layer to the light intensity to which the animal had been exposed. This appeared to be possible in two ways.

In the first analysis the block results for each animal could be combined and plotted against estimated retinal illumination (Fig. 4.43). The raw data from which Figure 4.43 is drawn are given in Appendix 3 along with the results of t tests comparing these results with the combined control results. As in the individual block results, animal results in which any of the features assessed were significantly different from the control results were more frequent in animals which had been exposed to the higher light intensities. However, the trend was once more not particularly marked. It was apparent, nevertheless, that at the higher light intensities both the scatter of the results and the standard deviations of the results increased. To analyse this finding the variance between the experimental results and the pooled control results were calculated. F, the variance ratio, was obtained by dividing the squared standard deviation of the experimental result by the squared standard deviation of the appropriate control result. Occasionally, this procedure had to be reversed, the squared control standard deviation becoming the numerator and the squared experimental standard deviation the denominator, as F must be equal to, or greater than 1. The animal results for receptor cell nuclei, receptor

cell cytoplasm, and Müller cell cytoplasm were then plotted against the estimated retinal illumination to which the animal had been exposed (Figs. 4.44, 4.45 and 4.46). The best straight line was fitted by linear least square regression. Only in the case of receptor cell cytoplasm was it possible to fit a straight line with a P value of less than 0.05 and in this case P lay between 0.05 and 0.01 (Fig. 4.45).

In the second analysis the results for all the blocks within an experimental group exposed to the same light intensity were combined and plotted against the estimated retinal illumination (Fig. 4.47). Results which differed significantly from the control results are shown encircled in Figure 4.47. As can be seen few of the results differ significantly from the control results shown on the y axis. However, it was again apparent that the standard deviations appeared to be larger for groups exposed to the higher light intensities. The variance ratios were calculated and plotted against the estimated retinal illumination as before. In this case positive correlations were obtained for both receptor cell nuclei and receptor cell cytoplasm. These were $0.05 > p > 0.01$ and $p < 0.001$ respectively. (Fig. 4.48)

These results and their implications are discussed at the end of the chapter.

As was expected, increasing intensity of illumination of the retina resulted in increasing damage to the retinal structure. In groups 6 and 5 (estimated retinal illumination 20.4 mWcm^{-2} and 23.2 mWcm^{-2} respectively) no departure from normal retinal structure could be detected by either light or electron microscopy. Ultrastructural changes were first observed in group 4 (estimated retinal illumination 28.9 mWcm^{-2}) and became more severe with increasing light intensity, until in group 1 (estimated retinal illumination 84.4 mWcm^{-2}) damage was detectable in all layers of the retina.

The initial site of damage was in some doubt as both the pigment epithelium and the receptor cells appeared to show ultrastructural abnormalities simultaneously. The pigment epithelium initially showed slight mitochondrial distension, rounding of the nuclei, and slight cytoplasmic rarefaction. These findings were in general agreement with those of Friedman and Kuwabara (1968), Tse (1973), Kuwabara and Okisaka (1976) and Fuller, Machemer, and Knighton (1978). In these studies the morphology of the outer segment damage was very similar to that seen in this investigation, although pigment epithelial damage was more variable in its appearance in the present study. Slight differences in morphology may be attributed to the disparate nature of species. Rabbits were used in this study while monkeys were the experimental animals employed in the investigations cited. Variations in light sources and exposure regimes may also account for some of these differences.

Lawwill (1973) has investigated the effects of 4 hour exposures to various intensities of white light and argon laser

(514.5nm wavelength) on the Dutch rabbit retina. Unfortunately comparisons cannot be drawn between Lawwill's study and the present study as in Lawwill's study the light damaged tissue was not examined histologically until one to four months after exposure.

The finding that the pigment epithelium and the photo-receptors appear to show ultrastructural damage simultaneously may be a reflection on their intimate structural and metabolic relation (Spitznas and Hogan, 1970 and Young and Bok, 1970) and possibly indicate a metabolic origin for light damage.

Although the pigment epithelium and the receptor cell outer segments began to show structural abnormalities simultaneously, cone cell outer and inner segments appeared to be more susceptible to damage than their rod cell counterparts. Severely damaged cone outer segments were found adjacent to only slightly damaged rod cell outer segments. A differential susceptibility of rod and cone cells to damage has been reported by Tso, Wallow and Powell (1973) in the retinae of rhesus monkeys following exposure to argon laser light. In the rhesus monkey's retina the increased sensitivity of the cone cell to damage by laser light was present throughout the structure of the cone photo-receptor. The inner and outer segments, the nuclei, and the synaptic pedicles all showed degenerative changes in advance of the corresponding regions of rod cells. In this study the increased sensitivity of the cone cells to damage was limited to their outer and inner segments. Frequently, in animals exposed to the higher light intensities, cone cell somata and receptor pedicles appeared to be more resistant to damage than the rod cell somata or spherules.

These differences in cone cell susceptibility to damage may again be attributable to species difference, light source differences or the time after exposure at which the tissue was examined histologically. In the study of Tso, Wallow and Powell (1973) the minimum time elapsing between exposure and histological examination was five hours. There was the possibility that further degenerative changes could take place during this time.

Tso, Wallow and Powell (1973) suggested that susceptibility of the cone outer segment to damage could be partially explained by their relation to the melanin granules of the pigment epithelium. In the rhesus monkey the melanin granules in the apical villi of the pigment epithelium appeared to surround the outer segments of the cone cells for greater distances than in the rabbit eye. The Melanin granules appeared to be present in greater numbers as compared with those present around the outer segments of rods. In photic injury, the radiant energy absorbed by the melanin granules would be converted to thermal energy which would damage the adjacent structures. Consequently, the outer segments of cone cells may be heated indirectly by surrounding melanin granules, and subsequently sustain more damage than the outer segments of rods. A similar argument was applied to the cone cell nuclei which lie adjacent to the outer limiting membrane. Here they were in closer proximity to the melanin granules of the pigment epithelium than were the rod cell nuclei, and were consequently more likely to be damaged by heat from the melanin granules. This was thought an unlikely explanation for the cone cell susceptibility to damage in the present study as the light intensities used, especially the lower ones, were unlikely to produce a significant rise in retinal temperature. (Some attempts at estimating the rise in retinal temperature during illumination, as well as by direct

measurement, have been made. These are given in Appendix 4.) Also, the dense packing of the melanin granules around the cone outer segment as seen in the rhesus monkey does not exist in the rabbit, as the rabbit cones have a much more rod-like appearance (Hughes, 1971, Bunt, 1978). It seems more likely that the susceptibility of the cone cells seen in this study was due to some structural, metabolic, or photochemical difference. It has been hypothesised that the cone cell outer segment membrane is a continuous structure and not formed of discrete discs enclosed in a membrane envelope (Young, 1965; Young and Droz, 1969; Young, 1969; Laties, Bok and Liebman, 1976 and Anderson, Fisher and Steinberg, 1978). This may also be true of the rabbit cone outer segment which showed a typical cone pattern of diffuse incorporation of labelled sugars and amino acids as was demonstrated by Bunt (1978). If the cone outer segment has greater continuity of its membranes than the rod it may be an inherently weaker structure. Localised damage to any one "disc" may affect neighbouring discs, because of the cones' continuity of membrane structure, and cause greater damage than would be produced in the discrete disc system of the rod outer segment.

Harwerth and Sperling (1971) demonstrated, in the rhesus monkey by psychophysical techniques, a loss of spectral sensitivity of over 90% following exposure to light of 6nm bandwidth centred on 463nm for 1.5 hours per day for seven consecutive days. This loss was in the blue region of the spectrum and it was postulated that the loss was produced by a selective destruction of a class of cones with their peak absorption at 445nm. These findings were later correlated histologically to selectively damaged cone cells in retina which had been subjected

to narrow bandwidth illumination (Sperling and Johnson, 1974).

Several investigators (Noel, Walker, Kang and Berman, 1966; Gorn and Kuwabara, 1967; Anderson, Coyle, and O'Steen, 1972; and Lawwill, 1973) have found that the degree of light damage produced by different wavelengths corresponds to the degree of visual effectiveness of the wavelength concerned. This may be a simplification. Blue light of short wavelengths, well below the peak absorption of the photo-pigments, has been shown to be extremely efficient in producing retinal damage (Ham Mueller and Sliney (1976) Ham, Ruffolo, Mueller, Clarke and Moon, 1978). It seems likely that the spectral composition of the light illuminating the retina will have relevance to the class (as defined by peak absorption) of photoreceptor which will be damaged.

In this study, where rabbit retinae were exposed to white light delivered through a fibre optic system, the selective cone damage seen at the lower intensities may be related to the spectral distribution of the light illuminating the retina. Due to the emission characteristics of the tungsten light source, the absorption characteristics of the fibre optic light guide, and the ocular media (see Appendix 2) considerably more energy was delivered to the retina at the red end of the spectrum than the blue. If some of the cones in the rabbit retina were absorbing light of longer wavelengths than the rods, their bleaching would be more extensive. Consequently, greater metabolic demands would be made on the cones. It therefore seemed likely that cone cells would have been damaged before adjacent rods, which could have been absorbing less light.

Any susceptibility of cone cells to damage may be enhanced by metabolic disturbances. Hansson (1970b) has shown that sustained light exposure inhibits the oxidative enzymes of the

retina. This depression of activity was first noted in the pigment epithelium, and shortly after in the inner segments. As these experiments were conducted on rats, which have virtually an all rod retina, no comparison between rods and cones could be drawn. However, Marshall, Mellerio and Palmer (1972) demonstrated accumulation of glycogen in the inner segments of damaged cones in pigeon retinae. This accumulation of glycogen may have been a result of light-induced disturbances of the oxidative enzymes of the inner segment and may have reflected an inability of the cell to utilise glycogen in its metabolism.

The cone cell may be more susceptible to light damage as a result of a combination of structural, photochemical or metabolic factors. A metabolic origin for light damage has been postulated by Noel, Walker, Kang and Berman (1966). They suggested that light could initiate destructive oxidising reactions in the retina. Photoreceptor discs are mostly composed of unsaturated fatty acids. The action of light on the photopigments begins a series of reactions which result in the production of some free radicals. These free radicals could initiate a chain reaction which, if unchecked by the presence of antioxidants such as vitamin E, could proceed to peroxidation of the lipid membranes. Noel, Walker, Kang and Berman (1966) reported negative results in effecting light damage by depriving animals of vitamin E or changing environmental oxygen tension. However, in vitamin E deficient monkeys, Hayes (1974) demonstrated outer segment damage to cones which was similar in appearance to light damage. Therefore peroxidation of the photoreceptor membranes remains a possibility.

Noel and Albrecht (1971) considered that retinol, from excessive rhodopsin bleaching, may be a retino-toxic agents. Free retinol is known to have membraneolytic effects on cells (Dingle and Lucy, 1965 and Daniel, Dingle, Sharman, and Moore, 1966). Noel and Albrecht (1971) found that vitamin A - deficient rats showed a degree of protection from light damage. These rats had reduced concentrations of rhodopsin for light to bleach and decreased concentrations of light-produced retinol. The authors were, however, forced to eliminate this loss of retinol as the factor of primary importance in protecting the vitamin A deficient rats. When the deficient rats were exposed for long periods of time, light damage did develop despite a depletion of retinol. They also noted that deficient animals were not protected if they had been kept in darkness continuously prior to exposure. Those animals, while having almost normal levels of rhodopsin, had low stores of retinol. The bleaching of rhodopsin by light temporarily increased retinol concentrations, but it was not thought to be the toxic agent responsible for light damage. These authors concluded that protection from light damage depends upon a state of "cell adaptation to light" which would be reflected by, but not determined by, the level of retinol.

At the higher light intensities in this study, groups 3, 2 and 1, increased damage to the pigment epithelium and receptor cells with increased intensity of illumination was apparent. The damage observed at the higher intensities was similar to that described by Grignolo, Orzalesi and Calabria (1966), Orzalesi, Grignolo and Calabria (1967); Orzalesi, Grignolo, Calabria and Castellazza (1967); and Orzalesi, Calabria and Grignolo (1970); after intravenous administration of sodium iodate, sodium fluoride diaminodiphenoxypentance and iodoacetic acid. All of these com-

pounds are metabolic inhibitors, preferentially affecting either the receptor cells or the pigment epithelium. The similarities between retinal tissues poisoned by metabolic inhibitors, and retinal tissues damaged by light, may reflect an underlying similarity in their mechanisms of producing cellular damage.

Impairment of mitochondrial function as seen by their swelling, coupled with enzymic inhibition as demonstrated by Hansson (1970a, 1970b), may lead to an imbalance in the electrolyte content of the cells. This probably occurs due to failure of membrane pumps, causing a subsequent accumulation of water in the cytoplasm. This mechanism may be responsible for the intracellular oedema seen, in this study, in retinae exposed to the higher light intensities. Similar mitochondrial changes and associated intracellular oedema have been described in the rabbit retina following anoxia (Webster and Ames, 1965) and following ischaemia (Johnson and Foulds, 1978). In the rat liver these changes have been described following anoxia (Oudea, 1963) ischaemia (Bassi, Bernelli-Zazzera, 1964) and hypoxia (Bassi, Bernelli-Zazzera and Cassi, 1960; Sulkin and Sulkin, 1965). Similar changes have also been reported in the brain tissues of hamsters following hypoxia (Hager, Hirschberger and Scholz, 1960).

In the normal eye the pigment epithelium is thought to be responsible for the maintenance of the blood retinal barrier (Noel, 1963; Shoise, 1970; Reyman, Spitznas and Straatsma, 1971b; Reyman and Bok, 1972; Raviola, 1977). In light induced damage to the retina, failure of the pigment epithelial enzymes and mitochondria may lead to the cell being unable to fulfil its role as a barrier epithelium.

It seems probable that a failure in the barrier function of the retinal pigment epithelium may lead to changes in the tonicity and osmolarity of the interphotoreceptor fluid. This could adversely affect the receptor cell outer segments. Structural changes in outer segments similar to those seen in this study have been described by Cohen (1971) who investigated the effects of osmotic stress on the structure of the receptor cell outer segments and discs.

In groups 1 and 2 there were frequently small focal regions of severe retinal damage. These small focal regions of damage were irregularly distributed within the area of illuminated retina. In these severely damaged regions the pigment epithelium contained vacuoles of flocculate material. The receptor cell outer segments were reduced to irregularly shaped membraneous bags" containing highly disorganised membrane material. The inner segments were usually swollen, and contained severely distended mitochondria. The cells of the inner layers of the retina often showed swollen electron lucent cytoplasm, clumping of the cell organelles within the cytoplasm, and swelling of their nuclei. These regions of severe retinal damage were often interspersed with regions of comparatively normal appearance. This extreme variation of damage within the experimental tissues was unexpected.

Initially, it was thought that the variation could have resulted from the presence of "hot spots" in the light incident on the retina. After consideration, this was thought to be an unlikely explanation as the end of the light guide was positioned within the front focal length of the eye. The front focal point of the rabbit eye, as determined by Hughs (1972) was 5.5mm in front of the corneal vertex, whereas the end of the light guide was positioned about 2mm in front of the corneal vertex. With this optical arrangement a focused image of the end plate of

the light guide could not be formed on the retina. The illumination of the retina would therefore be highly diffuse. This would eliminate the possibility of "hot spots", and regions of focal damage produced by them, arising.

Measurements of the energy distribution within the beam of light leaving the light guide, and its calculated distribution on the retina, are given in Appendix 2. From these calculations it was expected that the centre of the illuminated area was receiving a reasonably even distribution of light and that there would be a reasonably rapid reduction in energy at the edges of the illuminated area. It would also be expected that this distribution of illumination would give rise to a lesion with an even distribution of damage in the centre with reduced damage at the edges, finally, merging into normal retina.

The variation of damage seen within the experimental eyes may have resulted from an interaction of three factors. These are light induced metabolic damage, light induced thermal effects and lastly, the enhancement of metabolic or thermal effects by occlusion of the choriocapillaris. Occlusions of the choriocapillaris caused by degranulated platelets, inflammatory cells, or impacted red cells were almost invariably associated with regions of severe retinal damage. As the rabbit lacks a retinal circulation these occlusions could have given rise to small focal regions of ischaemic retina. Presumably, these regions would be more sensitive to light damage as they would already be in metabolic difficulties due to loss of their blood supply. The stimulus for the platelet and inflammatory cell response is unclear but it may have been in response to the metabolic by-products of the initial damage to the photoreceptors and pigment epithelium.

Moseley and Strang (1981) have calculated the expected rise in retinal temperature associated with constant illumination of the retina and various assumed values for choroidal blood flow. Moseley and Strang (1981) predicted that choroidal blood flow has a small effect, which becomes larger at higher levels of illumination, on retinal temperature. It seems probable that regions of retina overlying an occluded region of the choriocapillaris would be more susceptible to damage. Such regions of retina would be deprived of metabolites and probably subjected to elevated temperatures. Elevated temperature has been shown to greatly accelerate the appearance, and enhance the degree, of light damage (Noel, Walker, Kang and Berman, 1966; Friedman and Kuwabara, 1968; Grignolo, Orzalesi, Castellozzo and Vitone, 1969; and Hansson, 1970a).

During the course of the one hour exposures to light, regions of retina with a slightly impaired choroidal blood flow may have entered into a circle of increasing damage. Decreasing choroidal blood flow, caused by platelet aggregation or inflammatory cell invasion in response to the by-products of light damage, could lead to elevation of retinal temperature further accelerating the damaging processes. The more severely damaged retina may then induce further platelet aggregation within the choriocapillaris, decreasing blood flow to the adjacent retina still further.

The variation of damage seen within the experimental tissues led to considerable difficulties in any attempt to produce a quantitative measure of damage. Initially, it was considered possible to quantify changes in the pigment epithelium or the receptor cell inner and outer segments. Changes in the pigment epithelium, however, such as the number of phagosomes within each cell, were thought unsuitable for quantification. This was

because these features have been shown to be dependent on environmental conditions such as the time during the light/dark cycle at which the retinal tissues were fixed (La Vail, 1976b; Basinger, Hoffman and Mathes, 1976; Hollyfield, Besharse and Rayborn, 1976; Besharse, Hollyfield and Rayborn, 1977; and Young, 1978). Changes in the structure or appearance of the inner and outer segments were considered unquantifiable as their appearance was highly dependent on the plane of section. This difficulty was further compounded by the orientation of outer segments being frequently disturbed during dissection and subsequent tissue processing.

Ultimately, it was decided to quantify changes in the outer nuclear layer. This layer showed morphological changes after damaging light exposures which were reasonably consistent within each block. Also, the photoreceptors appear to be intimately associated with the primary pathological processes of light damage (Grignolo, Orzalesi, Castellazzo and Vitone, 1962; Kuwabara and Gorn, 1968; O'Steen, Shear and Anderson, 1972).

The features assessed within the outer nuclear layer are listed here:-

a) Pyknotic Receptor Cell Nuclei

These were often encountered in the groups exposed to the higher light intensities but their distribution and occurrence within groups 1, 2, 3 and 4 did not appear to be related to intensity.

b) Receptor Cell Nuclei

These appeared to show variation in size, often appearing distended or shrunken, in the groups exposed to the higher light intensities. This subjective finding was confirmed by analysis. The counts for receptor cell nuclei in groups 1 and 2 were not

infrequently below the control values (Fig. 4.43 and Appendix 3). As the counts for any feature were expressed as a percentage of the total points lying on the outer nuclear layer, and swelling of the outer nuclear layer was a common observation in the higher intensity groups, it would be expected that the number of points lying on the receptor cell nuclei would diminish. It was noted that there appeared to be an increase in the variance of the results. This was significant only when group results (all the animals at one intensity combined) were considered.

c) Receptor Cell Cytoplasm

This appeared to show increased electron lucency and often appeared distended in the higher intensity groups. Although there was a poor correlation between the results obtained and the intensity of light to which the animal had been exposed, there appeared to be agreement between the damage exhibited by block and the individual counts obtained for that particular block. For example block C2, animal 1.1 had exceptionally low counts for receptor cell nuclei ($27\% \pm 7.4\%$) and high counts for receptor cell cytoplasm ($52\% \pm 7.8\%$). The control values for these features were $51.1 \pm 6.4\%$ and $31.0 \pm 5.5\%$ respectively. The appearance of the tissue from which these results were obtained is shown in Figure 4.35. It can be seen that the counts for receptor cell nuclei and receptor cell cytoplasm did vary in accordance with the appearance of the tissue. Therefore, the inability to demonstrate unequivocally relations between the light intensity to which the tissues were exposed and the counts obtained for any feature within that tissue was not due to any inherent insensitivity of the counting method but was due instead to the variation within the experimental eyes.

d) Müller Cell Cytoplasm

The counts for Müller cell cytoplasm showed little variation from the values obtained for the control tissue, whether taken individually as results for a block or combined to give results for individual animals or groups. These results might, at first, confirm the subjective view that Müller cells were fairly resistant to damage. However, reproducibility tests showed considerable variation in the results for Müller cell cytoplasm. This may have masked any experimental result. The high variation in the Müller cell counts was thought to stem from the comparatively low counts obtained for them (15%-25%).

The counting method employed did appear to be sensitive enough to detect changes in the cellular relations within the outer nuclear layer. Calculations of the variance ratio for both the animal and group results (the group results being all the animals at a particular intensity) did imply that variation within the tissues of one animal and between animals tended to increase at higher light intensities. Sources of variation within the tissues have already been discussed. Variation between animals may be due to factors such as ocular transmission, size of the eye, and the accommodative state of the eye. Due to the double nature of the fibre optic light guide it was possible to illuminate the eyes of two rabbits simultaneously. This was done on occasion, the animals concerned being, Group 1: animals 2 and 3, Group 2: animals 3 and 4, Group 3: animals 1 and 2, Group 4: animals 1 and 2, and Group 5: animals 1 and 2. Even in the pairs of animals which were exposed simultaneously, there still existed considerable variation. This finding goes some way to reducing the disconcerting possibility that variation in the light intensity was underlying the variation seen in these experiments.

The point counting method employed in these investigations may not have been entirely successful due to the extreme variation within the tissues analysed but it would appear that it could be applied in other situations where the retinal changes are of a more uniform nature. These situations include, for example, retinal degeneration induced by acute ischaemia or metabolic poisons, such as sodium iodate, sodium fluoride, iodoacetic acid and diaminodiphenoxypentane.

The counts obtained for the features assessed were not converted to absolute measurements of area or volume. This was because counting system was primarily intended to give a repeatable method of assessing relative changes and variation within the tissue. Absolute measurements of cell area or volume were not required.

1



2



Fig. 4.1

(LD4.4 block D3). Light micrograph showing the appearance of the retina and choroid, after exposure to light intensity 4. OS: outer segments; PE: pigment epithelium; CC: chorio-capillaris (x 400).

Fig. 4.2

(LD4.1 block B4). Light micrograph showing a focal disruption of the pigment epithelium, after exposure to light intensity 4. Arrow: focal disruption of pigment epithelium (x 400).

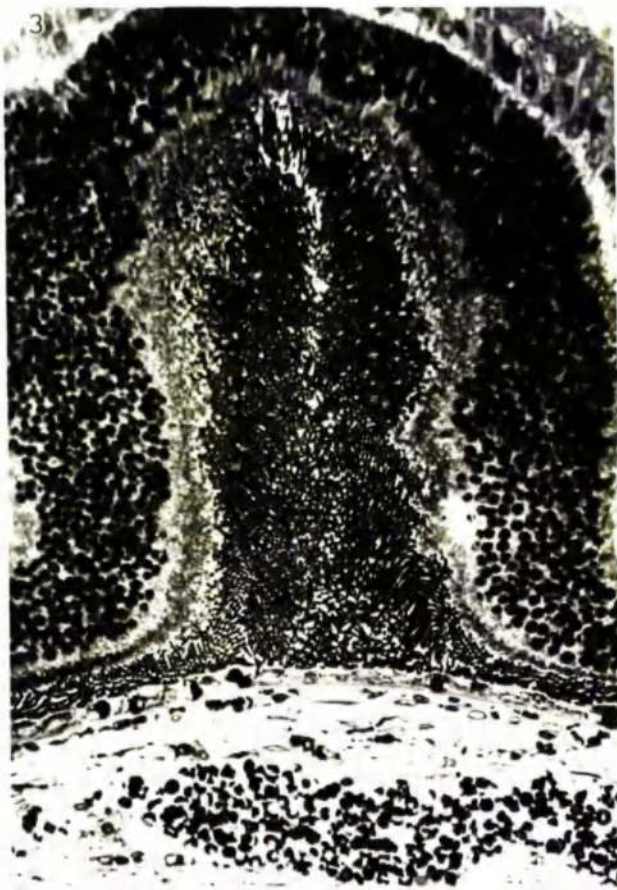


Fig. 4.3

(LD3.1 block B2). Light micrograph showing the appearance of a retinal fold, seen after exposure to light intensity 3. (x 250).

Fig. 4.4

(LD3.1 block A3). Light micrograph showing the appearance of the outer retina, after exposure to light intensity 3. OS: outer segments; PE: pigment epithelium (x 1,000).



Fig. 4.5

(LD3.2 block C2). Light micrograph showing a region of atypically pigmented pigment epithelium, after exposure to light intensity 3. PE: pigment epithelium; OS: outer segments; IS: inner segments; Arrows: pyknotic nuclei (x 400).

Fig. 4.6

(LD3.2 block B3). Light micrograph showing the appearance of the retina and choroid, after exposure to light intensity 3. PE: pigment epithelium; OS: outer segments; IS: inner segments; ONL: outer nuclear layer; Arrows: oedematous receptor synapses; IC: inflammatory cells (x 400).

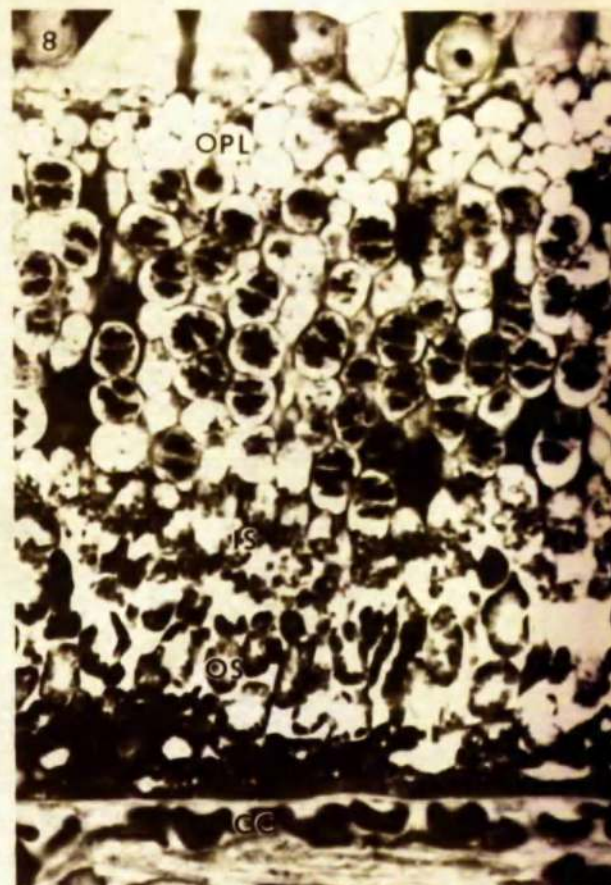
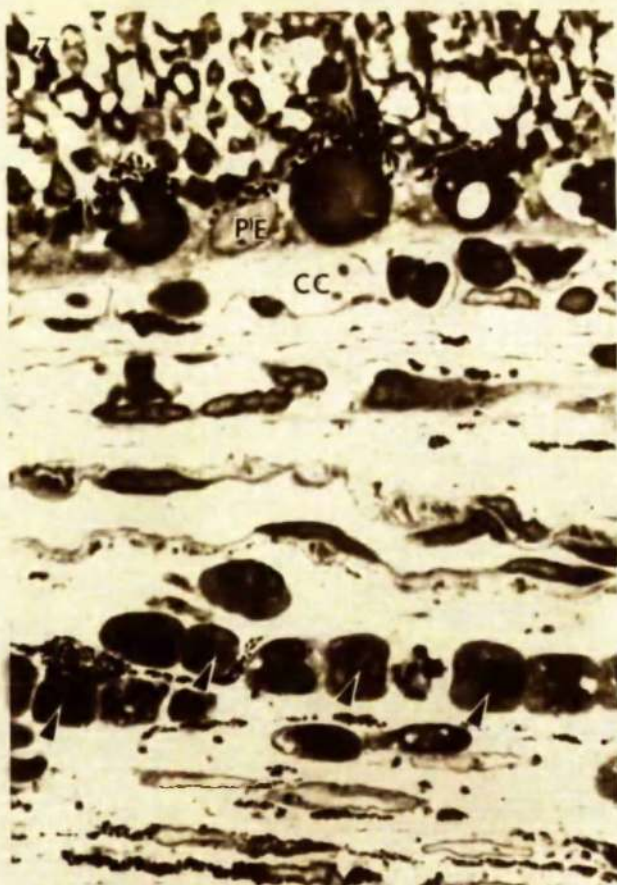


Fig. 4.7

(LD3.2 block B3). Light micrograph showing the presence of inflammatory cells, in one animal only, after exposure to light intensity 3. PE: pigment epithelium; CC: choriocapillaris; Arrows: inflammatory cells (x 1000).

Fig. 4.8

(LD2.1 block A3). Light micrograph showing the outer retina and choriocapillaris, after exposure to light intensity 2. CC: choriocapillaris; OS: outer segments; IS: inner segments; OPL: outer plexiform layer (x 1000).

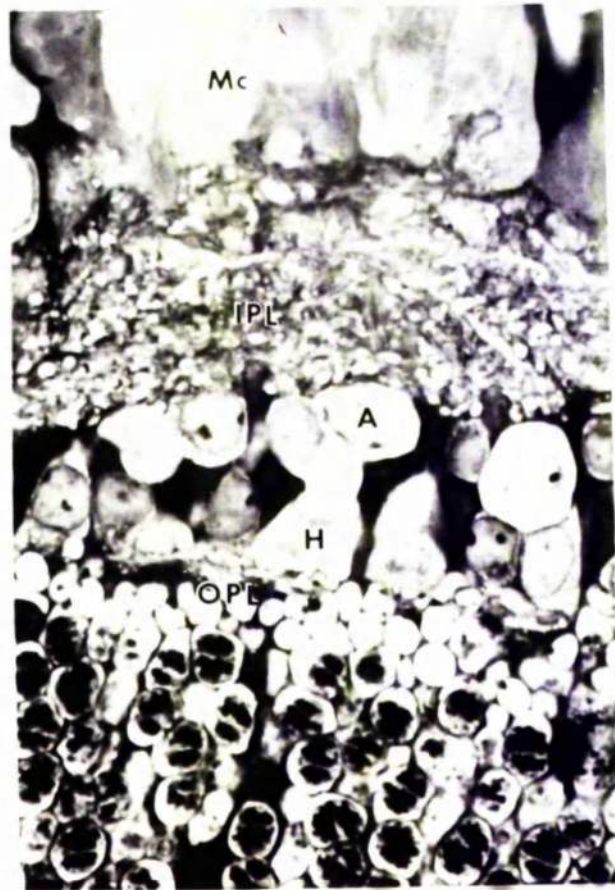


Fig. 4.9

(LD2.1 block A3). Light micrograph showing the inner retina, after exposure to light intensity 2. OPL: outer plexiform layer; H: horizontal cell; A: amacrine cell; IPL: inner plexiform layer; Mc: Müller cell cytoplasm (x 1,000).



Fig. 4.10

(LD2.1 block A3). Light micrograph showing the appearance of the choroid, after exposure to light intensity 2. PE: pigment epithelium; Arrows: platelets filling the choriocapillaris (x 1000).



Fig. 4.11

(LD 2.4 block B3). Light micrograph showing the appearance of the choroid, after exposure to light intensity 2. PE: pigment epithelium; IRC: impacted red cells (x 1,000).

Fig. 4.12

(LD1.1 block C2). Light micrograph showing the appearance of the neural retina, after exposure to light intensity 1. PE: pigment epithelial cell debris; OS: outer segments; IS: inner segments; ONL: outer nuclear layer; INL: inner nuclear layer (x 250).

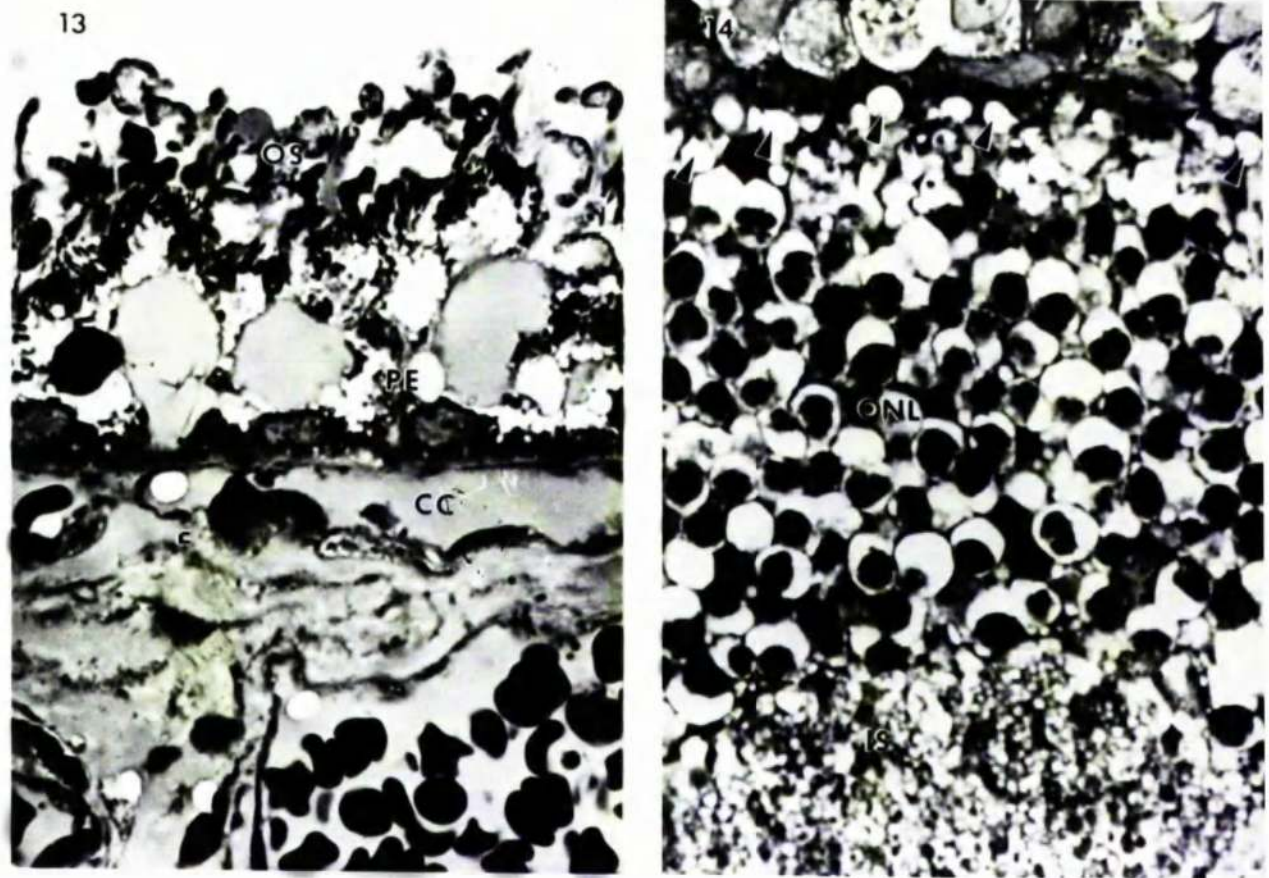


Fig. 4.13

(LD1.1 block C2). Light micrograph showing the appearance of the pigment epithelium and choroid, after exposure to light intensity 1. OS: outer segment material; PE: pigment epithelium; CC: choriocapillaris (x 1,000).

Fig. 4.14

(LD1.1 block C2). Light micrograph showing the appearance of the outer nuclear layer, after exposure to light intensity 1. IS: inner segments; ONL: outer nuclear layer; Arrows: oedematous receptor cell synapses (x 1000).

15



16



Fig. 4.15

(LD1.1 block C2). Light micrograph showing the appearance of the inner retina, after exposure to light intensity 1.

ONL: outer nuclear layer; OPL: outer plexiform layer; A: amacrine cell; M: Müller cell; H: horizontal cell; B: bipolar cell; IPL: inner plexiform layer; G : ganglion cell (x 1000).

Fig. 4.16

(LD1.1 block B1). Light micrograph of the inner retina, after exposure to light intensity 1. One of the macrophage like cells, occasionally present on the inner limiting membrane, can be seen. Arrow: macrophage like cell (x 1,000).



Fig. 4.17

(LD1.4 block B2). Light micrograph showing a region of choroid, after exposure to light intensity 1. CC: choriocapillaris. Arrows: platelets; IRC: impacted red cells (x 1000).

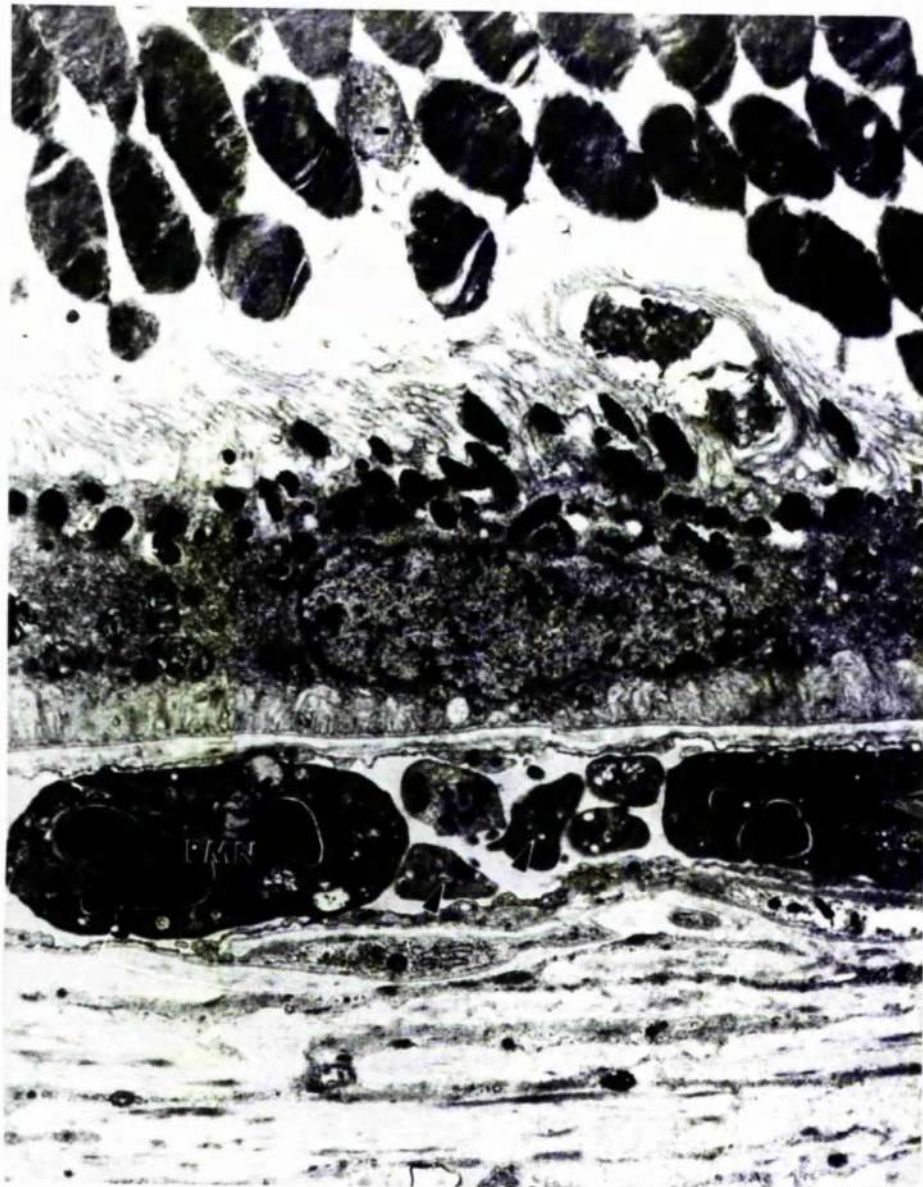


Fig. 4.18

(LD5.2 block B3). Electron micrograph showing the appearance of the pigment epithelium and choriocapillaris, after exposure to light intensity 5. A few degranulating platelets and inflammatory cells are present. PMN: polymorphonuclear leucocytes; Arrows: platelets (x 6,400).

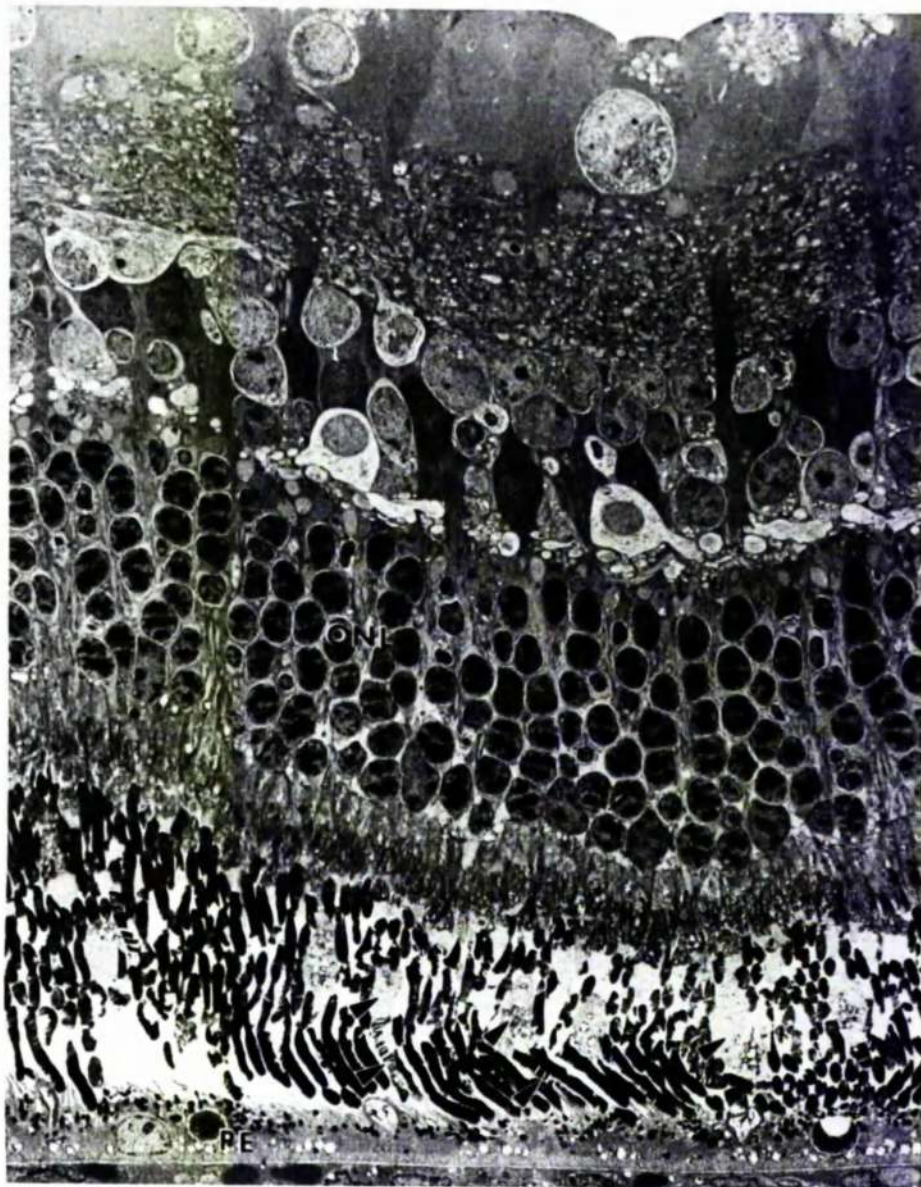


Fig. 4.19

(LD4.4 block B2). Low magnification electron micrograph of the retina, after exposure to light intensity 4. PE: pigment epithelium; Arrows: cone inner and outer segments; ONL: outer nuclear layer (x 900).



Fig. 4.20

(LD4.4 block B2). Electron micrograph showing the appearance of a disrupted pigment epithelial cell, after exposure to light intensity 4 ($\times 2,400$).

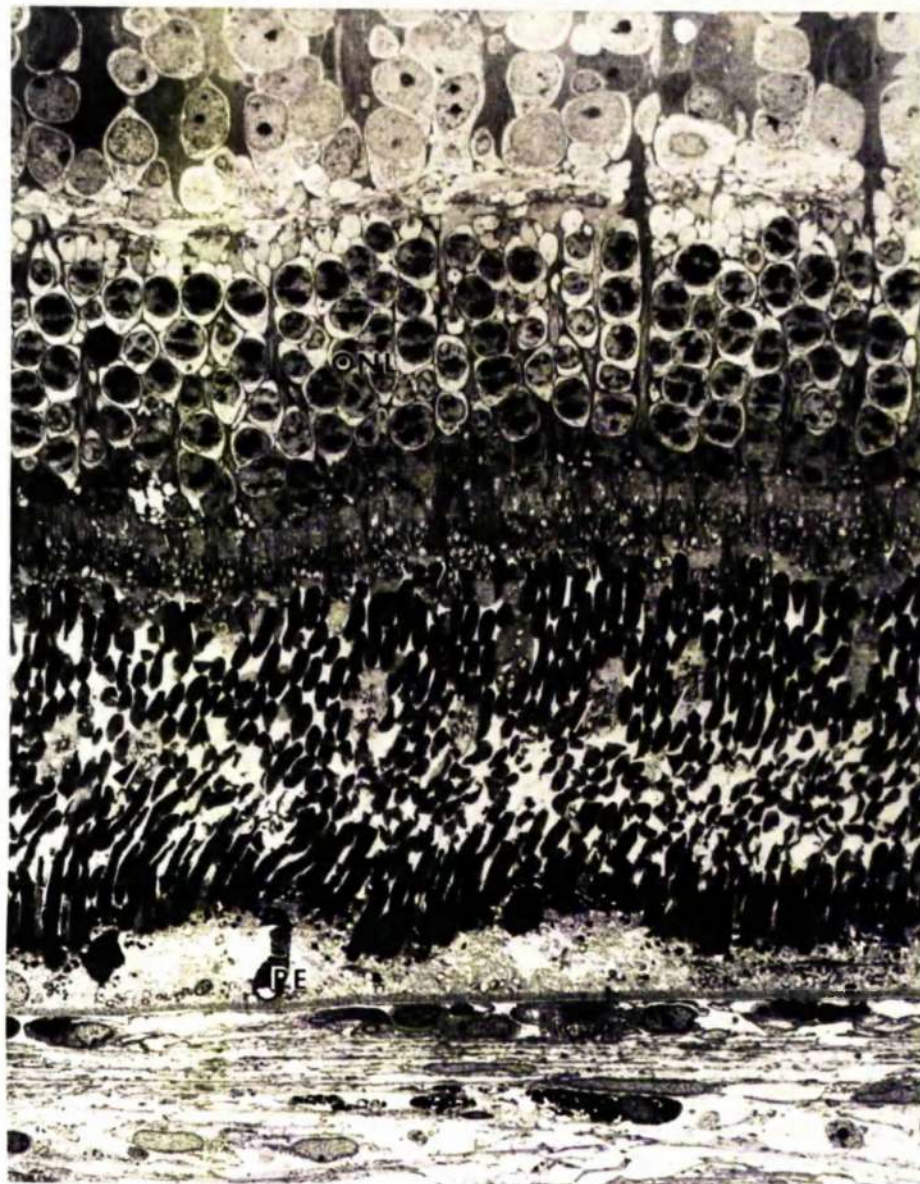


Fig. 4.21

(LD33 block A2). Electron micrograph showing the appearance of the outer retina, after exposure to light intensity 3. PE: pigment epithelium; Arrows: cone inner segments; ONL: outer nuclear layer (x 1,000).



Fig. 4.22

(LD3.3 block A2). Electron micrograph showing the appearance of the pigment epithelium, after exposure to light intensity 3. N: nucleus; Mt: mitochondrion; SER: smooth endoplasmic reticulum; BI: basal infoldings (x 7,000).



Fig. 4.23 a and b

(both LD3.3 block C2) Electron micrographs showing the variability in the appearance of the pigment epithelium, after exposure to light intensity 3. Ph: phagosomes; N: nucleus; Ev: electron-lucent vesicles; Mt: mitochondrion; Bl: basal infoldings (both x 3,600).

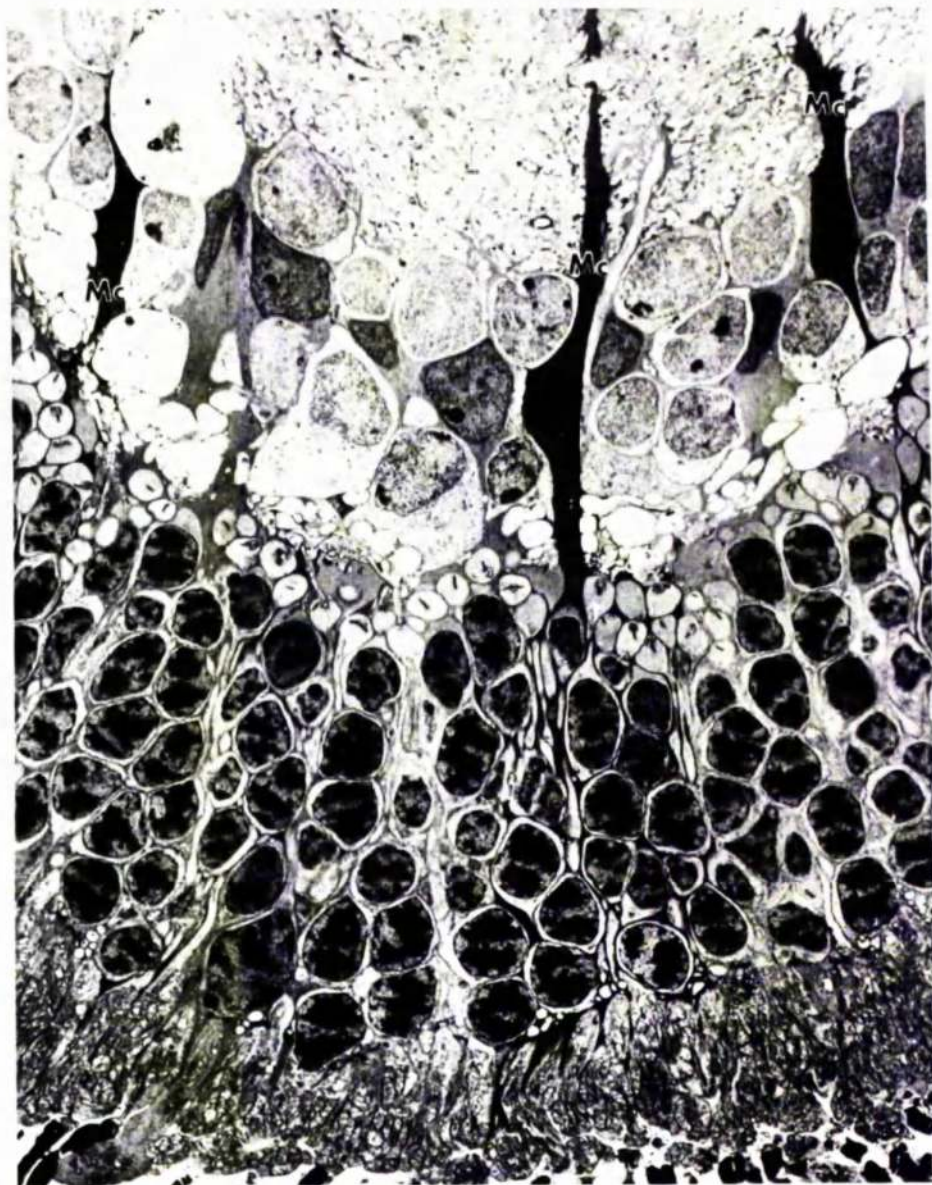


Fig. 4.24

(LD 3.3 block A1). Electron micrograph showing the appearance of the inner retina, after exposure to light intensity 3. Some of the Müller cells are densely stained demonstrating their extensive cytoplasm. Mc: Müller cell cytoplasm (x 1600).



Fig. 4.25

(LD3.2 block B3) Electron micrograph of the outer retina and choroid, after exposure to light intensity 3. ONL: outer nuclear layer; IS: inner segments; OS: outer segments; PE: pigment epithelium; Ma: macrophage; PMN: polymorphonuclear leucocyte (x 1,450).

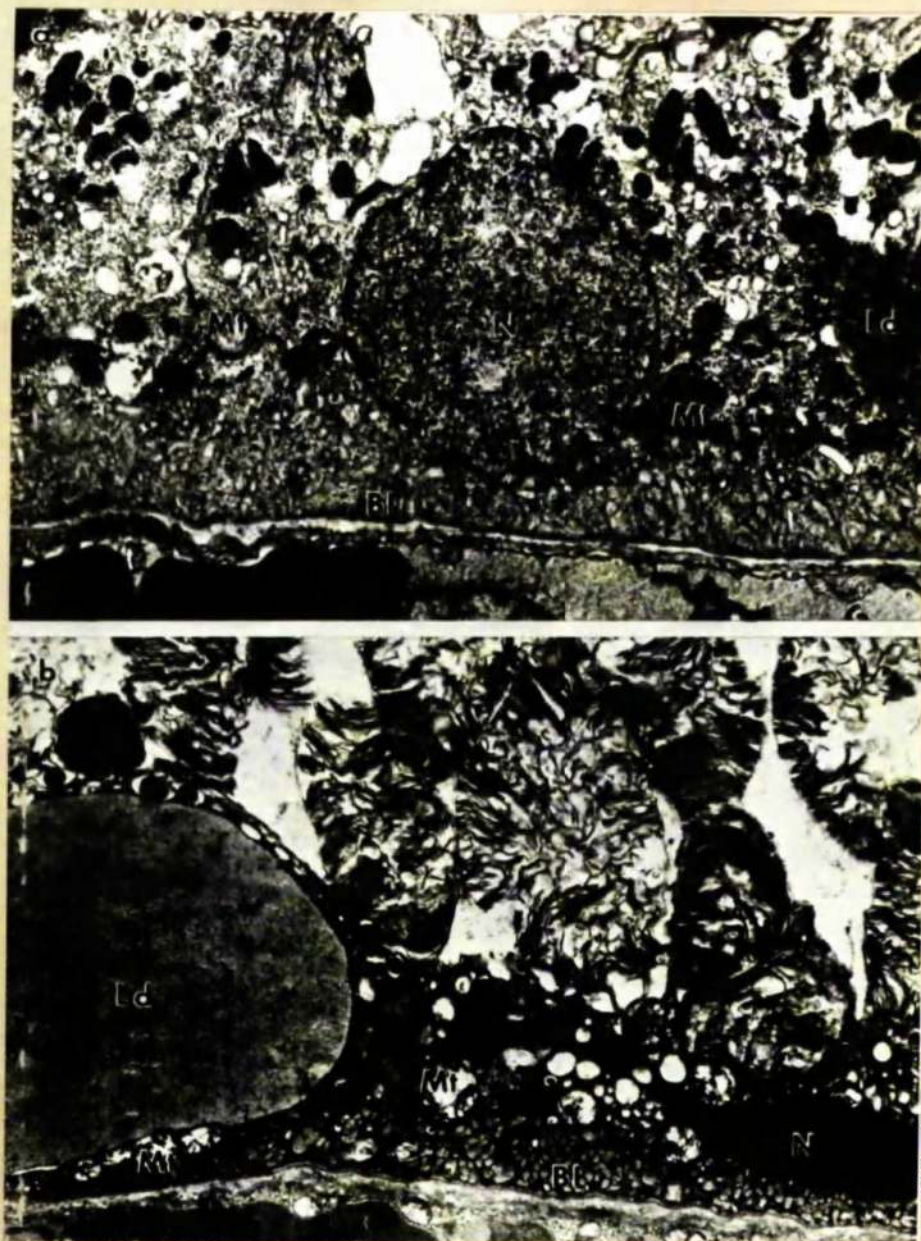


Fig. 4.26 a and b

(a. LD24 block B4. b. LD21 block A3). Electron micrographs showing the variability in the appearance of the pigment epithelium, after exposure to light intensity 2. N: nucleus; Mt: mitochondrion; Ld: lipid droplet; Bl: basal infoldings (both x 6,000).

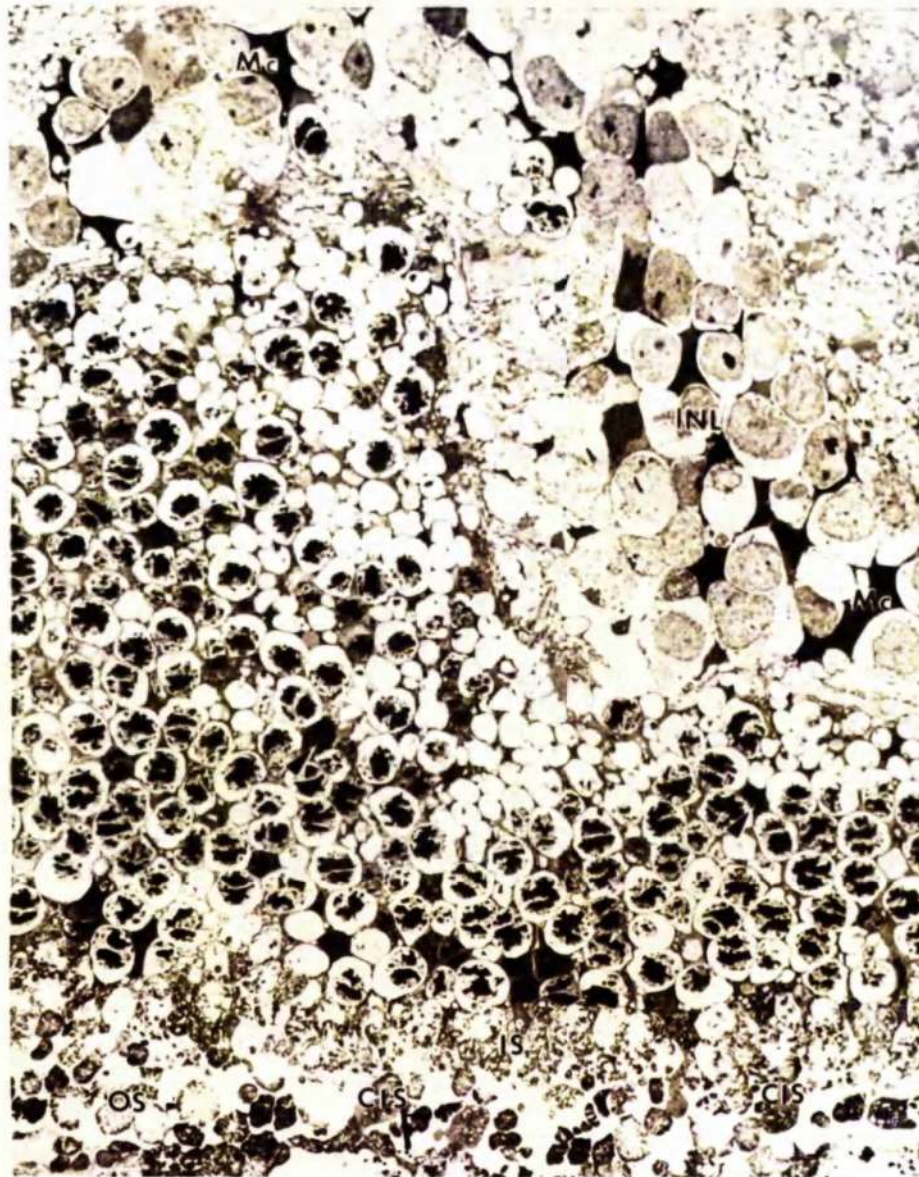


Fig. 4.27

(LD2.1 block A3). Electron micrograph showing the appearance of the neural retina, after exposure to light intensity 2. OS: outer segment material; CIS: cone inner segment; IS: inner segments; Arrows: pyknotic receptor cell nuclei; Mc: Müller cell cytoplasm; INL: inner nuclear layer (x 1,000).

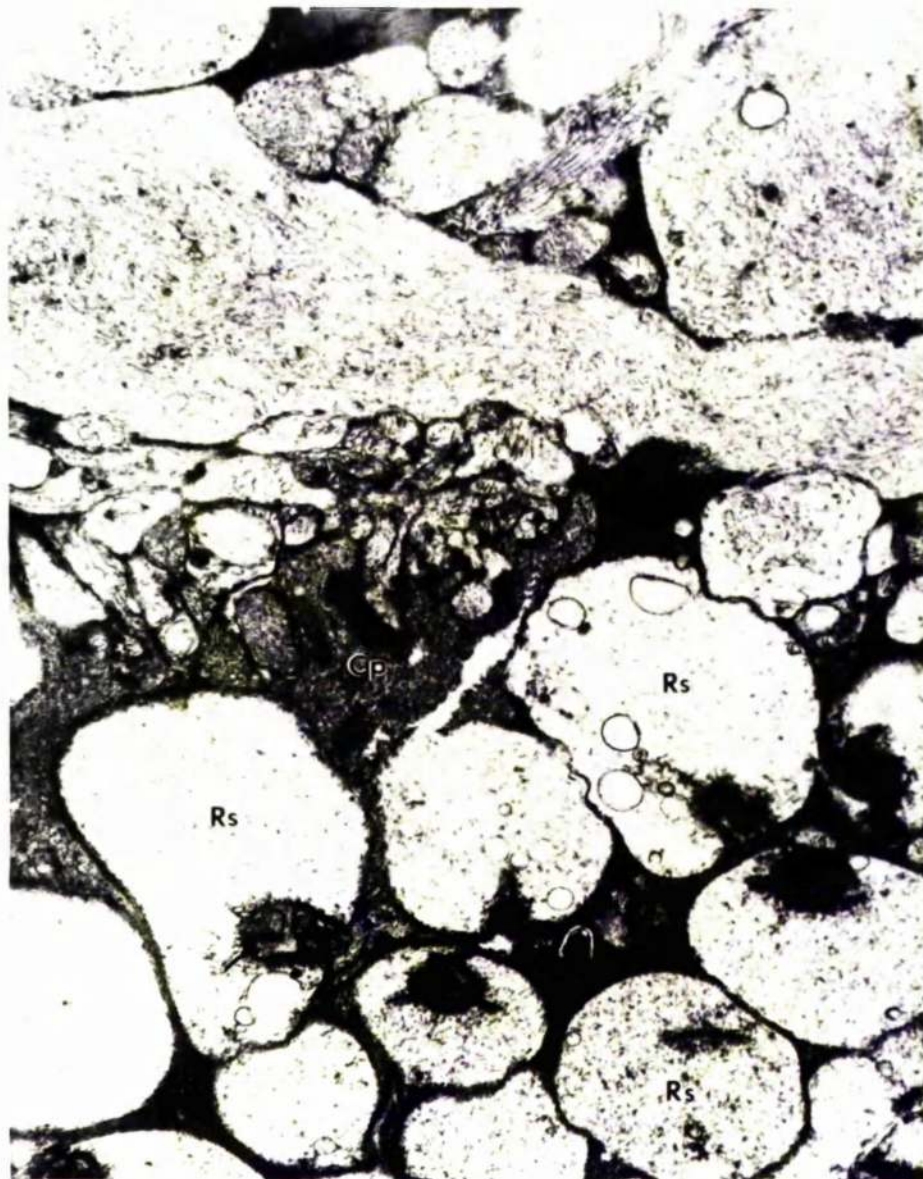


Fig. 4.28

(LD2.1 block A3). Electron micrograph showing the appearance of the outer plexiform layer, after exposure to light intensity 2. Cp: cone pedicle; Rs: rod spherule ($\times 10,500$).

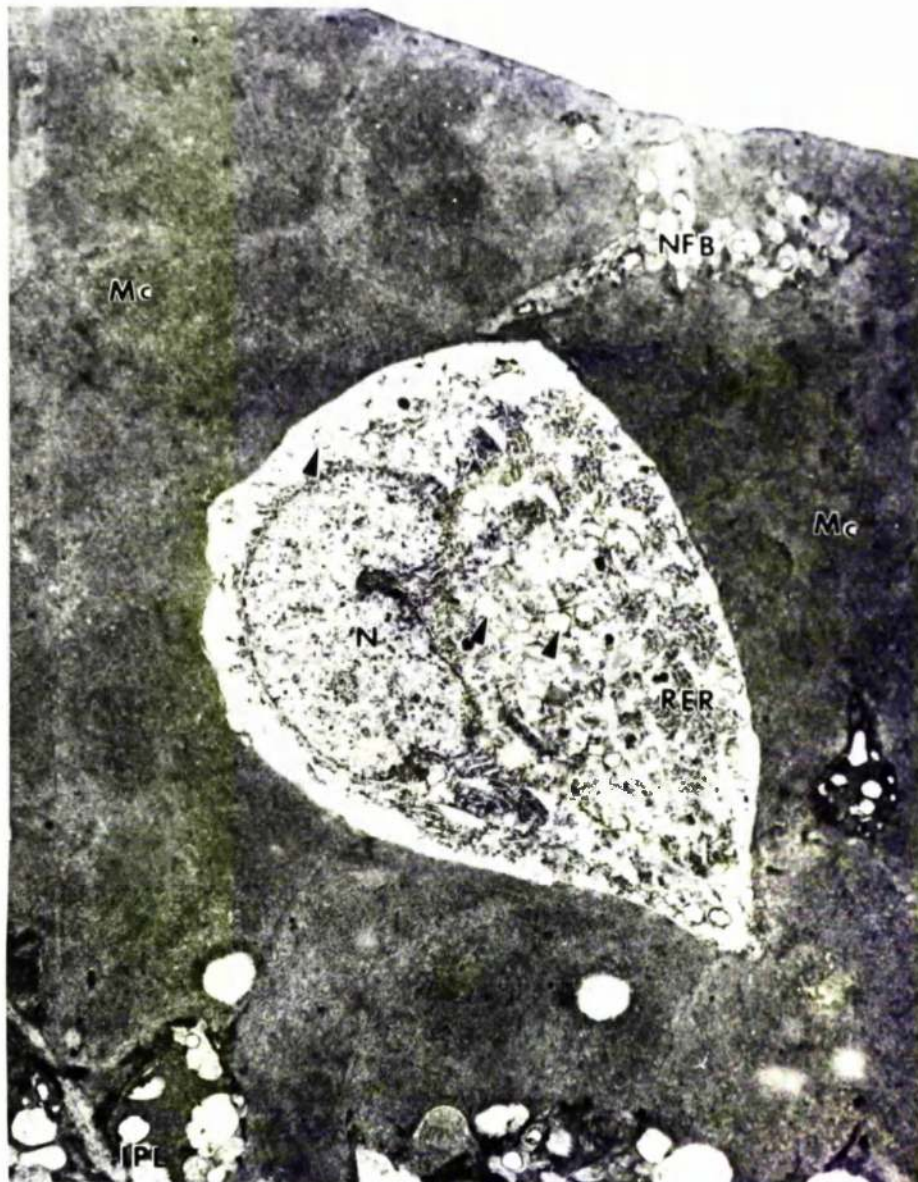


Fig. 4.29

(LD2.4 block B4). Electron micrograph showing the appearance of a ganglion cell, after exposure to light intensity 2. N: nucleus; Arrows: distended mitochondria; RER: rough endoplasmic reticulum; NFB: nerve fibre bundle; Mc: Müller cell cytoplasm; IPL: inner plexiform layer (x 3,300).



Fig. 4.30

(LD2.1 block A3). Electron micrograph showing the presence of degranulating platelets in the choriocapillaris, after exposure to light intensity 2. Arrows: platelets; PE: pigment epithelium; CC: choriocapillaris (x 1,700).



Fig. 4.31

(LD11 block C2). Electron micrograph showing the appearance of the choroid, after exposure to light intensity 1. There are degranulating platelets in the choriocapillaris and deeper vessels. Blood borne inflammatory cells are evident in the large vessel. PE: pigment epithelium; BM: Bruch's membrane; Arrows: platelets; PMN: polymorphonuclear leucocytes; Mo: monocytes; L: possibly a lymphocyte (x 2,100).



Fig. 4.32

(LD 1.1 block C2). Electron micrograph showing the appearance of the outer retina and choriocapillaris, after exposure to light intensity 1. IS: inner segments; OS: outer segments; AS: apical surface of the pigment epithelium; N: pigment epithelium nucleus; V: vacuoles of flocculate material; BM: Bruch's membrane; CC: choriocapillaris (x 1,800).



Fig. 4.33

(LD11 block C2). Electron micrograph showing the appearance of the apical surface of the pigment epithelium, after exposure to light intensity 1. Ap: apical processes; OS: outer segment material; Mg: melanin granule (x11,000).

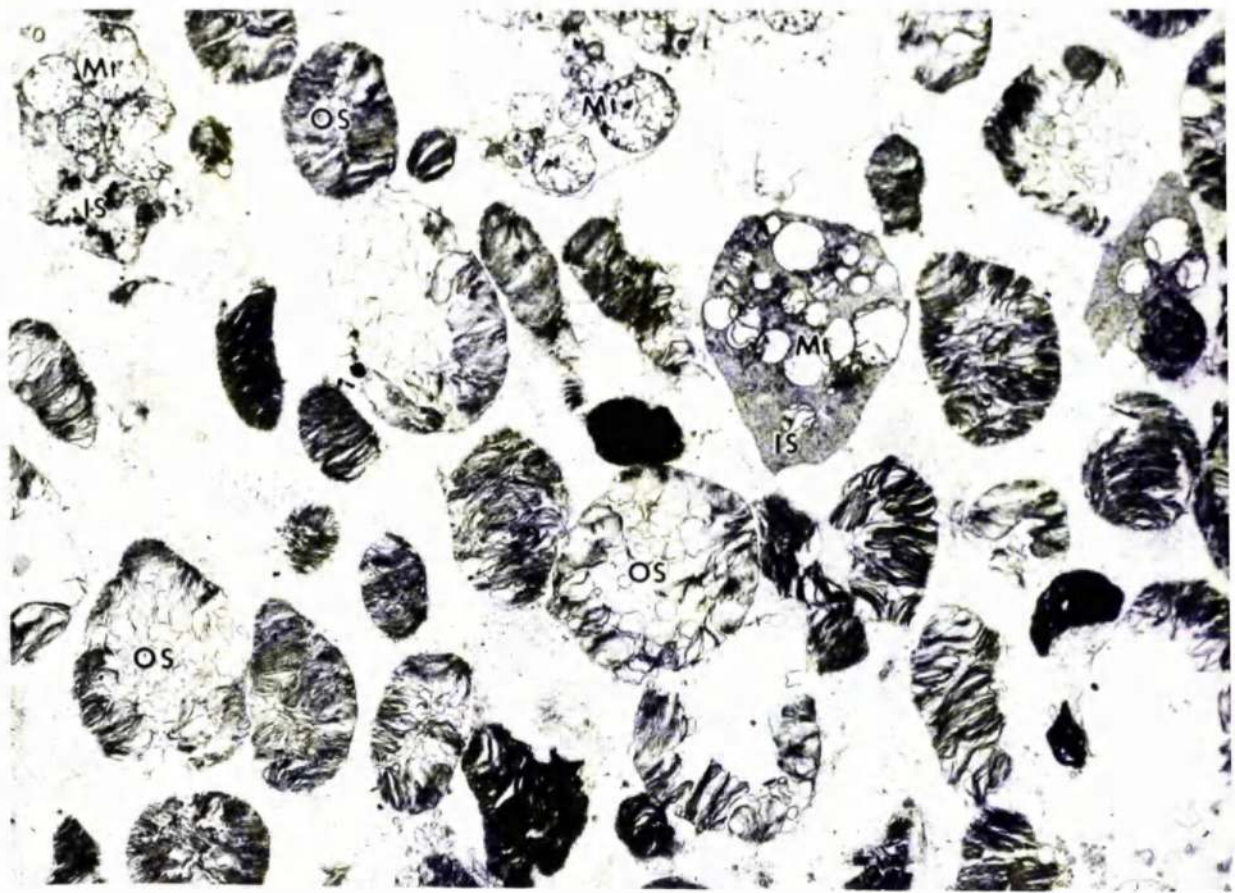


Fig. 4.34

(LD11 block C2). Electron micrograph showing the appearance of the photoreceptor debris in the subretinal space, after exposure to light intensity 1. OS: outer segment material; IS: inner segment; Mt: mitochondria (x 5,100).

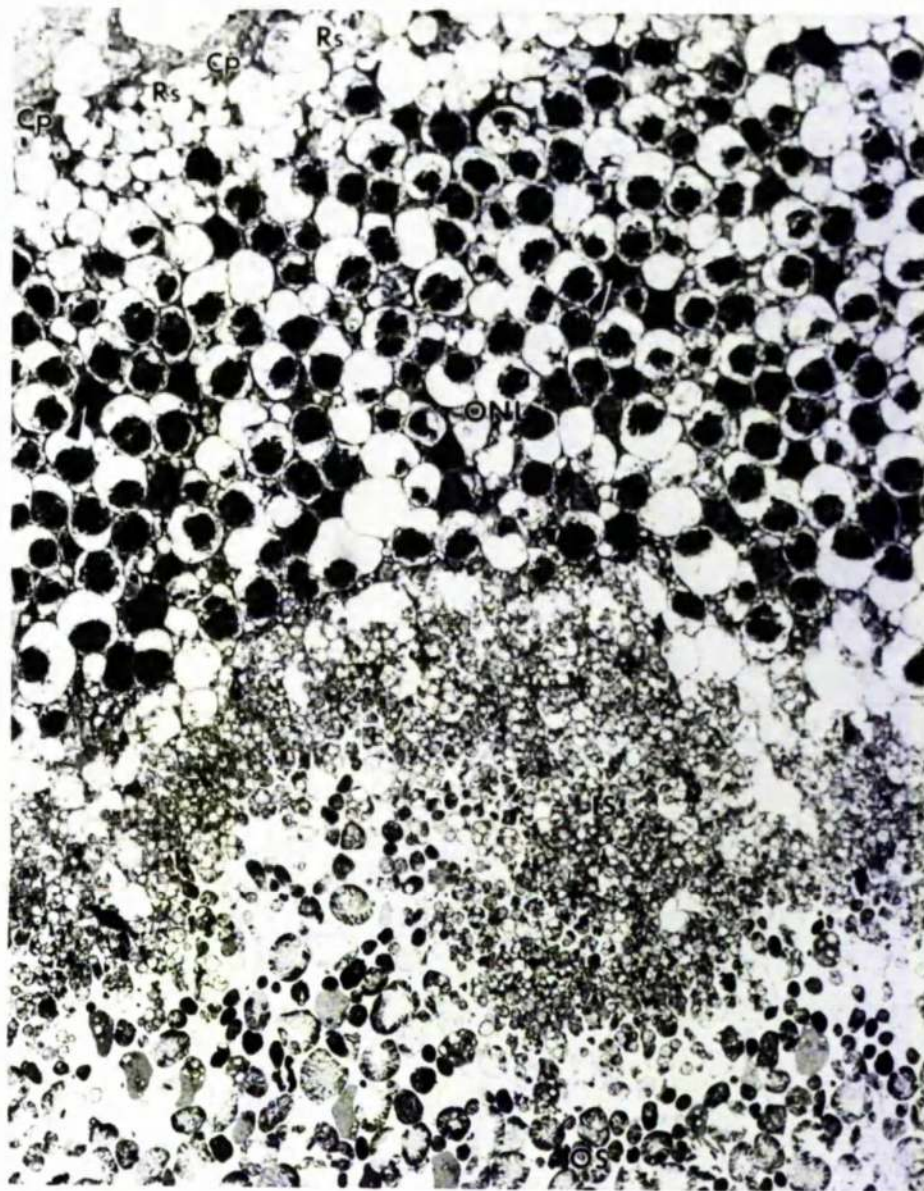


Fig. 4.35

(LD11 block C2). Electron micrograph showing the appearance of the receptor cells, after exposure to light intensity 1. OS: outer segment material; IS: inner segments; ONL: outer nuclear layer; Arrows: pyknotic nuclei; Rs: rod spherule ; Cp: cone pedicle (x 1,100).

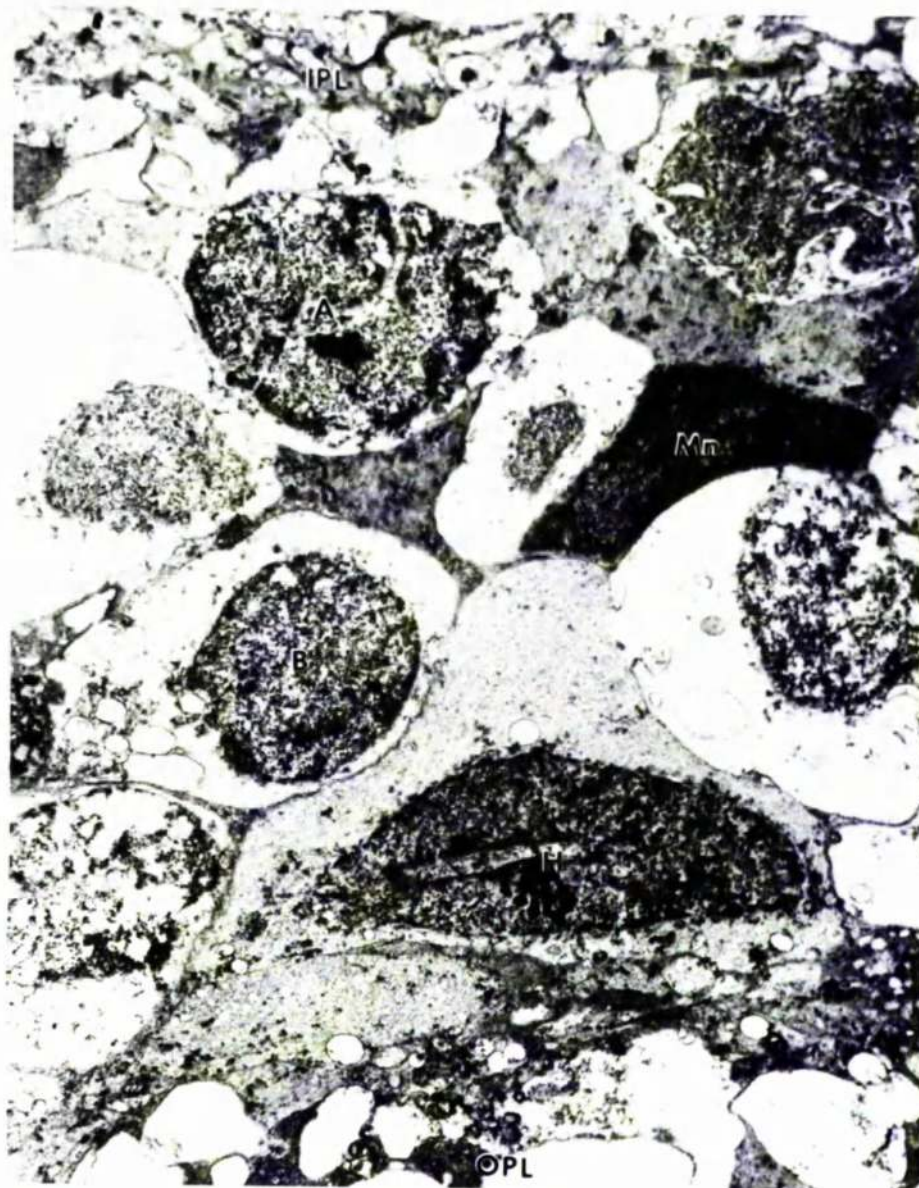


Fig. 4.36

(LD1.1 block C2). Electron micrograph showing the appearance of the inner nuclear layer, after exposure to light intensity 1. OPL: outer plexiform layer; H: horizontal cell; B: bipolar cell; Mn: Müller cell nucleus; A: amacrine cell; IPL: inner plexiform layer (x 4,900).



Fig. 4.37

(LD1.1 block C2). Electron micrograph showing the appearance of the inner retina, after exposure to light intensity 1. The Müller cell cytoplasm contains numerous electron-lucent vesicles, and small electron-dense granules. Mc: Müller cell cytoplasm; Ev: electron-lucent vesicles; Arrows: electron dense granules; G : ganglion cell; IPL: inner plexiform layer (x 3,700).

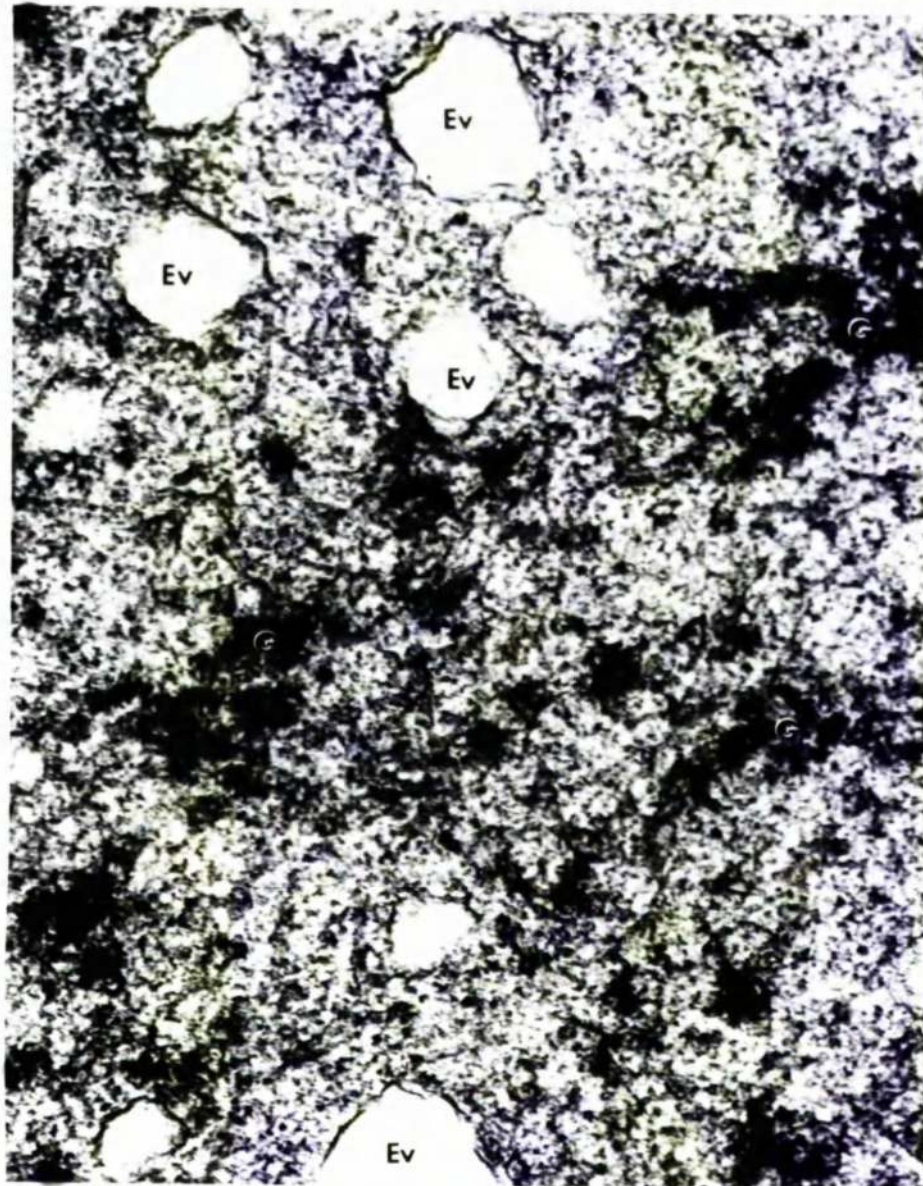


Fig. 4.38

(LD1.1 block C2). Higher magnification electron micrograph of the Müller cell cytoplasm shown in figure 4.37. G: electron-dense granules; Ev: electron-lucent vesicles, possibly distended tubules of smooth endoplasmic reticulum (x 66,000).



Fig. 4.39

(LD1.1 block C2) . Electron micrograph showing the appearance of the choriocapillaris and choroidal stroma, after exposure to light intensity 1. CC: choriocapillaris; Ec: endothelial cell; Arrows: endothelial cell blebs; F: fibroblast (x 3,800).

QUALITATIVE ASSESSMENT OF "WORST CASE" DAMAGE
TO VARIOUS RETINAL COMPONENTS

Degree of Damage		P.E. Pigment Epithelium					C.P. Cone Pedicles				
○	Normal	R.O.S. Rod Outer Segments					H.B.A. Horizontal Bipolar Amacrine Cells				
+	Slight	R.I.S. Rod Inner Segments					I.P.L. Inner Plexiform Layer				
++	Moderate	R.S. Rod Somata					G.C. Ganglion Cells				
+++	Severe	R.Sp. Rod Spherules					M.C. Müller Cells				
++++	Very Severe	C.O.S. Cone Outer Segments					C.I.S. Cone Inner Segments				

GROUP NO.		P.E.	R.O.S.	R.I.S.	R.S.	R.Sp.	C.O.S.	C.I.S.	C.S.	C.P.	H.B.A.	I.P.L.	G.C.	M.C.
	6	○	○	○	○	○	○	○	○	○	○	○	○	○
	5	○	○	○	○	○	○	○	○	○	○	○	○	○
	4	+	+	+	○	○	++	++	○	○	○	○	○	○
	3	++	++	++	++	+	+++	+++	+	○	○	○	○	+
	2	+++	+++	+++	+++	++	+++	+++	+++	+	+	+	+	+
	1	++++	++++	++++	++++	+++	++++	++++	++++	++	+++	++	++	++

Fig. 4.40

Table giving a qualitative assessment of the worst damage seen within any group.

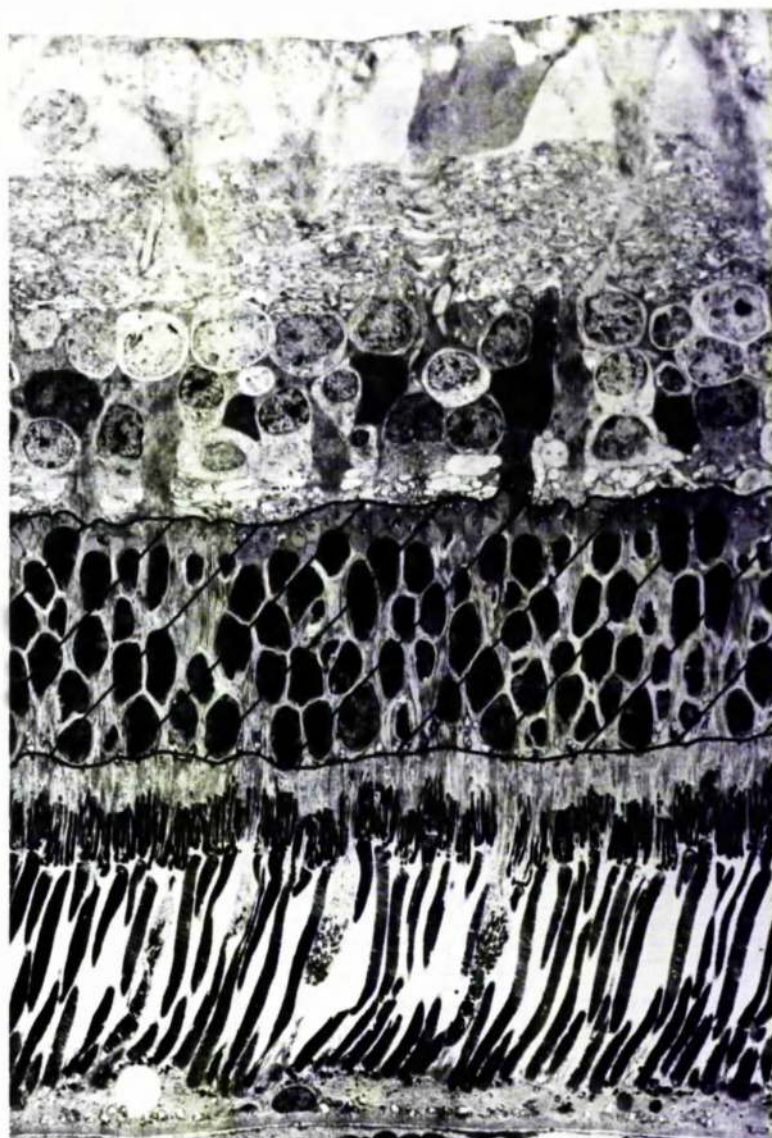
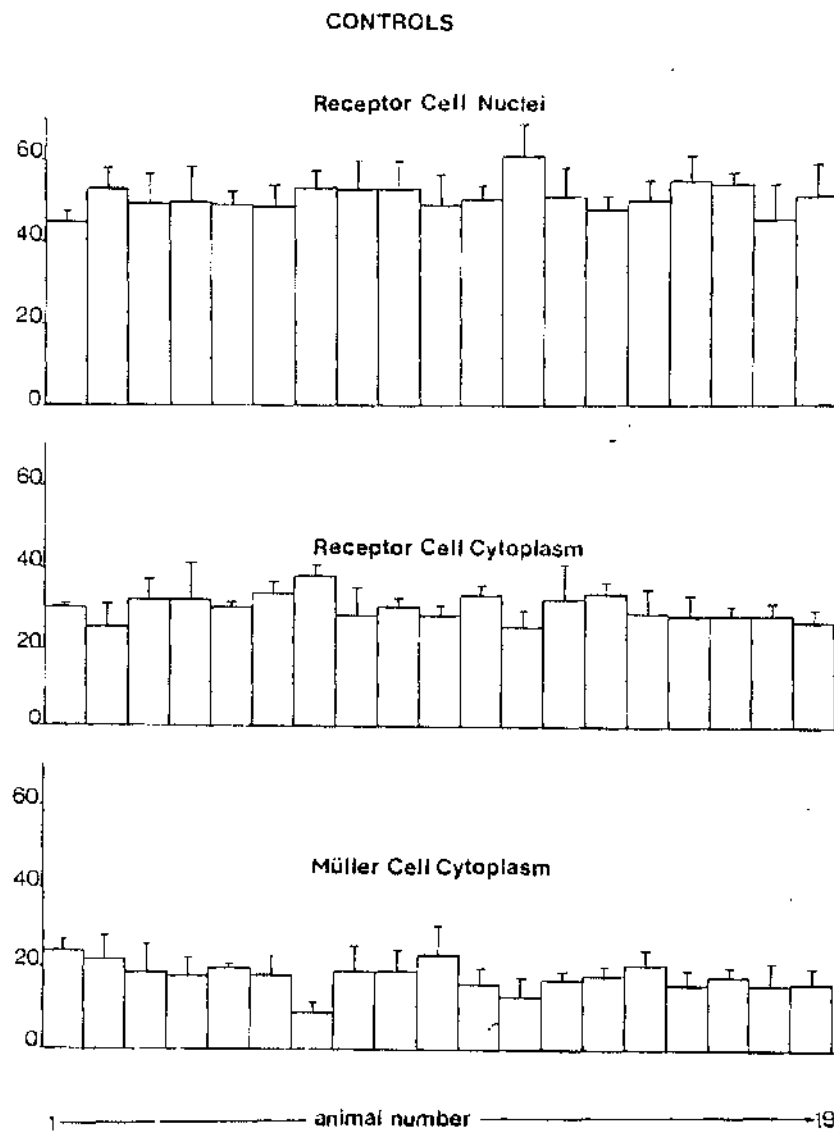


Fig. 4.41

Electron micrograph showing the area defined as the outer nuclear layer for the purposes of quantification.



COMBINED CONTROL RESULTS

	RCN	RCC	MCC
\bar{x}	51.1	31.0	17.7
SD	6.4	5.5	5.6

Fig. 4.42

Figure showing the results obtained, by the point counting method, within the control tissue.

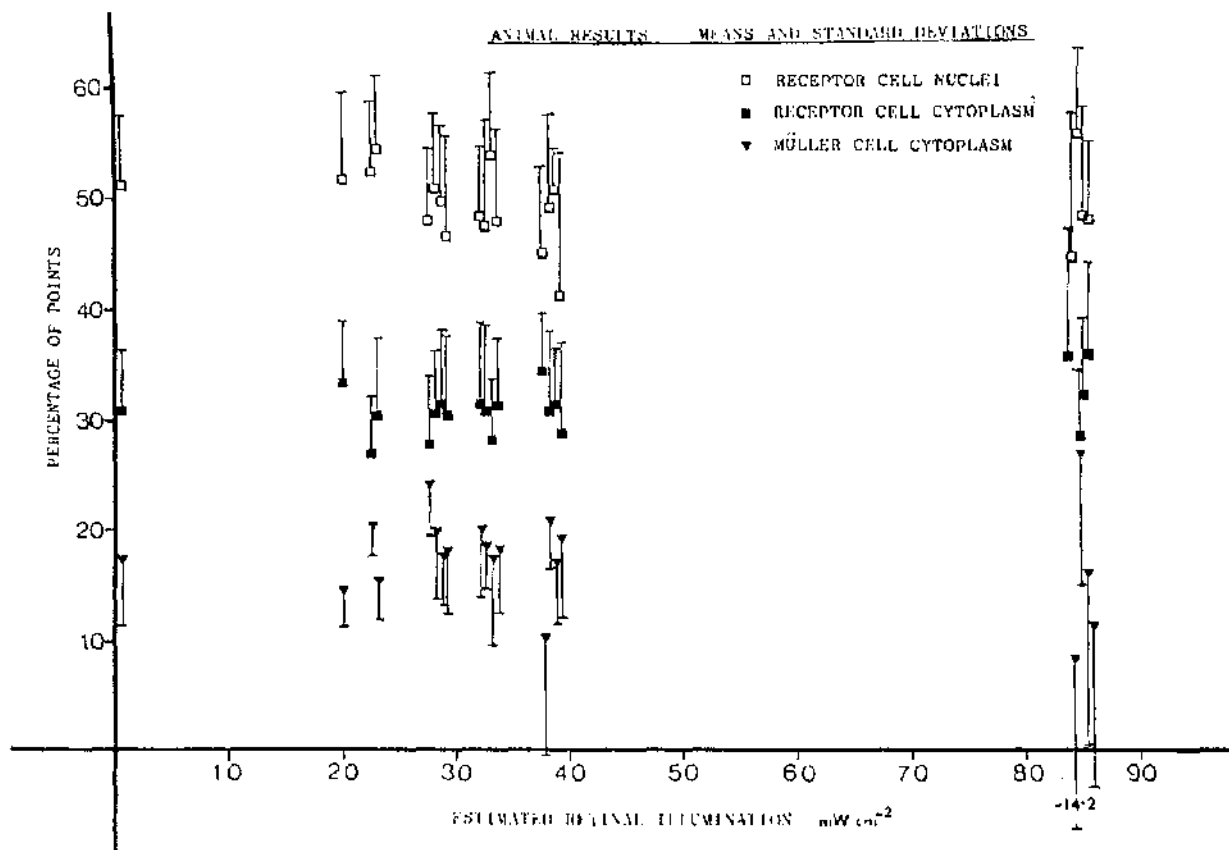


Fig. 4.43

Figure showing the experimental results for the three features assessed within the outer nuclear layer. The percentage of points landing on each feature of interest, in each animal, are plotted against the estimated retinal illumination. The control results are shown on the y axis.

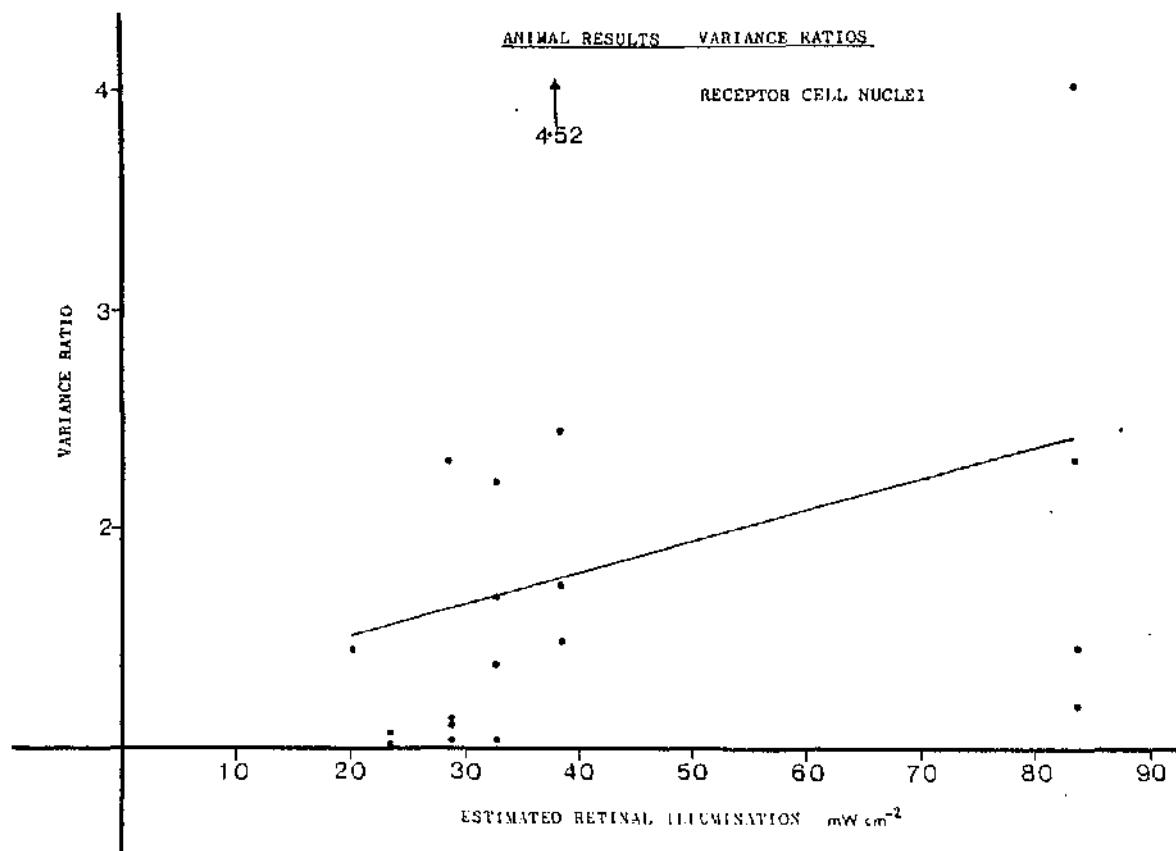


Fig. 4.44

Graph of the F ratios of the animal results for receptor cell nuclei plotted against estimated retinal illumination. The line fitted by linear least square regression is not significant at the 5% level.

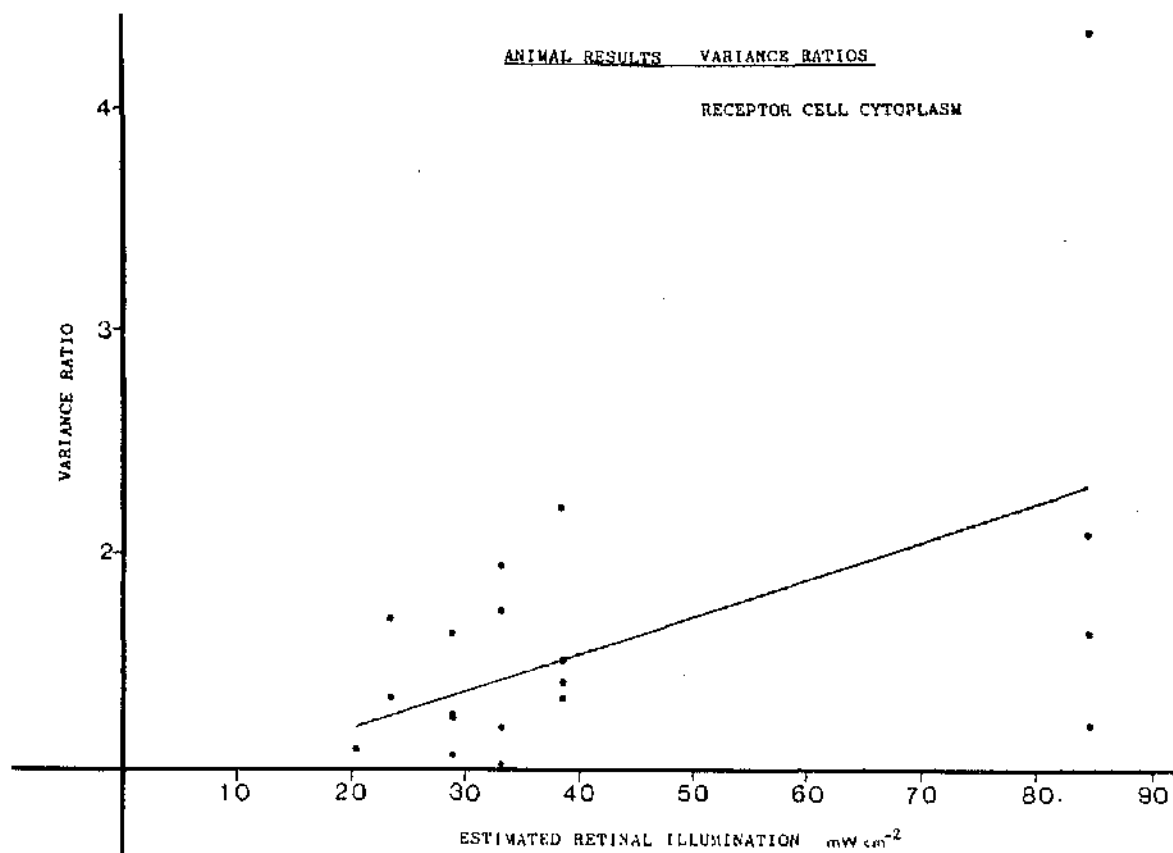


Fig. 4.45

Graph of the F ratios of the animal results for receptor cell cytoplasm plotted against estimated retinal illumination. The line fitted by linear least square regression is significant ($0.05 > P > 0.01$).

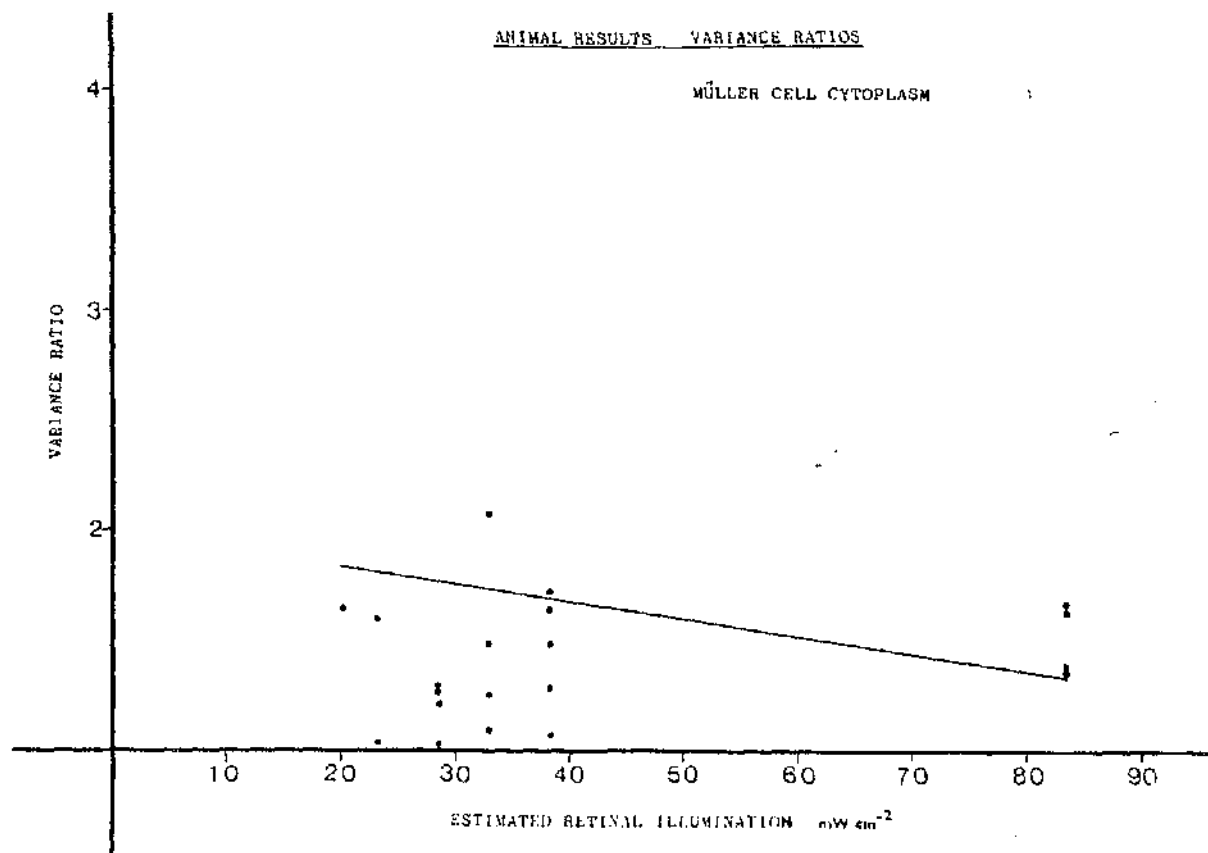


Fig. 4.46

Graph of the F ratios of the animal results for Müller cell cytoplasm plotted against estimated retinal illumination. The line fitted by linear least square regression is not significant at the 5% level.

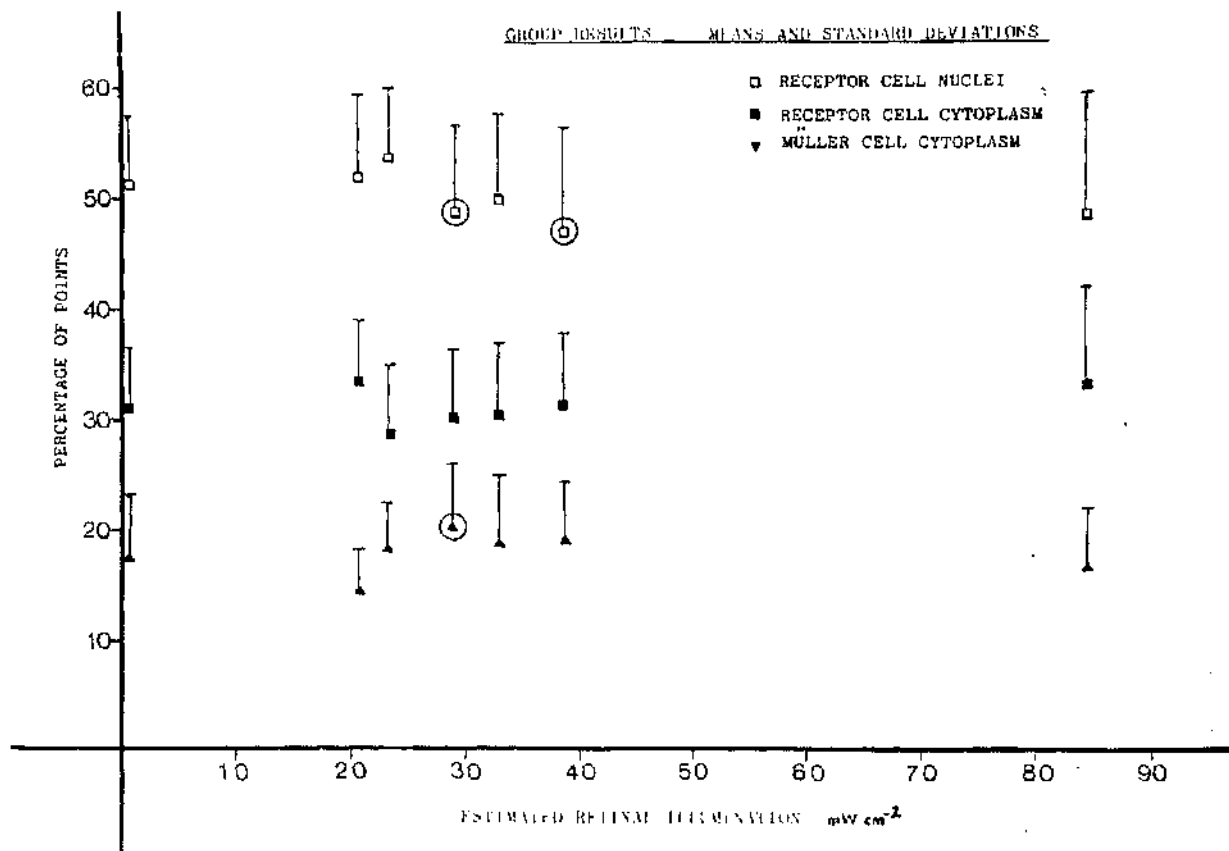


Fig. 4.47

Figure showing the experimental results for the three features assessed within the outer nuclear layer. The percentage of points landing on each feature of interest, in each group (all the animals at one intensity), are plotted against the estimated retinal illumination. The control results are shown on the y axis. Experimental results significantly different ($P < 0.05$) from the control results, using the Student t test, are circled.

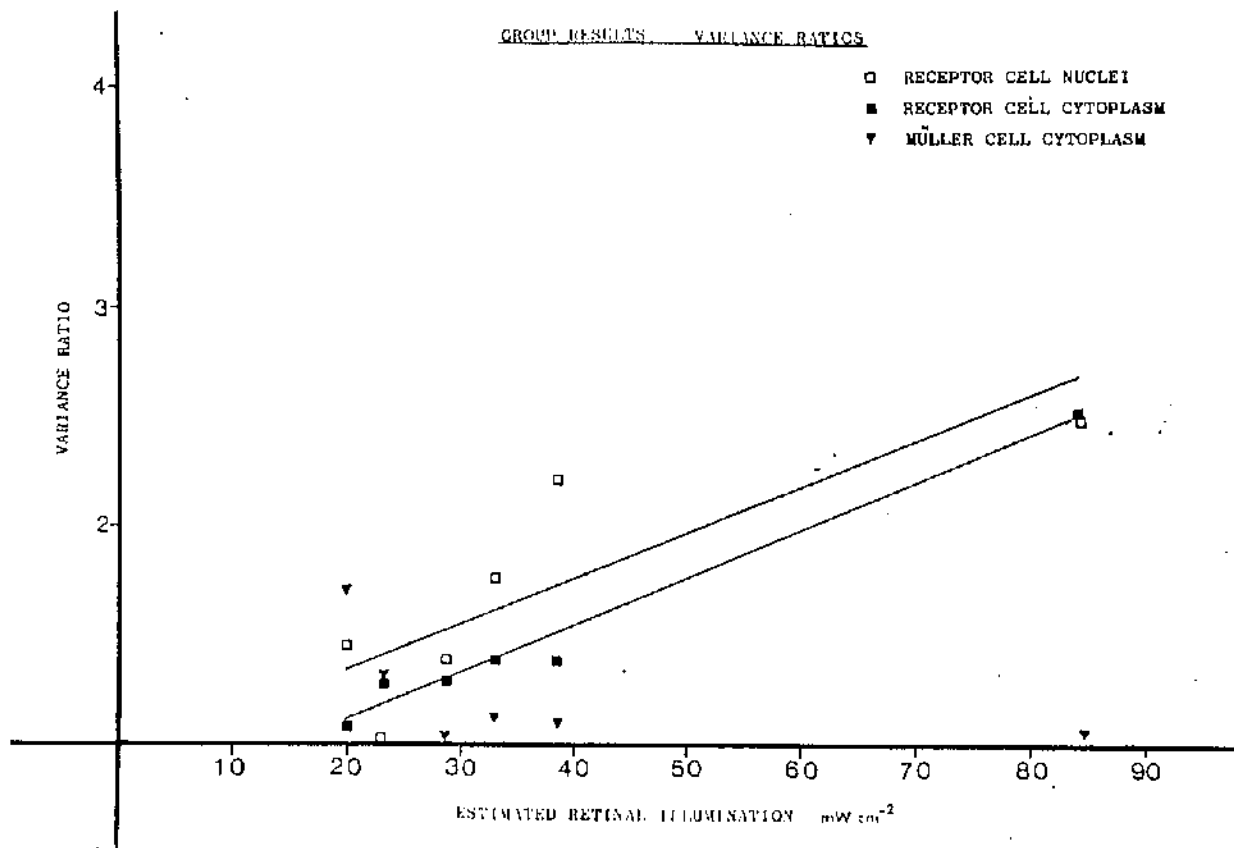


Fig. 4.48

Graphs of the F ratios of the group results for receptor cell nuclei, receptor cell cytoplasm and Müller cell cytoplasm plotted against the estimated retinal illumination. The straight lines fitted by linear least square regression, to the results for receptor cell nuclei and receptor cell cytoplasm are significant at the 5% level.

Receptor cell nuclei $0.05 > P > 0.01$. Receptor cell cytoplasm $P < 0.001$.

CHAPTER 5

RECOVERY OF THE RABBIT RETINA AND CHOROID FOLLOWING LIGHT DAMAGE

This chapter describes, by light and electron microscopy, the appearance of the retina and choroid following one hour exposures to light. The retinal and choroidal tissues were examined at various time intervals, up to 4 weeks, after the experimental exposure.

The previous chapter described the effects, on the retina and choroid, of one hour exposures to various intensities of white light. The two highest light intensities were selected for further investigation as they were already known to cause extensive damage to the photoreceptors and the pigment epithelium.

The aim of this investigation was to study the appearance of the retina and choroid, at various times after the photic insult, to determine the fate of the cellular debris, and the degree of recovery or repair which took place. The materials and methods are described in Chapter 2, Section 4. The details for each animal are given in Appendix 1.

Twenty eight animals were used. Fourteen animals were exposed to each light intensity for one hour. The estimated retinal illumination in the lower intensity group was 38.6mWcm^{-2} and 84.4mWcm^{-2} in the higher intensity group. They were allowed to recover for periods of 6 hours, 24 hours, 4 days, 1 week, 2 weeks or 4 weeks. After the appropriate recovery period the animals were killed. Retinal and choroidal tissues were then taken and examined by light and electron microscopy.

5.2 Recovery of the Rabbit Retina and Choroid Following Light Damage; Light Microscopy; Low Intensity Group.

As in the previous chapter considerable variation was seen between the tissue blocks examined. In some of the animals in the lower intensity group (animals 2/24h/2, 2/48h/1, 2/48h/2, 2/2W/1 and 2/4W/1) it was possible to determine which blocks

were taken from damaged regions. Damaged areas showed a whitish discolouration of the retina. These were often surrounded by areas of irregular pigmentation. After the longer recovery periods depressions were often noted in the inner surface of the retina. On examination by light microscopy these regions were found to be areas which had suffered a pronounced loss of retinal components. Figures 5.1, 5.2, 5.3 and 5.4 show the relation of damaged areas to the position of the blocks taken.

In the description of the retinal and choroidal tissues by light microscopy the lower intensity group (estimated retinal illumination 38.6mWcm^{-2}) will be described first.

5.2.1 Group 2; 6 Hours Recovery (2 animals).

No lesion of the retina was seen in either animal during dissection. Eight blocks from animal 2/6h/1 were examined by light microscopy. These were A2, A4, B3, C1, C2, C4, D3 and D4. Three of these blocks A2, B3 and C1 were of normal appearance. Blocks A4, C2, C4, D3 and D4 were of atypical appearance as they showed alterations of the outer retina and in two cases, D3 and D4, slight abnormalities in the appearance of the inner retina. The nuclei of the pigment epithelium were unusually rounded and the basal cytoplasm of the cells contained numerous unstained vesicles, which were probably swollen mitochondria (Fig. 5.5 and 5.6). In the damaged tissue the photoreceptor outer segments were disordered and irregular in appearance. The photoreceptor nuclei were of normal appearance. The receptor cell cytoplasm in the outer nuclear layer and the receptor cell synaptic regions did appear to be more lightly stained than normal. Occasionally, some of the cells of the inner nuclear layer were also unusually light in their staining. Cells with this lightly stained cytoplasm were identified as horizontal cells or, less often, as amacrine cells (Fig. 5.5).

In general, the appearance of the choroid was unremarkable. Blocks D3 and D4 (animal 2/6h/1) were exceptions however. These blocks showed the most extensive retinal damage seen in this group. The choriocapillaris and the deeper vessels of the choroid, adjacent to the damaged retina, appeared to be congested with red blood cells (Fig. 5.6).

5.2.2 Group 2; 24 Hours Recovery (2 animals).

On dissection of the retinal and choroidal tissues of animal 2/24h/2, a faint white mottled appearance was seen in row A (Fig. 5.1). No abnormalities of this tissue were detected by light microscopy. The light exposed retina of animal 2/24h/1 appeared normal and attached during dissection. However, all the blocks examined from animal 2/24h/1 showed some abnormalities of the receptor cells and pigment epithelium. Blocks A1, B1, and D1 all showed similar changes. The pigment epithelium appeared swollen and had lightly stained cytoplasm. The cytoplasm contained numerous small vesicles which were probably distended mitochondria. The nuclei of these pigment epithelial cells were rounded and showed marginal chromatin staining. They frequently contained a prominent nucleolus. The receptor cell outer segments showed slight disorganisation (Fig. 5.7). The majority of the receptor cell nuclei were usually normal in appearance although pyknotic nuclei were identified. The remainder of the retinal and choroidal tissues were of normal appearance.

A slightly different pattern of damage was seen in the region of the visual streak in block C1. The pigment epithelium was of two distinct appearances. In some instances intracellular swelling was severe, leaving rounded nuclei visible within clear cytoplasm (Fig. 5.8). In others, even in adjacent

cells, there was loss of cell volume and a marked increase in the density of staining. Cells with these appearances have already been described in Chapter 4 (see figures 4.2, 4.8, 4.20, 4.23 and 4.26). The receptor cells were virtually normal throughout their length, although there may have been slight disturbances of the outer segments. Some of the cells of the inner nuclear layer had swollen and pale staining cytoplasm. What were thought to be processes from these cells could be seen in the inner plexiform layer (Fig. 5.8). These cells were thought to be amacrine cells. The remainder of the retina and the choroid was of normal appearance.

The only abnormal block found in animal 2/24h/2, block B2, was of similar appearance to blocks A1, B1 and C1 from animal 2/24h/1.

5.2.3 Group 2; 48 Hours Recovery (2 animals).

In both animals slight abnormalities in the appearance of the retina in the experimental eyes were noted during dissection. In animal 2/48h/1 a small retinal fold was present in the area of block A2. In animal 2/48h/2 a slight pigmentary disturbance was seen in column 1 (Fig. 5.1) blocks A, B, C and D.

The only blocks examined, which exhibited unusual features, were blocks A2 (from both animals), block C2 from animal 2/48h/1 and B3 from animal 2/48h/2 (Fig. 5.1). Blocks C2 and B3 were similar in appearance to blocks A1, B1 and C1 from animal 2/24h/1 (described in the previous sub-section). All these blocks showed slight disturbances of the receptor cell outer segments and cellular swelling of the pigment epithelium.

The most noteworthy feature of this group was the presence of macrophage-like cells in the interphotoreceptor space. These were encountered in both animals, block A2 in each case (Fig.

5.9). The inner retina in these regions was normal in appearance. Abnormalities were limited to slight disturbances of the photoreceptor outer segments and the pigment epithelium. The latter were shrunken and densely stained, similar to that described for block C1 animal 2/24h/1. In addition to the macrophage-like cells seen in the interphotoreceptor space, small mononuclear cells could be identified within the structure of Bruch's membrane (Fig. 5.9). Their location within Bruch's membrane was not shown conclusively by light microscopy but was later confirmed by electron microscopy.

5.2.4 Group 2; 4 Days Recovery (2 animals).

No abnormality of retinal structure was detected during dissection in either animal. By light microscopy, the inner layers of the retina appeared normal in all blocks examined. The photoreceptor cells were also of normal appearance although slight folding of the outer nuclear layer was present in some blocks. This type of appearance was encountered in blocks C4 and D2 in animal 2/4D/1. Beneath these areas of retinal folding the pigment epithelium was highly irregular in appearance (Figs. 5.10 and 5.11). The irregular pigment epithelium showed a variety of appearances. Some cells had slightly rounded nuclei, while others appeared to contain numerous phagosomes (Fig. 5.10). In other areas the pigment epithelial cells contained vesicles. Very occasionally, what appeared to be a second irregular layer of pigment epithelial cells was present. It was not certain that these cells were of pigment epithelial origin, however (Fig. 5.11).

The choroid was of normal appearance in both animals in this group.

5.2.5 Group 2; 1 Week Recovery (2 animals).

The retinae of both animals appeared to be of normal appearance during dissection. Light microscopy revealed only minor disturbances of the photoreceptor cell outer segments. However, in one block (block C2 animal 2/1W/1), very small lesions of the pigment epithelium were observed. These lesions extended over only three to four pigment epithelial cells. These cells were highly vesiculated, had rounded nuclei, and appeared to be extruding their lipid droplets (Fig. 5.12). The chorio-capillaris immediately below such regions invariably contained impacted red cells or platelet thrombi (Fig. 5.12).

The remainder of the tissues examined by light microscopy were of normal appearance.

5.2.6 Group 2; 2 Weeks Recovery (2 animals).

In one animal, 2/2W/2, the retina appeared normal during dissection and on subsequent investigation by light microscopy.

In the other animal (2/2W/1) a whitish discolouration of the retina was seen in rows C and D (Fig. 5.1). By light microscopy several abnormalities in retinal structure were seen.

In block A2 there was a slight detachment of the neural retina. This detachment was associated with disturbances of the photoreceptor outer segments and the pigment epithelium. What appeared to be hyperplasia of pigment epithelium was noted as several layers of pigmented cells were present (Fig. 5.13 and 5.14).

Blocks taken from rows C and D showed varying degrees of abnormality being slight in the case of row C and more severe in the case of row D. Where these abnormalities were slight (Fig. 5.15) the pigment epithelium appeared normal. The photoreceptor cells showed some degenerative changes. Their outer segments appeared to be fragmented but did not appear as the vesicular structures more typical of light damaged outer segments.

Distended cone cell inner segments were identifiable among the outer segment material. However, the inner segments of the rods appeared normal. The nuclei of many of the receptor cells, probably of both rod and cone cells, were pyknotic. Many of the cell processes in the outer plexiform layer were swollen and lightly stained. These processes were tentatively identified as being receptor cell synaptic terminals and horizontal cell processes. Within the inner nuclear layer, some of the amacrine cells' nuclei were surrounded by very lightly stained cytoplasm. This pale staining of amacrine cell cytoplasm extended to their processes in the inner plexiform layer. The remainder of the retina, the Müller cells, the ganglion cells, and probably the bipolar cells, were of normal appearance (Fig. 5.15). As far as could be detected by light microscopy the choroid was of normal appearance.

Where the abnormalities of retinal structure were more severe, (row D) the pigment epithelium still appeared normal by light microscopy. However, the degenerative changes of the photoreceptor cells were much more pronounced than in row C. There was fragmentation of the photoreceptor cell outer segments and swelling of their inner segments. Distended mitochondria were probably present within the swollen inner segments. Within the outer nuclear layer virtually all the receptor cell nuclei were pyknotic. The receptor cell inner and outer receptor fibres were reduced to darkly stained strands. The resulting space between the "shrunken" receptor cells was filled with lightly stained Müller cell cytoplasm. With the exception of the Müller cells, virtually all the cells of the inner nuclear layer were swollen and had lightly stained cytoplasm. This cytoplasmic swelling appeared to extend as far as the cell processes of the inner plexiform layer. However, the ganglion cells and

the inner regions of the Müller cells had a normal appearance (Fig. 5.16).

5.2.7 Group 2; 4 weeks Recovery (2 animals)

During dissection of the tissue from animal 2/4W/1 a slight pigmentary disturbance of the retina was noted in the region which corresponded to block A2. This was not seen by light microscopy. However, on further examination by light microscopy, tissue from both animals showed a variety of structural abnormalities.

In animal 2/4W/1 the inner layers of the retina appeared normal. Abnormalities in retinal structure were confined to the outer retina. The receptor cells occasionally showed disturbances of their outer segments (Fig. 5.17). In such regions the pigment epithelial basal cytoplasm contained numerous clear vesicles. In other areas the disorganisation of the photoreceptor cell outer segments was more severe and many of the receptor cell nuclei were pyknotic (Fig. 5.18). In such areas the vacuolation of the pigment epithelial basal cytoplasm appeared to be more extensive, a greater proportion of the cytoplasm being involved. The choroid in both the regions described above was normal in appearance.

The morphology of the retina from animal 2/4W/2 was very similar to that already described for animal 2/4W/1. Disturbances of the outer segments and pigment epithelium were common. However, in one region (block D2) the degenerative changes of the retina appeared to be more extensive than those already described. The neural retina was detached. The receptor cells' outer segments were swollen and highly disorganised and their inner segments contained distended mitochondria. Within the

outer nuclear layer many of the receptor cell nuclei were pyknotic. Within the inner nuclear layer, the horizontal and amacrine cells had swollen and lightly stained cytoplasm. This cytoplasmic swelling of the amacrine and horizontal cells was also present in their processes in the inner plexiform layer (amacrine cells) and outer plexiform layer (horizontal cells) (Fig. 5.19).

The retinal pigment epithelium in this region was slightly abnormal in appearance. There were many small vesicles in the basal cytoplasm. These were thought to be swollen mitochondria. The choriocapillaris and choroidal vessels below these regions of pigment epithelium were frequently filled with impacted red cells (Fig. 5.20).

5.3 Recovery of the Rabbit Retina and Choroid Following Light Damage; Light Microscopy; High Intensity Group

At least four blocks were examined from each experimental eye. In all but one animal (1/2W/1) these blocks were selected from areas which showed abnormal appearance during dissection (Figs. 5.1, 5.2, 5.3 and 5.4). The experimental eyes in this group were exposed to light which produced an estimated retinal illumination of 84.4 mWcm^{-2} .

5.3.1 Group 1; High intensity (2 animals).

In both animals lesions of the retina were seen during dissection of the retinal and choroidal tissues (Fig. 5.2). In both animals tissue blocks were taken from within the confines of the lesion. In animal 1/6h/1, blocks A2, B2, C2 and D3 and in animal 1/6h/2, blocks A2, B2, C2 and D4, were selected. In both animals considerable variation was seen in the tissue examined, although the overall pattern of damage was quite similar in both animals. The severely damaged pigment epithelium

was similar in both animals. It contained numerous densely stained bodies, which were presumably receptor cell debris, as well as a few pale stained vacuoles which occupied a large proportion of the cells' cytoplasm. Complete vacuolation of the pigment epithelium was seen very rarely (Fig. 5.21).

The damage to the photoreceptors was extensive. Both the inner and outer segments were disrupted. The majority of the receptor cell nuclei were pyknotic. The pyknotic nuclei were surrounded by a halo of swollen cytoplasm. Occasionally the oedema of the receptor cell cytoplasm extended as far as the outer plexiform layer (Fig. 5.21). Surprisingly, the inner layers of the retina appeared normal apart from very infrequent pyknotic nuclei in the inner nuclear layer. As far as could be discerned by light microscopy the choroid was of normal morphology.

The remainder of the retina examined showed only slight disturbances of the pigment epithelium and receptor cell outer segments apart from one region, block D4 in animal 1/6h/2. Within this block the choriocapillaris and the deeper vessels of the choroid were filled with impacted red cells (Fig. 5.22). Immediately above this area of choroid the pigment epithelium was densely stained and contained numerous distended mitochondria. The detached (probably artifactual) neural retina showed disturbances of the receptor cell outer segments. The remainder of the tissue, the inner regions of the receptor cells and the inner retina, were of normal appearance.

5.3.2 Group 1; 24 Hours Recovery (2 animals)

Lesions of the retina were seen during dissection in both animals. Tissue blocks were selected from within these areas. In animal 1/24h/1, blocks A1 and B2, showed extensive damage. The appearance of these two blocks was similar to all the tissue examined from animal 1/24h/2. In these areas the pigment epithelium was reduced in thickness and showed little intracellular detail. In some regions the pigment epithelium was separated from Bruch's membrane by a fibrous material (Fig. 5.23). The receptor cell inner and outer segments were highly disorganised. The subretinal space was completely filled with photoreceptor cell inner and outer segment debris (Fig. 5.23). Virtually all of the receptor cells' nuclei were pyknotic and were surrounded by oedematous cytoplasm. The cells of the inner nuclear layer showed various changes. Some cells contained pyknotic nuclei within swollen cytoplasm while others showed only slight oedema of their cytoplasm. Oedema of cell processes was present throughout the inner plexiform layer. The cell type to which they belonged was not known. The ganglion

cells were well preserved. The Müller cell cytoplasm of the innermost retina was very lightly stained and greatly distended. However, the nerve fibre layer, and the inner limiting membrane, retained their normal morphology (Fig. 5.24).

The choriocapillaris below these extensively damaged regions of retina contained numerous mononuclear cells. The deeper vessels, and the remainder of the choroid were of normal morphology.

5.3.3 Group 1; 48 Hours Recovery (2 animals)

Lesions of the retina were visible during dissection of the tissues in both animals. In animal 1/48h/1 a large area of retina was damaged (Fig. 5.2). By light microscopy it was seen that the retina and choroid of animal 1/48h/1 were far more severely damaged than the retina and choroid of animal 1/48h/2.

The tissue blocks examined from animal 1/48h/1 were A3, B2, C1 and D2. Block B2, virtually from the centre of the lesion (Fig. 5.2), exhibited extremely severe damage to the retina and choroid. The pigment epithelium was densely stained, shrunken, and lacked any intracellular detail. The lipid droplets and melanin granules could still be identified, however (Fig. 5.25). The receptor cells were separated from the pigment epithelium by a layer of lightly stained flocculate material which contained approximately spherical, densely stained bodies, which may have been outer segment material. The receptor cells showed degenerative changes throughout their length. The inner and outer segments were reduced to a layer of vesicular debris. All the receptor cell nuclei were pyknotic. These pyknotic nuclei were surrounded by extensive Müller cell cytoplasm. Oedematous cells, and cells with pyknotic nuclei, were present throughout the inner retina. The innermost regions of the Müller cells were so extensively swollen that the inner limiting membrane and the nerve fibre layer appeared to be separated from the remainder of the retina (Fig. 5.25). The choriocapillaris and some of the deeper choroidal vessels appeared to be completely blocked with platelets and impacted red cells.

Blocks A2 and C1, both from peripheral regions of the lesion in animal 1/48h/1, were similar in appearance. The damage seen in these blocks was similar to the worst damage observed in animal 1/48h/2. As in the tissues already described, the photoreceptors and the pigment epithelium were the most severely damaged retinal components (Fig. 5.26). Individual pigment epithelial cells were conspicuous due to rounding of the cells' apical cytoplasm. These cells appeared to have fine cytoplasmic bridges extending across a separation between themselves and Bruch's membrane. The cells' cytoplasm contained densely stained inclusions and lipid droplets (Fig. 5.26). The receptor cells' inner segments appeared to be greatly reduced in length and their connection to any of the outer segment material was uncertain. Most of the receptor cell nuclei were pyknotic, although some nuclei of more normal appearance were also present. Loss of receptor cell cytoplasm, and replacement by Müller cell cytoplasm, was common throughout the outer nuclear layer.

The cells of the inner retina were mostly of normal appearance although slightly oedematous cells could be identified within the inner nuclear layer.

The choroidal vessels below these less severely damaged areas of retina differed markedly from those described for the more severely damaged regions. The deeper vessels were normal in appearance but the choriocapillaris was filled with mononuclear cells (Fig. 5.26).

The retinal and choroidal tissues surrounding the lesion in animal 1/48h/1, and the remainder of the tissue examined from animal 1/48h/2, were similar in appearance. Slight abnormalities of the receptor cells were present. The receptor cells' nuclei and cytoplasm were unusually densely stained.

There appeared to be a loss of outer segment material, and consequently many of the inner segments did not appear to process outer segments (Fig. 5.27). In all regions described the inner retina, the pigment epithelium, and the choroid appeared normal by light microscopy.

5.3.4 Group 1; 4 Days Recovery (2 animals).

Extensive lesions of the retina were seen during dissection in both animals (Fig. 5.3). As in the previous section the appearance of the tissue varied with the position from which the tissue was selected. The appearances of the tissues could be divided into two main categories: firstly, severely damaged areas and secondly, transitional areas between damaged and normal tissue.

The severely damaged areas of retina and choroid were of differing appearances. Areas similar to the severely damaged areas seen after 48 hours of recovery were present. These areas showed extensive damage to the entire neural retina. The choriocapillaris and the larger vessels of the choroid were occluded by impacted red cells (Fig. 5.28). In regions where the choroidal circulation appeared to be patent mononuclear cells were present within the choriocapillaris, and also throughout the inner layers of the choroid. The inner retina in these regions was still characterised by the presence of numerous degenerative cells. The outer retina, however, showed considerable change. The subretinal space was filled with macrophagic cells. These cells contained abundant phagosomes, which were presumably filled with photoreceptor debris (Fig. 5.29).

Regions of gliotic retina were present adjacent to the areas of macrophagic activity. In these gliotic regions the macrophagic removal of cellular debris appeared to be complete. There was extensive loss of receptor cells. Müller cell cytoplasm was extensive within the outer nuclear layer and appeared to compensate for the loss of receptor cells by filling the spaces between the surviving receptor cells. Müller cell nuclei were thought to be frequently observed in the remnants of the outer nuclear layer (Fig. 5.30). Where complete destruction of the pigment epithelium had occurred large pigmented cells were seen above Bruch's membrane. In other areas, presumably where the initial damage had been less severe, pigment epithelial cells and receptor cells were present. In these regions the receptor cells lacked both inner and outer segments (Fig. 5.30).

Transitional zones between lightly damaged and severely damaged retina were often surprisingly abrupt (Fig. 5.31). These transitional zones only extended over a few hundred microns of retina. The morphology of these areas was highly variable but generally the reappearance of receptor cells was intimately associated with the presence of viable pigment epithelium. The degree of photoreceptor cell loss and loss of other retinal cells was highly variable. This loss of cellular content was usually compensated for by expansion of Müller cell cytoplasm. This expansion of cytoplasm into the outer nuclear layer was often accompanied by a migration of the Müller cell nucleus into the outer nuclear layer. (Fig. 5.31)

In transitional zones the appearance of the choroid was also variable. It often appeared normal but as regions of more extensively damaged retina were approached mononuclear cells became increasingly common within its blood vessels (Fig. 5.31).

5.3.5 Group 1; 1, 2 and 4 Weeks Recovery (6 animals)

It was thought practical to describe the appearance of the tissues from these animals together as their appearance was, in many respects, similar. All of the animals in these three recovery periods, except animal 1/1W/2, had lesions of their retinae which were obvious during dissection (Fig. 5.3 and 5.4). Tissue examined by light microscopy was selected from areas within and around the visible lesions in all the animals except 1/1W/2. In animal 1/1W/2 they were selected randomly as no lesion was visible.

Extensively damaged photoreceptors, and associated debris within the subretinal space, were not observed at any recovery period longer than four days. The appearance of the tissues from these three recovery periods was divisible in three categories.

1. Areas of complete photoreceptor, and pigment epithelial cell loss.
2. Areas of partial photoreceptor loss.
3. Areas of pigment epithelial proliferation.

Areas where there was complete loss of the receptor cell and pigment epithelial cells were identified in animals 1/1W/1, 1/2W/1, 1/2W/2 and 1/4W/2. During dissection these areas of retina appeared to be of normal colouration, but of reduced thickness. Light microscopy of such regions revealed that the inner retina, from the inner nuclear layer to the inner limiting membrane, was only slightly abnormal in appearance (Fig. 5.32). However, the photoreceptors and the pigment epithelial cells were completely absent. The receptor cells and pigment epithelial cells were replaced by Müller cell cytoplasm. Within this cytoplasm, what were taken to be, Müller cells' nuclei were seen. Large pigmented cells were commonly seen adjacent to Bruch's membrane. By light microscopy it was impossible to decide whether these were surviving pigment epithelial cells or pigment

laden macrophages (Fig. 5.33).

There were occasional thickenings of Bruch's membrane (Fig. 5.32 and 5.33). In these areas the choriocapillaris was absent, or if present contained mononuclear cells (Figs. 5.32 and 5.33).

In the areas of partial photoreceptor loss the survival of some of the photoreceptors appeared to be intimately associated with the presence of pigment epithelial cells. In some sections a few photoreceptor cells extended beyond the edge of the surviving pigment epithelium. Their inner and outer segments were, however, directed toward the surviving pigment epithelial cells (Fig. 5.34).

In some areas there appeared to be pigment epithelial proliferation. This was not a certainty as it was extremely difficult to distinguish between pigment laden macrophages and atypical pigment epithelial cells. An area which was thought to show pigment epithelial proliferation is shown in Figure 5.35. Such areas were often associated with folding or detachment of the neural retina. These proliferated pigment epithelial cells were quite different from the cells which were thought to be pigment laden macrophages. These macrophages occurred throughout the outer retina of the later recovery periods (Fig. 5.36: one week recovery, and Fig. 5.37: four weeks recovery). The proliferated pigment epithelial cells were spindle shaped and contained only moderate quantities of melanin (Fig. 5.35). The pigment laden macrophages were considerably larger and usually contained massive amounts of melanin (Figs. 5.36 and 5.37).

The choroid in these animals at the later recovery periods was usually unremarkable. Only the choriocapillaris showed any variation. Occasionally it was completely absent (Fig. 5.37), or if present it contained scattered mononuclear cells

(Figs. 5.31 and 5.32).

5.4 Recovery of the Rabbit Retina and Choroid Following Light Damage; Electron Microscopy; Low Intensity Group

This section describes, by electron microscopy, the areas previously described by light microscopy. Any features of the tissues which were not seen by light microscopy, and which are of interest, will be described. As in the preceding section the appearance of the tissues will be first described for the group exposed to the lower intensity (estimated retinal illumination 38.6 mWcm^{-2}).

5.4.1 Group 2: 6 Hours Recovery

After six hours recovery damage was often restricted to the pigment epithelium and photoreceptors. In some areas the entire retina was abnormal (Fig. 5.38 - Light microscopy of this region was shown in Figs. 5.5 and 5.6). The damage to the pigment epithelium, and photoreceptor inner and outer segments, was similar in appearance to that seen in the higher intensity groups immediately after the one hour exposure to light. There was considerable swelling of the pigment epithelial cells' mitochondria. The rod outer segments had focal disturbances of their disc stacks. The mitochondria of the rod inner segments were slightly distended. Cone cells' outer segments were unidentifiable. Their inner segments were greatly distended and contained severely swollen mitochondria (Figure 5.39).

Much of the Müller cell cytoplasm within the outer nuclear layer was electron-lucent and severely swollen. Distended Müller cell mitochondria could be seen close to the outer limiting membrane. The receptor cells' nuclei and their synapses were reasonably normal in their appearance (Fig. 5.40).

The ganglion cells and the majority of the cells of the inner nuclear layer showed considerable swelling of their cytoplasm and cell processes in the plexiform layers (Fig. 5.38). The Müller cells, apart from swelling of their cytoplasm in the outer nuclear layer, were normal in appearance (Fig. 5.38).

The choroid was generally of normal appearance. In regions of more pronounced retinal damage, however, choroidal vessels were often occluded with impacted red cells or platelet thrombi (Fig. 5.38).

5.4.2 Group 2; 24 Hours Recovery

Twenty four hours after the light exposure degenerative changes were apparent in the pigment epithelium, and in the receptor cells (Fig. 5.41: Light microscopy was shown in Fig. 5.7). The pigment epithelium contained numerous electron lucent vesicles. Some of these were distended mitochondria while the others appeared to be regions of cytoplasmic rarefaction (Fig. 5.41). The majority of the pigment epithelial cells' cytoplasm was granular in appearance, although regions of more normal cytoplasm were found around the nuclei. The pigment epithelial nuclei were unusually rounded in appearance (Fig. 5.41). Morphological changes were also apparent in the apical surface of the pigment epithelium. The apical villi were reduced or flattened against the apical surfaces of the cells. The villi no longer interdigitated with the photoreceptor cells' outer segments (Fig. 5.41). The damage to the photoreceptor cell outer segments was similar to that seen after six hours recovery. Here again, the cone cells' inner and outer segments were more severely damaged than those of the rod cells. The outer nuclear layer contained a few pyknotic and disintegrating nuclei (Fig. 5.41).

In all the tissues examined from these two animals both the inner retina and the choroid were of normal appearance.

5.4.3 Group 2; 48 Hours Recovery

In both animals disturbances of retinal structure were limited to the receptor cell outer segments and to the pigment epithelium (Fig. 5.42). The receptor cell outer segments showed disturbances of their disc stacking. Macrophages were present among the outer segments in a few sections. These contained what was thought to be receptor cell outer segment material (Fig. 5.43. Light microscopy was shown in Fig. 5.9). The pigment epithelium in these damaged areas was degenerative and showed complete loss of cellular architecture (Fig. 5.44).

Cells had been seen below the degenerative pigment epithelium by light microscopy. By electron microscopy these were seen to be enclosed within the structure of Bruch's membrane. They were usually found immediately below the basement membrane of the pigment epithelium (Figs. 5.42 and 5.44). Cells of similar appearance were seen both within and external to the choriocapillaris (Fig. 5.44). On the basis of their size, nuclear shape and chromatin pattern, and their cytoplasmic inclusions, these cells were thought to be monocytes.

5.4.4 Group 2; 4 Days Recovery

In these animals, both the neural retina and the choroid were normal in appearance. However, abnormalities of the pigment epithelium were encountered (Fig. 5.45 a and b). In regions of abnormal pigment epithelium the neural retina was detached. These detachments may have been artifactual. The retina, although detached, was normal in appearance apart from some slight disorganisation of the most distal regions of the photoreceptor outer

segments. The atypical pigment epithelium had two distinct appearances. In some areas its cytoplasm was packed ^{with} phagosomes (Fig. 5.45a and 5.46). These phagosomes probably contained outer segment material. In other areas the pigment epithelium appeared to be "budding" cells (Fig. 5.45b and 5.47). These "budding" cells appeared to be pinched off at the level of the junctional complex (Fig. 5.47). These regions of atypical pigment epithelium were only found in association with retinal folds or detachments of the retina.

5.4.5 Group 2; 1 Week Recovery

As stated in the section on the light microscopy, the tissue from these animals was unremarkable. Only one block showed a focal lesion of the pigment epithelium. The light microscopy of this region is shown in Figure 5.12. Sections suitable for electron microscopy were fortunately obtained from this region (Fig. 5.48). There were slight irregularities of the outer segments of the photoreceptors. Damage was, however, far more conspicuous within the pigment epithelium. There was extensive vacuolation of the cytoplasm. This may have been produced by distension of the smooth endoplasmic reticulum. There was also slight swelling of the pigment epithelial cells' mitochondria (Fig. 5.48).

The choriocapillaris beneath these damaged pigment epithelial cells contained impacted red cells. Platelets, as seen by light microscopy (Fig. 5.12) were not seen by electron microscopy, however. (Fig. 5.48)

5.4.6 Group 2; 2 Weeks Recovery

Structural abnormalities were only seen in animal 2/2W/1 by light microscopy. In the other animal, 2/2W/1, the tissues appeared normal by light microscopy. Similarly, by electron microscopy, abnormalities of structure were only encountered

in animal 2/2W/1.

Two distinct appearances were seen within the damaged tissues: firstly, areas of retinal folding, or slight detachment, with associated pigment epithelial disturbances and secondly, areas of general degenerative change throughout the entire retina.

In the areas showing pigment epithelial disturbances the inner retina was of normal appearance. However, slight irregularities of the receptor cell outer segments did occur (Fig. 5.49. Light microscopy was shown in Figs. 5.13 and 5.14). By electron microscopy abnormalities of structure were seen in the choriocapillaris, Bruch's membrane, and the pigment epithelium.

In the regions of pigment epithelial abnormality (Fig. 5.49), the choriocapillaris showed an unusual crenulation or folding of its lining endothelium (Fig. 5.50). This did not appear to affect the patency of the vessels. In these regions of pigment epithelial disturbances thickening of Bruch's membrane was a common finding. This was produced by a thickening of the inner collagenous layer (Fig. 5.50). In some sections cells were seen within this thickened region of Bruch's membrane. Very occasionally, cellular processes were observed passing through the elastic layer of Bruch's membrane and into the connective tissue of the choroid (Fig. 5.50). The regions of pigment epithelial hyperplasia which were seen by light microscopy (Figs. 5.13 and 5.14) appeared to consist of three types of cells. 1. cells which appeared to be pigment epithelium albeit of atypical appearance. 2. cells of unknown character, which were found between the pigment epithelium and Bruch's membrane. 3. macrophages or macrophage-like cells which were found on the apical surface of the pigment epithelium and in the subretinal space (5.50).

In areas of retinal degeneration there was extensive intracellular oedema of all retinal cells apart from the receptor cells. The receptor cell cytoplasm was shrunken and densely stained (Fig. 5.51). The pigment epithelium did not appear to be severely damaged but did show swelling of its mitochondria as well as slight rounding of its nuclei (Fig. 5.52). The photo-receptor damage was unusual and differed considerably from that seen immediately after light exposure. Outer segment damage was not severe. However, the inner segments were swollen, and contained severely distended mitochondria (Figs. 5.51 and 5.53). Many of the receptor cell nuclei, principally rod cell nuclei, were pyknotic. the cytoplasm of these cells with pyknotic nuclei was often shrunken and densely stained (Fig. 5.53). The rods' spherules were rounded and densely stained while the cone cells' pedicles were less severely damaged (Fig. 5.53).

The cells of the inner retina, except the Müller cells, showed intracellular oedema and distension of their mitochondria. Although the Müller cells, inwards from the inner nuclear layer, appeared normal their cytoplasm was occasionally physically displaced by the severely oedematous cells of the inner retina (Fig. 5.53). The Müller cells' cytoplasm in the outer nuclear layer was greatly distended. Within the cytoplasm adjacent to the outer limiting membrane were numerous vesicular structures. These were thought to be distended Müller cell mitochondria (Fig. 5.53). The choroidal tissues below these regions of degenerative retina were normal in appearance (Figs. 5.51 and 5.52).

5.4.7 Group 2; 4 Weeks Recovery

The appearance of the tissues four weeks after exposure to light can be divided into three categories. 1. abnormalities of the choroid. 2. abnormalities of the pigment epithelium, and the receptor cells. 3. degenerative changes of the retina and choroid.

In some areas the choroid contained numerous inflammatory cells. The majority of these cells were in the extravascular tissues. These cells were thought to be macrophages, but they varied in appearance from monocyte-like cells to mature macrophages, which contained numerous phagosomes (Fig. 5.54).

The majority of the retinal tissue examined by electron microscopy showed some abnormalities of the receptor cells and the pigment epithelial cells (Fig. 5.55). The pigment epithelial mitochondria were slightly distended, and mild distension of the smooth endoplasmic reticulum was present (Fig. 5.55). The rod outer segments showed focal irregularities. In these regions the discs were replaced by a flocculate material (Fig. 5.55). Cone cell outer segments were absent or greatly reduced. Their inner segments were greatly distended and contained swollen mitochondria (Fig. 5.55).

Retinal degeneration similar to that described in the previous section (2weeks recovery) was also seen in this group. The retinal oedema and the distension of the Müller cells' cytoplasm within the outer nuclear layer was not so marked, however (Fig. 5.56). The pigment epithelium was again similar to that described previously although the choroidal vessels were more severely damaged. These contained impacted red cells and there was severe damage to the endothelial cells lining these vessels (Fig. 5.57).

5.5 Recovery of the Rabbit Retina and Choroid Following Light Damage; Electron Microscopy; High Intensity Group.

As stated in the section on light microscopy four or more blocks were examined from each animal. This section describes the same tissue by electron microscopy. Emphasis is placed on features not seen by light microscopy.

5.5.1 Group 1; 6 Hours Recovery

In both animals the pattern of damage was quite similar. In animal 1/6h/1 blocks A2 and B2 showed severely damaged tissue. Similarly animal 1/6h/2, blocks A2 and B2, showed severe damage to the retina. The remainder of the blocks examined, animal 1/6h/1, blocks C2 and D3, and animal 1/6h/2, block C2 showed only slight abnormalities. The photoreceptor outer segments were mildly disturbed while the pigment epithelium's smooth endoplasmic reticulum was slightly swollen. Apart from these minor changes the tissues were otherwise normal in appearance. The single remaining block, animal 1/6h/2 block D4, exhibited a pattern of damage uncharacteristic of light damage. The appearance of this block will be described later.

In the severely damaged regions both the photoreceptors and the pigment epithelium were highly abnormal. The inner nuclear layer, and the remainder of the retina, were of normal appearance (Fig. 5.58).

The pigment epithelium exhibited a variety of structural changes. The apical processes were disorganised or lost. The melanin granules were scattered throughout the cytoplasm. The mitochondria, although still present in the basal cytoplasm, were small and their internal matrix was densely stained. There were large phagosomes of outer segment material within

the cytoplasm. The nuclei and basal infoldings of these cells retained their normal appearance (Fig. 5.59).

The receptor cells in these severely damaged regions had ruptured inner and outer segments. The majority of the receptor cells were pyknotic. Their perinuclear cytoplasm was either condensed around the nucleus or extremely oedematous (Fig. 5.58). The choroid, outer to these regions of damaged retina, was normal in appearance (Figs. 5.58 and 5.59).

The remainder of the tissue examined from these two animals was virtually normal apart from block D4 animal 1/6h/2. In block D4 the photoreceptor inner and outer segments were slightly damaged. Many of the outer segments were swollen and showed disorganisation of their discs. The inner segments showed only slight swelling of their mitochondria. The remainder of the retinal tissue was unremarkable although there may have been slight intracellular oedema of the neural elements of the inner nuclear layer, and the ganglion cells (Fig. 5.60). The appearance of the pigment epithelium and choriocapillaris was of more interest. The pigment epithelium showed considerable swelling of its mitochondria, some of which were ruptured (Fig. 5.61). The smooth endoplasmic reticulum was swollen and the cisternae of rough endoplasmic reticulum were distended (Fig. 5.61). The vessels of the choriocapillaris were unusual in appearance. The vessels were uniformly filled with a densely stained material, which was thought to be haemoglobin derived from lysed red cells (Fig. 5.61). The endothelial cytoplasm was irregularly swollen and extended into the lumen of the vessels (Fig. 5.61).

5.2.2 Group 1; 24 Hours Recovery

The majority of the tissue examined from these animals was reasonably similar in appearance. However, some variation in the degree of damage to the retina and pigment epithelium was apparent. Blocks A1 and B2 from animal 1/24h/1, and all four blocks examined from animal 1/24h/2, showed severe damage. Within these tissue blocks the retina showed degenerative changes throughout its thickness (Figs. 5.62 and 5.63). In the regions of most severe damage the pigment epithelium was reduced to a thin layer of granular material. This material showed little evidence of cellular architecture apart from melanin granules and lipid droplets (Figs. 5.62 and 5.64). Occasionally this type of degenerative pigment epithelium was separated from Bruch's membrane by plasma-like material which contained a network of fibrous material, probably fibrin (Fig. 5.65).

In regions where the pigment epithelium had survived, it was similar in appearance to that seen after 6 hours of recovery (compare Figs. 5.59 and 5.66). The mitochondria were small with a densely stained matrix. The apical processes were lost, and melanin granules were distributed throughout the cytoplasm (Fig. 5.66).

The receptor cells' inner and outer segments were similar in appearance to those seen in severely damaged regions after six hours of recovery (compare Figs. 5.58 and 5.62). However, the outer nuclear layer was considerably different. The majority of the receptor cell nuclei were pyknotic. These pyknotic nuclei were surrounded^{by} highly oedematous cytoplasm. In some regions of the outer nuclear layer receptor cell membranes had ruptured, producing cystic spaces containing pyknotic nuclei (Figs. 5.62 and 5.63). The receptor cell synapses were identifiable within

the outer plexiform layer. Those of the cone cells appeared to be better preserved than those of the rods (Fig. 5.63).

The cells of the inner nuclear layer were highly variable in appearance. Some horizontal and amacrine cells had pyknotic nuclei within severely swollen cytoplasm. Other cells, thought to be bipolar cells, had shrunken intensely stained cytoplasm and pyknotic nuclei (Fig. 5.63). Some of the cell processes within the inner plexiform layer were swollen. These swollen processes presumably belonged to amacrine or bipolar cells: the ganglion cells were relatively normal, apart from a few cells in which the cytoplasm stained more intensely than normal. Throughout the retina the Müller cells were normal in appearance although their cytoplasm was markedly displaced, in the outer nuclear layer, by the highly oedematous cytoplasm of the receptor cells (Fig. 5.63). At the level of the outer limiting membrane, Müller cell processes could be seen extending into the sub-retinal space. Inner to the outer limiting membrane the Müller cells' cytoplasm was densely stained and contained many mitochondria (Fig. 5.67).

Below these damaged regions of retina, fibrin clots often occluded the choriocapillaris (Figs. 5.62 and 5.64). Where the choriocapillaris was patent, it contained many mononuclear cells (Figs. 5.66 and 5.68). The vast majority of these mononuclear cells were thought to be monocytes. Cells of a more macrophagic appearance were seen within the choroidal stroma and between the vessels of the choriocapillaris (Fig. 5.68).

5.5.3 Group 1; 48 Hours Recovery

Severe damage, similar to that described in the previous section, was seen only in one of the animals. This was animal 1/48h/1 blocks B2 and C2. In another two blocks, blocks A2 in animals 1/48h/1 and 1/48h/2, severe damage was restricted to the receptor cells and the pigment epithelium. In blocks D2, animal 1/48h/1, and C2, animal 1/48h/2, there was a loss of photoreceptor cells. The pigment epithelium, however, was intact. Blocks B2 and D2, animal 1/48h/2, were near normal in appearance; block B2 did show some abnormalities of the pigment epithelium which will be discussed later. In these two animals the degree of damage shown by a block correlated well with its position in the lesion (Fig. 5.2).

In the severely damaged areas, the appearance of the outer retina and choroid was similar to that seen in severely damaged regions twenty four hours after exposure. However, there appeared to be extensive leakage of plasma through the damaged pigment epithelium. Fibrin fibres were present within the plasma in the subretinal space (Fig. 5.6). The receptor cells were virtually all degenerative. Many nuclei were pyknotic while others were disintegrating (Fig. 5.70). Müller cells' cytoplasm occupied most of the outer nuclear layer. It surrounded, or possibly contained, the receptor cell debris (Fig. 5.70). The numerous, small, densely stained structures seen external to the Müller cells' cytoplasm and within degenerate receptor cells were thought to be remnants of secondary lysosomes produced by the receptor cells (Fig. 5.71).

The inner nuclear layer showed changes which were similar to those observed in severely damaged areas after 24 hours recovery although cells in an advanced state of degeneration

were more common (Fig. 5.70). Within the inner plexiform layer a greater proportion of the cell processes were swollen (compare Figs. 5.70 and 5.63). The Müller cells had more extensive cytoplasm in both the inner and outer nuclear layers. This increase in cytoplasmic volume was accompanied by an increase in the size of the nucleus. The Müller cell nuclei also appeared to be occupying a more external position within the inner nuclear layer (Fig. 5.70).

The innermost regions of the retina, the ganglion cells and the inner regions of the Müller cells, were unusually in appearance. Many of the ganglion cells' mitochondria were swollen. The Müller cells' cytoplasm was of varying electron-density and contained electron-lucent vesicles. These may have been produced by distension of the Müller cell's smooth endoplasmic reticulum (Fig. 5.70).

Below these regions of severely damaged retina the choriocapillaris and the deeper vessels of the choroid showed extensive damage to their endothelium. The interior of these vessels were often filled with fibrin, various inflammatory cells, and degranulating platelets (Figs. 5.72 and 5.73).

Within the less severely damaged areas, the pigment epithelium and the photoreceptors appeared to be selectively damaged while the inner retina, the inner nuclear layer, the inner plexiform layer, and the ganglion cell layer, retained a more normal appearance. Intracellular oedema and distended mitochondria were present within the inner retina but the cells showing these features did not appear to be severely damaged (Fig. 5.74).

As in the severely damaged tissue, the Müller cells' nuclei were found more toward the outer aspect of the inner

nuclear layer. Occasionally, Müller cells' nuclei were identified within the outer nuclear layer. These cells were identified as Müller cells as, in some instances, their cytoplasm could be followed into the inner layers of the retina where its distribution was typical of Müller cells (Fig. 5.74).

The choriocapillaris beneath the less severely damaged regions of retina did not appear to have suffered much damage to its endothelium. Consequently, fibrin clots, degranulated platelets, and polymorphonuclear leucocytes were not seen in these areas. However, mononuclear cells were present within, and external to, the choriocapillaris. In some sections cells were seen within the structure of Bruch's membrane. They were found between the inner collagenous layer and the basement membrane of the pigment epithelium. In these areas the remainder of the choroid was normal in appearance (Fig. 5.75).

The more peripheral regions of the extensive lesion in animal 1/48h/1 (block D2). and the area of reduced retinal thickness in animal 1/48h/2 (block C2) were similar in appearance. Both the outer nuclear layer and the pigment epithelium were unusual in appearance. Some pyknotic nuclei were present in the outer nuclear layer but many of the receptor cell nuclei were normal in appearance (Fig. 5.76). The receptor cells' inner and outer segments were reduced. Much of the outer segment shrinkage appeared to result from breakdown of the receptor cells' disc membranes. However, the plasma membrane of the outer segment often appeared to be intact (Fig. 5.77). Other structures, possibly distended inner segments, were found adjacent to the pigment epithelium. These contained mitochondria or outer segment material.

The pigment epithelial cells were rounded and had lost their apical processes. Their nuclei were rounded, their mitochondria distended and their melanin granules were randomly distributed in the cells' apical cytoplasm (Fig. 5.77).

As in other tissues, within this group, after forty eight hours recovery, loss of receptor cells from the outer nuclear layer was associated with expansion of Müller cell cytoplasm. This increase in the quantity of Müller cell cytoplasm within the outer nuclear layer was accompanied by migration of the Müller cells' nuclei into the outer nuclear layer (Figs. 5.76 and 5.78). Much of the Müller cells' cytoplasm in the outer nuclear layer contained what was taken to be receptor cell debris (Fig. 5.78). In these areas both the inner retina and the choroid were of normal appearance.

In one of the blocks examined, animal 1/48h/2, block B2, the pigment epithelium was highly unusually in its appearance (Fig. 5.79). The cells were swollen, apical displacement of their cytoplasm accommodating the increased cell volume (Fig. 5.79 and 5.80). The nuclei of these cells were rounded and showed an unusual chromatin pattern (Fig. 5.80). Although present, the apical processes were much reduced in length. Melanin granules and a few phagosomes of outer segment material were present within the apical cytoplasm. In common with the normal appearance of the cell, the basal infoldings were present with their associated mitochondria. However, the mitochondria were slightly smaller and denser than normal. The junctional complexes were intact and particularly prominent due to the light staining of the cells cytoplasm (Fig. 5.80). the increased

cell size was probably due to the nuclear swelling and distension, or an increase in the amount of smooth endoplasmic reticulum. The surrounding retinal and choroidal tissues were unremarkable.

5.5.4 Group 1; 4 Days Recovery.

The appearances of the tissues from these animals can be divided into three groups: 1. blocks showing rapid transition from lightly to severely damaged tissue (animal 1/4D/1, blocks A2, B2 and D3). 2. blocks showing uniformly severe damage (animal 1/4D/1 block C2 and animal 1/4D/2 blocks B2 and C2). 3. blocks showing normal or near normal morphology (animal 1/4D/2 blocks A2 and D1). It was noted that the degree of damage exhibited by a block matched well the region of the lesion from which it was taken (Fig. 5.3).

In regions of rapid transition from lightly to severely damaged tissue, many of the patterns of damage seen throughout the lesion were present within the one block. For example, figures 5.81, 5.82 and 5.83 show fields taken from adjacent 100 mesh grid squares. The distance between these fields was around 300 μ m. At the outer edges of the lesion the only signs of damage were slight irregularities in the disc stacking of the rod and cone outer segments. Within the pigment epithelium rounding of the nuclei and an increase in the electron density of the mitochondria were the only abnormalities (Fig. 5.81). As the lesion was approached there was a striking loss of photoreceptor cells (Fig. 5.82). Once again Müller cells had invaded the outer nuclear layer, filling the space once occupied by receptor cells (Fig. 5.82). At the edge of the lesion, the size of the individual pigment epithelial cells increased markedly. These cells often showed extension of their cytoplasm along

Bruch's membrane towards the centre of the lesion (Fig. 5.82).

Immediately within the edge of the lesion, the degenerative photoreceptor cells and pigment epithelial cells were similar in appearance to the severely damaged regions seen after twenty-four and forty-eight hours of recovery. Vacuolation and degeneration were still occurring within the inner and outer nuclear layers. Considerable quantities of photoreceptor and pigment epithelial cell debris were present (Fig. 5.83). Below the degenerate pigment epithelium long cytoplasmic processes were seen extending along Bruch's membrane (Figs. 5.83 and 5.84). It was thought that these processes were extensions of the viable pigment epithelium at the edge of the lesion. Below the severely damaged retina, at the edges of the lesion, numerous mononuclear cells were present within, and external to, the choriocapillaris (Fig. 5.83).

In one of the tissue blocks examined (animal 1/4D/1, block D3), there was, peripheral to the severely damaged tissue, an area of retina showing considerable photoreceptor loss (Fig. 5.85). Within this block, the repair of the damaged tissue was well advanced. Degenerate receptor cells were present although few in number. There was little, if any, photoreceptor debris seen within, or below, the outer nuclear layer. As in other regions of retina, previously described, replacement of receptor cells by Müller cell cytoplasm had occurred throughout the outer nuclear layer. Once again Müller cell nuclei were present within what remained the outer nuclear layer. The surviving photoreceptors showed a considerable reduction in the length of their inner and outer segments. This appearance may have been due, in part, to lack of orientation of the inner and outer segments (Fig. 5.86). The loss of receptor cells was reflected within

the outer plexiform layer, where there was a considerable reduction in the number of receptor cell synapses (Fig. 5.85). The remainder of the retina, the inner layers of the retina and the pigment epithelium, were normal in appearance, as was the choroid.

Within the lesions, the retina and the choroid showed uniform, severe damage. This severely damaged tissue could be divided into two categories. 1. Tissue taken from within the large lesion seen in animal 1/4D/1 showing little evidence of recovery. These blocks were similar in appearance to some of the severely damaged tissue examined after 24 hours recovery (Fig. 5.87). 2. Tissue taken from within the smaller lesion in animal 1/4D/1. Within this tissue, phagocytic cells were extremely common (Fig. 5.88). These different appearances were thought to be related to the patency of the choroidal vessels. Within the larger lesion the choriocapillaris was occluded by fibrin. The deeper vessels were filled with impacted red cells (Fig. 5.87). Within the smaller lesion, and toward the edges of the larger lesion, the vessels of the choriocapillaris were filled with mononuclear cells (Fig. 5.88). If, as was thought, these cells were monocytes, they could be the source of the macrophages seen within the damaged retinal tissues. After some of the earlier recovery periods (24 and 48 hours) mononuclear cells had been seen within the structure of Bruch's membrane. In a fortuitous section of the tissue from animal 1/4D/2 one of these cells was seen extending through all the layers of Bruch's membrane (Fig. 5.89). The two different appearances of the severely damaged retina stemmed from the degree of inflammatory cell invasion. This in turn would be related to the accessibility

of the damaged tissue to inflammatory cells. Access to the damaged tissue would be promoted by a patent choroidal circulation and inhibited by occlusion of the choroidal vessels.

In the retinal tissues well removed from the visible lesions (animal 1/4D/2, block D2) abnormalities in structure were limited to the outer segments (Fig. 5.90). The disturbances of disc stacking in the rods was more severe in the distal regions of the outer segment. The cone cells appeared to lack outer segments. Their inner segments were swollen and extended to the pigment epithelium (Fig. 5.90). However, some cone cell outer segment material could be identified at the level of the pigment epithelium. This material was identified as belonging to cone cells because of two reasons: its deep penetration into the pigment epithelium, and the numerous ensheathing pigment epithelial processes. These characteristics are typical of cone outer segments. The remainder of this tissue was normal in appearance.

5.5.5 Group 1; 1, 2 and 4 Weeks Recovery.

These three recovery periods were described together in the section on their light microscopic appearance. This approach will be adopted here as the tissues from these three recovery periods were found to have much in common.

Five of these six animals had lesions of the retina which were seen during dissection. The exception was animal 1/1W/2 in which no lesion was visible. The tissue examined from this animal appeared normal by both light microscopy but some pigment epithelial disturbances were seen by electron microscopy. The appearance of these tissues will be described later.

In all the tissue examined by electron microscopy no extracellular cell debris was seen. However, many cells contained phagosomes or secondary lysosomes.

The appearance of the tissues will be described under three main headings. 1. Areas showing complete loss of receptor cells and pigment epithelial cells. 2. Areas showing partial loss of photoreceptor cells. 3. Areas showing pigment epithelial proliferation or atypical macrophages.

Areas showing complete loss of photoreceptor cells and pigment epithelial cells were encountered in animals 1/1W/1, 1/2W/1, 1/2W/2, and 1/4W/2. The loss of the photoreceptor cells and pigment epithelial cells did not unduly affect the structure of the inner retina (Fig. 5.91). However, some loss of, and thickening of, cell processes within the inner plexiform layer was present. The absent photoreceptor cells and pigment epithelial cells were replaced by Müller cells' cytoplasm which came into direct contact with Bruch's membrane (Fig. 5.91). The Müller cells' cytoplasm immediately above Bruch's membrane was highly convoluted and formed numerous interdigitating processes. These processes contained scattered small mitochondria, and occasionally cisternae of rough endoplasmic reticulum (Fig. 5.92). Pigment laden cells were found near to Bruch's membrane (Fig. 5.92a). These cells were thought to be macrophages, rather than surviving pigment epithelium, as the melanin granules within their cytoplasm appeared to be undergoing degradation. Also, cells of this type were not seen in intimate association with Bruch's membrane as would be expected of pigment epithelial cells (Fig. 5.90a).

Bruch's membrane and the choroid in these regions were atypical. There was often considerable thickening of Bruch's

membrane. This appeared to be due to a marked increase in the amount of collagen present (Fig. 5.92a). This increase in collagen content was also present within the inner layers of the choroid (Fig. 5.92b). Within this tissue, and in tissue examined after shorter recovery periods, cells were seen within the structure of Bruch's membrane. Typically, these cells were mononuclear and had scant cytoplasm, which contained some of the organelles and inclusion bodies characteristic of monocytes. However, after the longer recovery periods, cells with more copious cytoplasm which contained melanin granules and possibly secondary lysosomes were encountered within the structure of Bruch's membrane (Fig. 5.92b).

Very occasionally, loss of cellular components extended beyond the receptor and pigment epithelial cells. In some instances there was complete loss of recognisable retinal components apart from ganglion cells (Fig. 5.93). This tissue appeared to be composed of highly disorganised Müller cells and large pigment-laden macrophages (Fig. 5.93). As in the regions of photoreceptor and pigment epithelial cell loss already described thickening of Bruch's membrane was common. As in the other areas, pigmented cells were found within the structure of Bruch's membrane. The choroid in these regions of gliotic retina frequently showed a marked increase in the amount of collagen present. In such regions there was also a reduction in both the size, and occurrence, of the vessels of the choriocapillaris (Figs. 5.93 and 5.94).

Regions showing reduced occurrence of photoreceptor cells were encountered in all animals examined 1, 2 and 4 weeks after exposure, with the exception of animal 1/1W/1. The degree of

photoreceptor loss was highly variable ranging from a slight to near complete loss. It became apparent that photoreceptors were only found in regions where the pigment epithelium had survived (Fig. 5.95). Four weeks after exposure photoreceptor cells showing recognisable inner and outer segments were only found in conjunction with pigment epithelium cells. Regions of a similar appearance were seen as early as four days after the light exposure (see Fig. 5.85). However, four days after exposure the regeneration of the photoreceptor inner and outer segments was less advanced. Four weeks after exposure, photoreceptor cells which were thought to have suffered a similar degree of damage had recognisable inner and outer segments below a well organised outer limiting membrane (Fig. 5.96a and b). The two regions compared were thought to have suffered a similar degree of damage as in both the inner retina, the choroid, the choriocapillaris, and the pigment epithelium were all of a similar appearance. Damage was restricted to the receptor cells, which, in both cases, had been so reduced in number as to comprise a layer of only one or two nuclei within the outer nuclear layer.

Macrophages were first seen in the interphotoreceptor space 24 to 48 hours after the light exposure. They were a common finding by the fourth day after exposure. After the longer recovery periods (1, 2 and 4 weeks) macrophages were often seen in areas which had suffered extensive loss of retinal elements. These macrophages were extremely large and packed with melanin (Fig. 5.93).

Regions of pigment epithelial proliferation or atypical macrophages were often associated with slight detachment of the neural retina. Some of these areas were thought, on

initial examination by light microscopy, to show pigment epithelial proliferation (Fig. 5.35). Examination by electron microscopy, however, failed to support this impression. Examination of block A3 from animal 1/1W/2 by electron microscopy (light micrograph Fig. 5.35) allowed the majority of the cells present below the neural retina to be identified as macrophages. These macrophages lay inner to a layer of atypical pigment epithelial cells (Fig. 5.97). It was thought that these cells were true macrophages of haemotogenous origin as some did not contain any melanin. Also, cells of a similar appearance could be identified within the choroid and Bruch's membrane (Fig. 5.98). The retina adjacent to these accumulations of macrophages showed only slight abnormalities of the receptor cell outer segments (Fig. 5.97). The choroid and the choriocapillaris below these regions of macrophage aggregation contained a few scattered mononuclear cells and macrophages. Bruch's membrane was slightly thickened and contained a few cells (Figs. 5.97 and 5.98).

The other region of suspected pigment epithelial proliferation, block C2 from animal 1/4W/2, (light micrograph Fig. 5.36) was again associated with a slight detachment of the neural retina. Unlike the area already described, block A3 animal 1/1W/2, loss of photoreceptor cells was evident (Fig. 5.99). The pigmented cells seen by light microscopy were identified as pigment laden macrophages. The remainder of the cells forming this area of "proliferation" were thought to be Müller cells (Fig. 5.100). Their nuclear shape and chromatin pattern, and their cytoplasmic organelles were very similar to the cells identified as Muller cells which had migrated into the outer

retina as seen in Figures 5.82, 5.85, 5.91 and 5.92.

Diagrammatic summaries of the findings for each tissue block examined in the animals exposed to both the lower and higher intensity are given in figures 5.101 and 5.102.

The ability of the retina to recovery after a damaging light exposure is of obvious importance. This is especially true when the levels of illumination produced by some modern diagnostic instruments are considered (Fig. 5.103). In Chapter Four it was shown that the degree of damage suffered by the retinal and choroidal tissues was related to the intensity of light to which the eye was exposed. The degree of recovery shown by the retinal and choroidal tissues was likely to be related to both the intensity of the light to which the eye was exposed, and to the length of time for which the recovery processes were active.

To assess the effects of these variables, light intensity and recovery period, two series of rabbits were exposed to one or other of the two highest light intensities. The two light intensities employed had already been shown to produce retinal damage. In the case of the higher light intensity choroidal damage was also expected. Retinal and choroidal tissues taken from the rabbits in both series were then examined, by light and electron microscopy, at various periods after the light exposure (6 hours, 24 hours, 48 hours, 4 days, 1 week, 2 weeks, or 4 weeks).

As was discussed in Chapter 4, the variation of damage seen, even within one eye, was considerable. However, the problem of tissue selection was simplified due to the visibility of lesions of the retina during dissection. These lesions were seen in five out of the fourteen animals in the lower light intensity group and thirteen out of the fourteen animals in the higher light intensity group. In eyes having visible lesions,

tissue blocks were selected from areas within and around the lesion. In eyes where no lesion was visible, the blocks examined were selected randomly from within the previously illuminated area.

As already discussed in Chapter 4, illumination of the retinal and choroidal tissues must result in slight temperature increases. In studies employing lasers or photocoagulators, pre-exposure fundus or body temperature has been found to be related to the threshold for production of a retinal lesion (Ward and Bruce, 1971a; Ward and Bruce, 1971b; Polhamus and Welch, 1975). This effect is related to the amount of energy required to raise the retinal temperature sufficiently for thermal damage to occur. The amount of energy required would be decreased at high body temperatures and increased at lower body temperatures. In this respect the effect appears to be purely physical.

In the long term experiments of Noel, Walker, Kang and Berman (1966); Friedman and Kuwabara (1968); Grigolo, Orzalesi and Vitone (1969) and Hannson (1970a) elevated body temperature during the light exposure increased the rate of appearance, and the extent of the retinal damage.

Many investigators have suggested that light damage is separate from thermal damage because the light levels are simply too low to cause denaturation of retinal proteins. Kuwabara and Gorn (1968) showed no appreciable increase in retinal temperature elevation under 1,000ft-c of illumination: light damage being produced by exposure to 750ft-c in their study. Harwerth and Sperling (1971) produced behavioral sensitivity shifts at power levels as low as one thousandth the level reported by Ham, Williams, Mueller, Guerry, Clarke and

Geeraetes (1966) for thermal damage, or for pigment epithelial damage as reported by Friedman and Kuwabara (1968).

The primary site of thermal damage is the pigment epithelium and is related to the density of melanin granules present (Geeraetes and Ridgeway, 1963; Ham, Wiesinger, Schmidt, Williams, Ruffin, Shaffer and Guerry, 1958; Lappin and Coogan, 1970). Thermal damage is greater in the more pigmented areas of an individual eye and greater in pigmented eyes than in albino eyes (Geeraetes, Williams, Chan, Ham Guerry and Schmidt, 1962; Geeraets and Ridgeway, 1963; Lappin and Coogan, 1970).

The damage observed in this study did not appear to be related to pigmentation, and was of a highly irregular nature, similar to that described by Lawwill (1973). Although heat released by the absorption of light cannot be ruled out (see Appendix 4) it seems more likely that the damage observed in this study was produced by excessive illumination rather than heating. Possible mechanisms underlying light damage have already been described in Chapter 4.

Immediately after exposure, and throughout the recovery periods, cell damage and cell loss was greater in the higher light intensity group. In the lower intensity group damage was mostly restricted to the photoreceptors and pigment. Damage to the inner retina was rare, but it did occur in some of the tissues examined after the longer recovery periods (one to four weeks). This will be discussed later. The milder changes in the appearance of the outer retina were in general agreement with those reported by Kuwabara and Okisaka (1976), Ham, Ruffolo, Mueller, Clarke and Moon (1978), and Fuller, Machemer and Knighton (1978) even although a considerable species difference between monkeys,

used in the investigations cited, and rabbits, used in this investigation, had been expected.

In the group exposed to the higher light intensity six hours, twenty four hours and forty eight hours of recovery were associated with extensive damage to the photoreceptors and the pigment epithelium. During the recovery periods of twenty four and forty eight hours degenerating cells were observed within the inner nuclear layer. Ultrastructural changes in the Müller cells and horizontal cells of human retina have been reported by Radnot, Jabbagy, Heszeiger and Lovas (1969). These changes were seen at the end of a forty three minute exposure to light and not after any recovery period. In this study the degenerating cells in the inner nuclear layer seen within forty eight hours after exposure to the higher intensity light, were horizontal, bipolar and amacrine cells. The Müller cells appeared to be surprisingly resistant to damage.

During the early stages of recovery, in regions of extensive damage to the outer retina, Muller cells appeared to be particularly active in the processes of repair. Their cytoplasm extended into the volume once filled by receptor cells. The Müller cells' cytoplasm in these areas contained phagosomes of receptor cell material. This expansion of the Müller cell cytoplasm into the outer nuclear layer was associated with migration of the Müller cells' nuclei into the area of expanding cytoplasm. The reason for this nuclear migration is not understood. In areas of extensive Muller cell replacement, the Müller cells were responsible for the preservation of the outer limiting membrane, which separated the degenerating outer retina from the surviving inner retina. Very similar findings were reported by Hansson (1970a). Hansson followed the pattern

of recovery of the rat retina following light damage produced at elevated body temperature. After two weeks of recovery, Hansson reported that, in regions showing complete loss of photoreceptors and pigment epithelium, the Müller cells apposed Bruch's membrane. Similar regions were seen in this study one week after exposure to the higher intensity. After longer recovery periods, Müller cell cytoplasm was found to extend through the outer limiting membrane and contact the apical surface of the pigment epithelium. These regions of Müller cell and pigment epithelial cell contact were only observed in regions of surviving receptor cell and pigment epithelial cells. The Müller cells' cytoplasm filled the enlarged spaces between the decreased numbers of receptor cell outer segments, in what could be termed the inter photoreceptor space. Complete loss of the receptor cells, and fusion of the Müller cells with the pigment epithelium, as described by Kuwabara and Gorn (1968), was not observed in this study. The survival of receptor cells appeared to be intimately associated with the presence of viable pigment epithelium. The importance of the retinal pigment epithelium in the maintenance of the retina has been stressed by Meier-Ruge (1969), Straatsma, Hall, Allan and Cresatelli (1969) and Hansson (1970a).

Lawwill (1973) investigated the effects on the rabbit retina of four hour exposures to both white light (xenon arc) and a monochromatic source (argon laser). In Lawwill's study the effects of the exposures were assessed by electroretinography, ophthalmoscopy, and histopathology. The tissue examined histologically was obtained from animals killed one to four months after exposure. Damage was assessed on a scale of 0 to 4+, with the rating determined by the most severe damage present in an eye. The criteria used by Lawwill are given below.

- + : mild oedema and disruption of the receptor cell layer.
- 1+ : oedema, disruption of receptor cell outer segments and early involvement of the pigment epithelium.
- 2+ : oedema, almost total disruption of the receptor cells with changes in the nuclei, and extensive pigment epithelial changes.
- 3+ : total loss of the receptors but with preservation of the inner nuclear layer.
- 4+ : complete loss of identifiable retinal structure.

In Lawwill's study, as in this study, there was considerable variation in the degree of damage suffered by the retina. Lawwill stated that the degree of damage appeared to be determined by the density of the photoreceptor cells. This would seem to be a reasonable proposition as the studies of Noel, Walker, Kang and Berman (1966), and Gorn and Kuwabara (1967) implied that the effectiveness of a light source in producing light damage is related to its efficiency in bleaching the photoreceptor pigments. If light damage is mediated by some by-product of rhodopsin bleaching, there would be more of this by-product in regions of high receptor density. (This does not take into account the extreme effectiveness of blue light in producing light damage. This has already been discussed in Chapter 4.) The area of greatest photoreceptor density in the rabbit eye is found in the region of the visual streak (Hughes, 1971). It was in that region that Lawwill found highest degree of damage. This finding was not confirmed by this study, but differences in the light sources, area of retinal illumination, and the length of the experimental exposure may account for this discrepancy.

The alterations in retinal structure seen by Lawwill ranged from slight oedema, associated with disturbances of the photo-receptors and pigment epithelium, to complete loss of retinal structure. Comparisons between Lawwill's study and this study are difficult as formaldehyde fixation and conventional histology were employed in Lawwill's investigation. There are, however, similarities in the appearance of the retinal tissues. In the low intensity group of this study, retinal damage was seen two to four weeks after exposure. This damage did not appear to be directly related to the light exposure as the retinac of animals examined up to about the second week of recovery appeared to be regaining their normal appearance. However, at the later recovery periods, two and four weeks, regions of damaged retina were seen in three out of the four animals. In such regions there was detachment of the neural retina and a generalised intra-cellular oedema of the retina. Frequently pyknotic receptor cell nuclei were seen. The appearance of the retina differed markedly from that produced by light damage. It was closer in appearance to that of rabbit retina exposed to periods of total acute ischaemia as described by Johnson (1974) and Johnson and Foulds (1978). The appearance of the retina after sixty to one hundred and twenty minutes of acute ischaemia (Johnson, 1974 and Johnson and Foulds, 1978) was very similar to that shown in Figures 5.51, 5.52 and 5.53. If ischaemia produces an appearance similar to that seen in this study, it seems likely that the underlying mechanisms of damage may be similar. Two of the four blocks exhibiting an "ischaemia" pattern of damage showed irregularities of the choroidal vasculature. There was either invasion of the choriocapillaris by inflammatory cells or blockage of the choriocapillaris by impacted red cells and platelets. The many ischaemic studies conducted in primates are not comparable, as primates possess a retinal circulation, which the rabbit

lacks. The presence or absence of a retinal circulation would be crucial in determining the sparing or loss of the inner retina following cessation of blood flow in the choroid.

The lower intensities employed by Lawwill (1973) resulted in what he terms 1+ and 2+ changes. These 1+ and 2+ changes were associated with disturbances of the retinal pigment epithelium. Similarly, in this study, disturbances of the retinal pigment epithelium were seen after the longer recovery periods in the lower intensity group. these regions of pigment epithelial disturbances were invariably associated with folding or detachment of the neural retina. Pigment epithelial disturbances of a similar appearance to those described in this study (Figs. 5.47, 5.49, 5.97 and 5.98) have been described in the rabbit retina, following experimental retinal detachment (Johnson and Foulds, 1977) and in the rhesus monkey retina following retinal detachment (Machemer, 1968; Kroll and Machemer, 1968; and Machemer and Laqua, 1975).

In this and other studies, regions of suspected pigment epithelial proliferation or "budding", described by Johnson and Foulds (1977), have been associated with the presence of macrophages in the sub-retinal space. In a study of the rabbit pigment epithelium following photocoagulation Gloor (1969) observed mitosis and proliferation of the pigment epithelium. He concluded that pigment epithelial mitosis and proliferation gave rise to the macrophages seen in his study. Gloor proposed the term "pigment epithelial macrophage" as the name for a pigment epithelial cell which behaves like a macrophage. In 1975 Mandelcorn, Machemer, Fineberg and Herch demonstrated proliferation of intravitreal retinal pigment epithelial cell autotransplants, in rhesus monkey eyes. Perhaps more conclusively Mueller-Jensen, Machemer and Azarnia (1975) demonstrated similar proliferation and redifferentia-

tion of rabbit retinal pigment epithelial cells autotransplanted in cell tight diffusion chambers. This approach removed the possibility of secondary contamination of the transplanted cells, but did not remove the possibility that the cells were contaminated in the first place by cells of other than pigment epithelial origin. These studies strongly suggest that the retinal pigment epithelium of the rhesus monkey and the rabbit are capable of proliferation and redifferentiation into macrophage-like cells. this was obviously one source of the macrophages seen in this study.

In both the lower and higher light intensity groups macrophages were observed among the photoreceptor and pigment epithelial cell debris. In both groups they were present within twenty four to forty eight hours. In the higher intensity group they were particularly numerous by the fourth day of recovery. The origin of these macrophages is in some doubt. As already suggested the retinal pigment epithelium could, either by proliferation or budding, give rise to these cells. Such an origin for the macrophages seen in this study was considered. However, it was thought unlikely that the majority of the macrophages seen in this study originated from the pigment epithelium for the following reasons:

- 1) No mitotic figures were ever observed within the pigment epithelium or the retina. The fact that none were seen does not preclude their existence. this finding is in contrast to the observations of Ishikawa, Uga and Ikai (1973), Ishikawa and Ikai (1974) and Wallow Tso and Fine (1975) all of whom reported mitotic figures in the retina following photocoagulation.

- 2) In the regions of greatest damage macrophages were common. In these areas the pigment epithelium had been destroyed by the photic insult. Therefore it could not be the source of

these macrophages. Proliferation of retinal pigment epithelial cells at the edges of the lesion and subsequent migration of pigment epithelial macrophages was never observed. Sliding of surviving pigment epithelial cells beneath degenerate pigment epithelium was seen at the edges of the lesions (Fig. 5.84).

The macrophages seen within the retina were thought to be of haemotogenous origin for the following reasons:

- 1) Beneath severely damaged regions of retina, where macrophages were plentiful, mononuclear cells filled the vessels of the choriocapillaris and were common in the extravascular tissues of the choroid. If, as was thought, these cells were monocytes, they represented a source for the macrophages seen in the subretinal space.

- 2) the mononuclear cells were also observed within the structure of Bruch's membrane. They usually lay immediately below the basement membrane of the pigment epithelium. On one occasion a favourable section revealed one of these cells penetrating the complete thickness of Bruch's membrane (Fig. 5.89). As the nucleus of the cell remains in the plane of section throughout the region of penetration of Bruch's membrane it is apparent that Bruch's membrane does not represent a barrier to the migration of these mononuclear cells from the choroid into the retina.

Following retinal detachment in the rabbit cells of haemotogenous origin have been seen within the structure of Bruch's membrane, and among proliferated retinal pigment epithelial cells (Johnson and Foulds, 1977). Following mixed sympathetic and lens induced ophthalmitis cells of haemotogenous origin have been observed below the basement membrane of the pigment epithelium (Lee and Grierson, 1977).

During the early stages of phagocytosis of receptor cell and pigment epithelial cell debris, forty eight hours to four days after the photic insult, macrophages were very common. These phagocytic cells were ultrastructurally very similar to those described by Hannson (1970a). Hannson thought that the phagocytosing cells were partly derived from glial cells in the inner half of the retina and possibly from blood cells, as in the case of brain macrophages (Konigsmark and Sidman, 1963). In the study of Hannson the phagocytosing cells appeared during the second day of recovery and rapidly removed the cell debris. Most of the cell debris was removed within one week and little remained thereafter. These observations of Hannson are very similar to what was seen in the higher intensity group of this investigation. There were, however, some differences. According to Hannson the phagocytosing cells first appeared in the inner retina and migrated outward into the photoreceptor debris. Similarly, in another light damage study in the rat, O'Steen and Lytle (1971) first noted the presence of phagocytosing cells in the outer plexiform and receptor cell layers. In a later paper, (O'Steen and Karciglu, 1974) light damaged rats were injected intravenously or intravitreally with fine carbon particles in an attempt to follow the pattern of invasion, migration and egression of the carbon filled phagocytes in eyes with degenerate retinae. They concluded that retinal debris was removed by two populations of cells: mononuclear cells of vascular origin, and pigment epithelial cells. Following retinal damage, mononuclear cells were first detected in the vitreous body.

At later recovery periods they were seen progressively deeper in the inner plexiform layer and out to the bipolar layer, where they were seen within, or partially within, the retinal

capillaries. They concluded that these mononuclear cells entered the eye through the central retinal artery or its capillaries, and left through the central retinal vein. They also concluded that phagocytic cells did not leave the retina by way of the choroidal circulation, as following intravitreal injection of carbon particles, phagocytes containing carbon particles were never observed in the choroid or choroidal vessels. In the study of O'Steen and Karcioglu, pigment epithelial cells which had proliferated by mitotic activity, occurred as single cells separated from Bruch's membrane by the photoreceptor debris. After direct exposure to carbon particles, pigment epithelial cell phagosomes contained both carbon and lamellated discs of outer segment material. They could not determine whether these cells left the eye through the retinal capillaries or returned to Bruch's membrane to re-establish continuity in the pigment epithelium.

The ultrastructure of the phagocytic cells seen in the studies of Hannson (1970.a), O'Steen and Lytle (1971) and O'Steen and Karcioglu (1974) and their period of peak activity (2-4 days after the initial damage to the retina) was very similar to that seen in this study. However, in the studies cited, the phagocytic cells entered and left the retina via the central retinal artery and the central retinal vein. In this study it appears that the majority of the phagocytic cells entered the retina from the choroidal circulation, passing through Bruch's membrane. This difference in the behaviour of the phagocytic cells can probably be explained by the fact that the rat possesses a retinal circulation which the rabbit lacks. If the phagocytosing cells are of haemogenous origin in both the rat and the rabbit, they have little option in the rabbit but to enter the retina from the

choroidal circulation. It is possible that blood borne cells could enter the rabbit retina from the vessels of the medullated nerve fibres. Mononuclear cells were observed around the vessels in this area and among the fibres of the cortical vitreous. It was thought unlikely however, that these cells would make any significant contribution to the population of phagocytosing cells.

O'Steen and Karioglu (1974) reported that, following intra-vitreous injection of carbon particles, carbon containing phagocytes were never observed in the choroid. They concluded that it was unlikely that retinal phagocytes escaped from the retina by passing through Bruch's membrane and into the choroidal circulation. However, from the results of this study, it was thought that the retinal phagocytes left the site of damage via Bruch's membrane and the choriocapillaris. In figure 5.92b a cell containing pigment epithelium like melanin granules can be seen within the structure of Bruch's membrane. It was thought that cells of this nature had been previously active phagocytes (hence the melanin), which were leaving the site of retinal damage, and migrating toward the choroidal vasculature.

Pigment containing macrophages were a common feature of the choroid in the higher intensity group. It was thought that some of these cells may have been retinal phagocytes, which had migrated back into the choroid. It is possible, however, that cells such as the one shown in Figure 5.92b may be migrating into the retina, and not out of it. The melanin content of the cells being derived from damaged choroidal melanocytes.

Invasion of the retina by phagocytic cells which appear to originate in the choroid and enter the retina through Bruch's membrane has been observed in rabbit retinae damaged by diamino-diphenoxypentane. (Orzalesi, Grignolo, Calabria, Castellazzo,

1967) but not those damaged by sodium iodate or fluoride (Grignolo, Orzalesi and Calabria, 1966, Orzalesi, Grignolo and Calabria, 1967). Hansson (1970a). Hansson and Sourander (1970) reported, following light induced retinal degeneration in the rat, lipid laden macrophages passed through an apparently intact Bruch's membrane to appear in the choroid, often perivascularly. Following exposure of monkey eyes to light from an indirect ophthalmoscope Tso (1973) concluded that the phagocytic cells left the site of injury by way of the choroidal vasculature. It seems possible that the pattern of phagocyte invasion and egression is related to the extent of retinal and choroidal damage produced by the light exposure, or other insult employed. In the present study and that of Hansson (1970a) choroidal damage was occasionally encountered. Complete loss of the choriocapillaris was seen in this study, and invasion of the damaged choriocapillaris by mesenchymal cells was observed by Hansson (1970a). Phagocytes leaving the retina might be influenced by the degree of damage present, not only in the retina, but also in the choroid. It is interesting to note that the retinal degeneration induced by diaminodiphenoxypentane (Orzalesi, Grignolo, Calabri and Castellazzo, 1967) results in rapid and complete destruction of the pigment epithelium. The degeneration induced by iodate or fluoride result in a patchy destruction of the pigment epithelium. It appears that where there was complete destruction of the pigment epithelium non-native phagocytic cells invade the retina and are active in the removal of cellular debris. If pigment epithelial cells survive, these surviving cells become more macrophagic in character and are active in the removal of cellular debris, without any assistance from non-native phagocytic cells. Similar results are obtained following retinal degeneration induced

by iodoacetic acid (Orzalesi, Calabria and Gignolo, 1970). Iodoacetic acid appears to be highly specific in its action, causing destruction of the receptor cells by leaving the pigment epithelium and inner retina intact. Following poisoning by iodoacetic acid, receptor debris is removed by pigment epithelial cells and Müller cells. It appears that the fate of the pigment epithelium, following administration of retino-toxic compounds, or exposure to damaging illumination, is important in determining which cells are responsible for the phagocytosis of cell debris. If the pigment epithelium survives, it and possibly the Müller cells, are responsible for the removal of debris. If the pigment epithelium is destroyed, non-native cells invade the retina and are responsible for the removal of cell debris.

One further piece of evidence points to a haemotogenous origin for the phagocytic cells seen in this study. Phagocytic cells were usually most numerous at the edges of severely damaged regions. It was thought that this vigorous response was due to the patency of the surrounding choroidal vessels. In the centre of severe lesions the choroidal vessels were occluded by impacted red cells, fibrin clots and degranulated platelets. Therefore, if the phagocytic cells were of haemotogenous origin, they would be far more numerous at the edges of the lesions where they had easier access to the damaged tissues. As already stated, this was in fact seen.

In the immediate effects study it was thought that occlusion of the choriocapillaris, or deeper choroidal vessels, would give rise to regions of increased retinal damage due to the combined effects of light exposure and ischaemia. This process was also thought to be responsible for the areas of extreme retinal damage seen in the recovery series of experiments.

In the group exposed to the higher light intensity, after one, two or four weeks recovery, regions of complete loss of photoreceptor and pigment epithelial cells were seen. In these areas there was, occasionally, an associated loss of the choriocapillaris. It was usually replaced by fibroblasts and collagen fibres, Bruch's membrane, adjacent to these areas, showed a highly irregular thickening. The collagenous layers of Bruch's appeared to have increased markedly in thickness. The source of this collagen is in some doubt. The cells seen within Bruch's membrane may have been responsible, but this is highly unlikely if they were monocytes. The two remaining possibilities are: 1) It was produced by choroidal fibroblasts. 2) It was secreted by the Müller cells, which had replaced the outer retina. Fibroblastic invasion of Bruch's membrane following the passage of the mononuclear cells would be the most favourable alternative.

Thickening of Bruch's membrane, with or without loss of the choriocapillaris, must have a considerable effect on the diffusion of metabolites and metabolic by-products to and from the retina. It seems very likely that the condition of Bruch's membrane will exert a considerable influence on the degree of recovery achieved by the retina.

In the non-survival series of experiments it was found that the cone cells' outer and inner segments were more susceptible to light damage than their rod equivalents. Similar findings have been reported in pigeon retinae damaged by continuous illumination from fluorescent lamps (Marshall, Mellerio and Palmer, 1972). Curiously the increased sensitivity of the cone cell outer segment does not appear to influence the survival of the cell or its eventual regeneration of outer segment material. In a study of light damaged rats supposedly lacking photoreceptors Anderson and O'Steen

(1972) demonstrated that the rats possessed both black/white and pattern recognition. It was later demonstrated by La Vail (1976a) that there were in fact surviving photoreceptor elements in the chronically light damaged rat retina. These surviving elements were later identified as cones (Cicerone, 1976). In this investigation, in the group exposed to the higher light intensity, cones were frequently encountered among the surviving photoreceptor cells. They could be identified as cones on the basis of their nuclear chromatin pattern and the presence of synaptic pedicles. They appeared to comprise far more than their predicted 8% of the photoreceptor population (Hughes, 1971). To account for this discrepancy it is necessary only to hypothesise selective loss of rod photoreceptor cells.

In the high intensity group, regeneration of photoreceptor outer segment material began about one week after the photic insult. It still appeared to be progressing four weeks after the photic insult. Therefore the regeneration of the outer segments appeared to be considerably slower than that predicted by the studies of Young (1967); Bok and Hall (1971); La Vail, Sidman and O'Neil (1972); and Wyse (1980). These studies indicated a complete turnover of the rat outer segment in about nine days. In the higher intensity group of this study, the surviving photoreceptors still appeared abnormally short, even after twenty eight days of recovery. This discrepancy in the rate of outer segment regeneration was probably due to damage of the inner segment and even the cell body of the receptor. Thus the repair processes would be more involved and consequently take longer. Also complete regeneration of an outer segment is probably more demanding than the gradual turnover of an already existing outer segment.

There remains the possibility that some of the degenerative changes seen within the experimental tissue were the result of age changes. Light damage and age changes, in the rat, have been shown to produce a similar morphology (Weisse and Stotzer, 1974).

Age changes in the rat take several years to develop. The longest survival period employed in this investigation was twenty eight days and control eyes were usually of normal appearance. Therefore it can be concluded that the changes seen in the experimental eyes in this study were attributable to light exposure or to its secondary effects.

Figures 5.1 to 5.4 show the positions of the retinal lesions seen during dissection. If no lesion was seen during dissection no diagram is shown. The key shown below refers to all four figures.

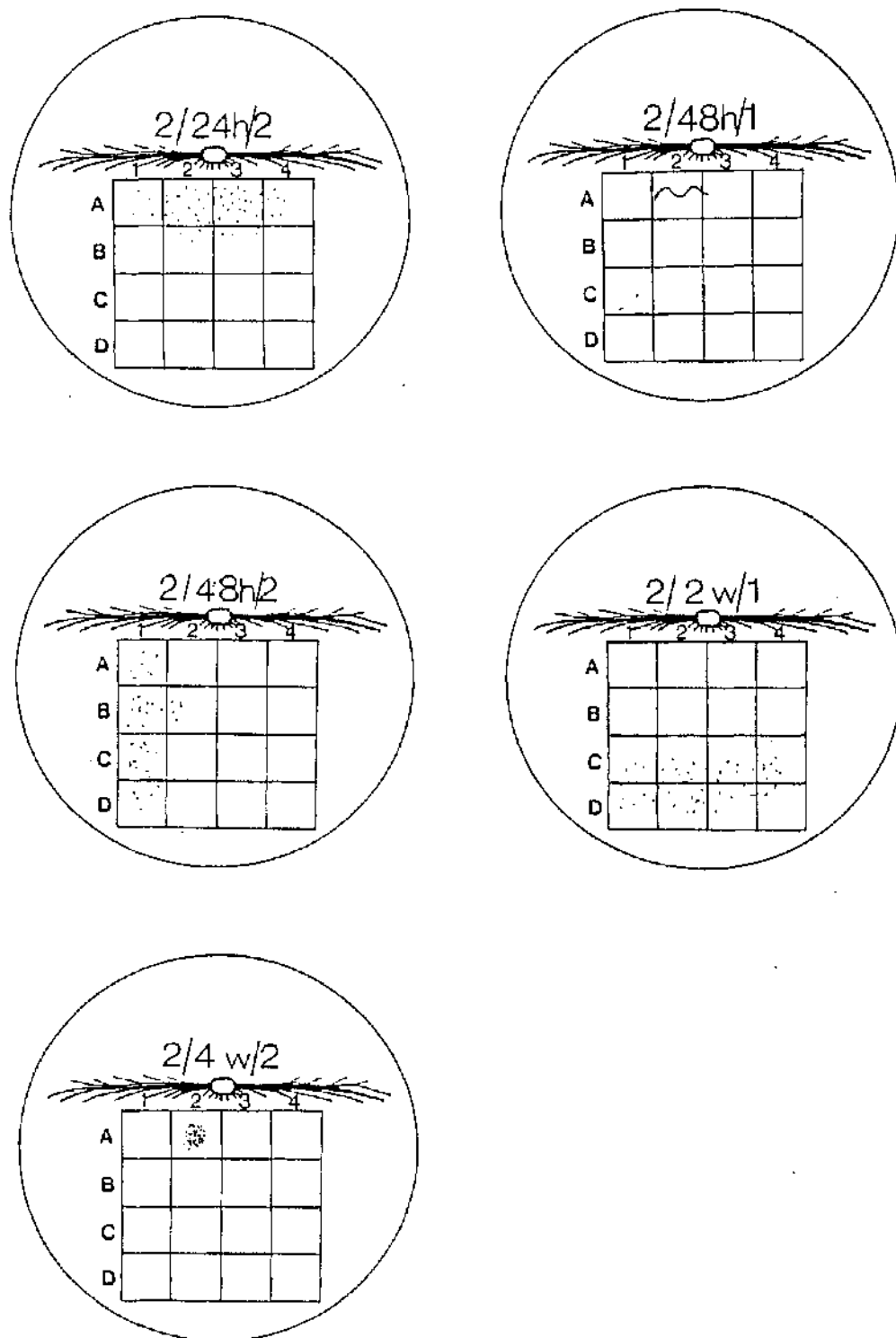


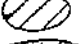
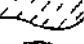



Figure 5.1

KEY

-  PIGMENTARY DISTURBANCE
-  RETINAL FOLD
-  AREA OF WHITE DISCOLOURATION
-  AREA OF PATCHY DISCOLOURATION
-  AREA OF REDUCED RETINAL THICKNESS

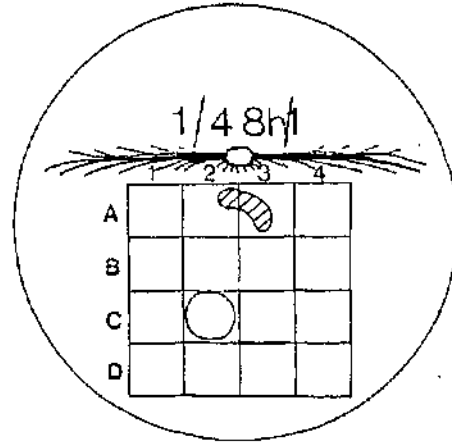
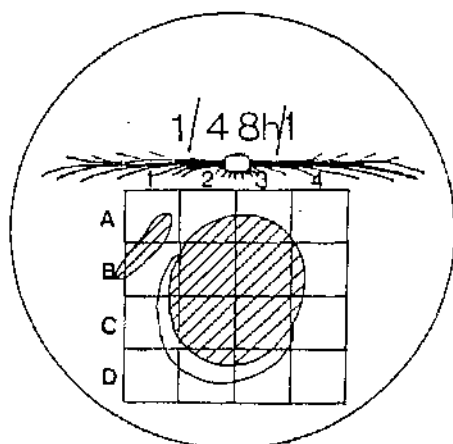
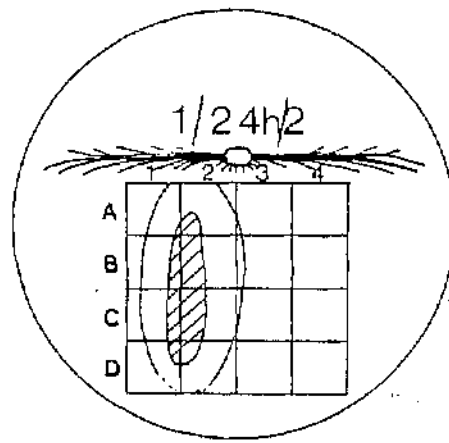
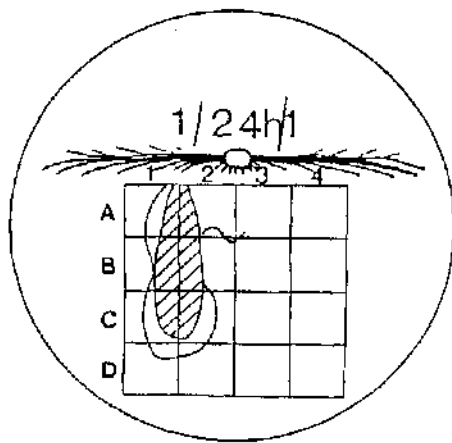
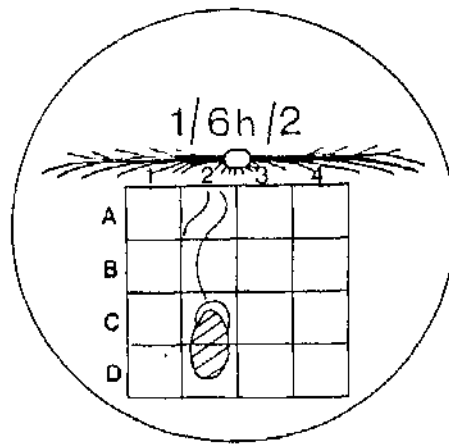
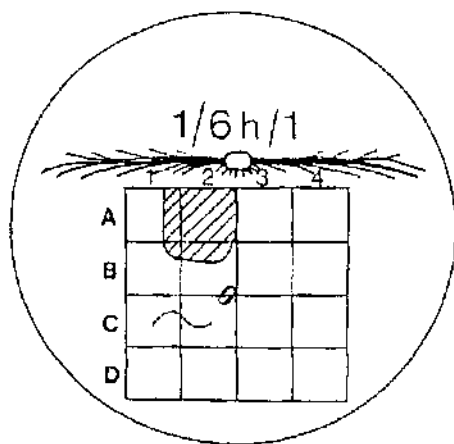


Figure 5.2

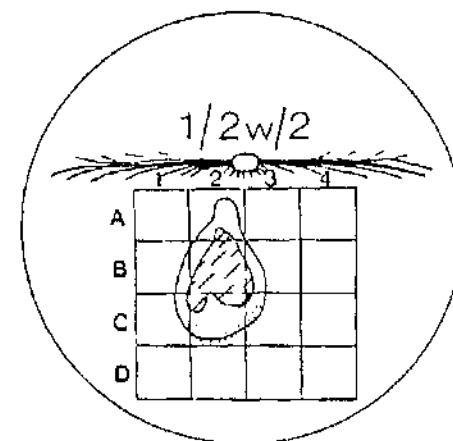
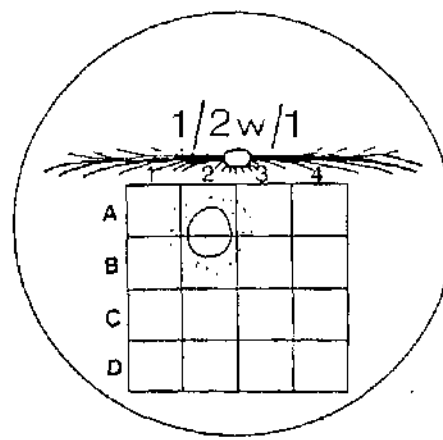
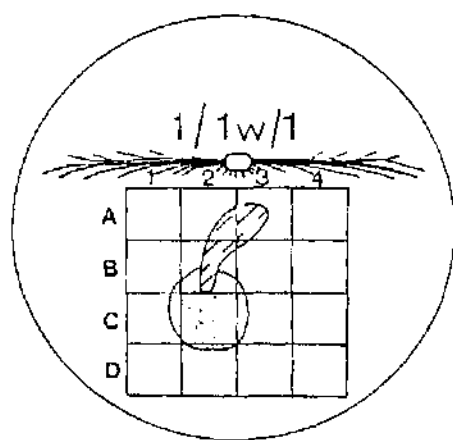
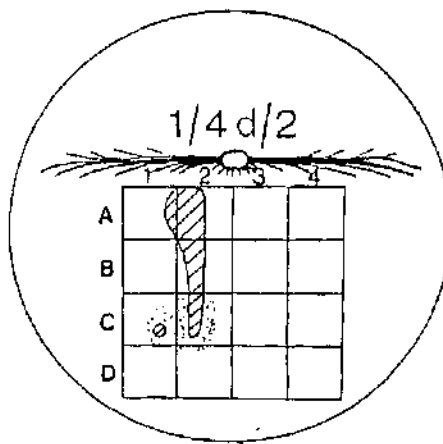
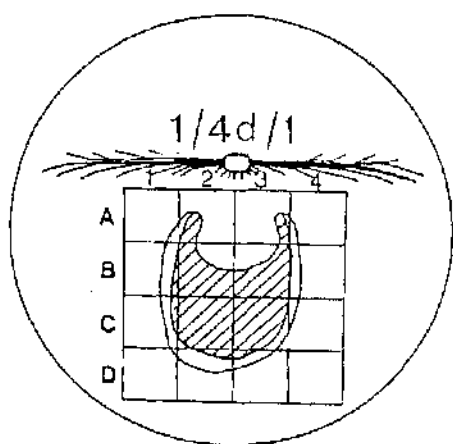


Figure 5.3

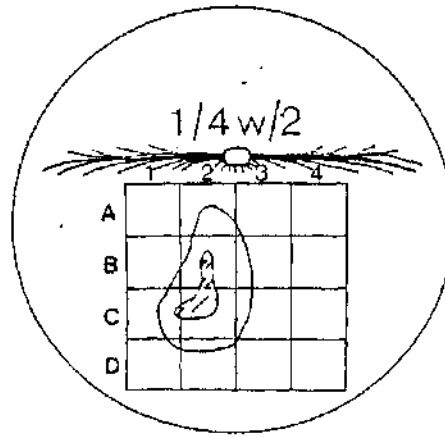
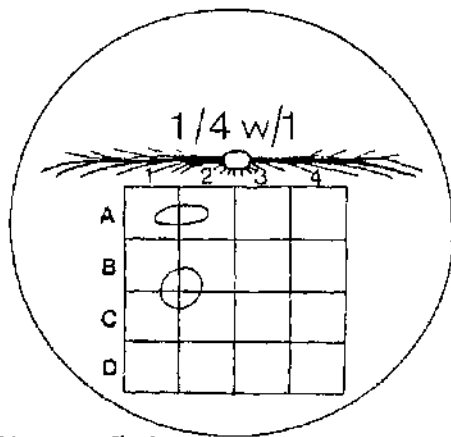


Figure 5.4

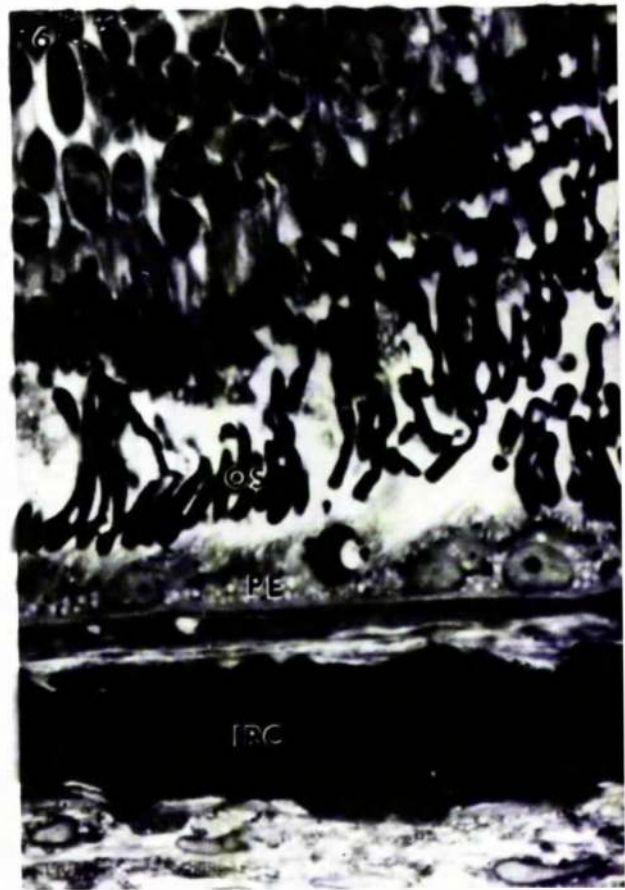
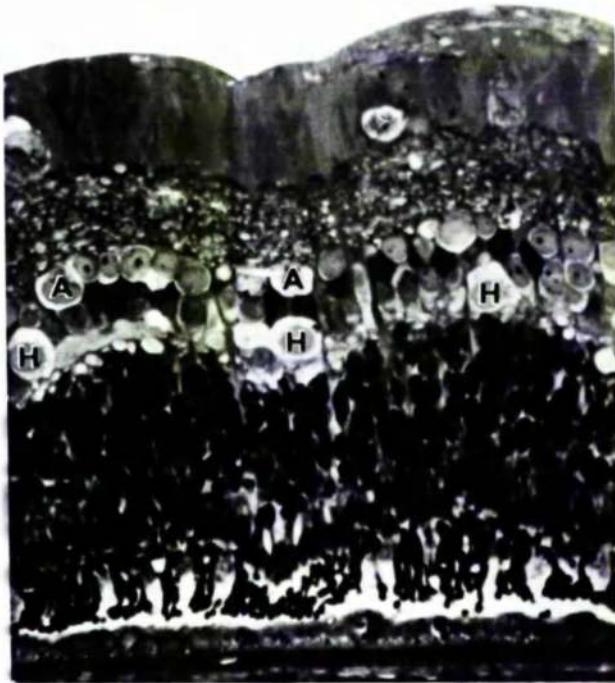


Figure 5.5 (2/6h/1 block D4). Light micrograph showing the appearance of the retina, six hours after exposure to light of the lower intensity. A: amacrine cell; H: horizontal cell (x 400).

Figure 5.6 (2/6h/1 block D4). Light micrograph showing the appearance of the outer retina, six hours after exposure to light of the lower intensity. OS: outer segments; PE: pigment epithelium; IRC: impacted red cells (x 1000).

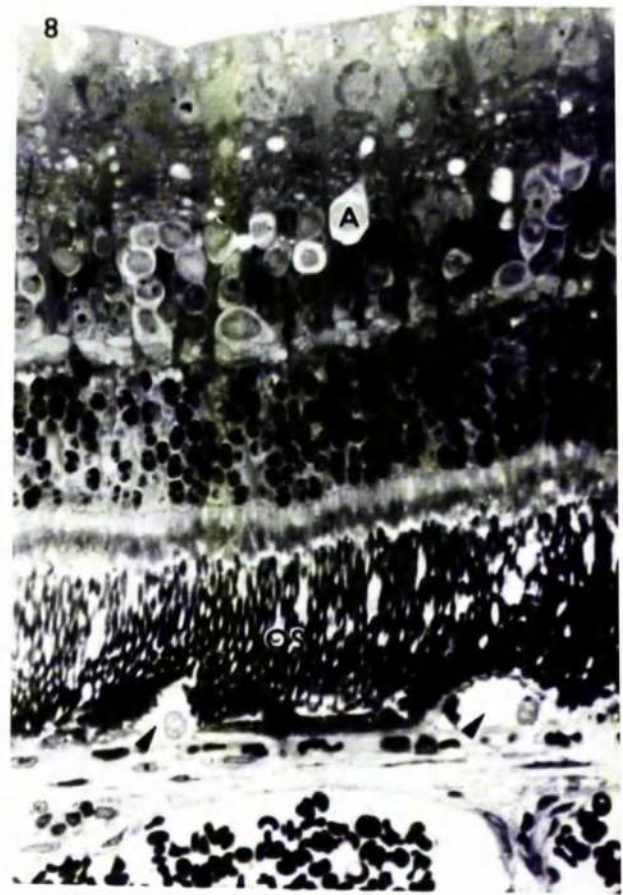
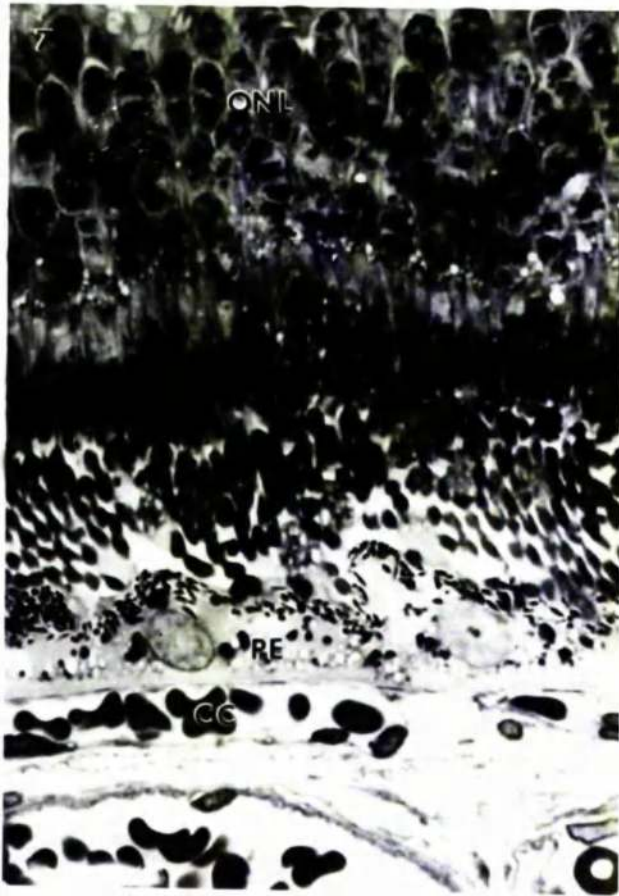


Figure 5.7 (2/24h/1 block D2). Light micrograph showing the outer retina and the choriocapillaris, twenty four hours after exposure to light of the lower intensity. ONL: outer nuclear layer; PE: pigment epithelium; CC: choriocapillaris (x 1000).

Figure 5.8 (2/24h/1 block C1). Light micrograph showing the retina, twenty four hours after exposure to light of the lower intensity. Arrows: disrupted pigment epithelial cells; OS outer segments; A: amacrine cell (x 400).

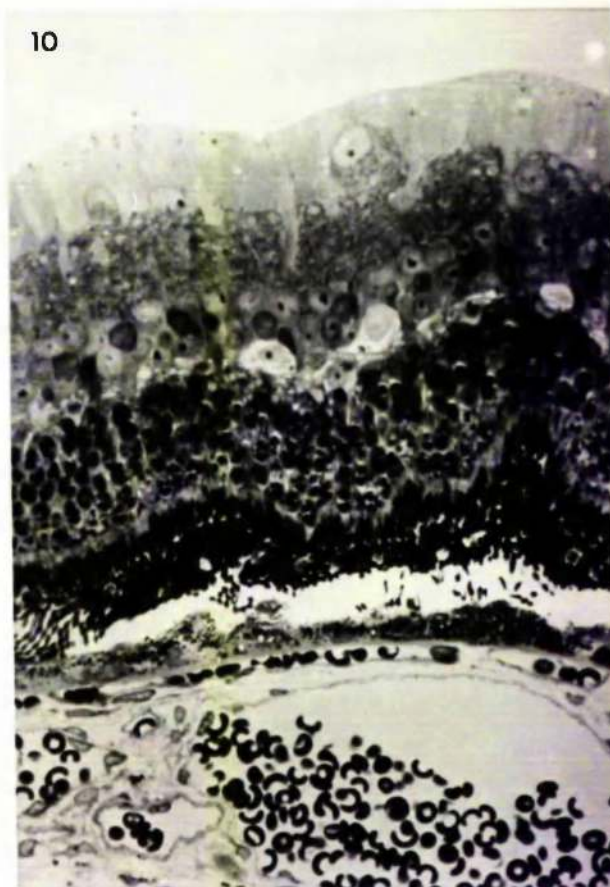


Figure 5.9 (2/48h/1 block A2). Light micrograph showing the outer retina, forty eight hours after exposure to light of the lower intensity. Ma:macrophage; PE: pigment epithelium; Arrow: Mononuclear cell within Bruchs membrane (x 1,000).

Figure 5.10 (2/4D/1 block C4). Light micrograph showing the retina and choroid, four days after exposure to light of the lower intensity. Numerous phagosomes are present within the pigment epithelium (x 400).

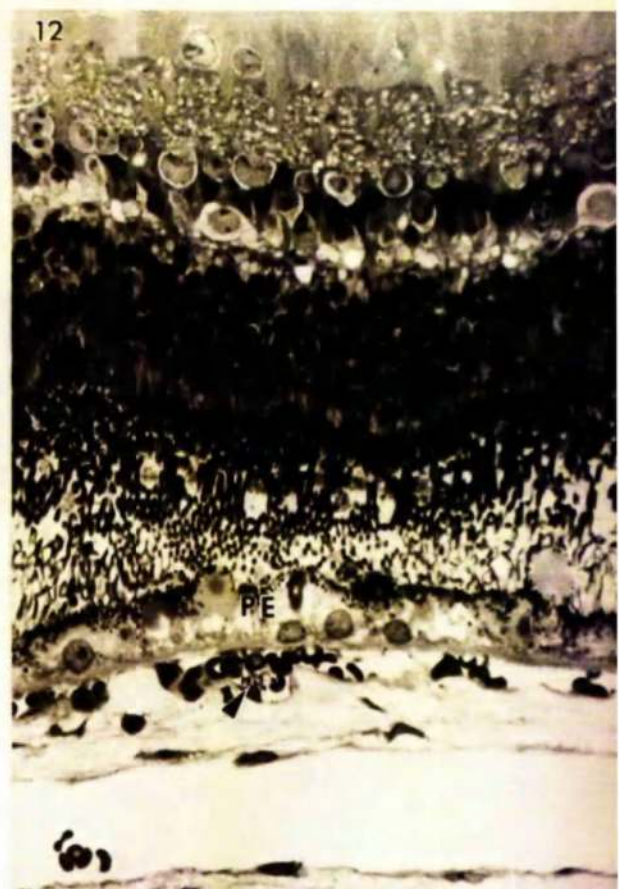


Figure 5.11 (2/4D/2 block A1). Light micrograph showing the appearance of the outer retina, four days after exposure to light of the lower intensity. One of the cells forming the irregular layer above the pigment epithelium is shown. PE: pigment epithelium (x 1000).

Figure 5.12 (2/1W/1 block C2). Light micrograph showing the appearance of the retina, one week after exposure to light of the lower intensity. There is a small lesion of the pigment epithelium overlying a vessel of the choriocapillaris. The vessel contains a small thrombus of red cells and platelets. PE: pigment epithelium; Arrow: thrombosed vessel (x 400).

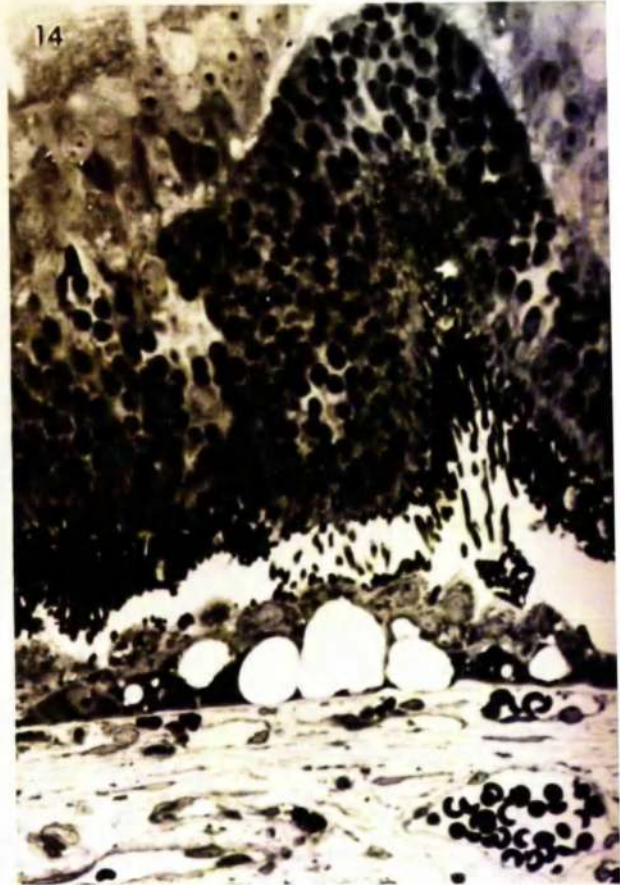
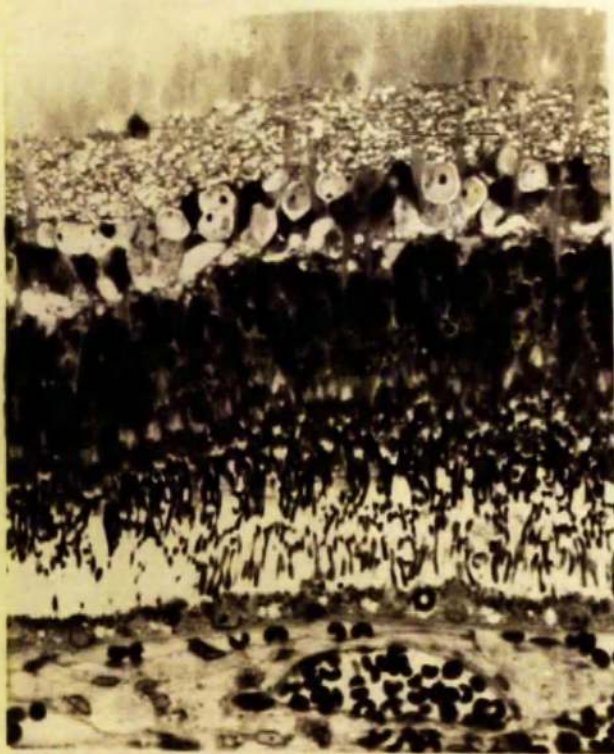


Figure 5.13 (2 /2W/1 block A2). Light micrograph of the retina, two weeks after exposure to light of the lower intensity, showing possible hyperplasia of the pigment epithelium (x 400).

Figure 5.14 (2/2W/1 block A2). Light micrograph of the retina, two weeks after exposure to light of the lower intensity. The remainder of the area seen in figure 5.13 is shown (x 400).

15



16

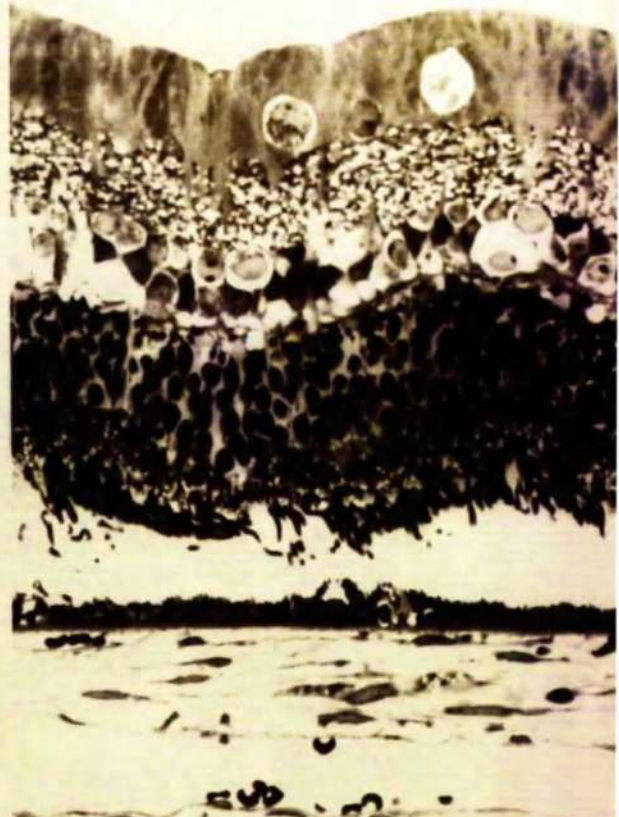


Figure 5.15 (2/2W/1 block C1). Light micrograph showing the appearance of the retina, two weeks after exposure to light of the lower intensity. There is slight oedema of the entire retina (x 400).

Figure 5.16 (2/2W/1 block D3). Light micrograph showing the appearance of the retina, two weeks after exposure to light of the lower intensity. There is prominent oedema of the inner retina. Many of the receptor cell nuclei are pyknotic (x 400).

17



18

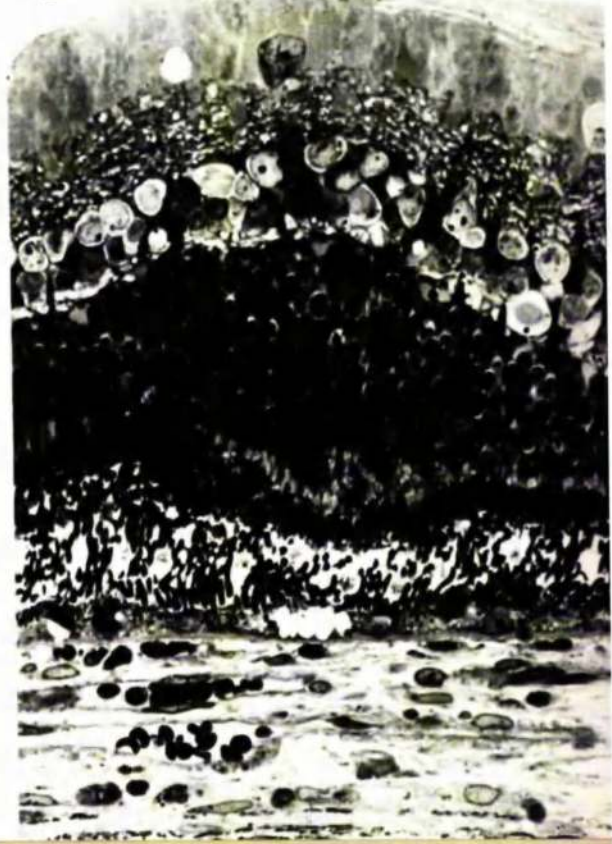


Figure 5.17 (2/4W/1 block A2). Light micrograph showing the appearance of the retina, four weeks after exposure to light of the lower intensity. There are minor disturbances of the outer retina. The pigment epithelium is vacuolated. Arrows: vacuoles (x 400).

Figure 5.18 (2/4W/1 block C2). Similar to figure 5.17 but showing greater disturbances of the outer segments and more extensive vacuolation of the pigment epithelium (x 400).



20



Figure 5.19 (2/4W/2 block D2). Light micrograph showing degenerative changes within the retina, four weeks after exposure to light of the lower intensity (x 400).

5.20 (2/4W/2 block D2). Light micrograph showing the appearance of the pigment epithelium and the choroid, underlying regions of retina such as shown in figure 5.19. The pigment epithelium contains many small vacuoles. The choroidal vessels are filled with impacted red cells. PE: pigment epithelium; IRC: impacted red cells (x 400).

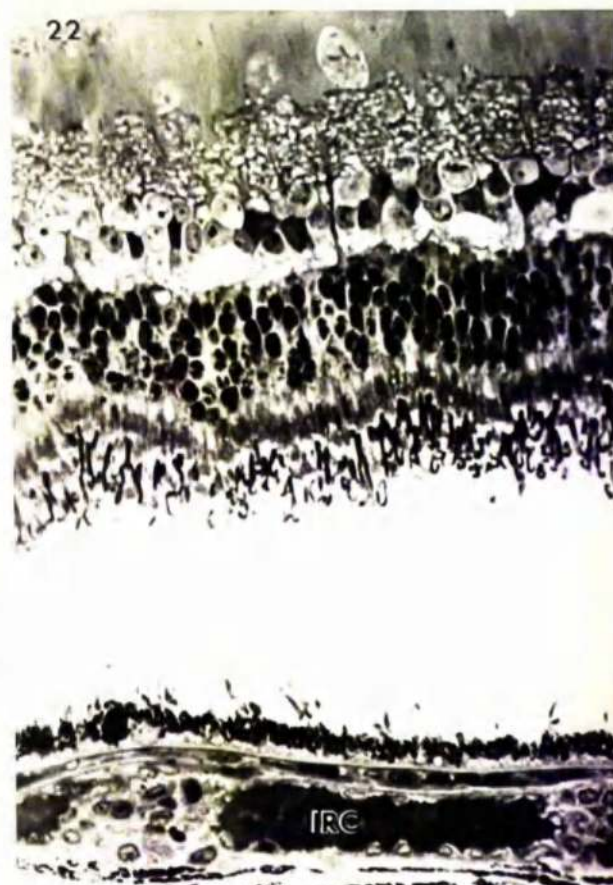


Figure 5.21 (1/6h/1 A2) Light micrograph showing the appearance of the retina and choroid, six hours after exposure to light of the higher intensity. Many of the receptor cell nuclei are pyknotic. There is a considerable amount of photoreceptor debris present. INL: inner nuclear layer; ONL: outer nuclear layer (x 250).

Figure 5.22 (1/6h/1 block D4). Light micrograph of the retina and choroid, six hours after exposure to light of the higher intensity. Areas of retina showing slight intracellular oedema were often adjacent to regions of choroid in which the blood vessels were filled with impacted red cells. IRC: impacted red cells (x 400).

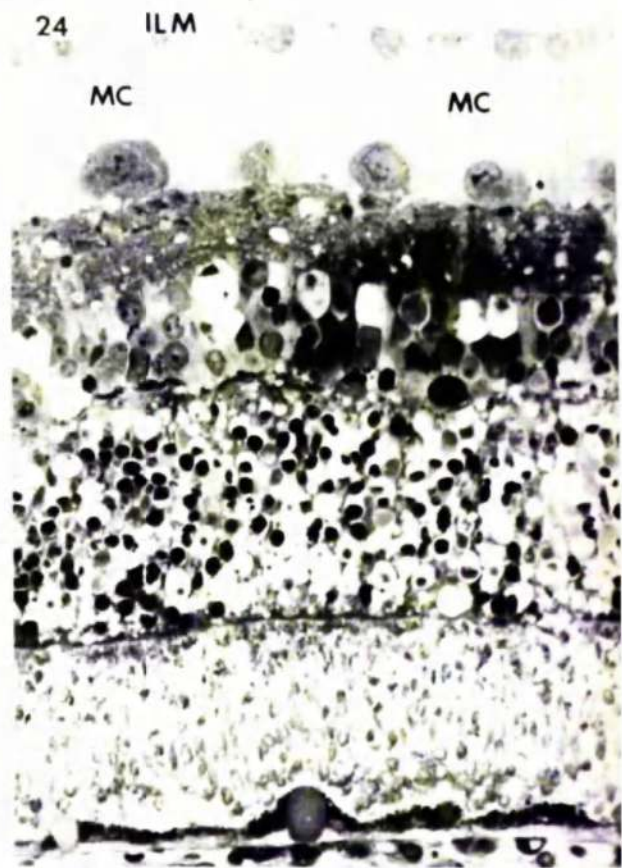
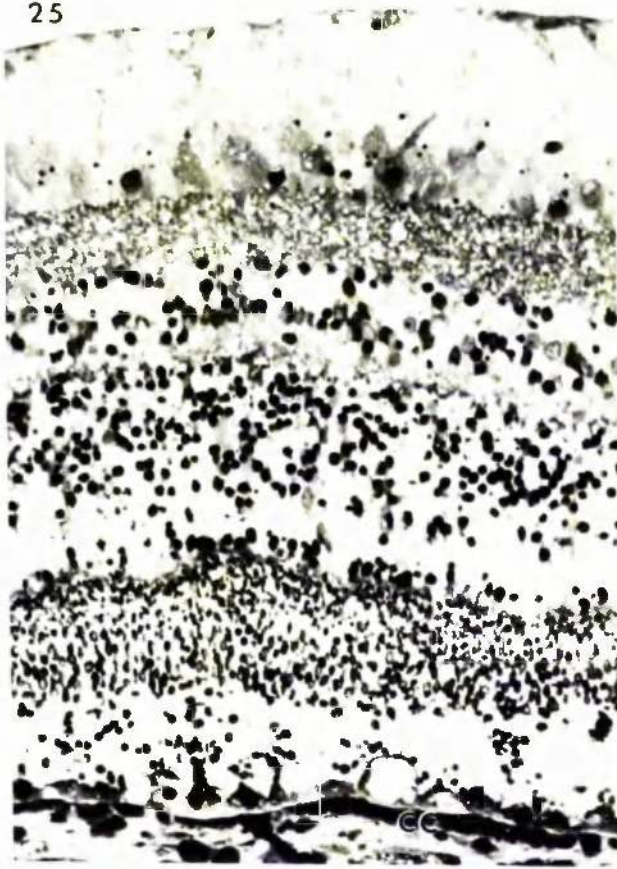


Figure 5.23 (1/24h/2 block A2). Light micrograph of the retina, twenty four hours after exposure to light of the higher intensity. Pyknotic nuclei are present in both the inner nuclear layer and the outer nuclear layer. Severely damaged pigment epithelium is separated from Bruch's membrane by a fibrous material. INL: inner nuclear layer; ONL: outer nuclear layer; PE: pigment epithelium; FM: fibrous material (x 400).

Figure 5.24 (1/24h/2 block B1). Light micrograph of the retina, twenty four hours after exposure to light of the higher intensity. Cellular damage is evident in all layers of the retina. ILM: inner limiting membrane; MC: Muller cell cytoplasm (x 400).

25



26



Figure 5.25 (1/48h/1 block B2). Light micrograph showing the appearance of the retina and choroid forty eight hours after exposure to light of the higher intensity. There is extensive damage to both the neural retina and the pigment epithelium. The choriocapillaris is occluded by platelets and red cells. CC: choriocapillaris (x 400).

Figure 5.26 (1/48h/1 block A3). Light micrograph showing the appearance of the retina and choroid, forty eight hours after exposure to light of the higher intensity. In the less severely damaged regions the inner retina was of more normal appearance. However, there was still extensive damage to the outer retina. The vessels of the choriocapillaris are filled with mononuclear cells (x 250).



Figure 5.27 (1/48h/1 block D2). Light micrograph showing the appearance of the retina, in a peripheral region of the lesion, forty eight hours after exposure to light of the higher intensity. There are pyknotic nuclei within the outer nuclear layer. The receptor cell outer segments are reduced in length. ONL: outer nuclear layer; OS: outer segments (x 400).

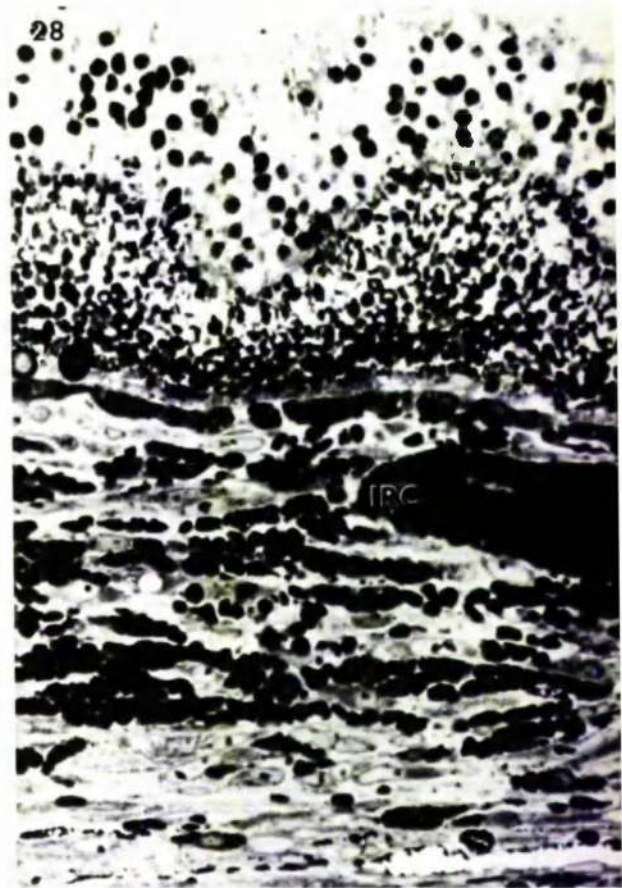


Figure 5.28 (1/4D/1 block C3). Light micrograph showing the appearance of the outer retina and choroid, in the centre of a lesion, four days after exposure to light of the higher intensity. There is severe damage to the outer retina. The choroidal vessels are filled with impacted red cells. IPC: impacted red cells (x 400).

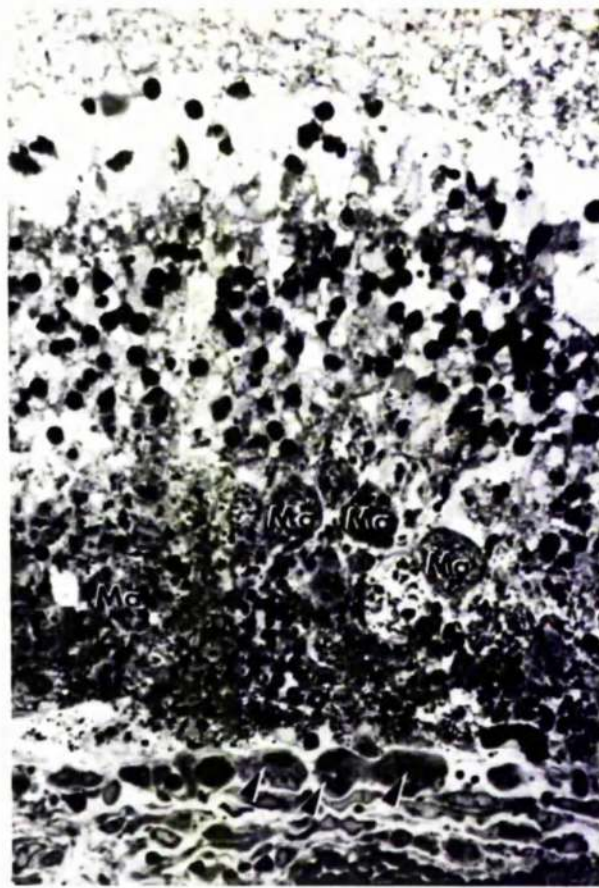


Figure 5.29 (1/4D/1 block D3). Light micrograph showing the appearance of the outer retina and choroid, at the edge of a lesion, four days after exposure to light of the higher intensity. The sub-retinal space is filled with macrophages. The choriocapillaris contains many mononuclear cells. Ma: macrophages; Arrows: mononuclear cells (x 400).

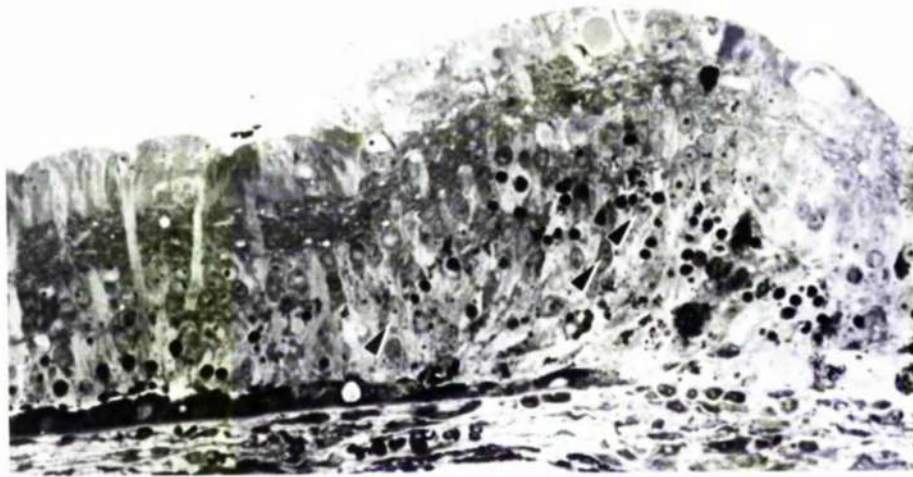


Figure 5.30 (14D71 block D3). Light micrograph showing the appearance of the retina, in a peripheral region of the lesion, four days after exposure to light of the higher intensity. Much of the outer retina has been replaced by Müller cell cytoplasm. Arrows; Müller cell nuclei (x 250).

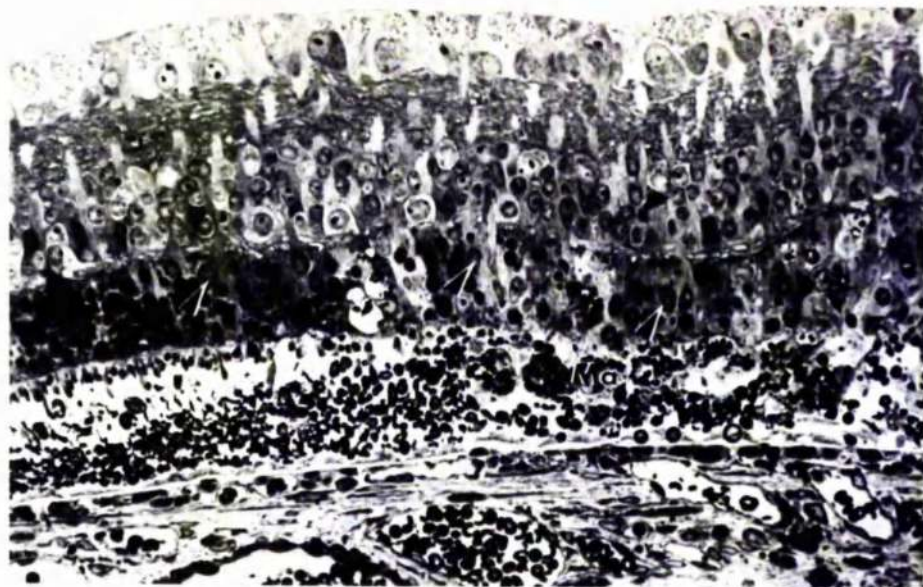


Figure 5.31 (1/4D/1 block D3). Light micrograph showing the appearance of the retina and choroid, four days after exposure to light of the higher intensity. In the region shown there is a rapid transition from mild to severe damage. Where there is extensive loss of photoreceptor cells, Müller cells are present within the outer nuclear layer. Arrows: Müller cells; Ma: macrophage (x 250).

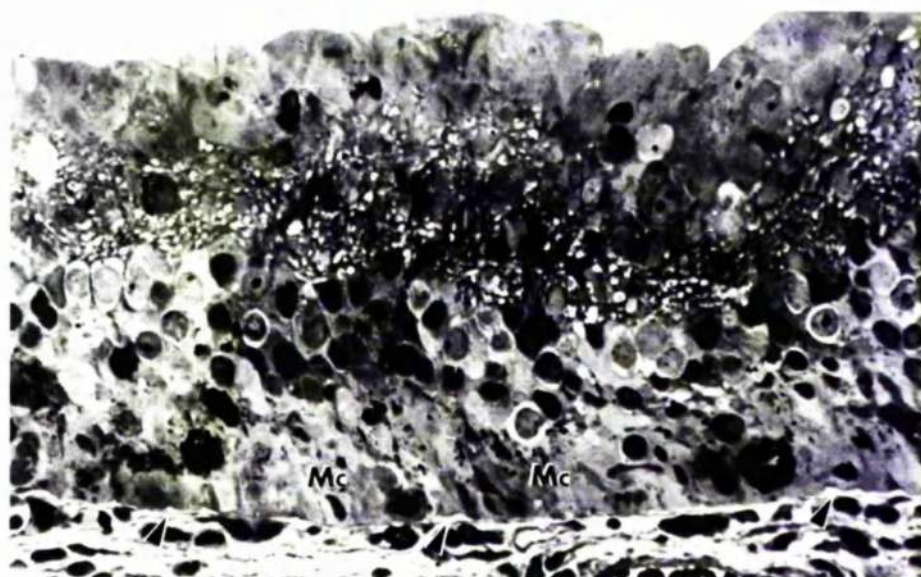


Figure 5.32 (1/2W/2 block C2). Light micrograph showing the appearance of the retina, two weeks after exposure to light of the higher intensity. There is complete loss of the photoreceptors and the pigment epithelium. Müller cells' cytoplasm occupies all of the outer retina. Mc: Müller cell cytoplasm; Arrows: thickenings of Bruch's membrane (x 400).

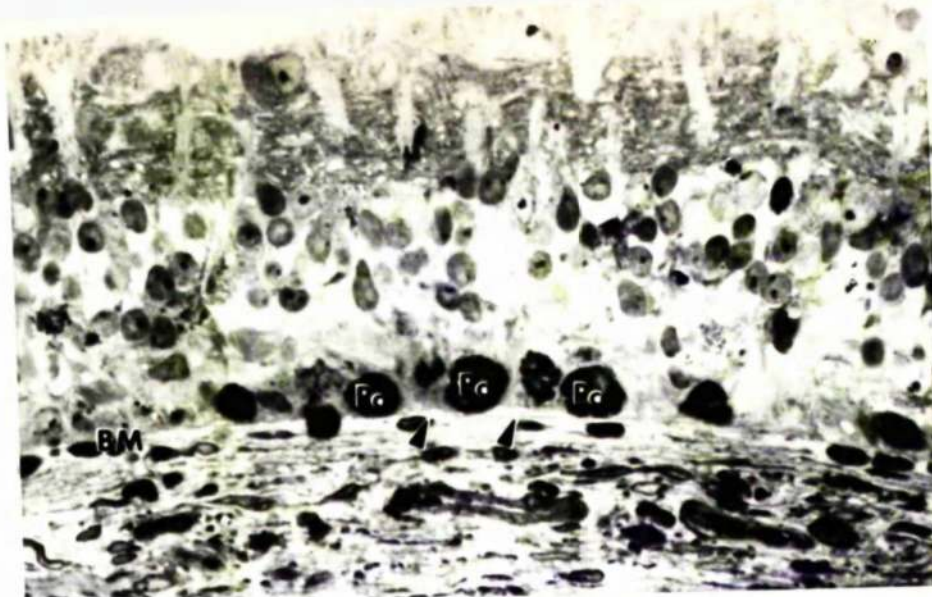


Figure 5.33 (1/4W/2 block C2). Light micrograph showing the appearance of the retina and choroid, four weeks after exposure to light of the higher intensity. As shown in figure 5.32, the outer retina has been replaced by Müller cell cytoplasm. Adjacent to Bruch's membrane are large pigmented cells. It is thought that these cells are macrophages but this is not certain. Pc: pigmented cells (x 400); B.M. Bruch's membrane; Arrows: thickenings of Bruch's membrane (x 400).



Figure 5.34 (1/4W/2 block D2). Light micrograph showing an area of partial photoreceptor loss, four weeks after exposure to the higher intensity. The presence of photoreceptors is intimately associated with the presence of pigment epithelial cells (x 250).

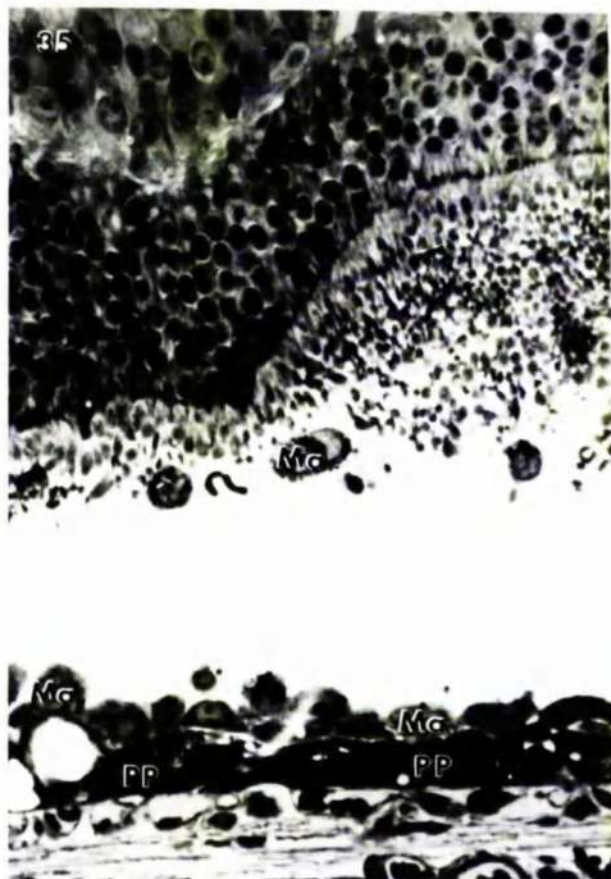


Figure 5.35 (1/1W/2 block A3). Light micrograph of the retina, one week after exposure to the higher intensity, showing an area of suspected pigment epithelial proliferation. Ma: macrophage; PP: proliferated pigment epithelium (x 400).

Figure 5.36 (1/4W/2 block C2). Light micrograph of the retina, four weeks after exposure to light of the higher intensity. The pigmented cells are different in appearance to those seen in figure 5.35. These large pigmented cells are thought to be macrophages. Pc: pigmented cells (x 400).

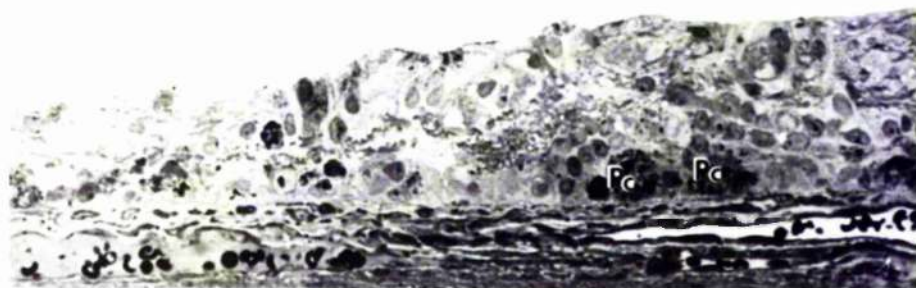


Figure 5.37 (F4W2 block D2). Light micrograph of the retina and choroid, ten weeks after exposure to light of the higher intensity. The region shown has suffered considerable loss of retinal cells. Large pigmented cells, probably macrophages, are present adjacent to Bruch's membrane. The choriocapillaris is absent in the region shown. Pc: pigmented cells (x 250).

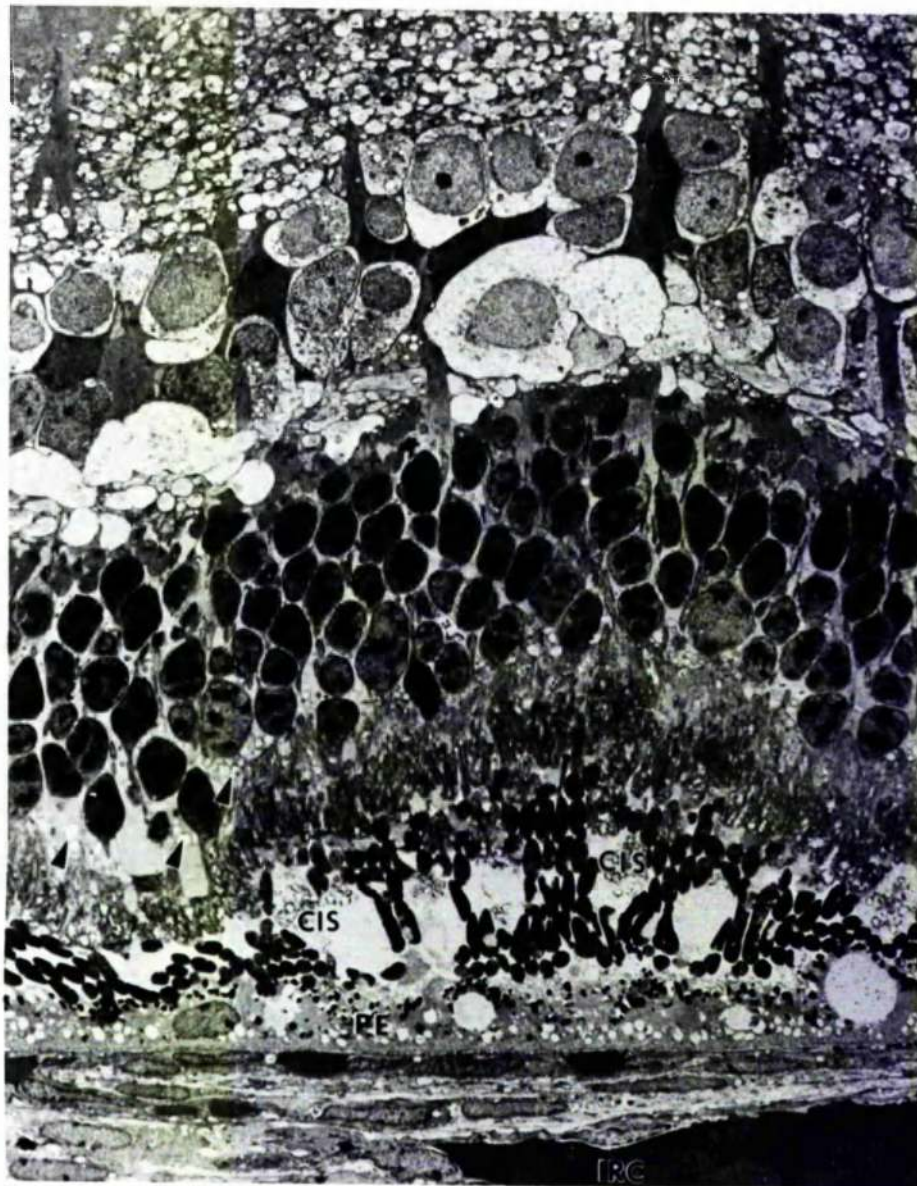


Figure 5.38 (2/6h/1 block D4). Electron micrograph showing the appearance of the retina and choroid, six hours after exposure to light of the lower intensity. PE: pigment epithelium; CIS: cone inner segment; Arrows: swollen Muller cell mitochondria; IRC: impacted red cells (x 1,000).



Figure 5.39 (2/6h/1 block D4). Electron micrograph showing the pigment epithelium and receptor cell inner and outer segments, six hours after exposure to light of the lower intensity. ROS: rod outer segment; CIS: cone inner segment; Mt: mitochondria; Ld: lipid droplet; N: nucleus (x 3,600).

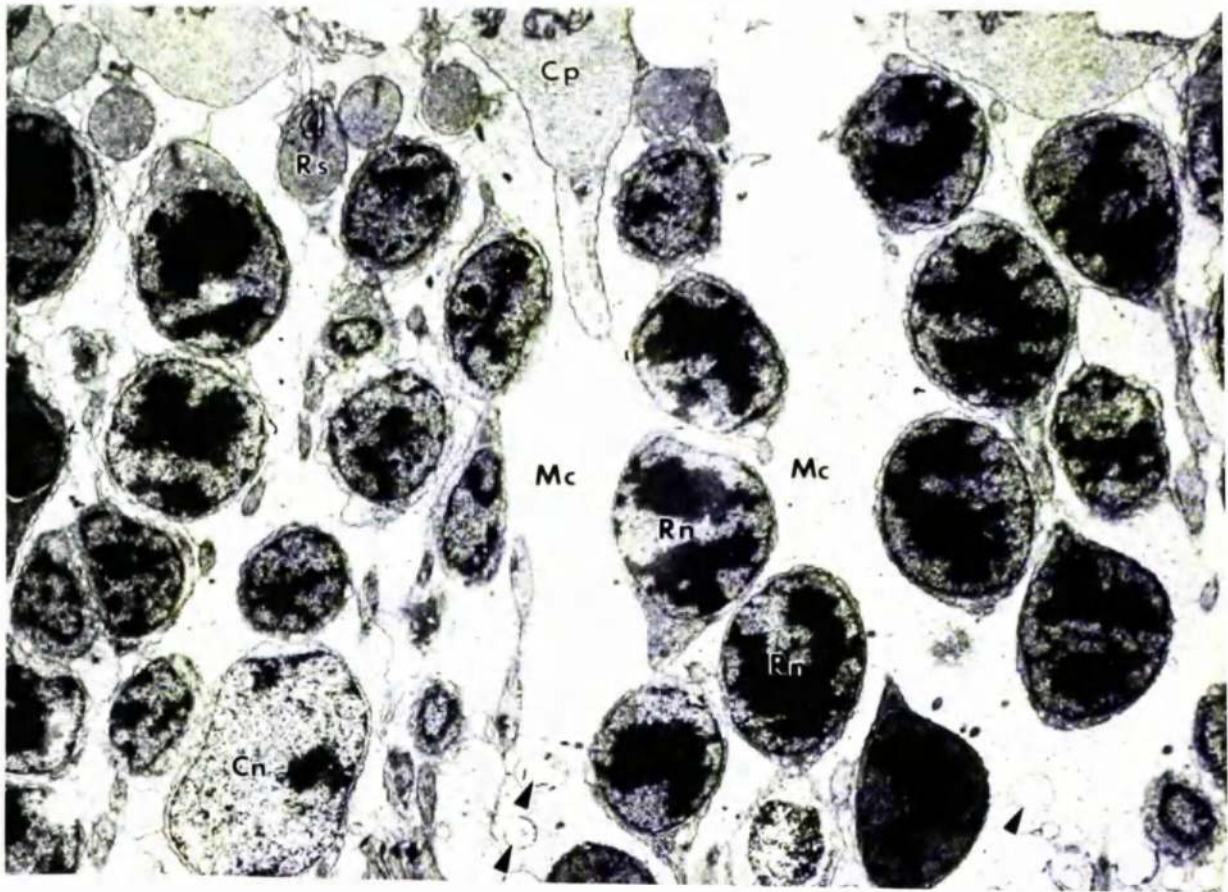


Figure 5.40 (2/6h/1 block D4). Electron micrograph showing the outer nuclear layer and the outer plexiform layer, six hours after exposure to light of the lower intensity. Rn: rod nucleus; Cn: cone nucleus; Mc: Müller cell cytoplasm; Cp: cone pedicle; Rs: rod spherule; Arrows: distended Müller cell mitochondria ($\times 3,600$).

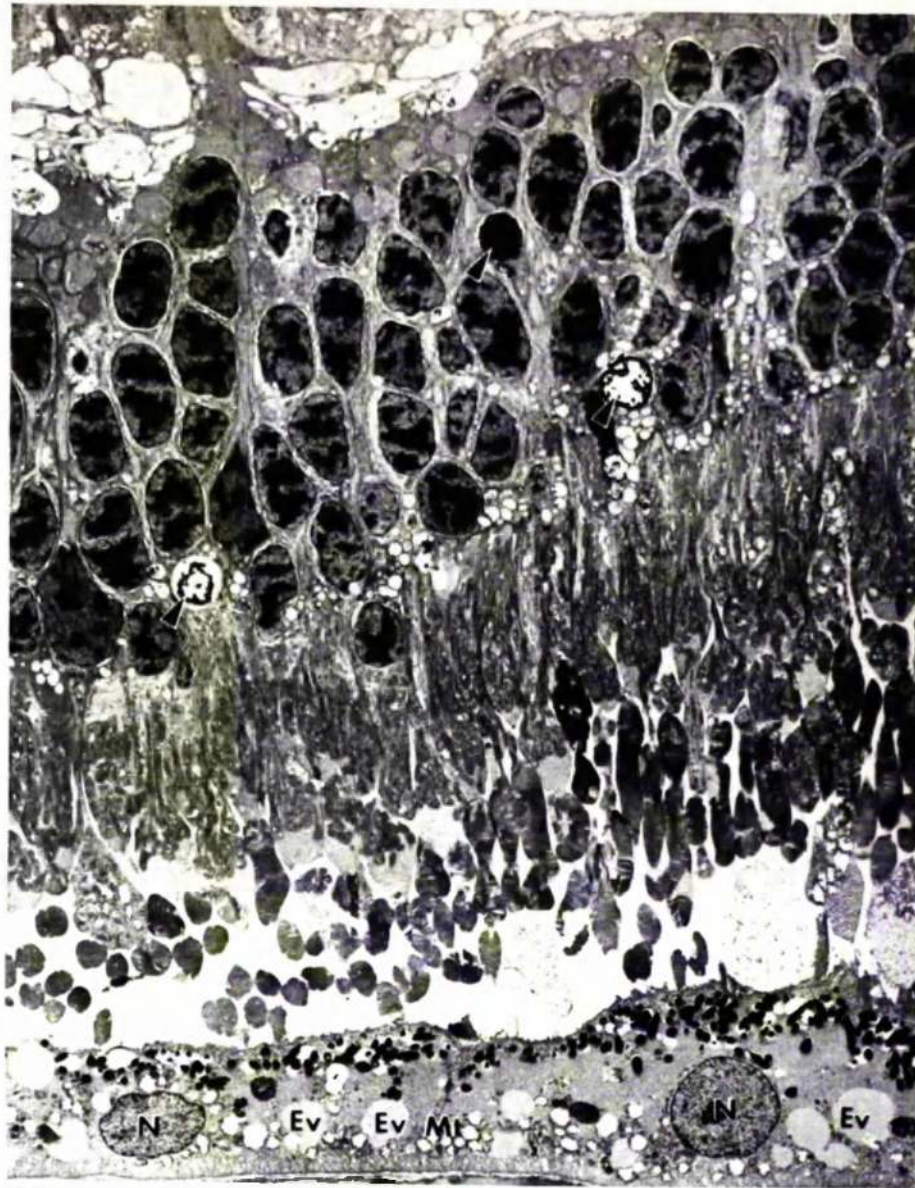


Figure 5.41 (2/24h/1 block D1). Electron micrograph showing the appearance of the outer retina, twenty four hours after exposure to light of the lower intensity. Ev: electron lucent vesicles; Mt: mitochondria; N: pigment epithelial nucleus; CIS: cone inner segment; Arrows: disintegrating receptor cell nuclei (x 1900).

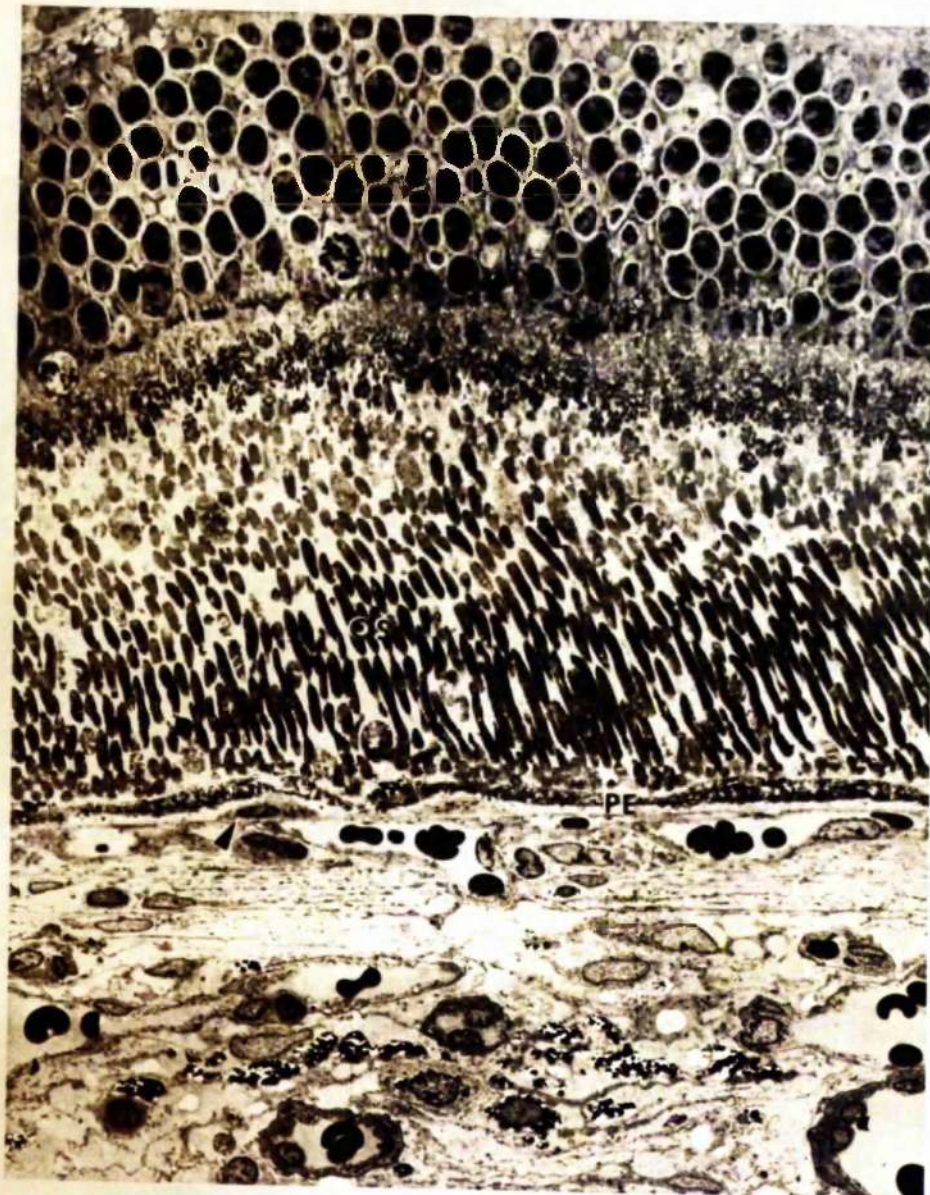


Figure 5.42 (2/48h/2 block A2). Electron micrograph showing the appearance of the outer retina and choroid, forty eight hours after exposure to light of the lower intensity. OS: outer segments; PE: pigment epithelium; Arrow: cell in Bruch's membrane ($\times 1,000$).

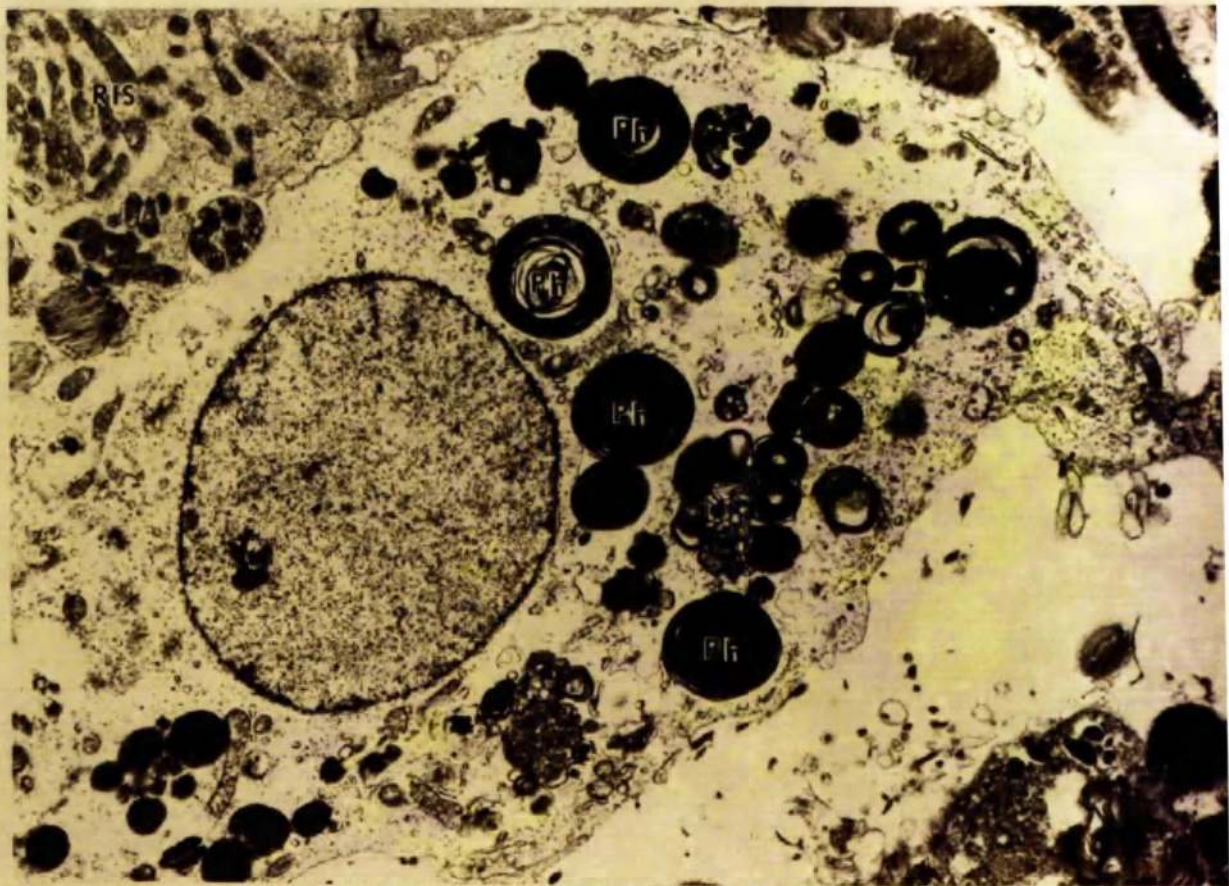


Figure 5.43 (2/48h/2 block A2). Electron micrograph of a macrophage, seen in the subretinal space, forty eight hours after exposure to light of the lower intensity. RIS: rod inner segment; Ph: phagosomes of receptor cell material ($\times 6,000$).

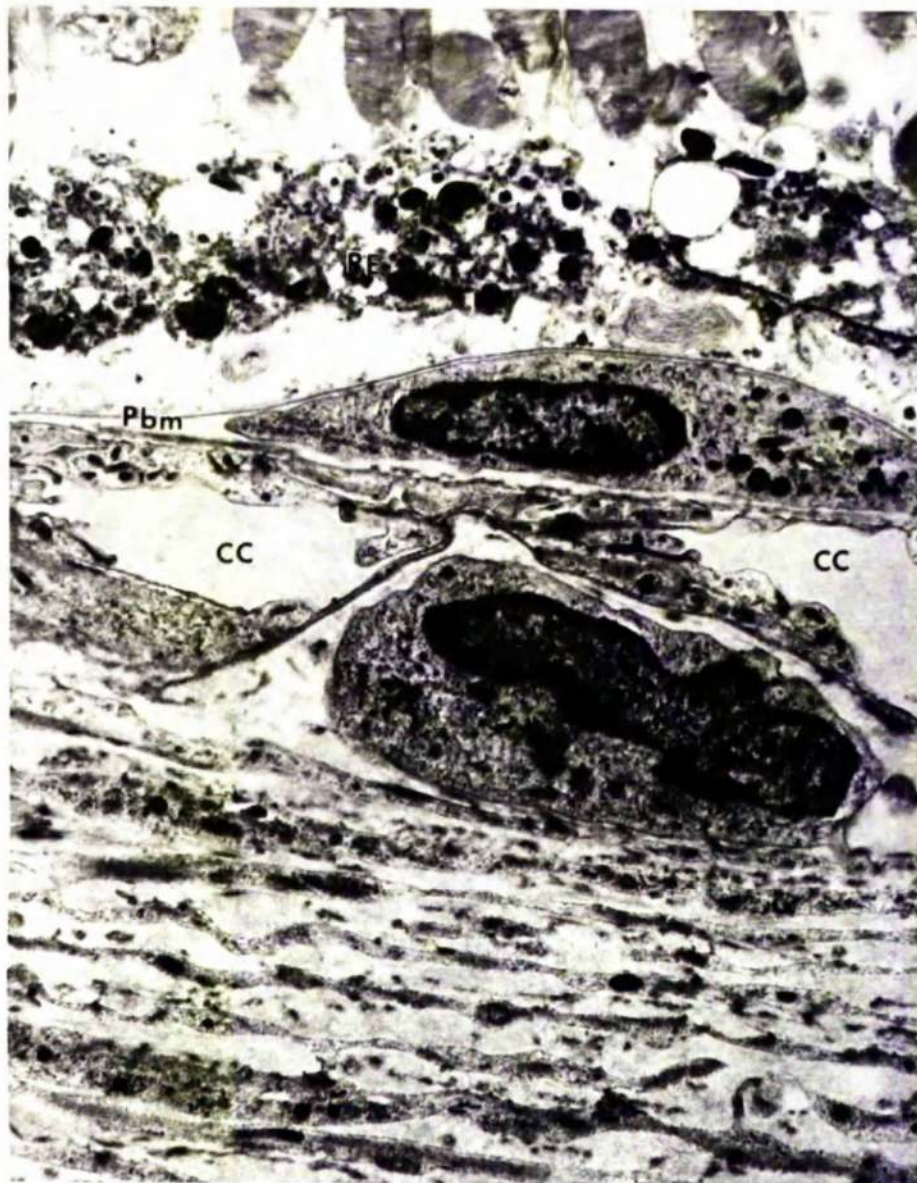


Figure 5.44 (2/48h/2 block A2). Electron micrograph showing the cell seen in Bruch's membrane in Figure 5.42 at higher power. PE: pigment epithelium; Pbm: pigment epithelium basement membrane; CC: choriocapillaris (x 7,600).

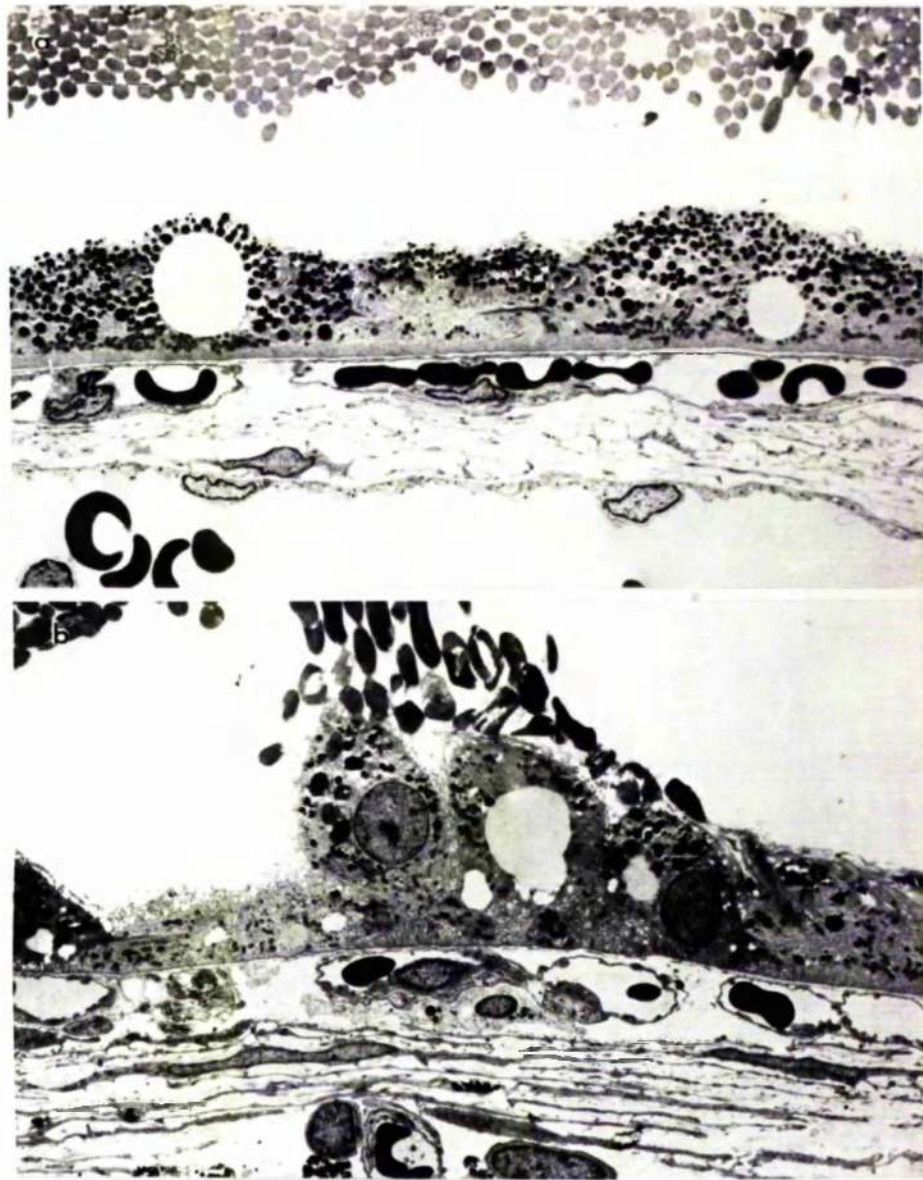


Figure 5.45 a. (2/4D/1 block C4); b. (2/4D/1 block A2). Electron micrographs showing the appearances of the pigment epithelium, four days after exposure to light of the lower intensity. In a. the pigment epithelium is packed with phagosomes. In b. there appears to be "budding" of the pigment epithelium (both x 1500).

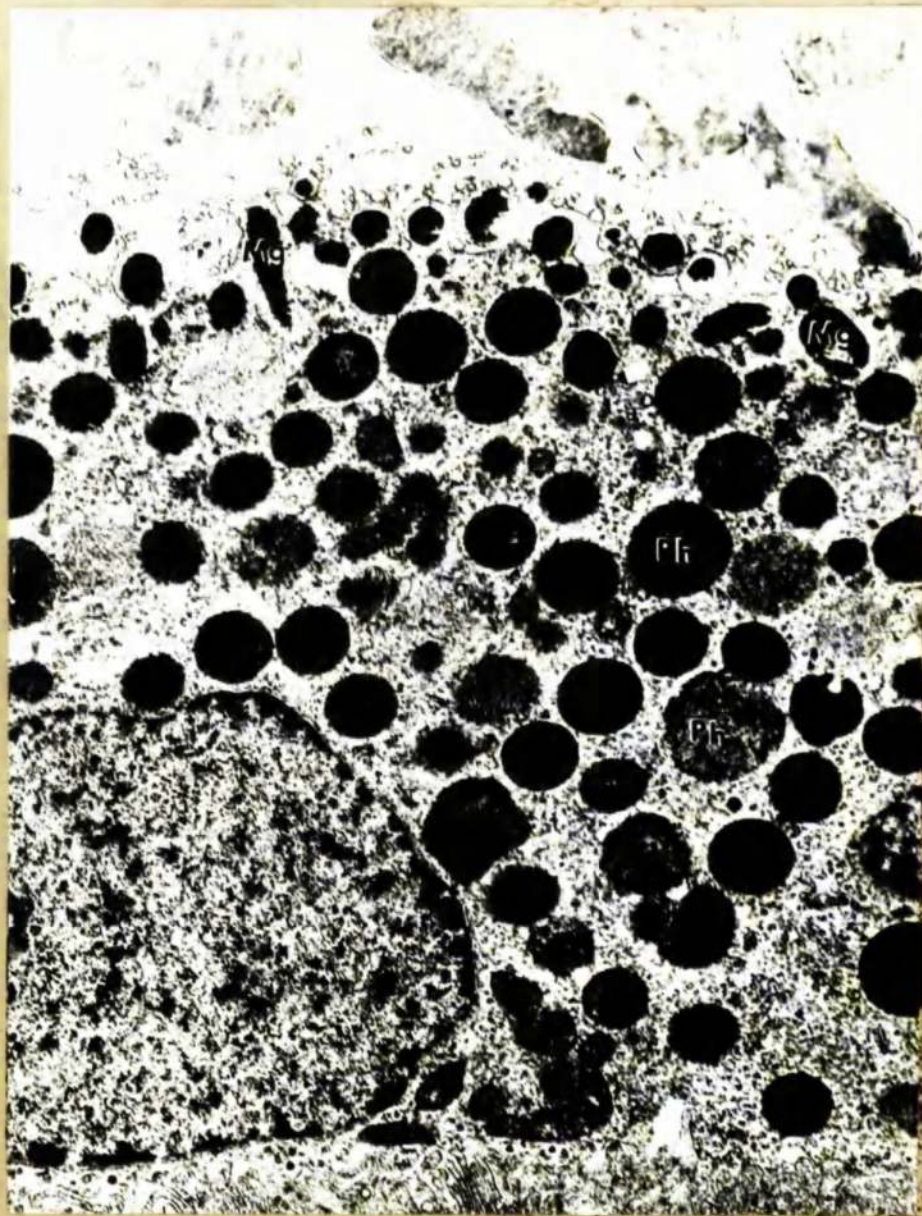


Figure 5.46 (2/4D/1 block C4). Electron micrograph, at higher magnification, of pigment epithelium shown in Figure 5.45a. Ph: phagosomes; Mg: melanin granules (x 16,500).

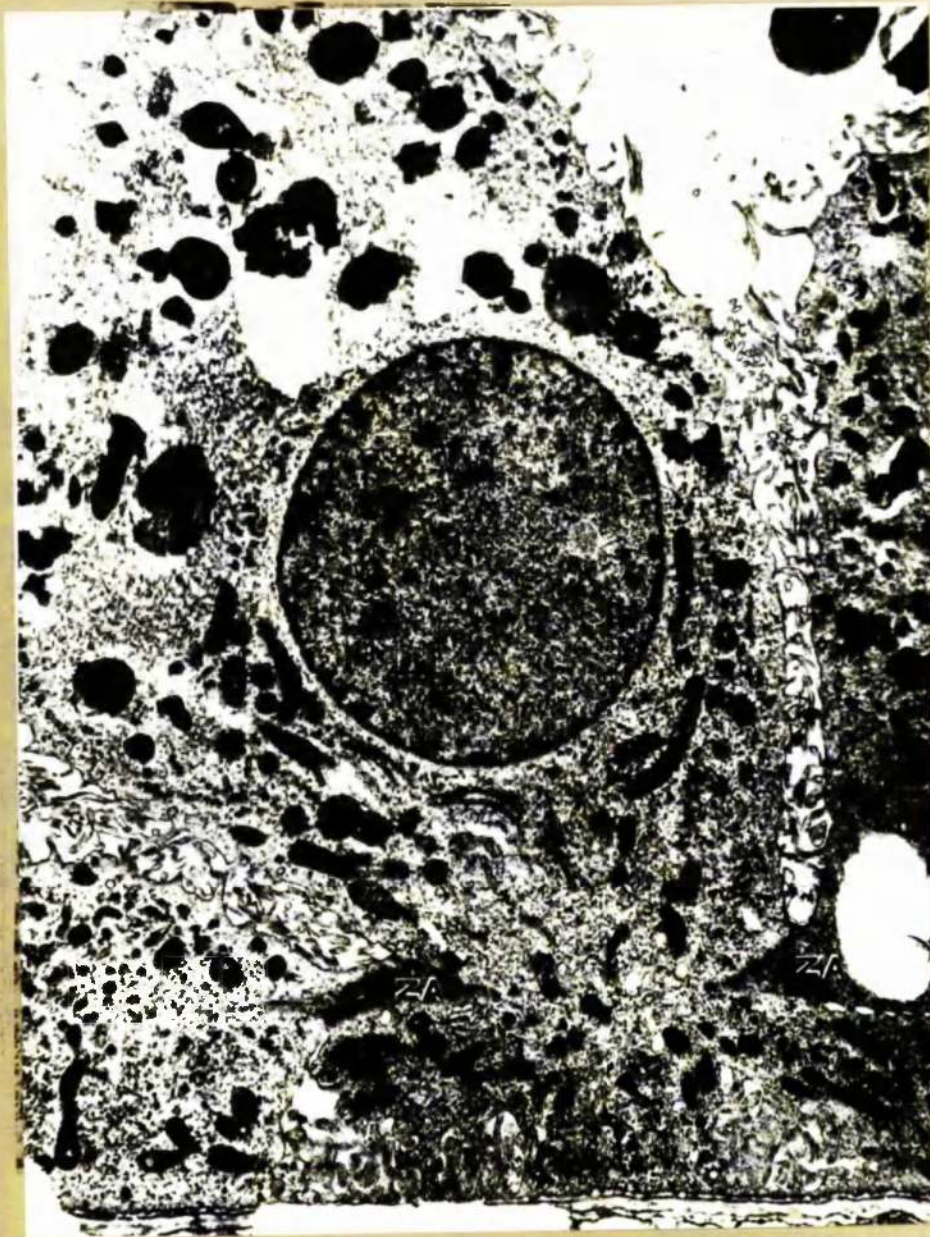


Figure 5.47 (2/4D/1 block A2). Electron micrograph, at higher magnification, of the pigment epithelium shown in Figure 5.45b. The cell appears to be constricted at the level of the zonula adhaerens. ZA: zonula adhaerens (x 6,600).

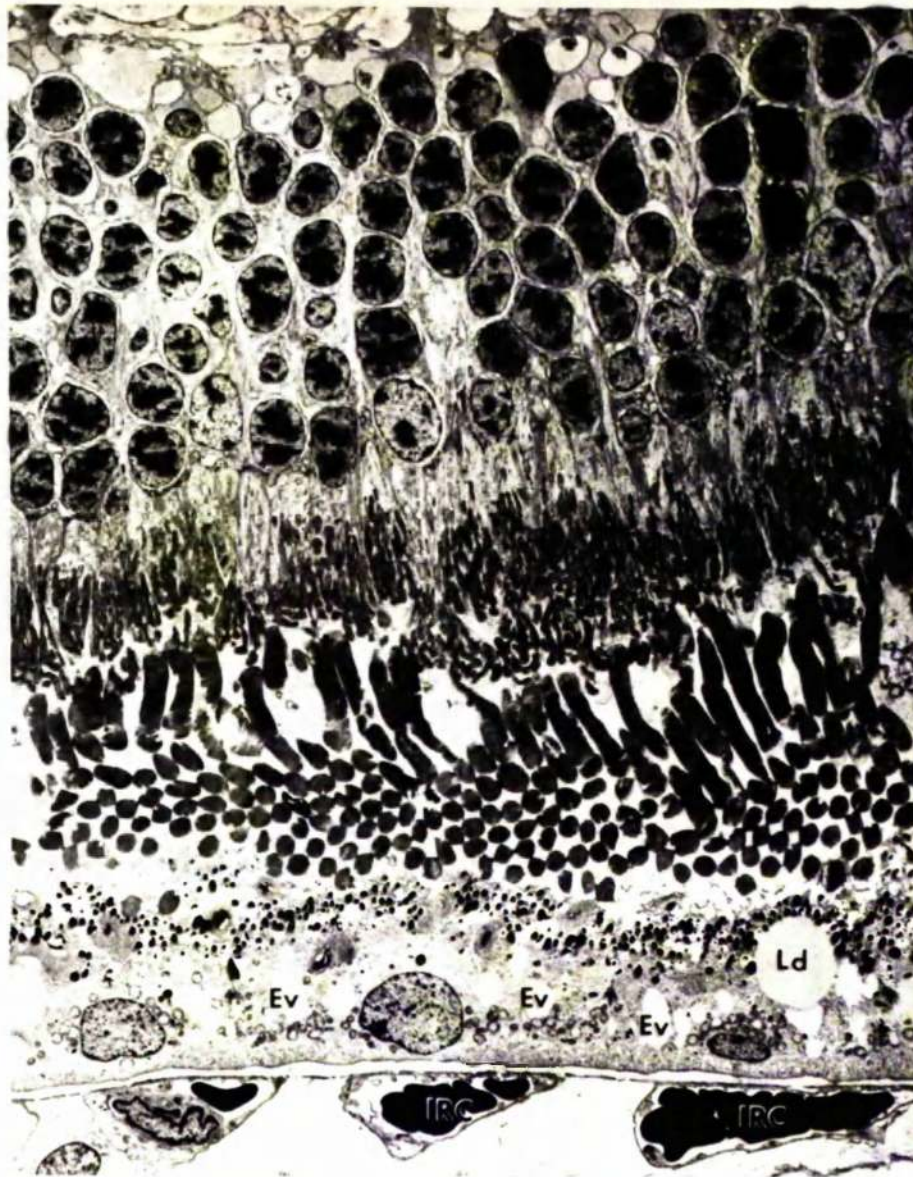


Figure 5.48 (2/1W/1 block C2). Electron micrograph of the outer retina, one week after exposure to light of the lower intensity. Abnormalities of the pigment epithelium were only seen adjacent to regions of occluded choriocapillaris. Ev: electron lucent vesicle; Ld: lipid droplet; IRC: impacted red cells (x 1,700).

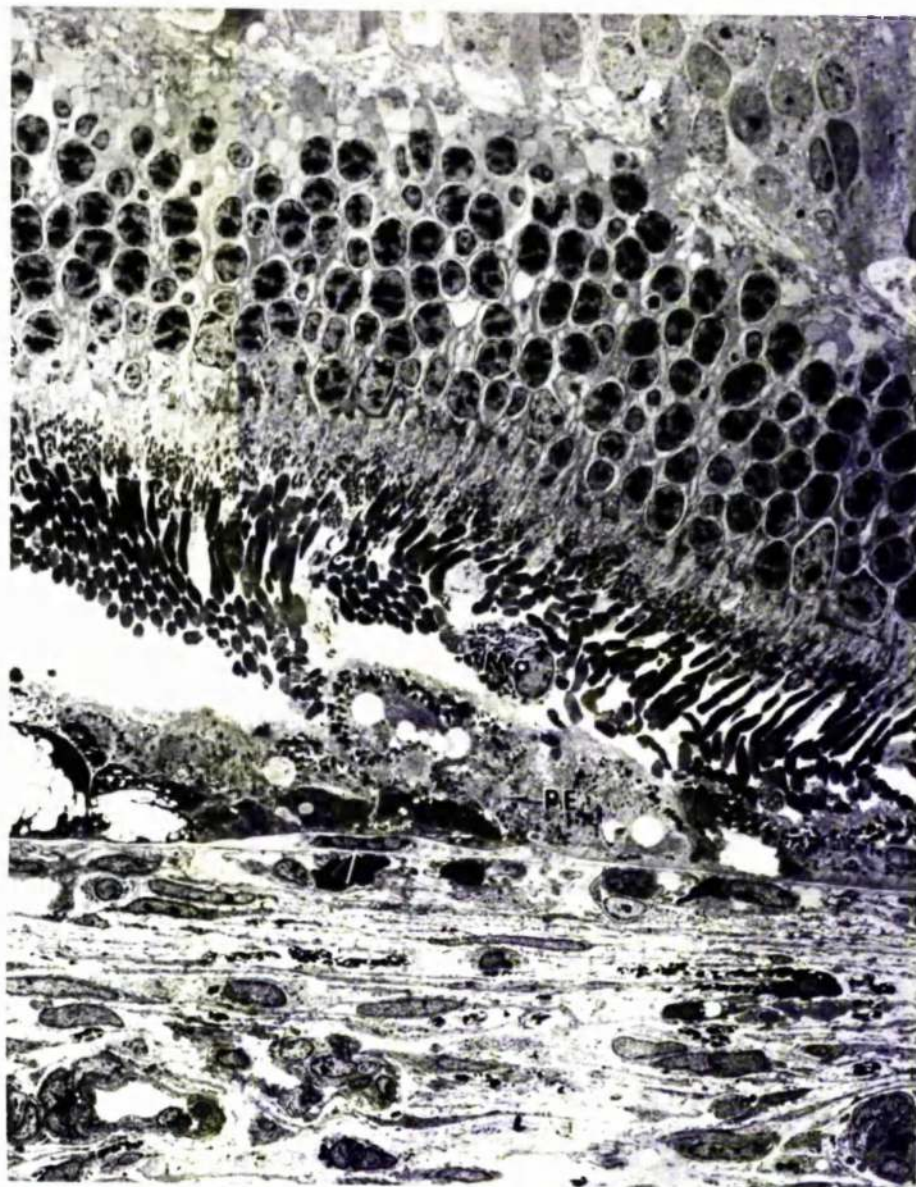


Figure 5.49 (2/2W/1 block C2). Electron micrograph of the outer retina and choroid, two weeks after exposure to light of the lower intensity. By light microscopy this region was thought to show pigment epithelial proliferation. Ma: macrophage; PE: pigment epithelium; Arrow: cell within Bruch's membrane ($\times 1,000$).

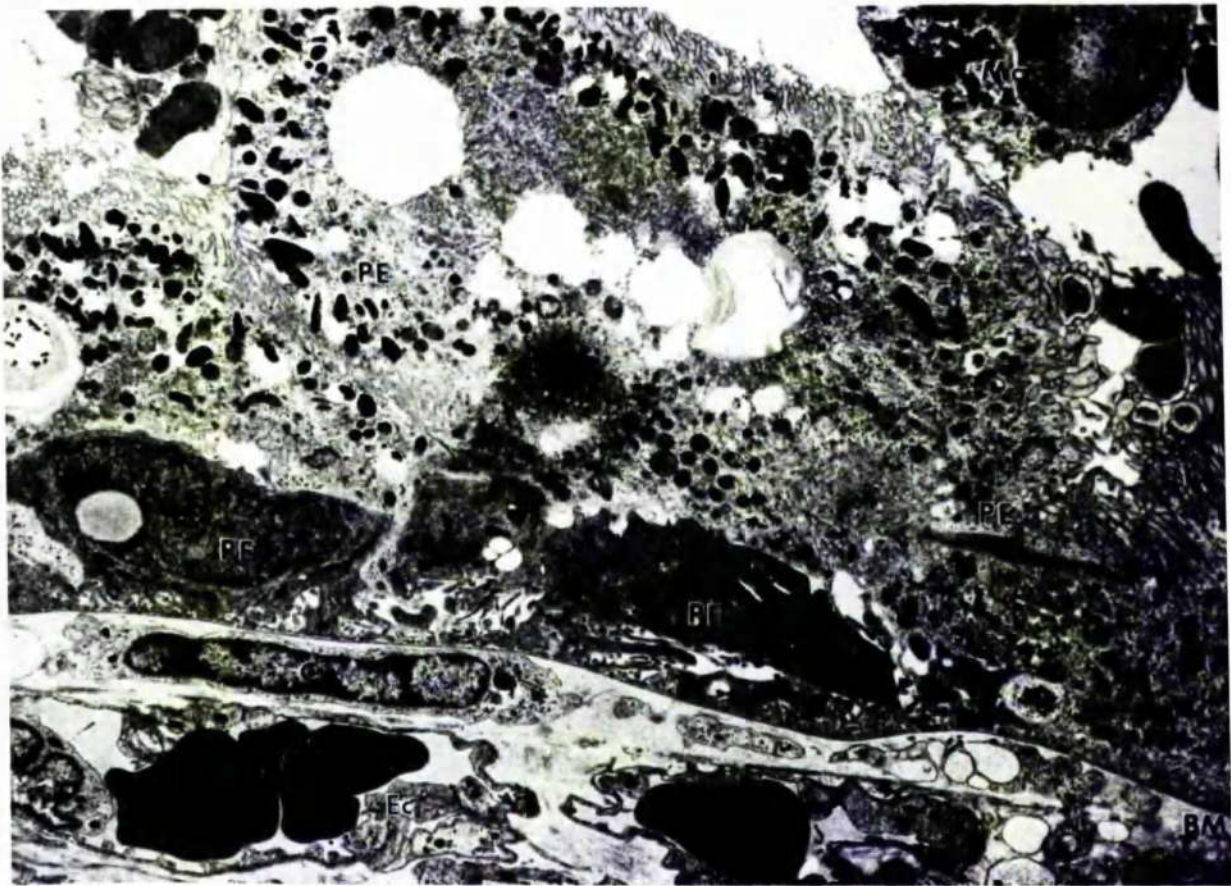


Figure 5.50 (2/2W/1 block C2). Electron micrograph, at higher magnification, of the region shown in figure 5.49. A cell is present within Bruch's membrane. BM: Bruch's membrane; Ec: endothelial cell cytoplasm; Ma: macrophage; PE: pigment epithelium; C: cell of unknown origin (x 3,800).

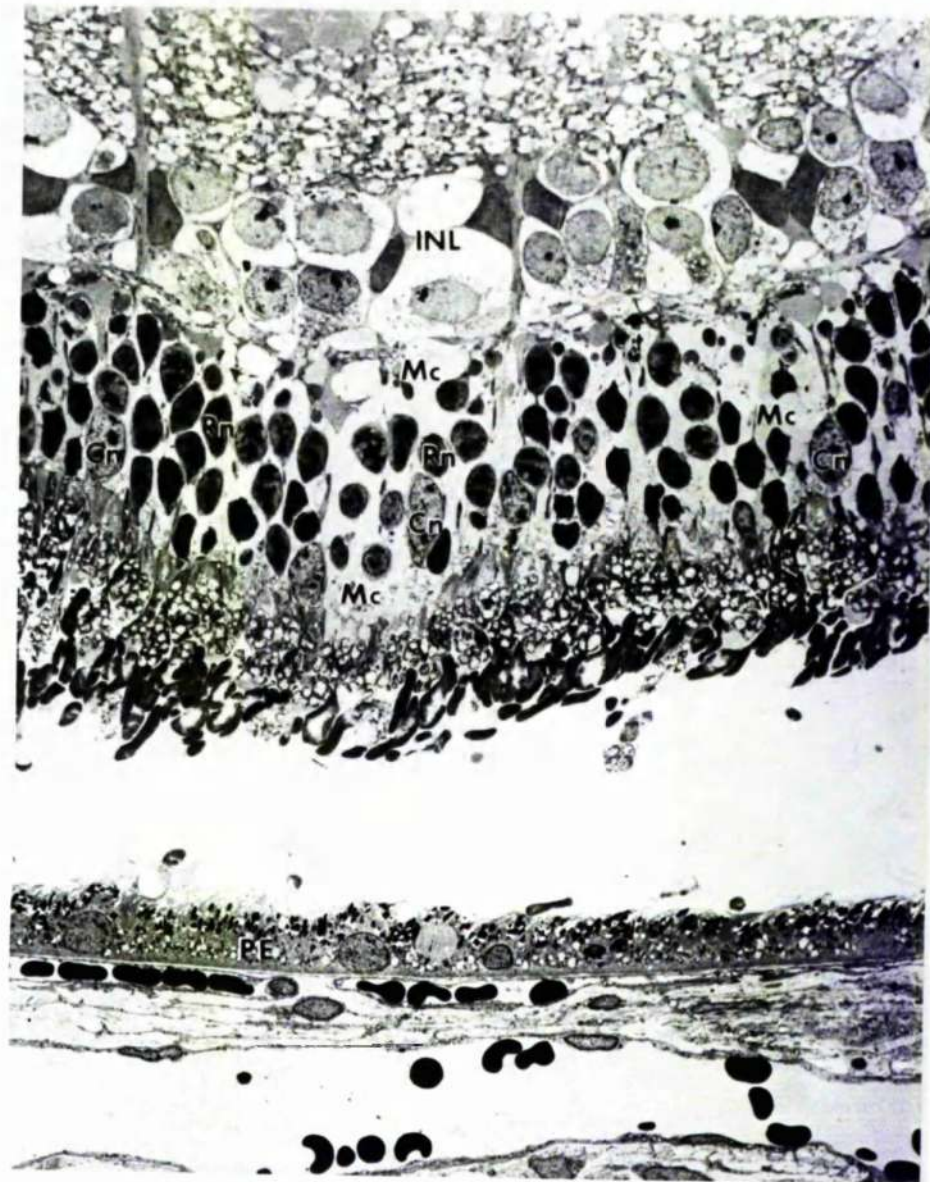


Figure 5.51 (2/2W/1 block D3). Electron micrograph showing the appearance of the retina and choroid, two weeks after exposure to light of the lower intensity. There is intracellular oedema of the inner nuclear layer. Receptor cell cytoplasm is shrunken and densely stained. INL: inner nuclear layer; Rn: rod nucleus; Cn: cone nucleus; Mc: Müller cell cytoplasm; PE: pigment epithelium (x900).

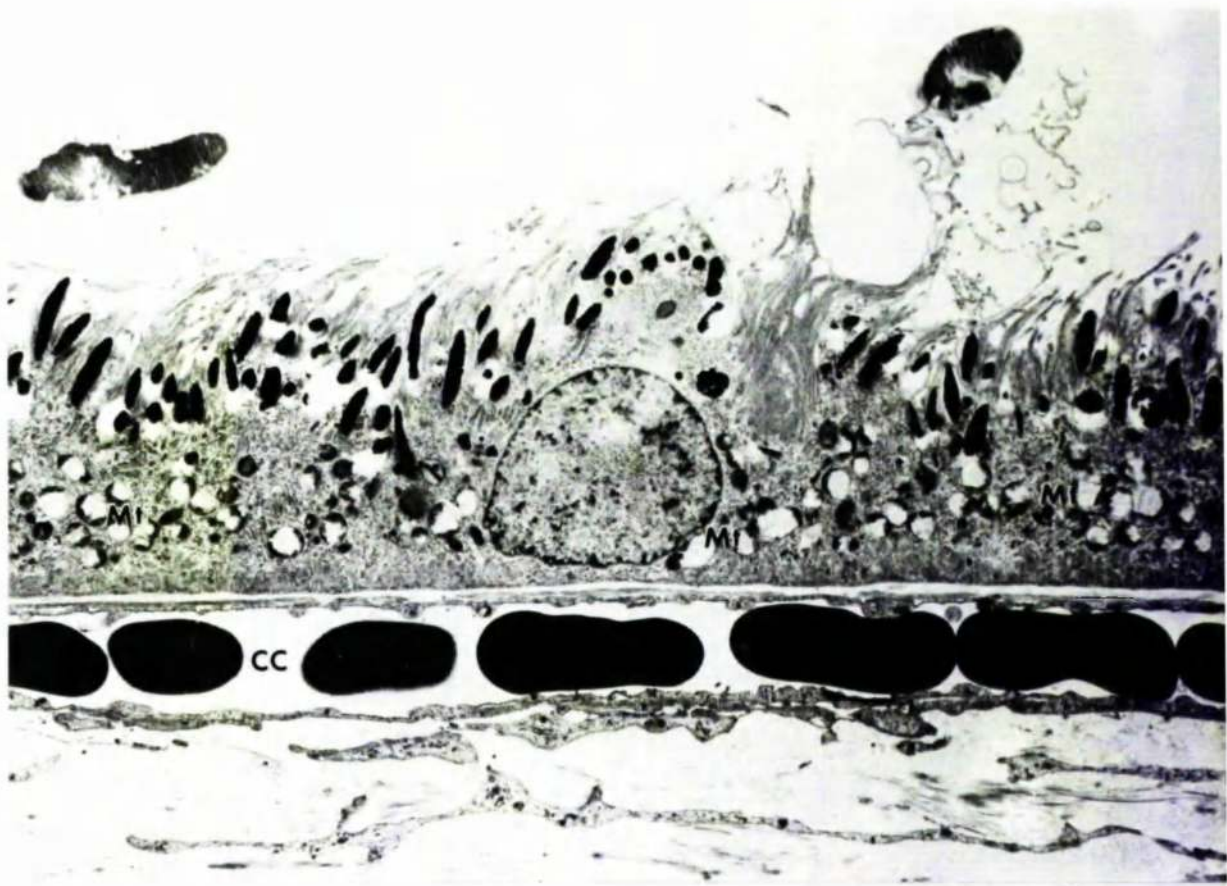


Figure 5.52 (2/2W/1 block D3). Electron micrograph showing, at higher magnification, the pigment epithelium seen in Figure 5.51. The cell is nearly normal in appearance apart from distension of its mitochondria. Mt: swollen mitochondria; CC: chorio-capillaris (x 3,800).

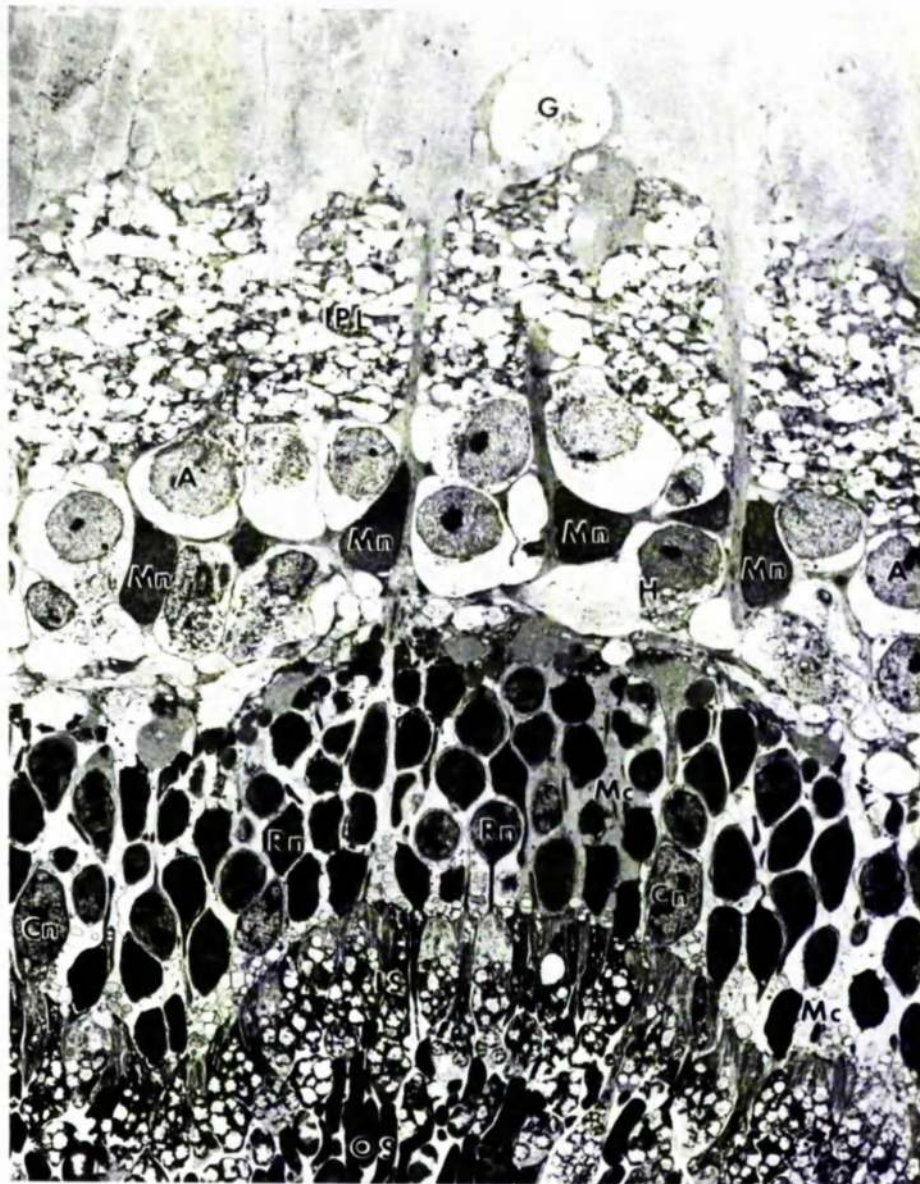


Figure 5.53 (2/2W/1 block D3). Electron micrograph showing, at slightly greater magnification, the inner retina shown in Figure 5.51. OS: outer segments; IS: inner segments; Rn: rod nucleus; Cn: cone nucleus; Mc: Müller cell cytoplasm; Mn: Müller cell nucleus; A: amacrine cell; H: horizontal cell; IPL: inner plexiform layer; G: ganglion cell ($\times 1,200$).



Figure 5.54 (2/4W/1 block A4). Electron micrograph showing the appearance of the choroid, four weeks after exposure to light of the lower intensity. Extra-vascular inflammatory cells are abundant. Ma: macrophage (x 1,650).



Figure 5.55 (2/4W/1 block D2). Electron micrograph showing the appearance of the outer retina, four weeks after exposure to light of the lower intensity. PE: pigment epithelium; Ld: lipid droplet, SER: smooth endoplasmic reticulum; ROS: rod outer segment; Arrows: flecculate material within rod outer segments; CIS: cone inner segment (x 3,700).



Figure 5.56 (2/4W/2 block D2). Electron micrograph showing degenerative changes in the neural retina, four weeks after exposure to light of the lower intensity. G: ganglion cell; A: amacrine cell; H: horizontal cell; M: Müller cell; ONL: outer nuclear layer; IS: inner segments; OS: outer segments ($\times 1,000$).

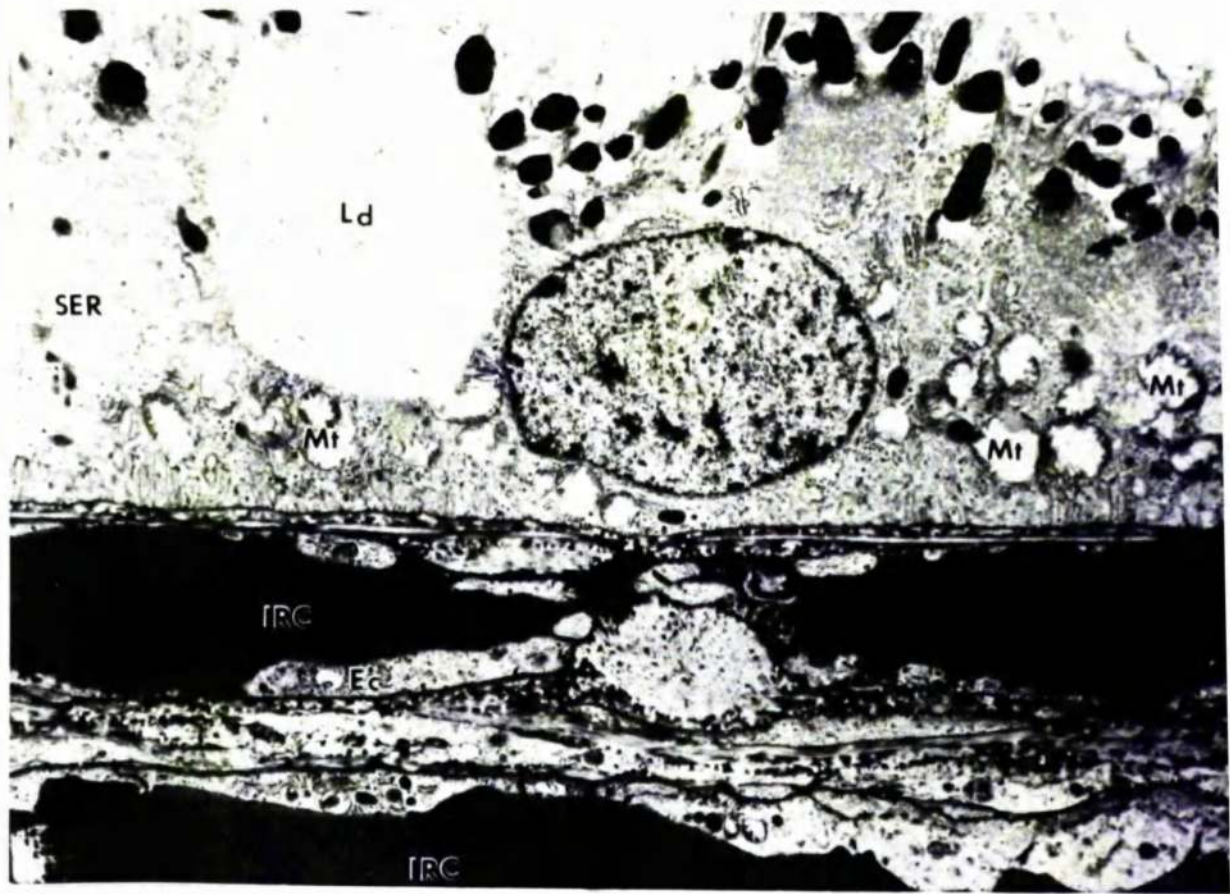


Figure 5.57 (2/4W/2 block D2). Electron micrograph showing the appearance of the pigment epithelium and choriocapillaris, in an area of retinal degeneration, four weeks after exposure to light of the lower intensity. SER: smooth endoplasmic reticulum; Ld: lipid droplet; Mt: mitochondria; Ec: endothelial cell cytoplasm; IRC: impacted rod cells (x 3,200).

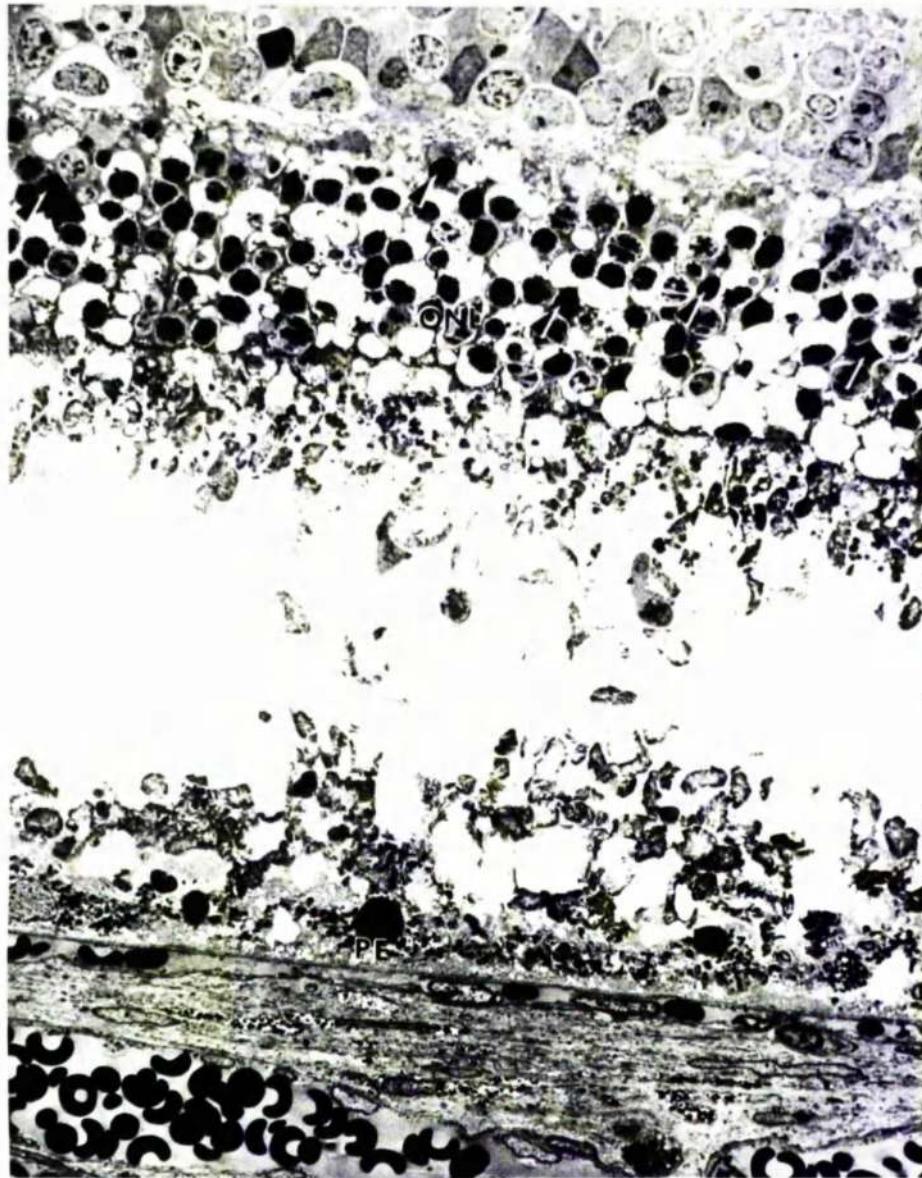


Figure 5.58 (1/6h/1 block B2). Electron micrograph showing the appearance of the outer retina and choroid, six hours after exposure to light of the higher intensity. ONL: outer nuclear layer; Arrows: pyknotic receptor cell nuclei; PE: pigment epithelium (x 900).

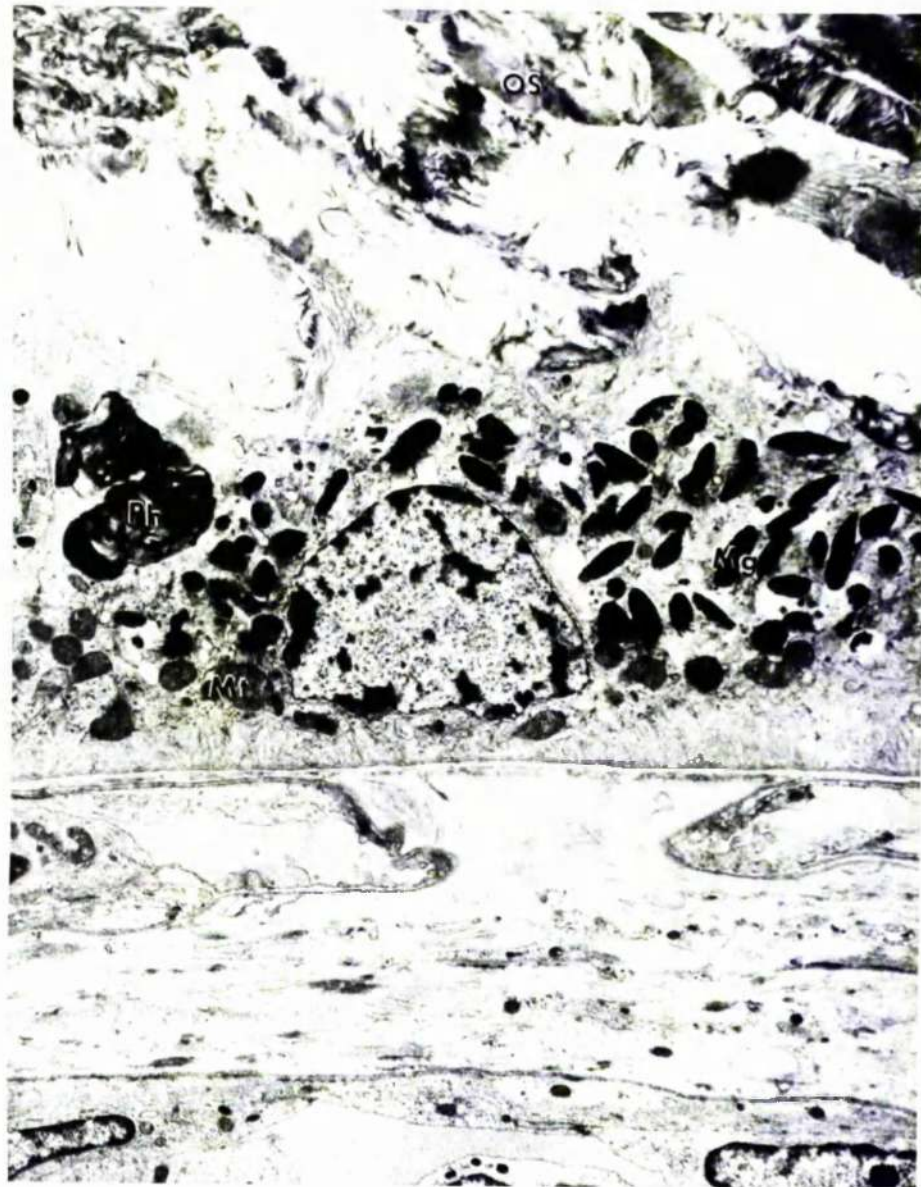


Figure 5.59 (1/6h/1 block B2). Electron micrograph showing the appearance of the pigment epithelium, six hours after exposure to light of the higher intensity. Ph: phagosome; Mt: mitochondria; Mg: melanin granules; OS: outer segment material ($\times 5,500$).

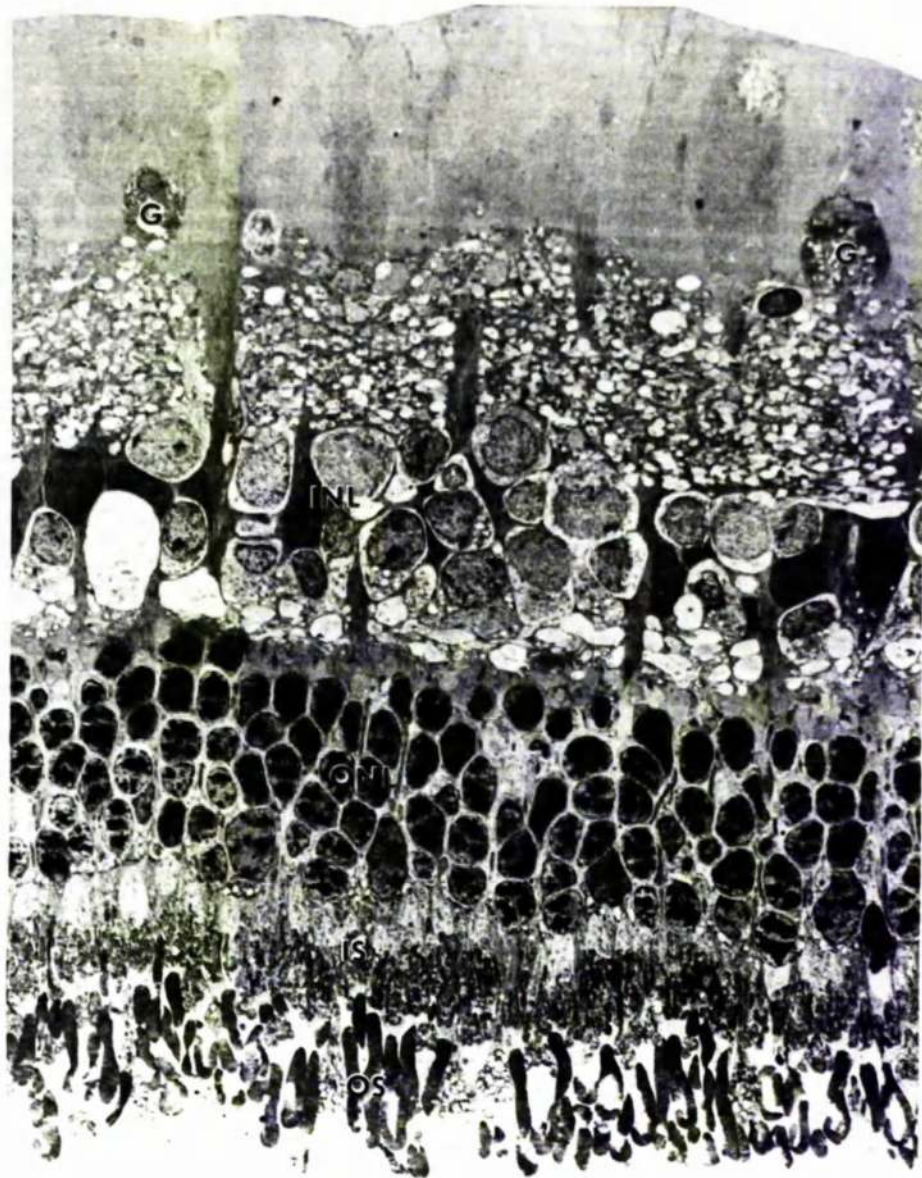


Figure 5.60 (1/6h/2 block D4). Electron micrograph of the neural retina six hours after exposure to light of the higher intensity. The pattern of damage is not characteristic of that produced by light. G: ganglion cell; INL: inner nuclear layer; ONL: outer nuclear layer; IS: inner segments; OS: outer segments (x 1,200).

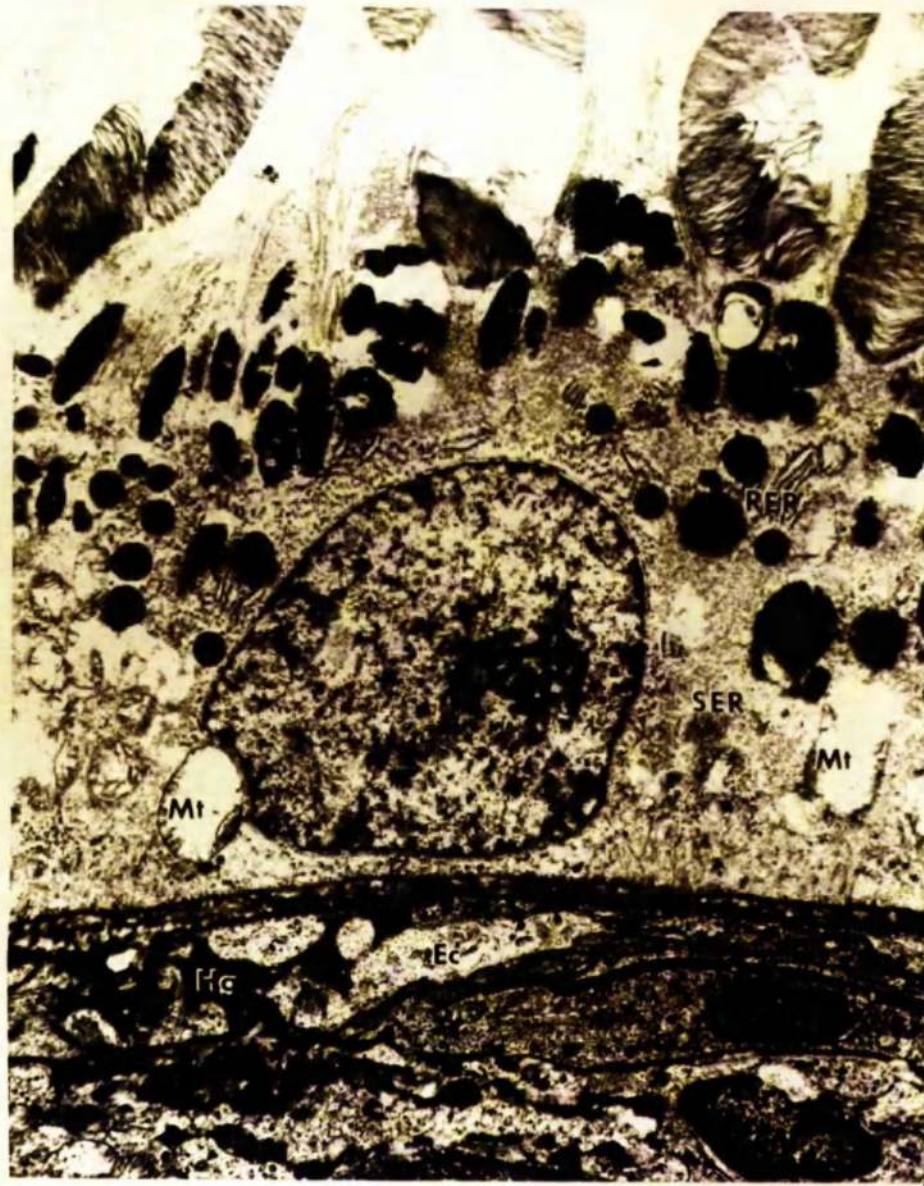


Figure 5.61 (1/6h/2 block D4). Electron micrograph showing the appearance of the pigment epithelium, adjacent to areas of retinal degeneration, six hours after exposure to light of the higher intensity. Mt: mitochondria; RER: rough endoplasmic reticulum; SER: smooth endoplasmic reticulum; Ec: endothelial cytoplasm; Hg: densely staining material thought to be haemoglobin or one of its breakdown products (x 8,800).

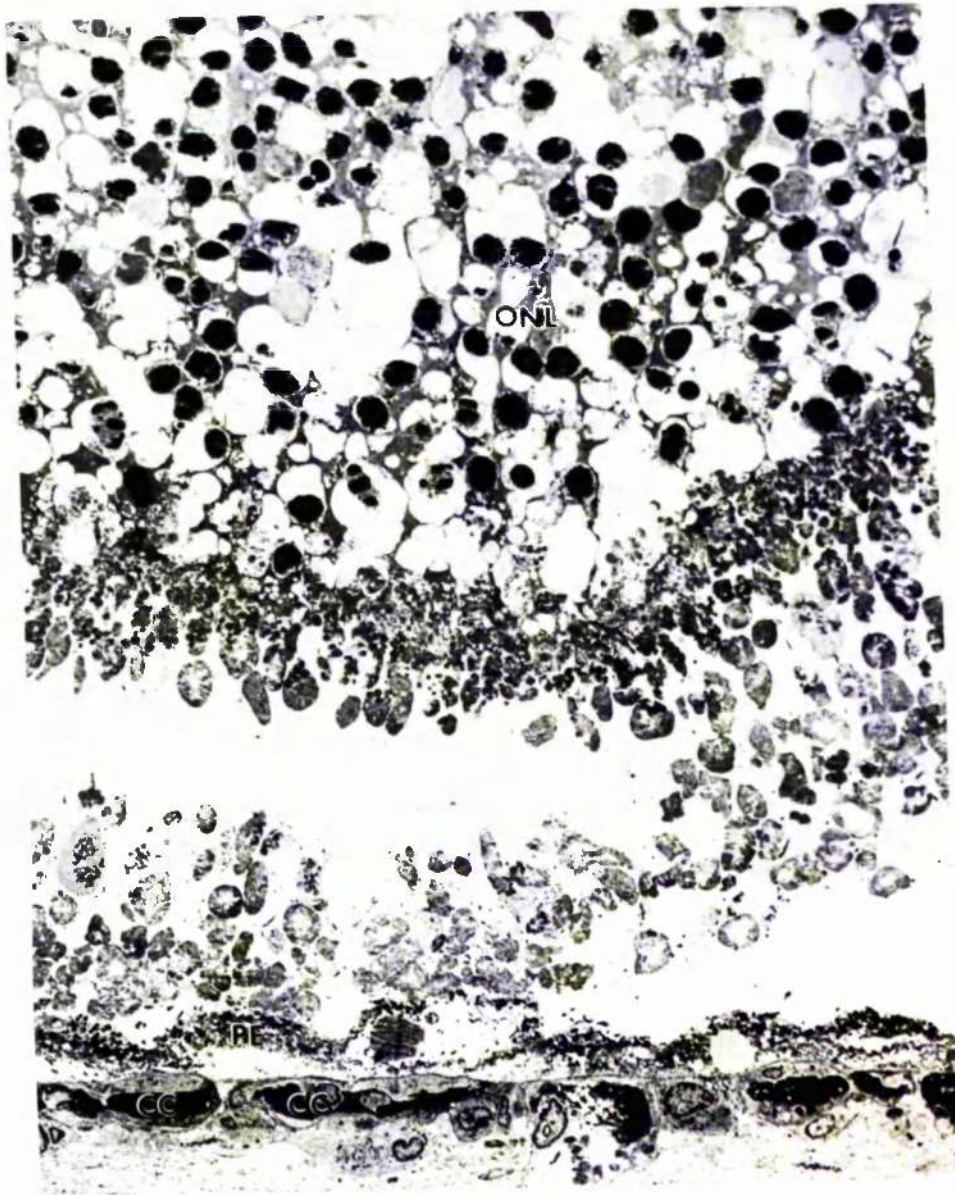


Figure 5.62 (1/24h/1 block B2). Electron micrograph showing the appearance of the outer retina and choriocapillaris, twenty four hours after exposure to light of the higher intensity. CC: choriocapillaris; PE: pigment epithelium; ONL: outer nuclear layer (x 1,100).

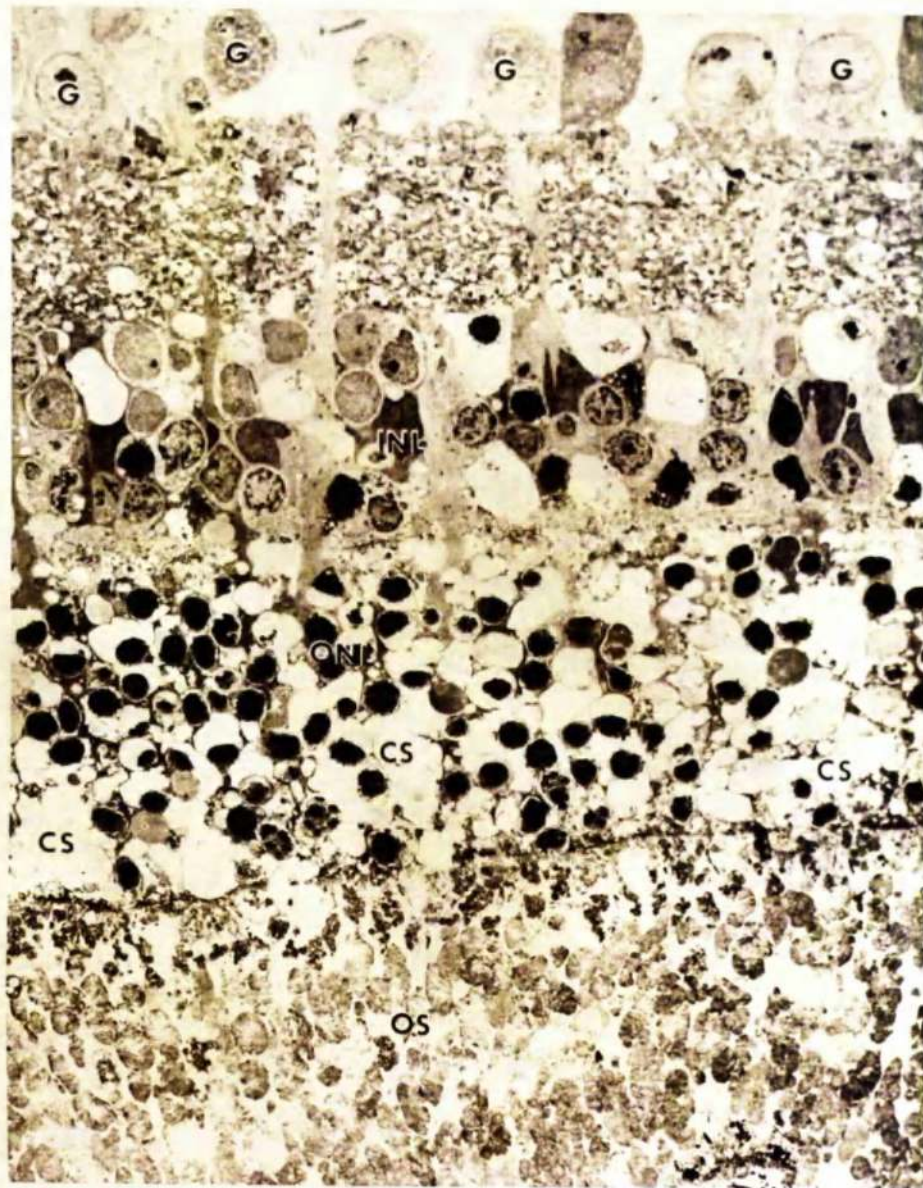


Figure 5.63 (1/24h/2 block A2). Electron micrograph showing the appearance of the neural retina, twenty four hours after exposure to light of the higher intensity. G: ganglion cell; INL: inner nuclear layer; ONL: outer nuclear layer; CS: cystic spaces; OS: outer segment material (x 950).



Figure 5.64 (1/24h/1 block B2). Electron micrograph showing the appearance of the pigment epithelium and choriocapillaris, twenty four hours after exposure to light of the higher intensity. PE: pigment epithelium; Fi: fibrin (x 2,200).



Figure 5.65 (1/24h/1 block A2). Electron micrograph showing the presence of plasma and fibrin, between Bruch's membrane and the pigment epithelium, twenty four hours after exposure to light of the higher intensity. Ff: fibrin (x 9,000).

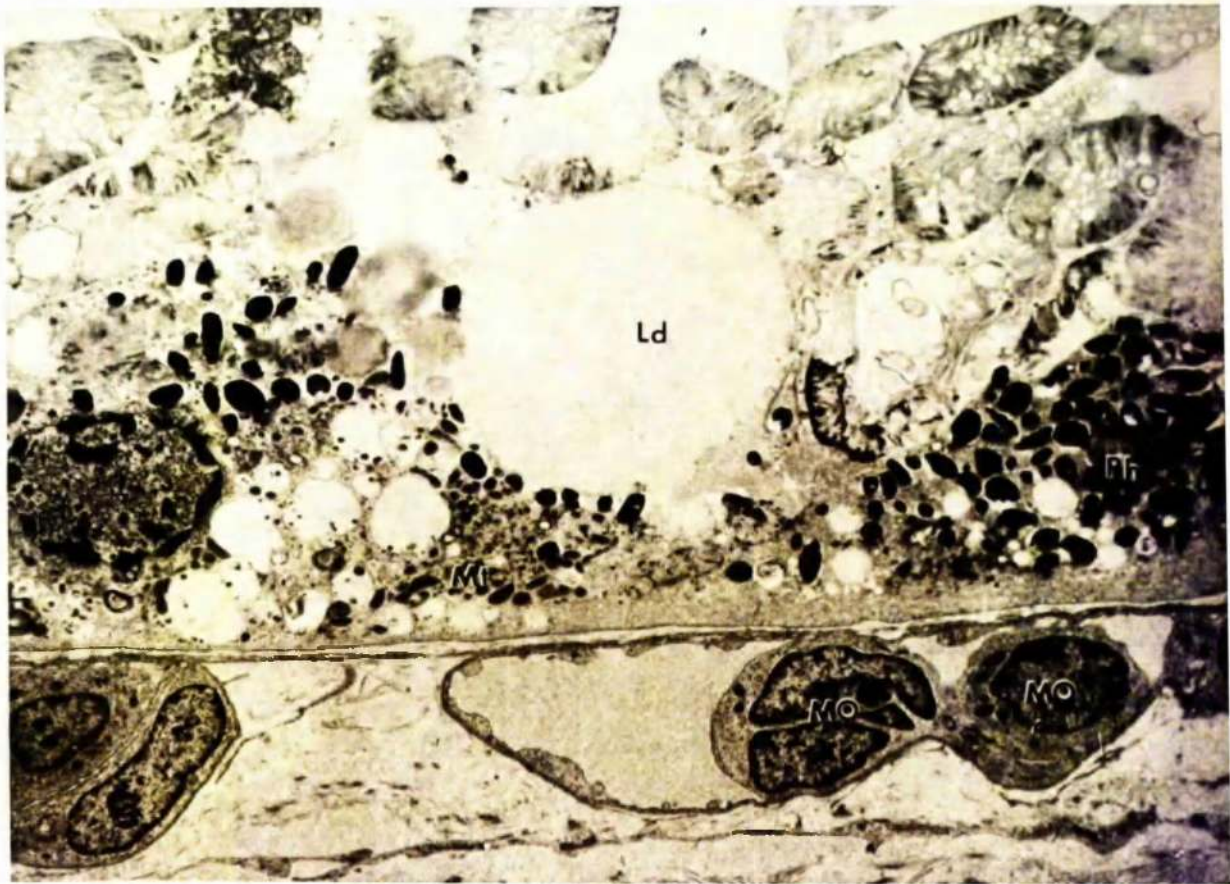


Figure 5.66 (1/24h/2 block C2). Electron micrograph showing the appearance of surviving pigment epithelium, twenty four hours after exposure to light of the higher intensity. Mt: mitochondria; Ld: lipid droplet; Ph: phagosome; MO: mononuclear cell (x 3,800).

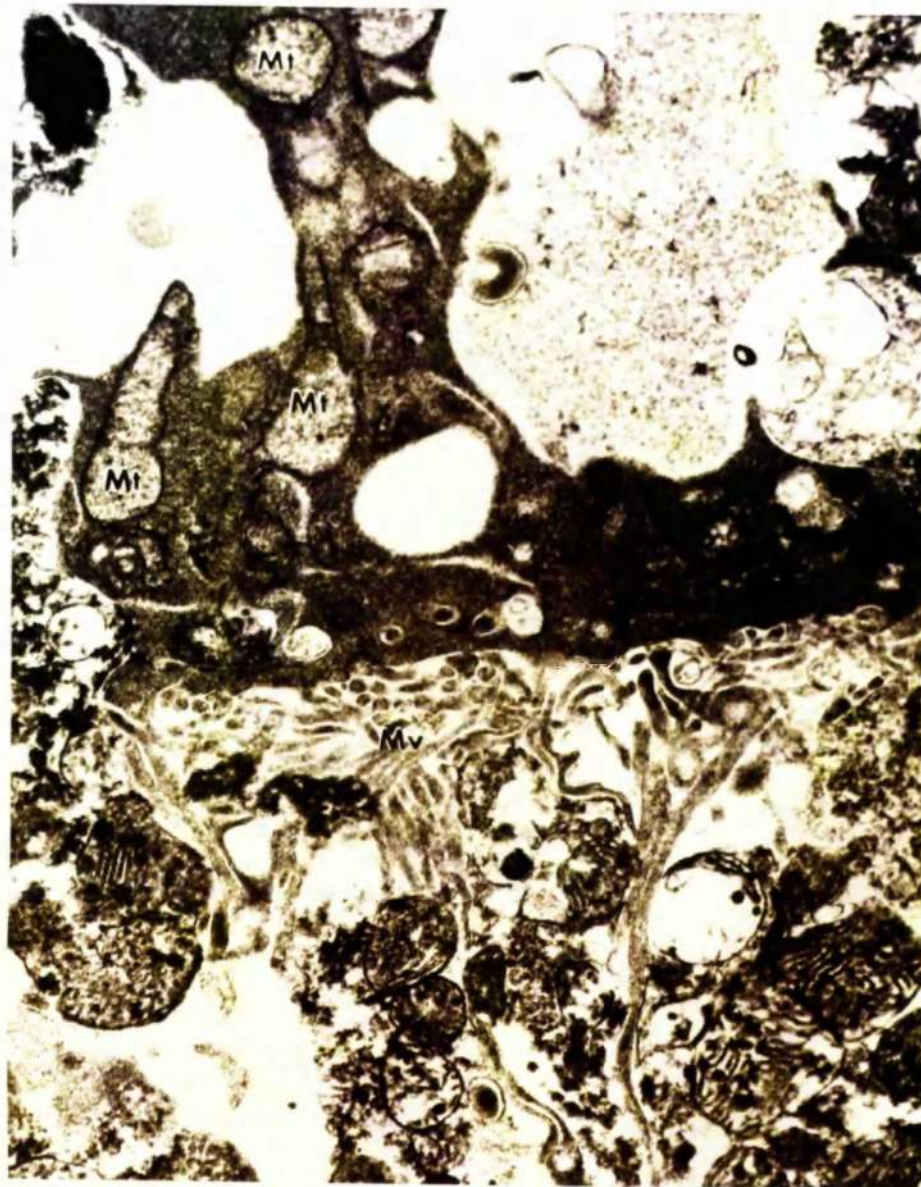


Figure 5.67 (1/24h/2 block C2). Electron micrograph showing the appearance of Müller cells' cytoplasm at the level of the outer limiting membrane, twenty four hours after exposure to light of the higher intensity. Mv: Microvilli; Mt: mitochondria (x 18,000).

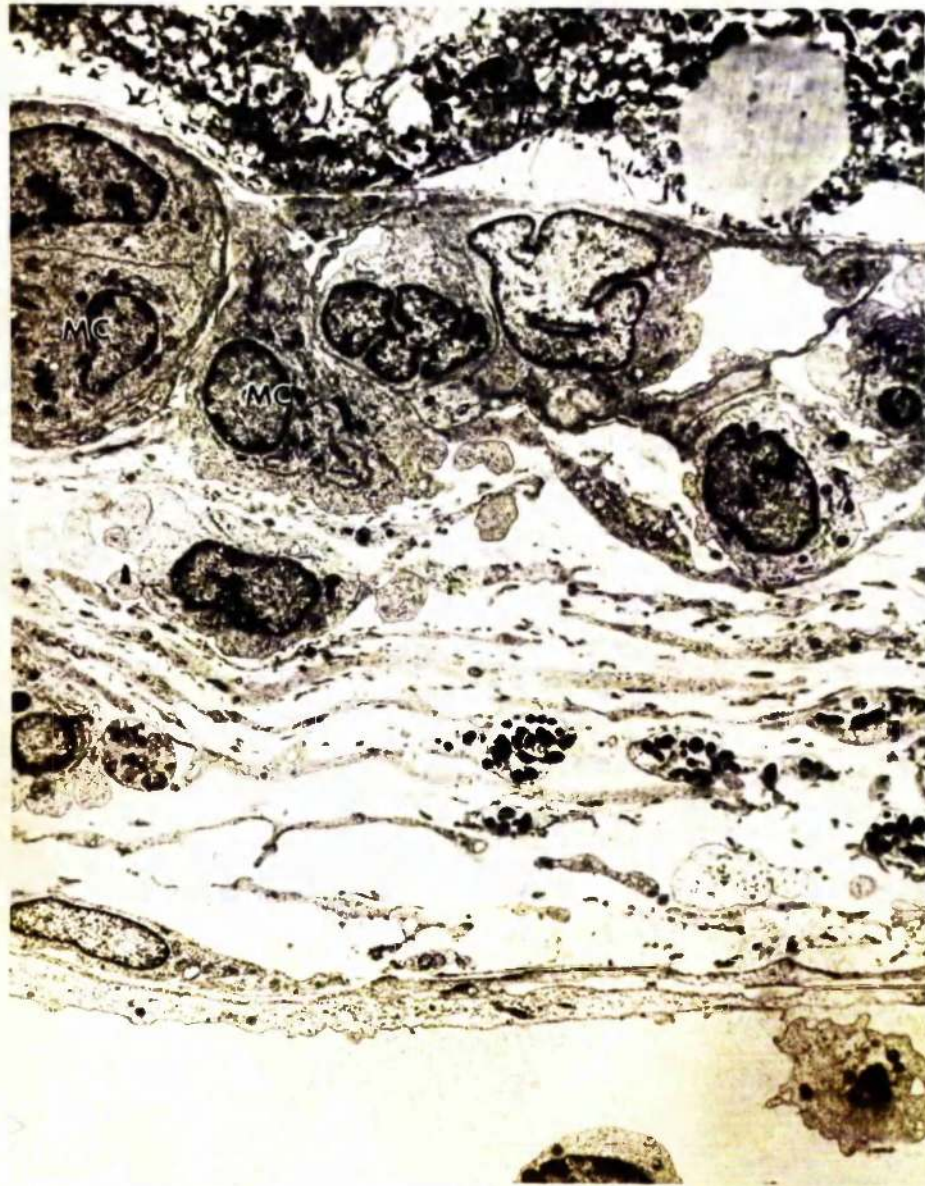


Figure 5.68 (1/24h/1 block B1). Electron micrograph showing the appearance of the choriocapillaris, twenty four hours after exposure to light of the higher intensity. Cells, thought to be monocytes, are present within, and between, the vessels of the choriocapillaris. MC: monocyte (x 3,700).

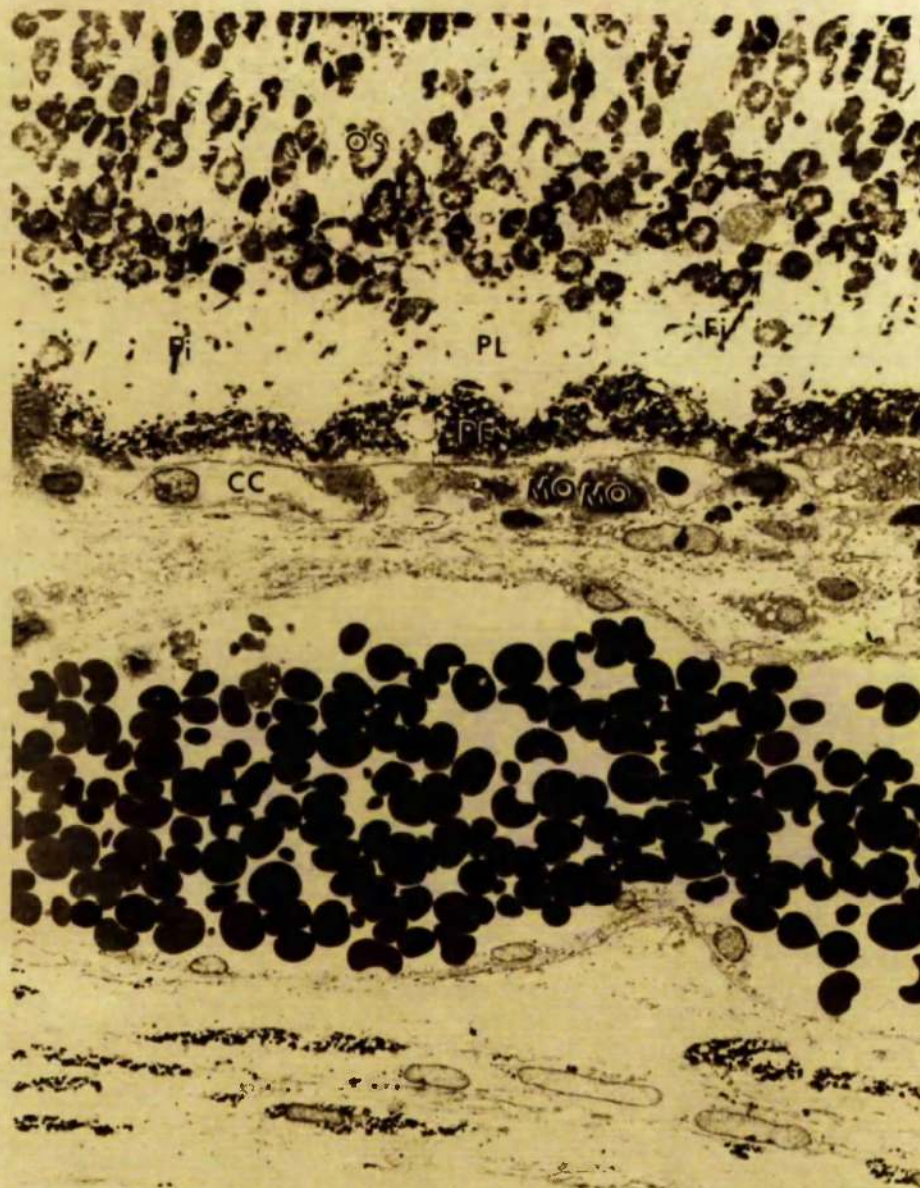


Figure 5.69 (1/48h/1 block C1). Electron micrograph of the outer retina and choroid, forty eight hours after exposure to light of the higher intensity. OS: outer segment material; PE: pigment epithelium; CC: choriocapillaris; MO: mononuclear cells; PL: plasma; Fi: fibrin (x 1,000).



Figure 5.70 (i/48h/1 block C1). Electron micrograph showing the appearance of the inner retina, forty eight hours after exposure to light of the higher intensity. Arrows: pyknotic and disintegrating nuclei; Mc: Müller cell cytoplasm; Mn: Müller cell nucleus; G: ganglion cell (x 1,200).

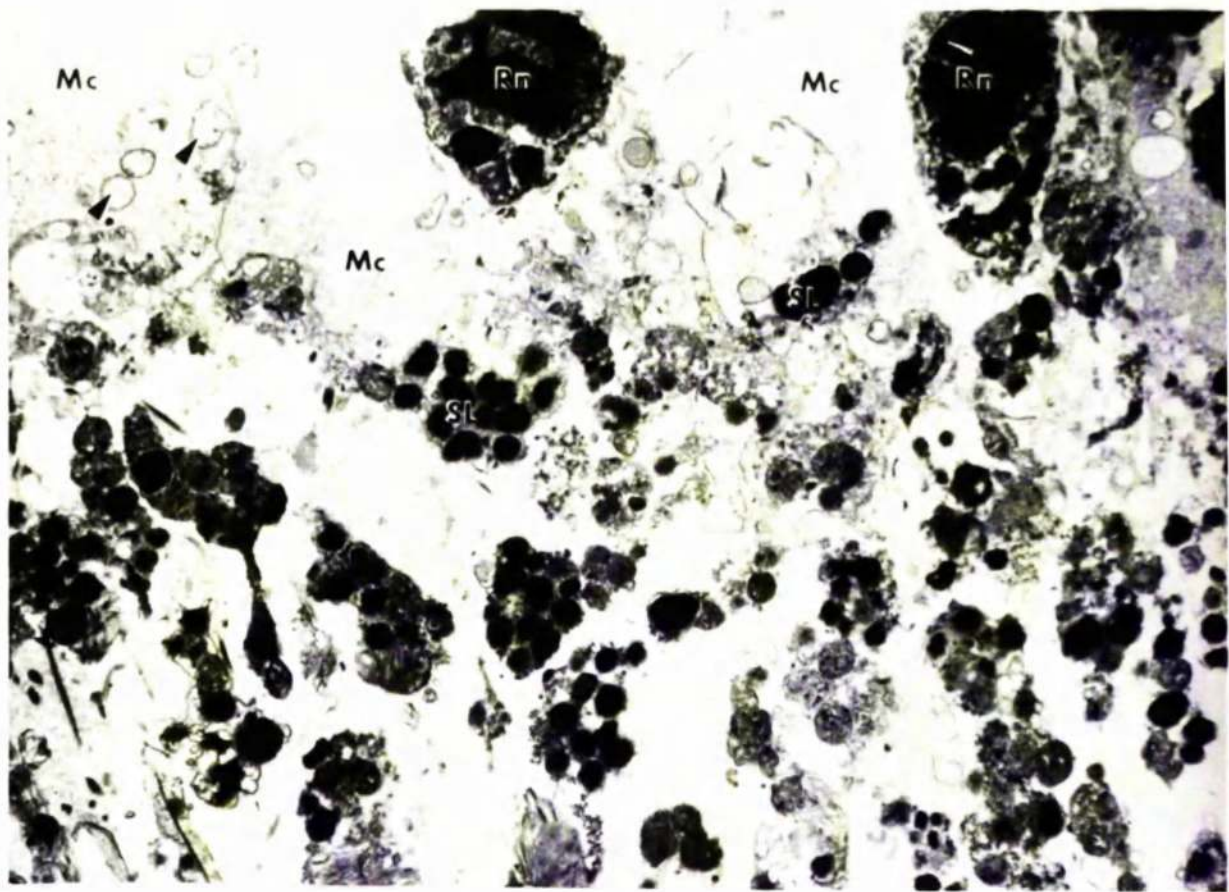


Figure 5.71 (1/48h/1 block C1). Electron micrograph showing the appearance of the retina, in the region of the outer limiting membrane, forty eight hours after exposure to light of the higher intensity. Rn: rod nucleus; Mc: Müller cell cytoplasm; Arrows: Müller cell mitochondria; SL: secondary lysosomes (x 4,600).

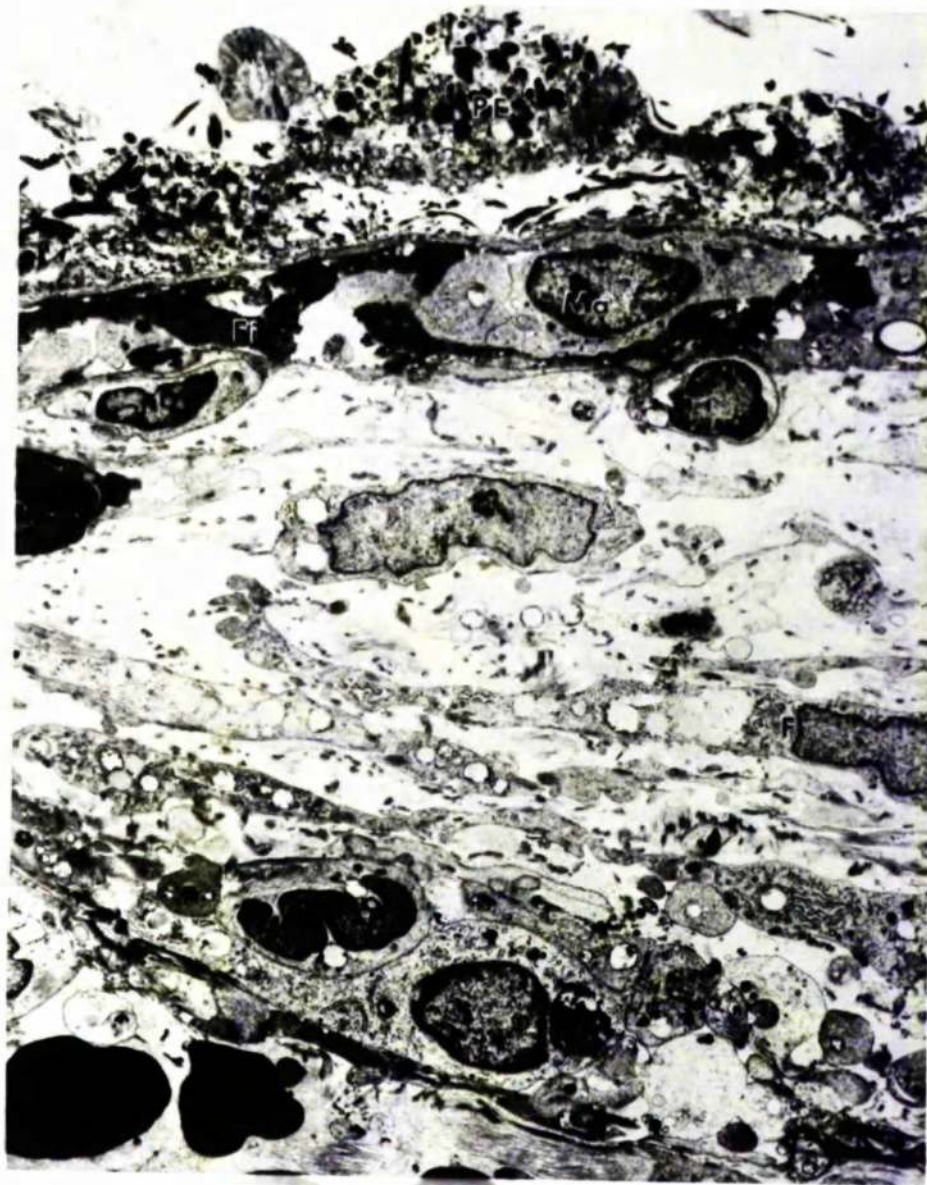


Figure 5.72 (1/48h/1 block B2). Electron micrograph of the pigment epithelium and choroid, forty eight hours after exposure to light of the higher intensity. PE: pigment epithelium; Ma: macrophage; F: fibroblast; Fi: fibrin (x 3,500).

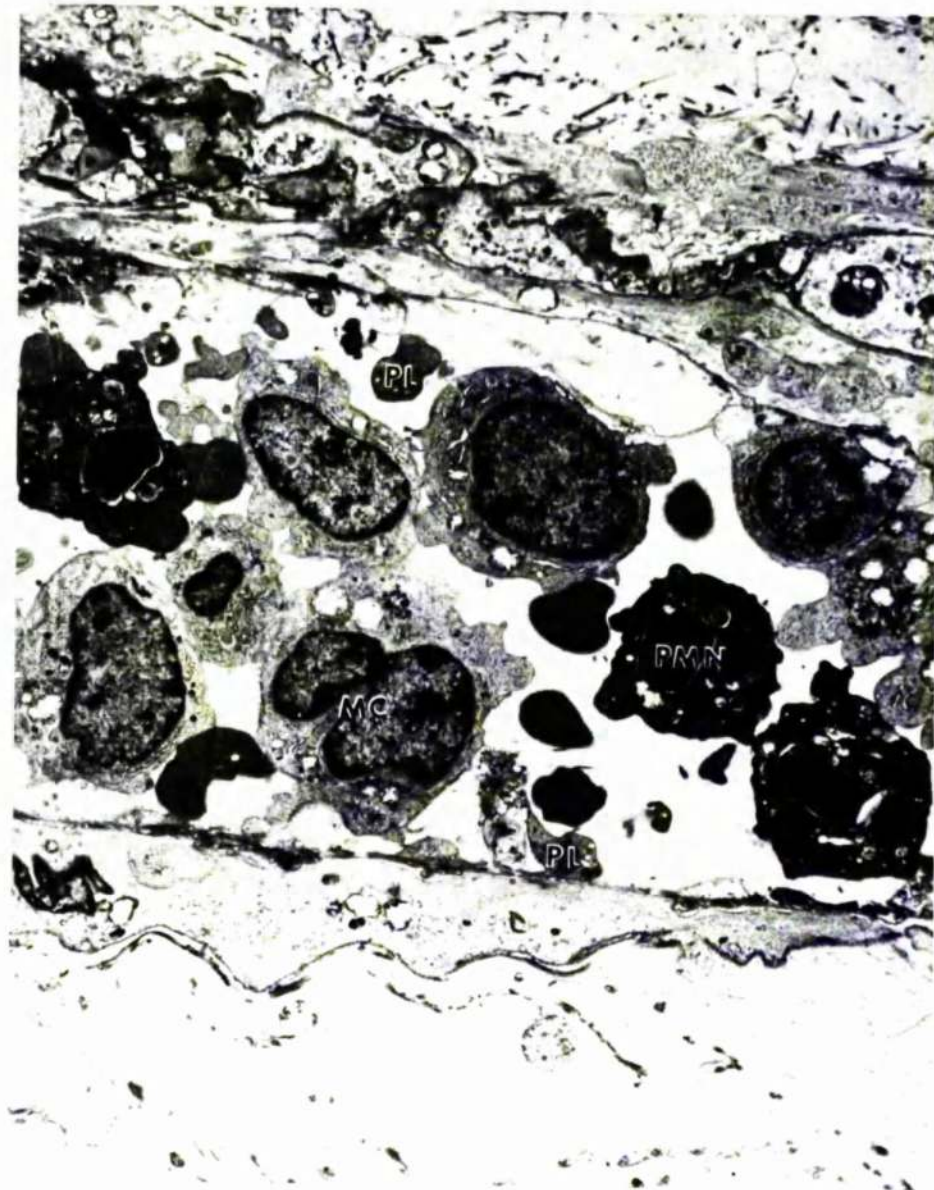


Figure 5.73 (1/48h/1 block B2). Electron micrograph of a choroidal venule, forty eight hours after exposure to light of the higher intensity. The lining endothelium is severely damaged and many inflammatory cells fill the lumen of the vessel. PMN: polymorphonuclear leucocyte; MC: monocyte; PL: platelet (x 3,600).

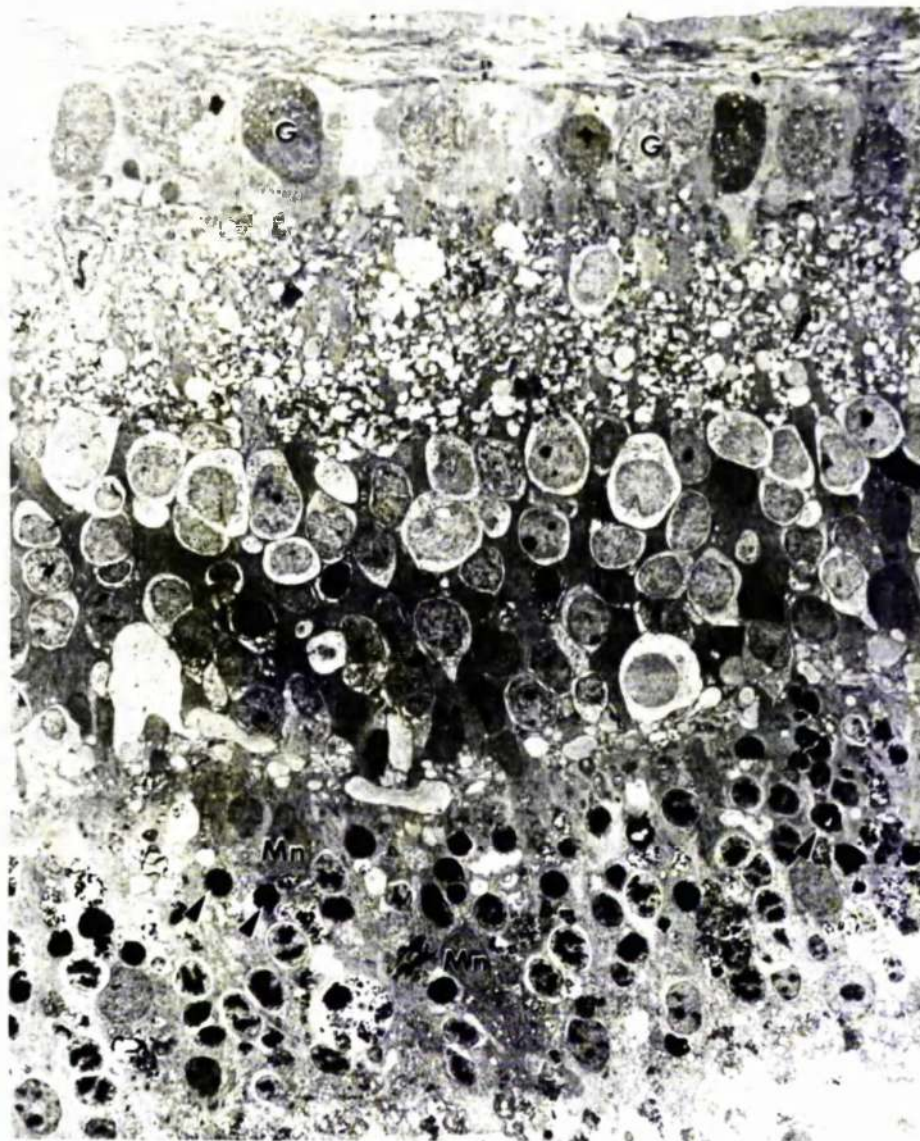


Figure 5.74 (1/48h/1 block A2). Electron micrograph showing a less severely damaged region of neural retina, forty eight hours after exposure to light of the higher intensity. G: ganglion; Mn: Müller cell nucleus; Arrows: pyknotic, and disintegrating, receptor cell nuclei (x 900).

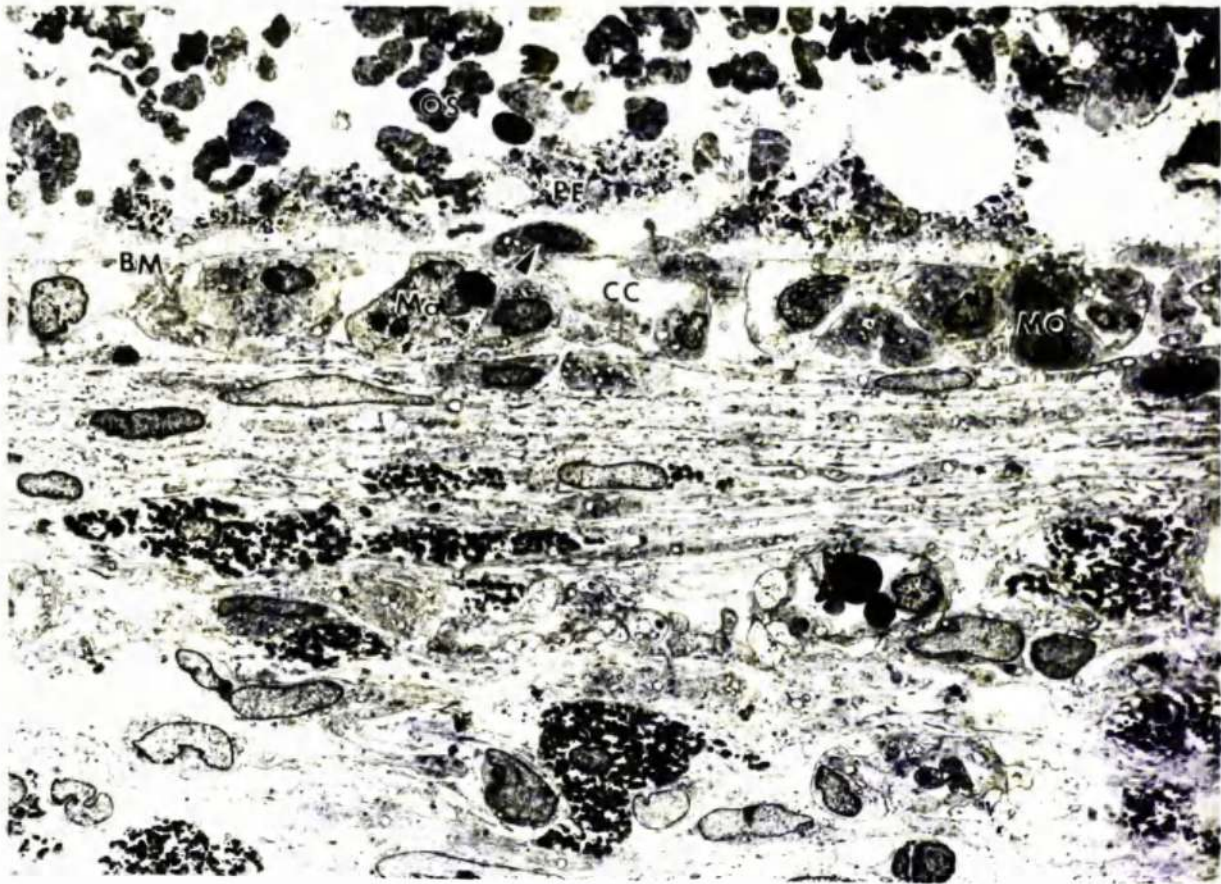


Figure 5.75 (1/48h/1 block A2). Electron micrograph showing the appearance of the pigment epithelium and choroid, forty eight hours after exposure to light of the higher intensity. OS: outer segment material; PE: pigment epithelium; CC: choriocapillaris; BM: Bruch's membrane; Ma: macrophage; MO: mononuclear cell between vessels of the choriocapillaris; Arrow: cell within Bruch's membrane (x 1,500).

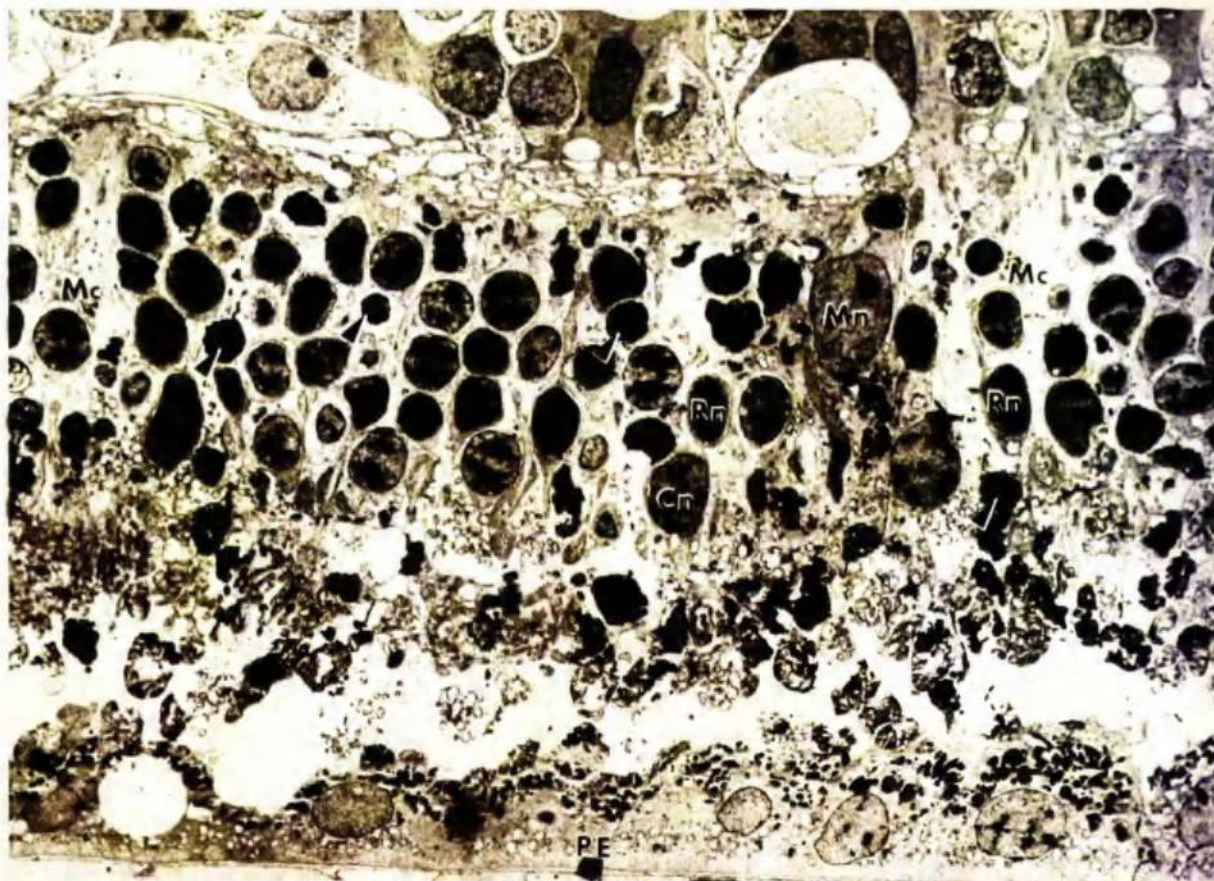


Figure 5.76 (1/48h/1 block D2). Electron micrograph showing the appearance of the outer retina, in a peripheral region of a lesion, forty eight hours after exposure to light of the higher intensity. Arrows: pyknotic and disintegrating nuclei; Rn: rod nucleus; Cn: cone nucleus; Mn: Müller cell nucleus; Mc: Müller cell cytoplasm; PE: pigment epithelium (x 1,400).



Figure 5.77 (1/48h/1 block D2). Electron micrograph, showing at higher magnification, the outer retina seen in Figure 5.76. IS: inner segment; OS: outer segment material; PE: pigment epithelium (x 3,500).

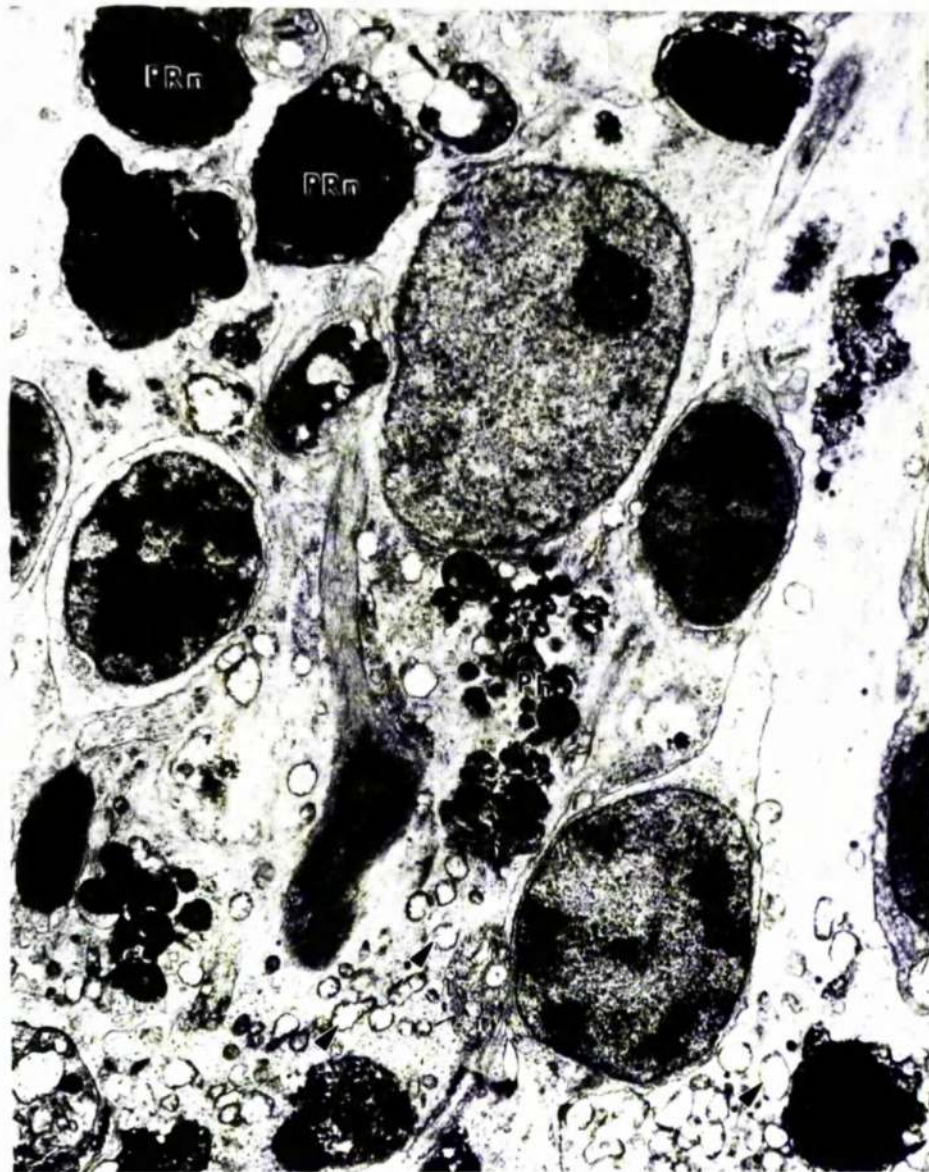


Figure 5.78 (1/48h/1 block D2). Electron micrograph showing, at higher magnification, one of the Müller cell nuclei observed within the outer nuclear layer in Figure 5.76. Mn: Müller cell nucleus; PRn: pyknotic rod nucleus; Ph: phagosomes of receptor cell material; Arrows: distended Müller cell mitochondria (x 4,600).

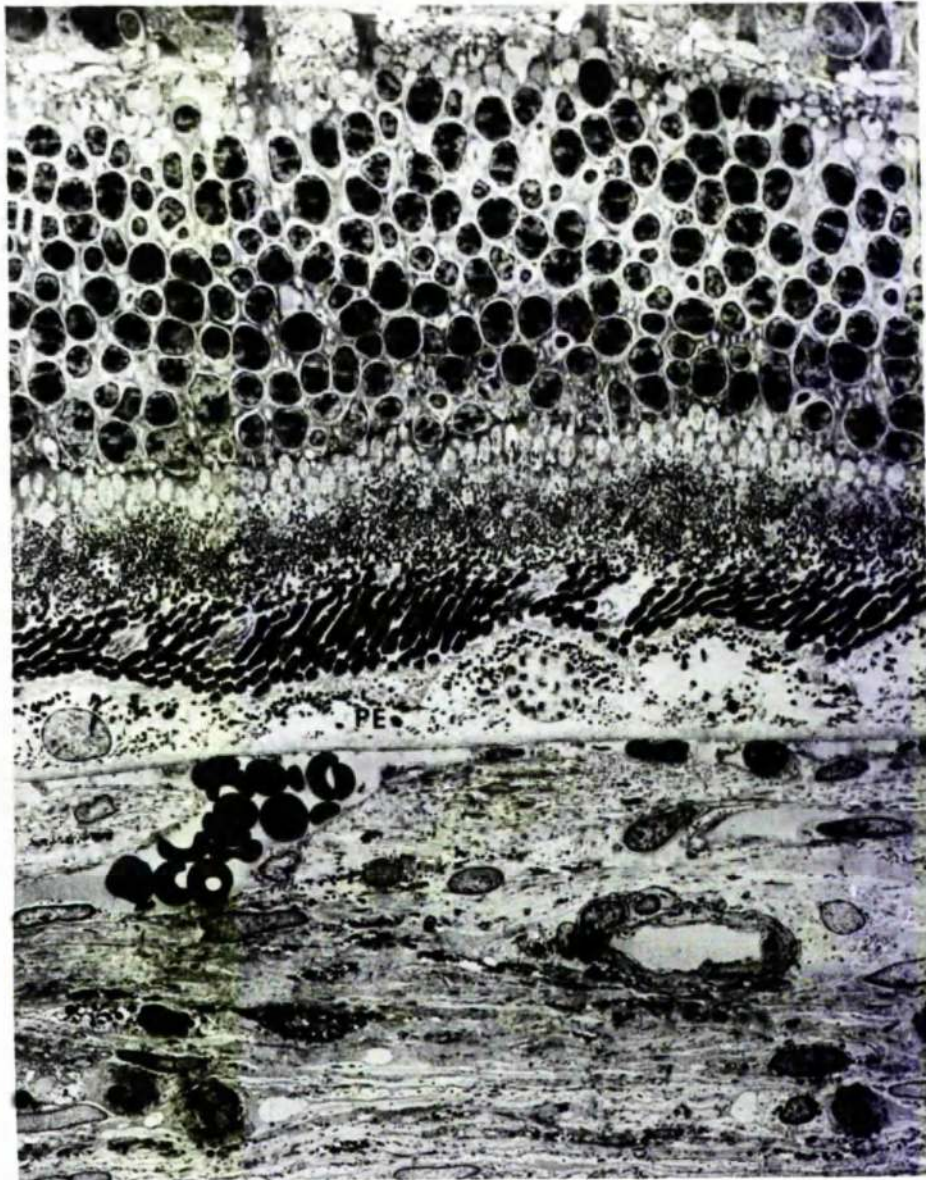


Figure 5.79 (1/48h/2 block B2). Electron micrograph of the outer retina and choroid, forty eight hours after exposure to light of the higher intensity. The neural retina does not appear to have suffered any damage but the pigment epithelium is highly unusual in appearance. PE: pigment epithelium (x 1,000).

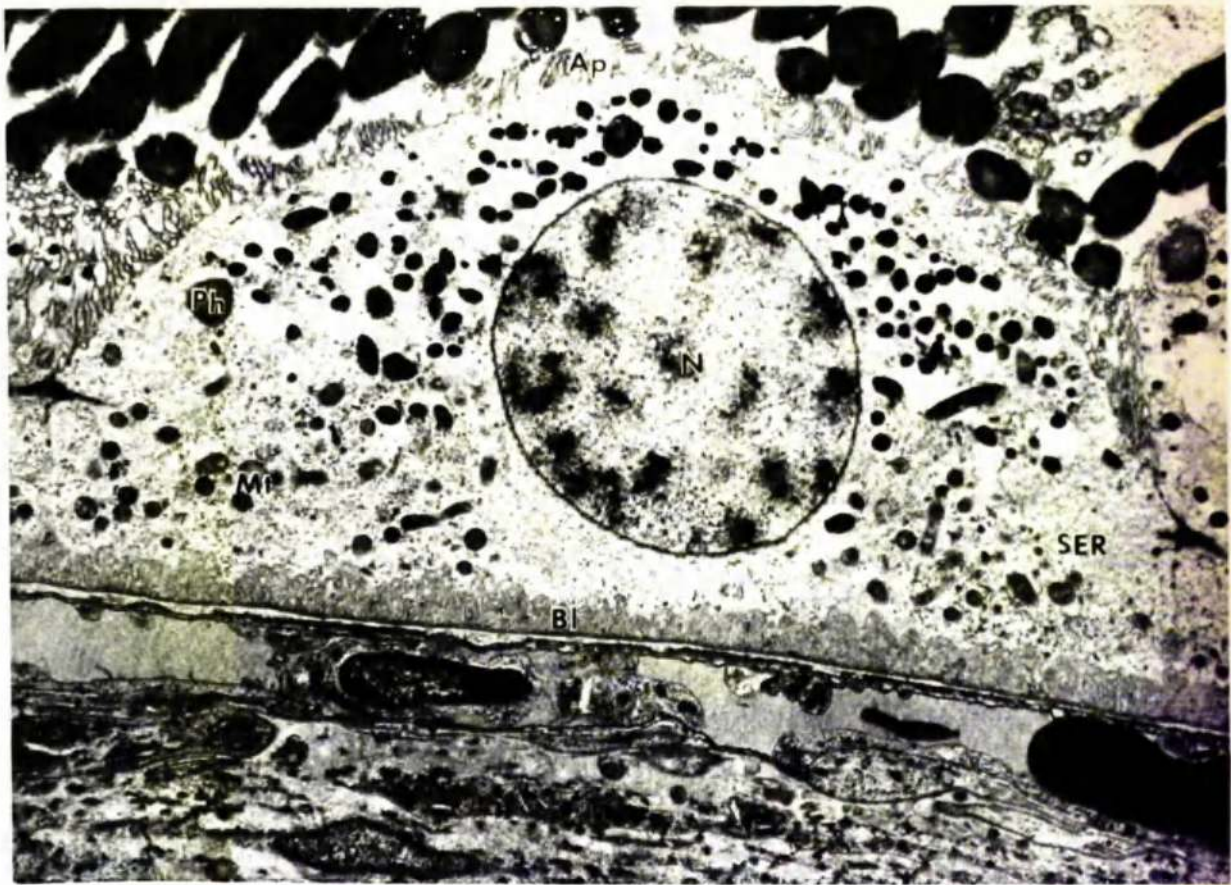


Figure 5.80 (1/48h/2 block B2). Electron micrograph, at higher magnification, of the pigment epithelium shown in Figure 5.79. Ap: apical processes; Ph: phagosome; Mt: mitochondria; SER: smooth endoplasmic reticulum; Bl: basal infoldings; N: nucleus ($\times 8,000$).

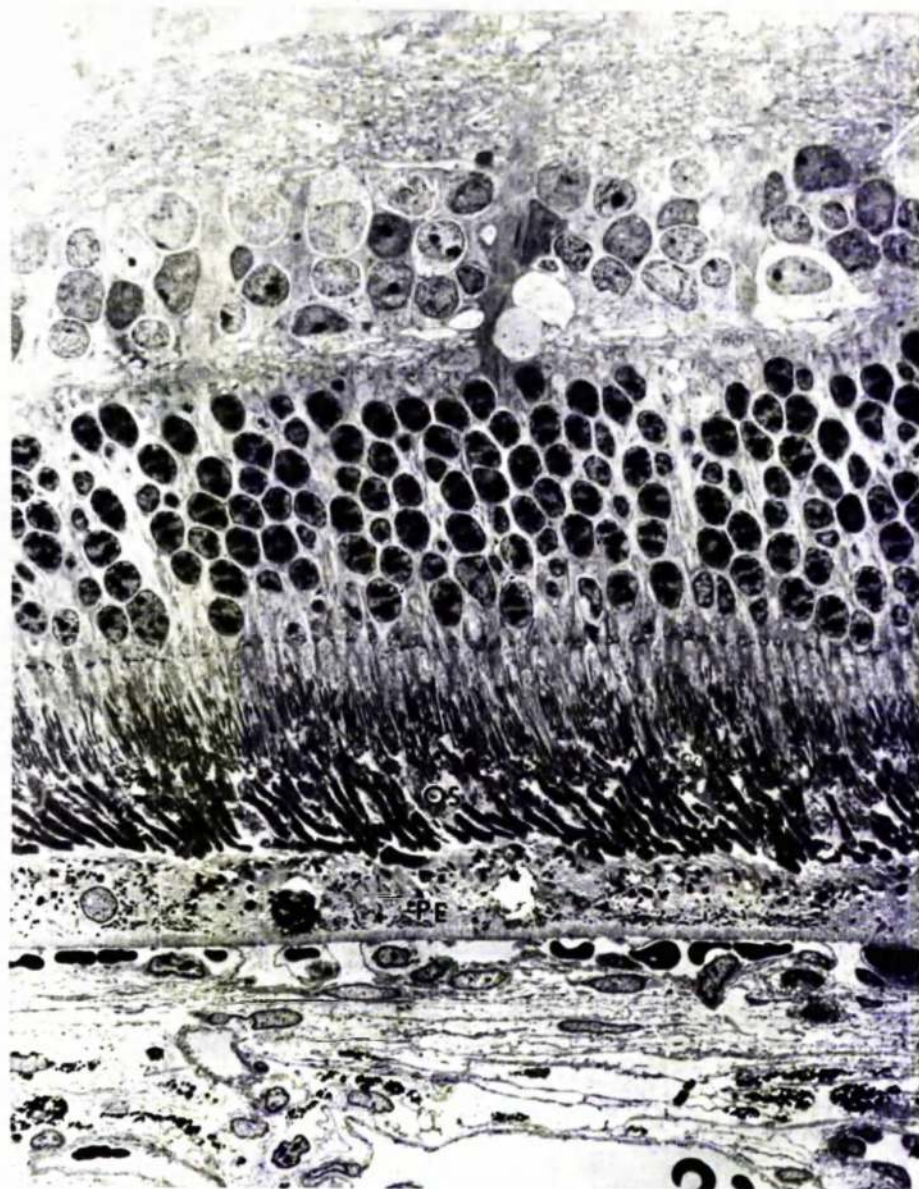


Figure 5.81 (1/4D/1 block B3). Figures 5.81, 5.82 and 5.83 are electron micrographs of the same tissue block. The fields shown are approximately 300 μ m apart. Figure 5.81 shows the appearance of the retina and choroid, at the extreme edge of a lesion, four days after exposure to light of the higher intensity. Structural abnormalities are limited to the outer segments and the pigment epithelium. OS: outer segments; PE: pigment epithelium. (x 900).

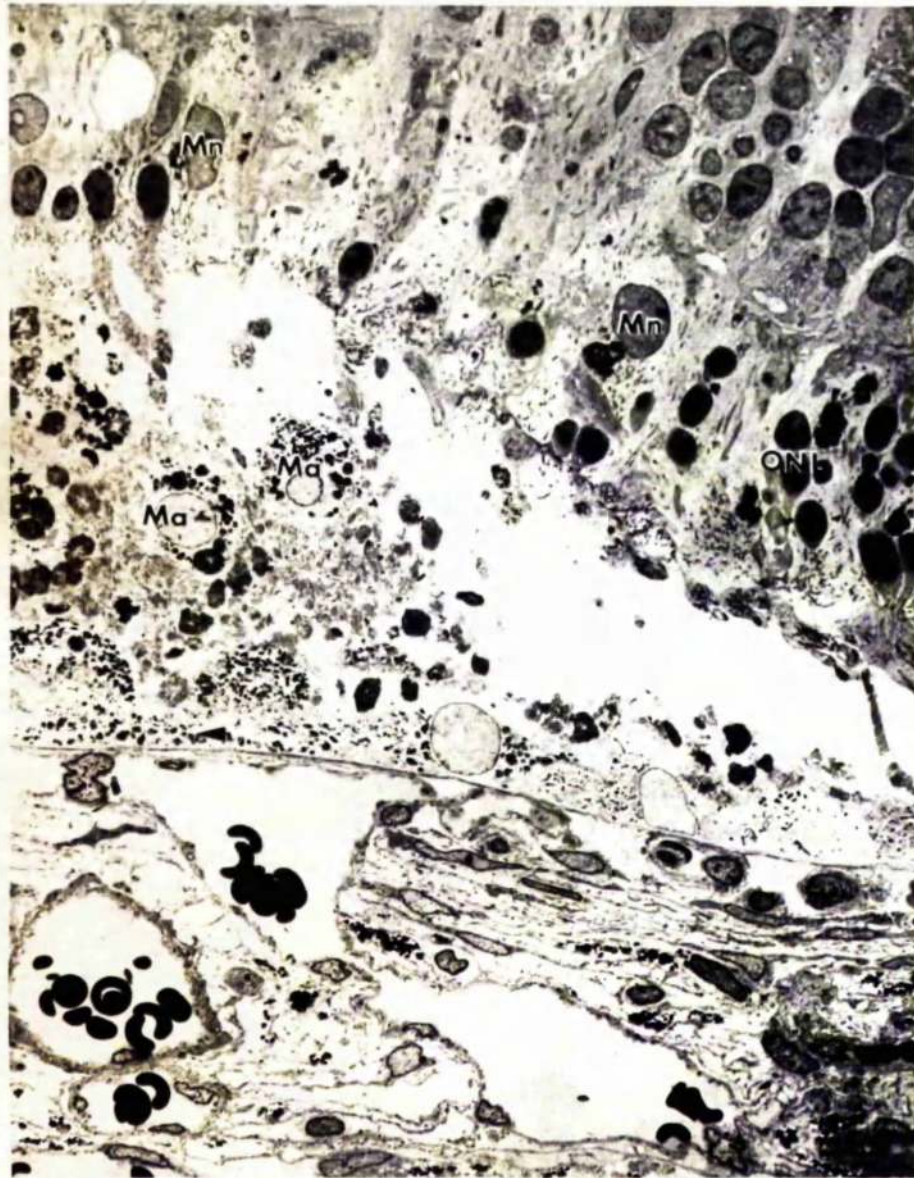


Figure 5.82 (1/4D/1 block B3). Electron micrograph showing the appearance of the retina and choroid four days after exposure to light of the higher intensity. The field shown is approximately 300 μ m further toward the lesion than the field shown in Figure 5.81. There is a loss of photoreceptor cells. Macrophages are plentiful in the subretinal space. The pigment epithelium is greatly extended in direction of increasing severity of damage. Arrow: pigment epithelial extension; Ma: macrophage; Mn: Müller cell nucleus; ONL: outer nuclear layer (x 900).

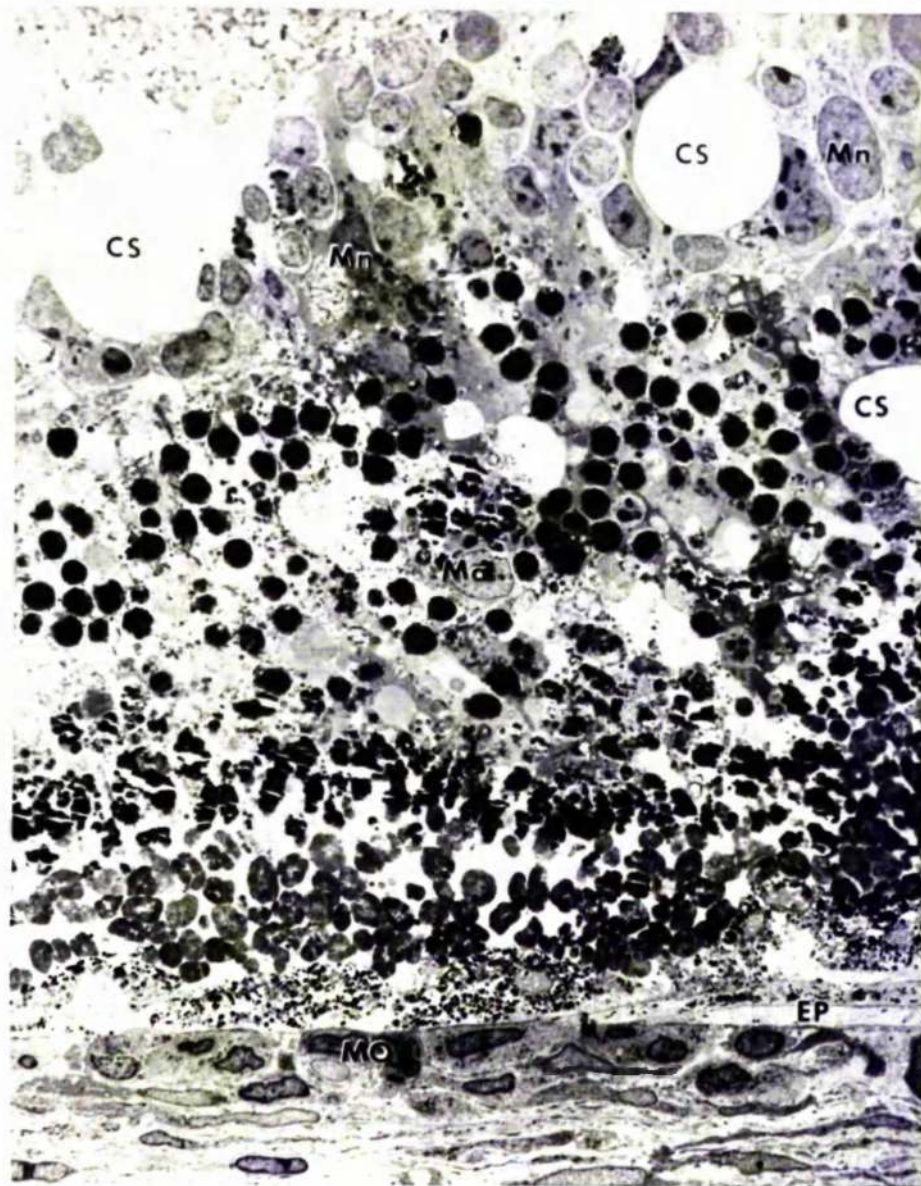


Figure 5.83 (1/4D/1 block B3). Electron micrograph showing the appearance of the retina, and choroid, four days after exposure to light of the higher intensity. The field shown is approximately 300 μ m further into the lesion than that shown in Figure 5.82. The retina has suffered considerably more damage. The vessels of the choriocapillaris are filled with mononuclear cells, probably monocytes. MO: mononuclear cells; Ma: macrophage; Mn: Müller cell nucleus; CS: cystic spaces; EP: extensions of the pigment epithelium. (x 900)



Figure 5.84 (1/4D/1 block B3). Electron micrograph, showing at higher magnification, the pigment epithelial processes seen in Figure 5.83. The processes appear to extend along Bruch's membrane below the degenerate pigment epithelium. DPE: degenerate pigment epithelium; EP: extensions of viable pigment epithelium (x 2,000).

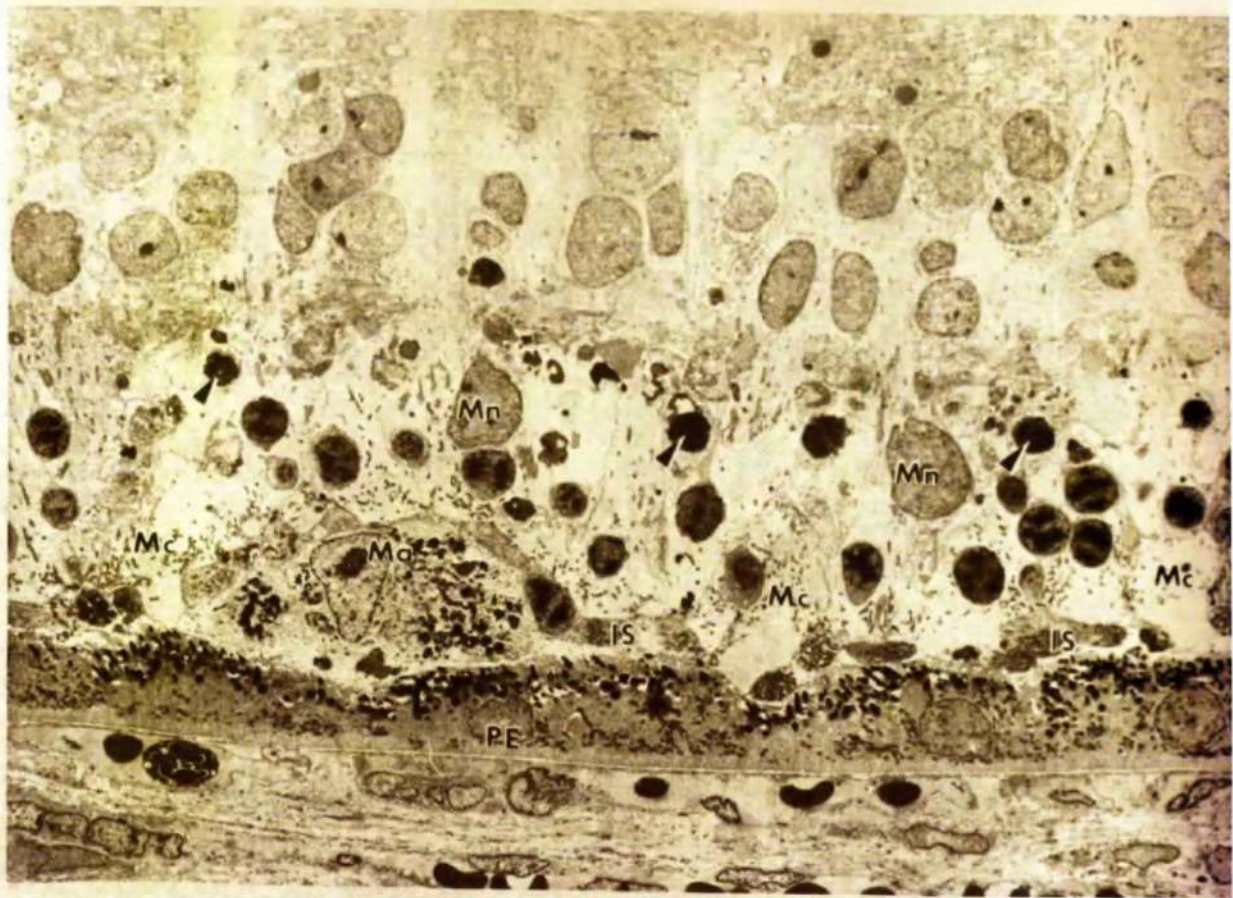


Figure 5.85 (1/4D/1 block D3). Electron micrograph showing the appearance of the retina, four days after exposure to light of the higher intensity. In the region shown there is considerable photoreceptor loss. Arrows: pyknotic and degenerating receptor cell nuclei; Mn: Müller cell nucleus; Mc: Müller cell cytoplasm; Ma: Macrophage; IS: inner segment; PE: pigment epithelium (x 1,350).

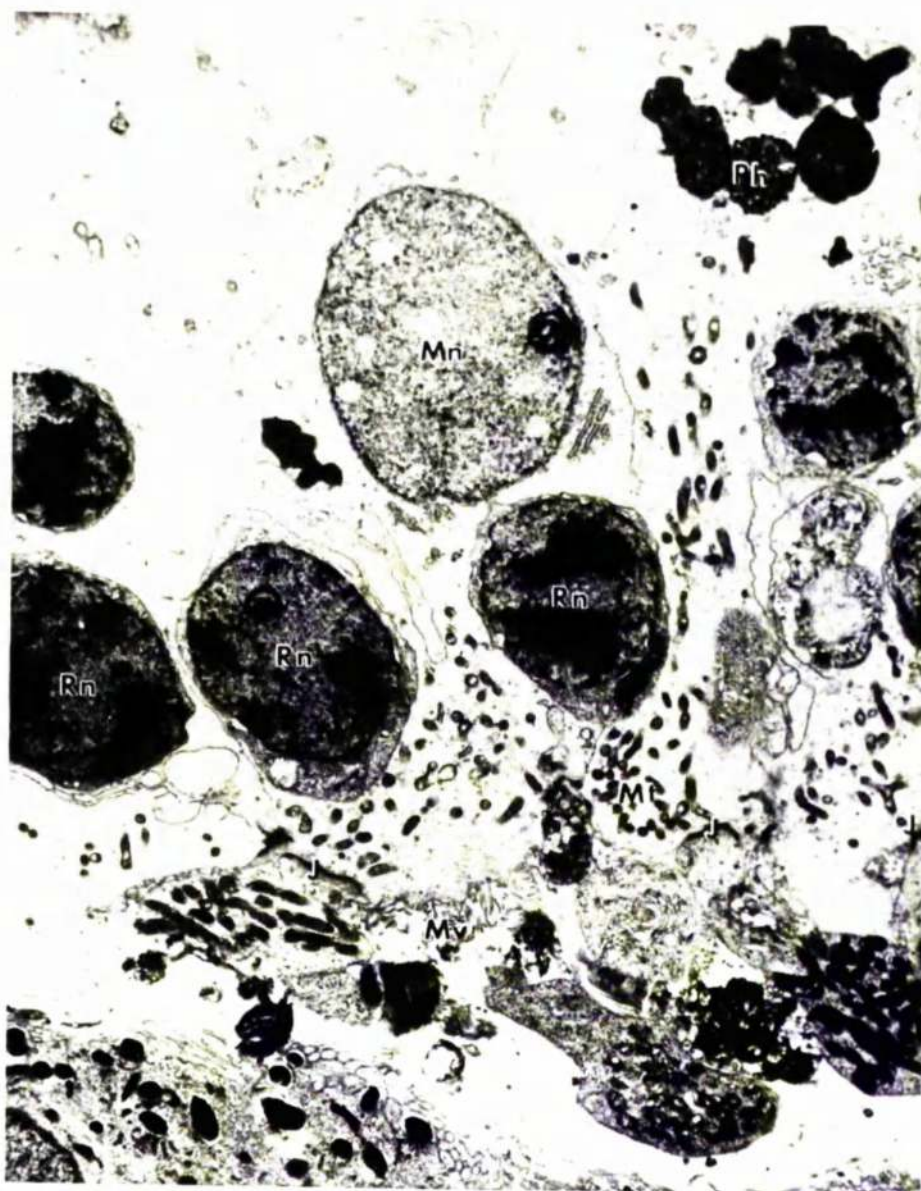


Figure 5.86 (1/4D/1 block D3). Electron micrograph showing, at higher magnification, the appearance of the surviving photoreceptors, four days after exposure to light of the higher intensity. Rn: rod nucleus; Mn: Müller cell nucleus; Mv: Müller cell micro villi; Mt: mitochondria (Müller cell); Ph: phagosome; J: cell junctions of outer limiting membrane (x 3,000).



Figure 5.87 (1/4D/1 block C2). Electron micrograph showing the appearance of the outer retina and the choroid, four days after exposure to light of the higher intensity. The field shown is from the centre of the lesion. ONL: outer nuclear layer; OS: outer segment material; PE: pigment epithelium; CC: chorio-capillaris; IRC: impacted rod cells (x 850).

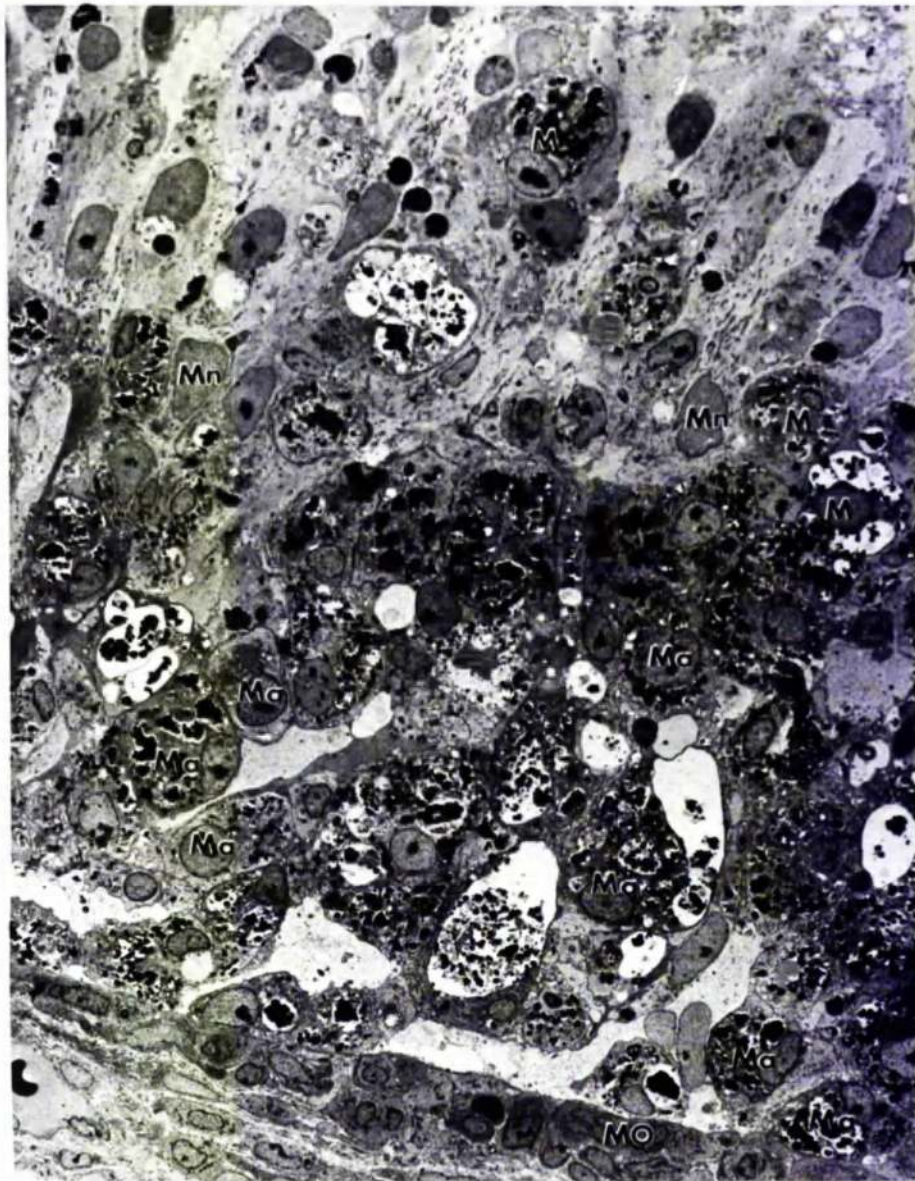


Figure 5.88 (1/4D/2 block C2). Electron micrograph showing the appearance of the retina and the choroid, four days after exposure to light of the higher intensity. The tissue shown is from a smaller lesion than that shown in Figure 5.87. Macrophages are abundant within the outer retina, some are present within the inner nuclear layer. The choriocapillaris is filled with mononuclear cells. Ma: macrophage; Mn: Müller cell nucleus; MO: mononuclear cell (x 850).

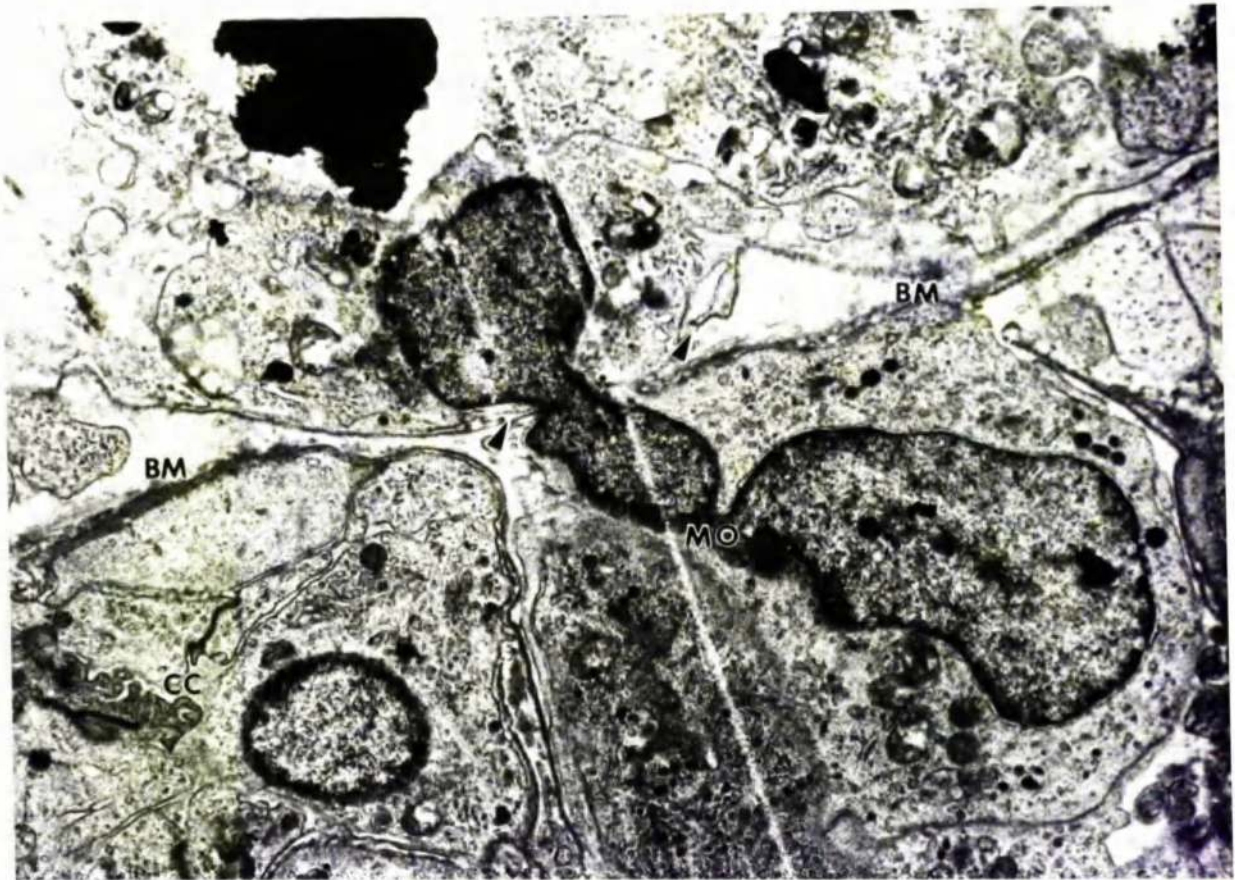


Figure 5.89 (1/4D/2 block B2). Electron micrograph showing a mononuclear cell passing through Bruch's membrane, four days after exposure to light of the higher intensity. MO: mononuclear cell; BM: Bruch's membrane; Arrows: pigment epithelial basement membrane; CC: choriocapillaris (x 8,600).



Figure 5.90 (1/4D/1 block D1). Electron micrograph showing a mildly damaged region of outer retina, four days after exposure to light of the higher intensity. There are disturbances of the rod outer segments. The pigment epithelial mitochondria are more densely stained than normal. ROS: rod outer segment; CIS: cone inner segment; COS: cone outer segment; Mt: mitochondria (x 3,500).

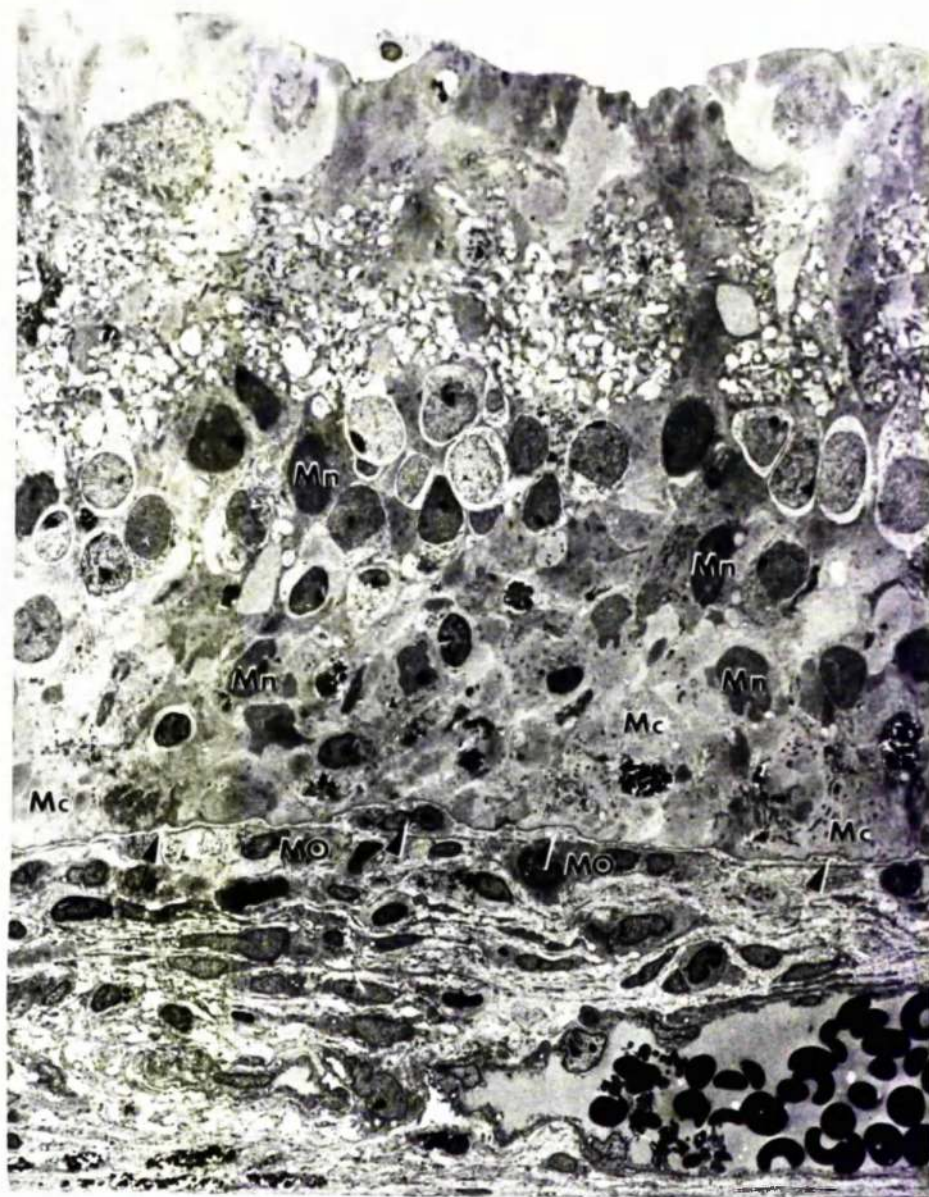


Figure 5.91 (1/2W/2 block C2). Electron micrograph of the retina and the choroid, two weeks after exposure to light of the higher intensity. The photoreceptors and the pigment epithelium are completely absent. Müller cell cytoplasm is in direct contact with Bruch's membrane. There are thickenings, and cellular infiltration, of Bruch's membrane. Macrophages and mononuclear cells are common in the inner regions of the choroid. Mn: Müller cell nucleus; Mc: Müller cell cytoplasm; Arrows: thickenings of, and cell within, Bruch's membrane; MO: mononuclear cells (x 1,000).

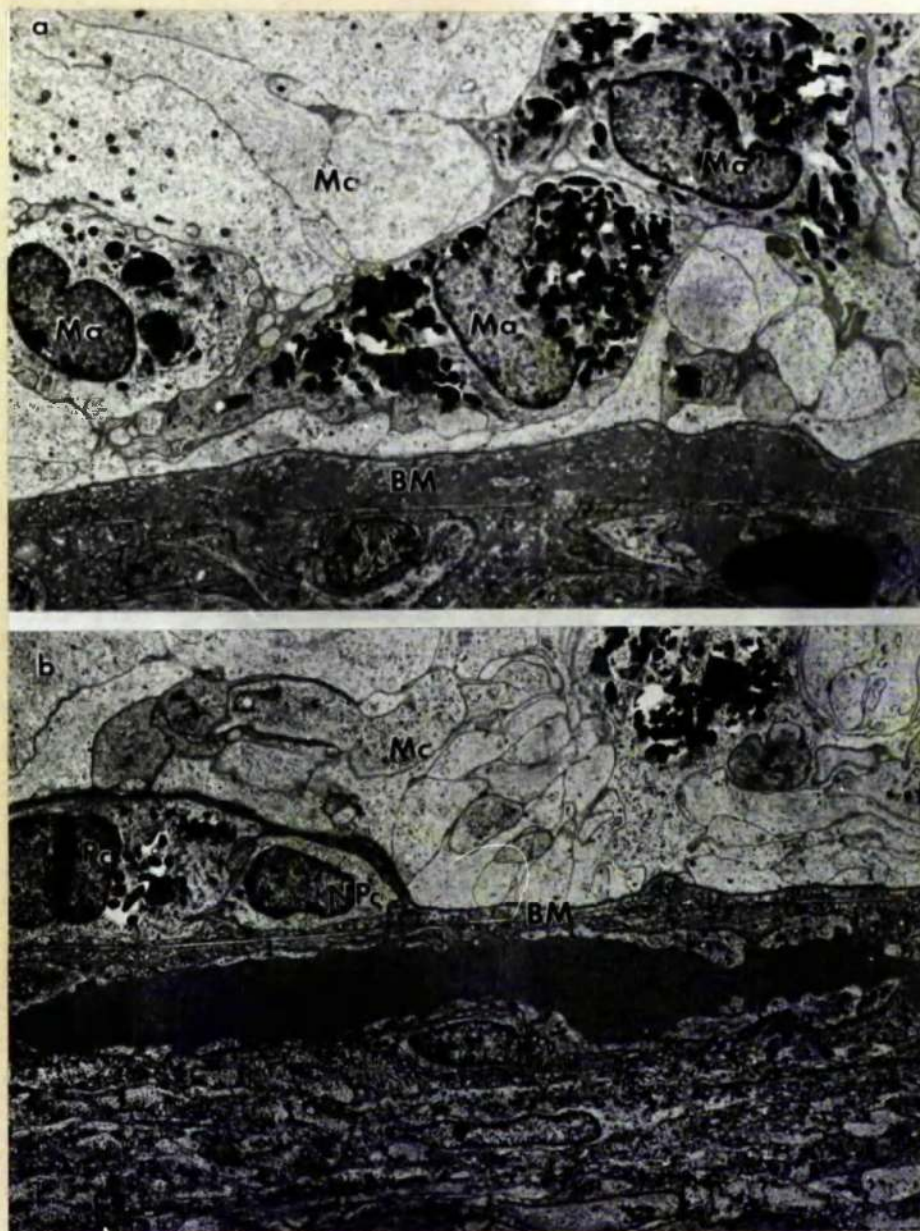


Figure 5.92 a and b (both 1/1W/1 block C2). a) Electron micrograph showing the appearance of the Müller cell cytoplasm, in an area of complete photoreceptor and pigment epithelial loss, one week after exposure to light of the higher intensity. Mc: Müller cell cytoplasm; BM: thickened Bruch's membrane; Ma: macrophage. (x 2,600). b) Same as a) but showing the presence of pigmented and non-pigmented cells within the structure of Bruch's membrane. Mc: Müller cell cytoplasm; Pc: pigmented cell; NPc: non-pigmented cell; BM: Bruch's membrane (x 2,600).



Figure 5.93 (1/4W/2 block D2). Electron micrograph showing the appearance of the retina, in a region of profound cellular loss, four weeks after exposure to light of the higher intensity. G: ganglion cell; Mn: Müller cell nucleus; Mc: Müller cell cytoplasm; Pc: pigmented cells, thought to be macrophages; BM: Bruch's membrane; Arrow: pigmented cell within the structure of Bruch's membrane (x 1,800).

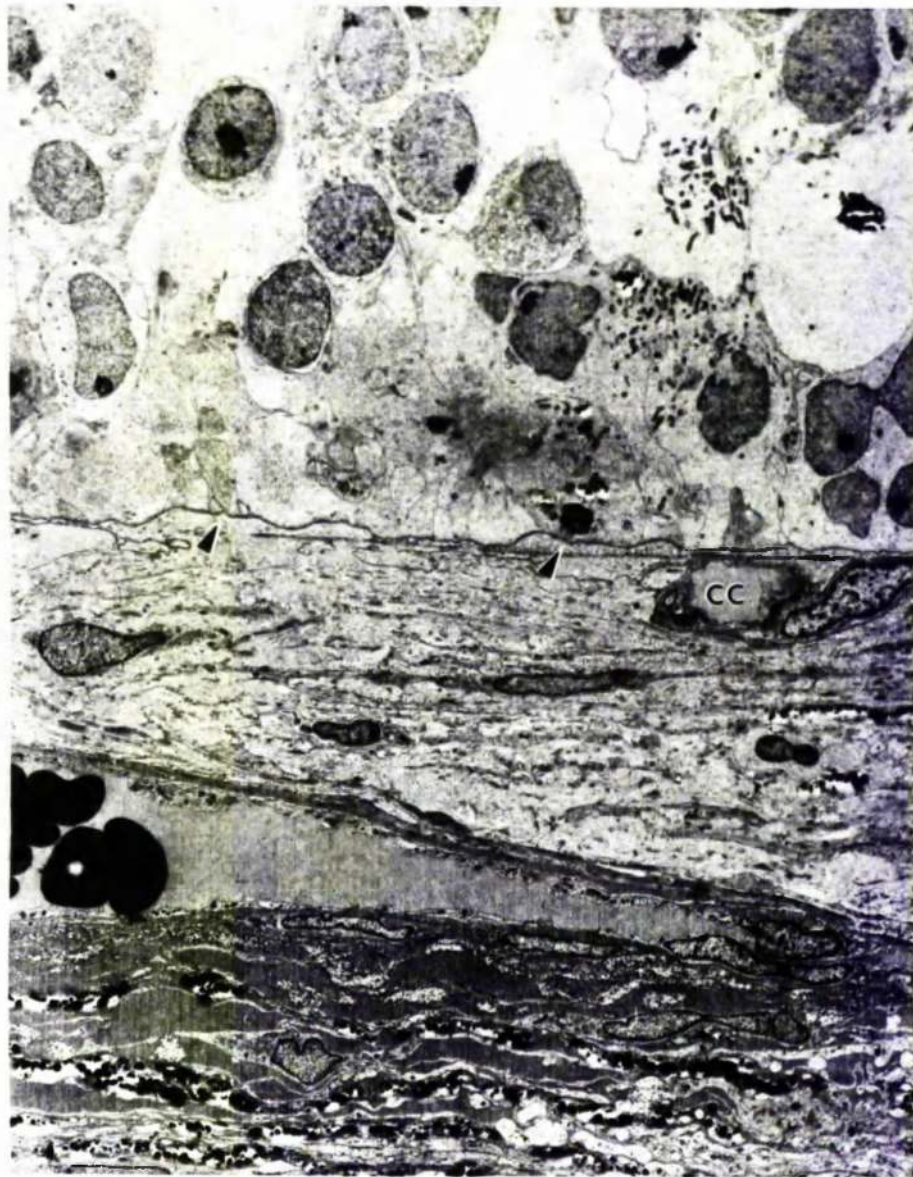


Figure 5.94 (1/4W/2 block C2). Electron micrograph showing the appearance of Bruch's membrane and the choroid, in an area of receptor and pigment epithelial cell loss, four weeks after exposure to light of the higher intensity. There are thickenings of Bruch's membrane. The choriocapillaris is absent, or of highly atypical appearance. Arrows: thickenings of Bruch's membrane; CC: greatly reduced vessel of the choriocapillaris. The endothelial cells show crenellation of their nuclei which suggests contraction of the cells (x 2,000).

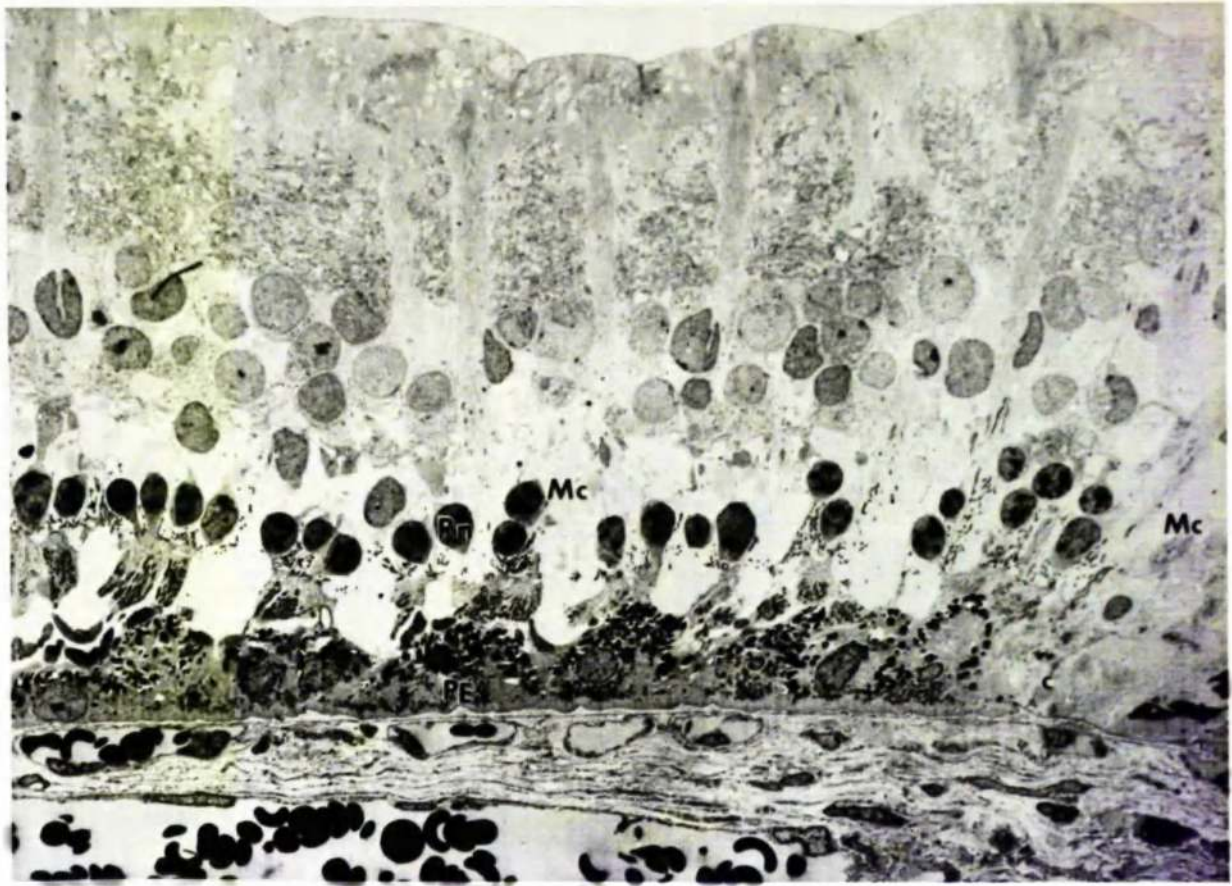


Figure 5.95 (1/4W/2 block D2). Electron micrograph showing the appearance of the retina and the choroid, four weeks after exposure to light of the higher intensity. Surviving photoreceptors occur only in association with viable pigment epithelium. Rn: rod nucleus; PE: pigment epithelium; Mc: Müller cell cytoplasm (x 900).

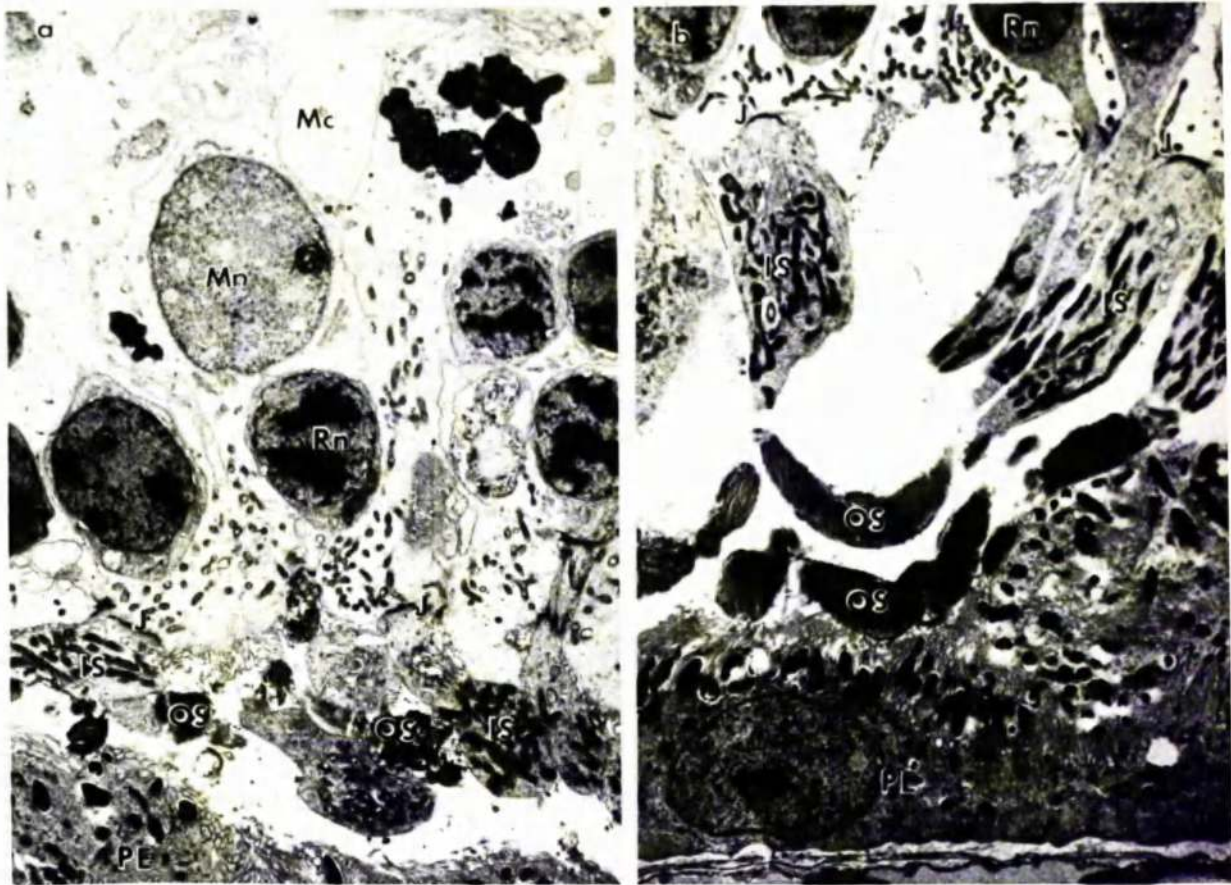


Figure 5.96 (a) 1/4D/1 block D2; b) 1/4W/2 block D3). Electron micrographs showing the appearance of the rod inner and outer segments, a) 4 days and b) 4 weeks, after exposure to light of the higher intensity. The regions shown are thought to have suffered a similar degree of initial damage. Rn: rod nucleus; IS: inner segment; OS: outer segment; Mn: Müller cell nucleus; Mc: Müller cell cytoplasm; J: junctions of the outer limiting membrane; PE: pigment epithelium (both $\times 3,100$).

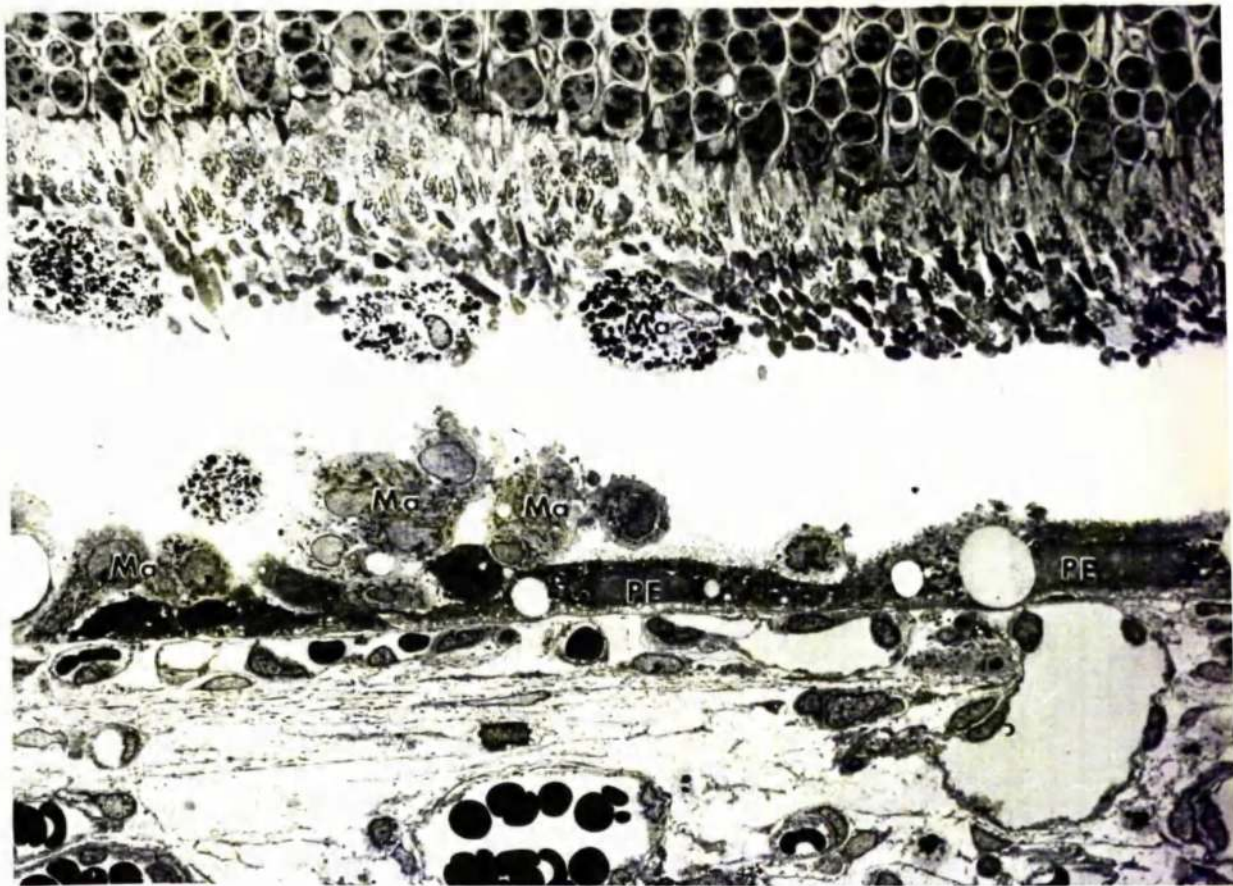


Figure 5.97 (1/1W/2 block A3). Electron micrograph showing an area of suspected pigment epithelial proliferation, one week after exposure to light of the higher intensity. By light microscopy this area was thought to show pigment epithelial proliferation. Electron microscopy suggested that the majority of the cells were macrophages. PE: pigment epithelium; Ma: macrophage ($\times 850$).

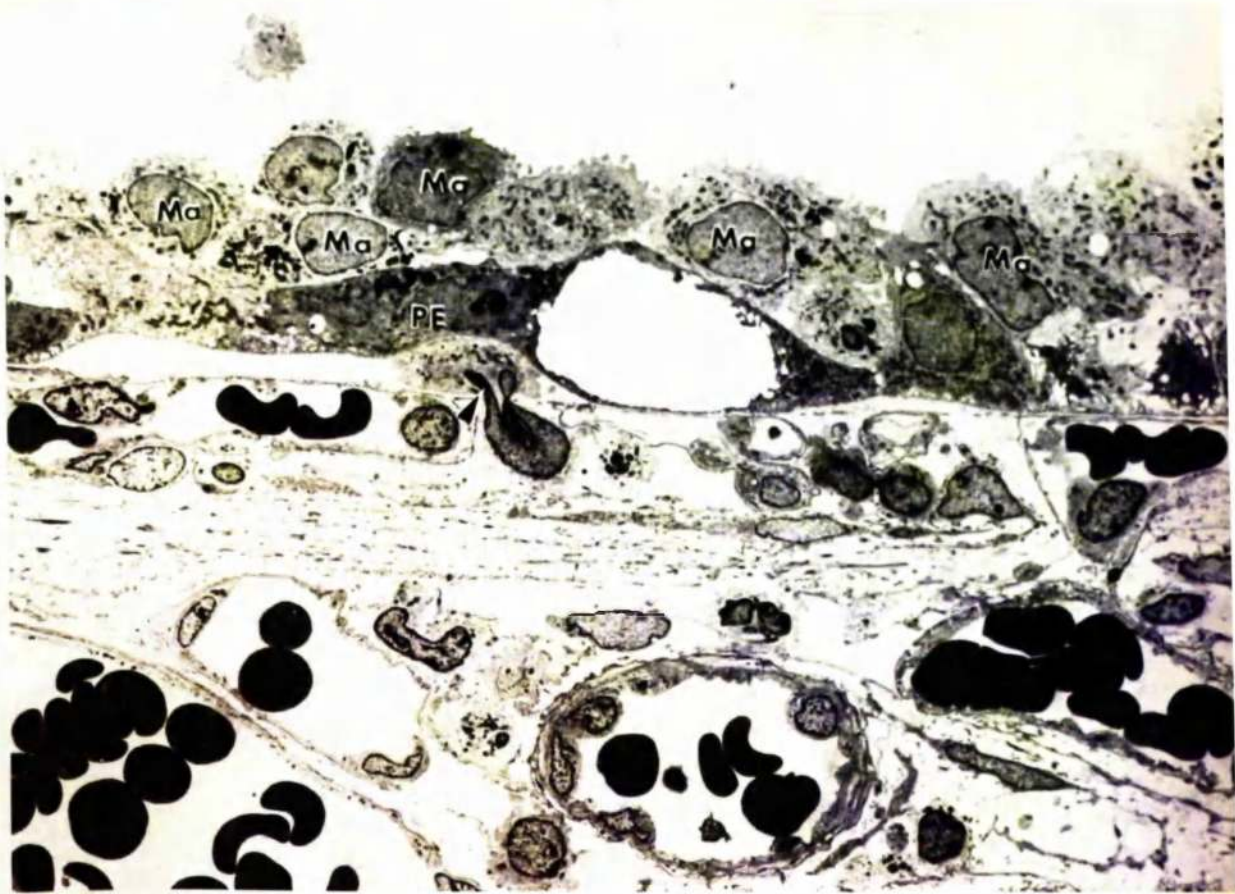


Figure 5.98 (1/1W/2 block A3). Electron micrograph showing, at slightly higher power, a region of suspected pigment epithelial proliferation one week after exposure to light of the higher intensity. The majority of the cells present are thought to be macrophages. A similarity of the cells in the retina, to the cell between Bruch's membrane and the choroid, is apparant. PE: pigment epithelium; Ma: cells thought to be macrophages; Arrow: cell partly within Bruch's membrane (x 1,200).

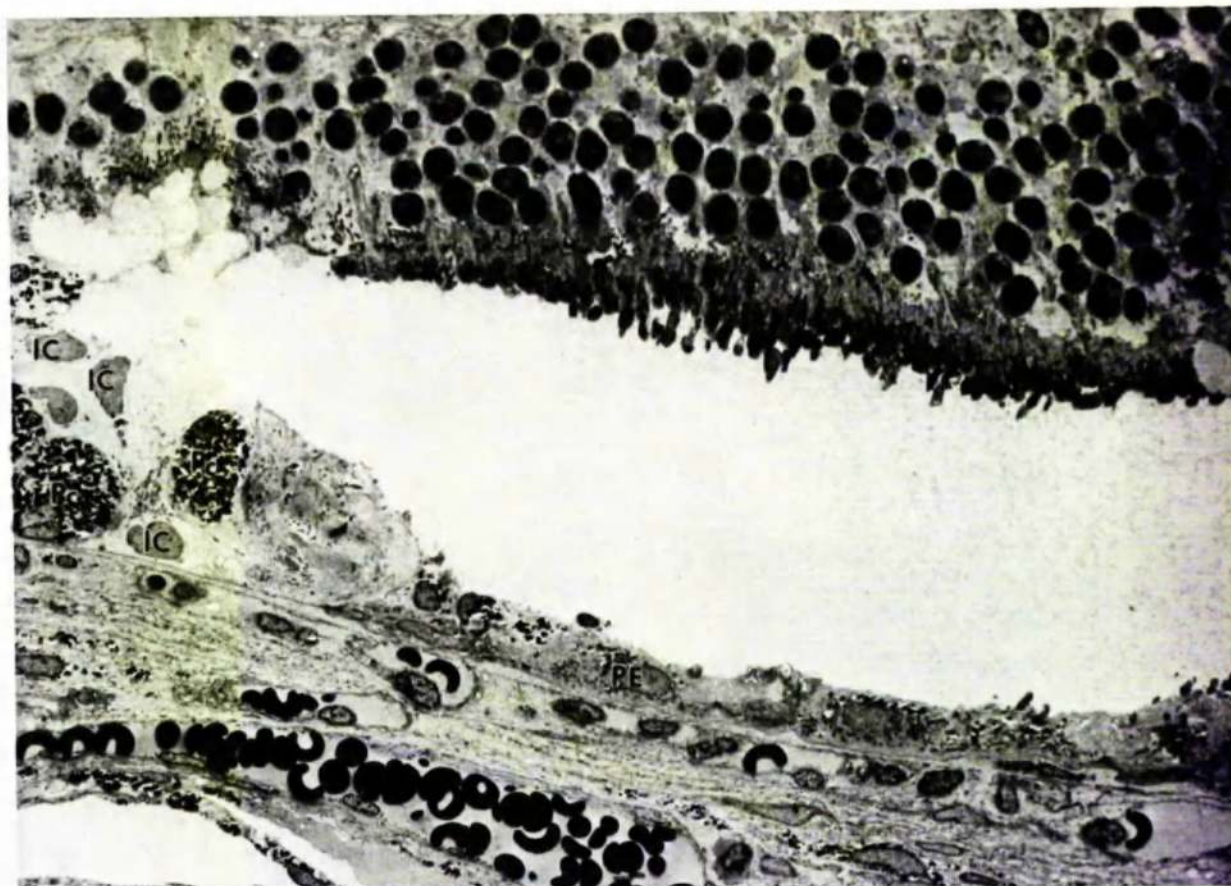


Figure 5.99 (1/4W/2 block C2). Electron micrograph showing an area of suspected cell proliferation, four weeks after exposure to light of the higher intensity. The cells within this region of suspected proliferation were of two types: large pigmented cells, and irregularly shaped non-pigmented cells. PE: pigment epithelium; Pc: pigmented cell; IC: irregularly shaped cell ($\times 1,200$).

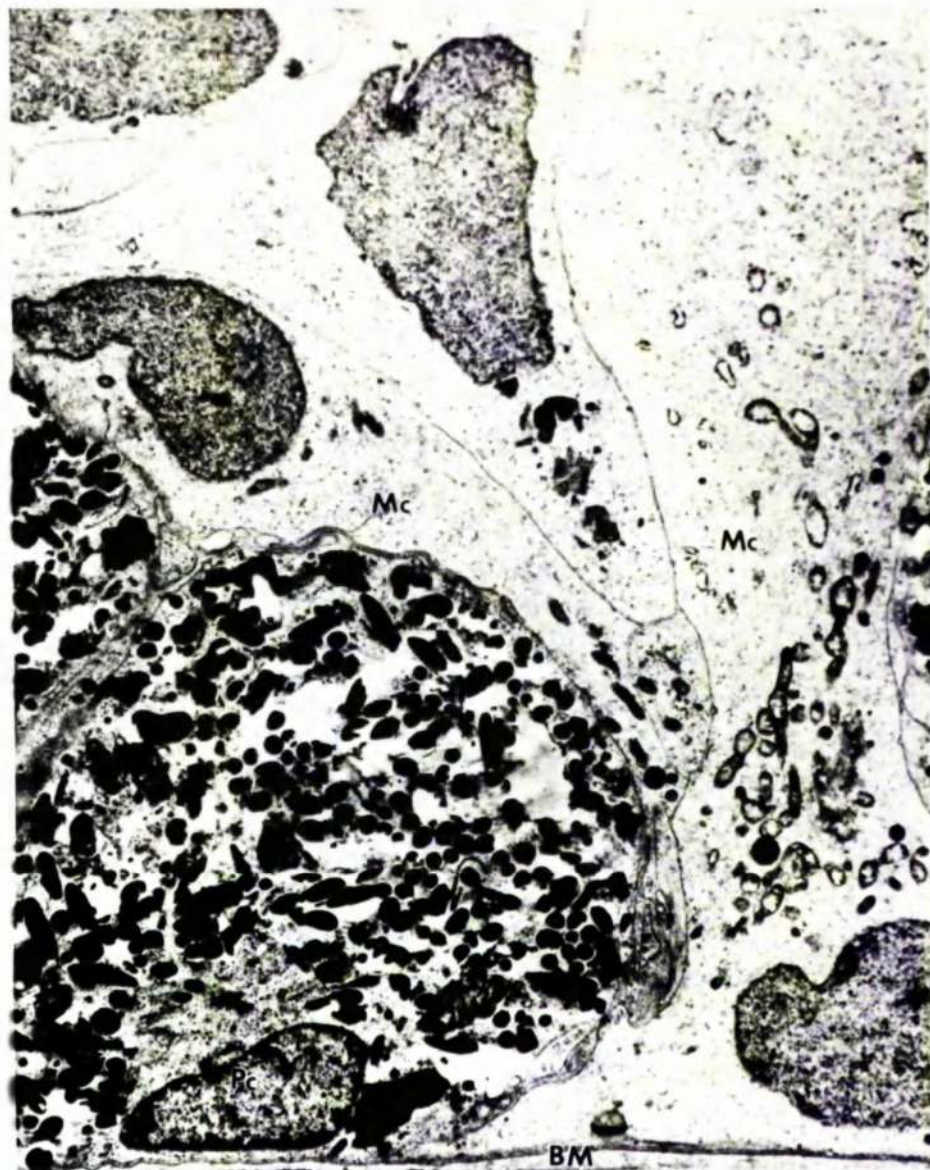


Figure 5.100 (1/4W/2 block C2). Electron micrograph showing, at higher power, the area of suspected proliferation seen in Figure 5.99. The larger pigmented cells are thought to be pigment laden macrophage. The irregularly shaped cells, on the basis of their nuclear appearance, cytoplasmic appearance, and their ability to fuse with Bruch's membrane, are thought to be Müller cells. Mc: Müller cell cytoplasm; Pc: pigment laden macrophage; BM: Bruch's membrane ($\times 4,300$).

[illegible]

Diagrammatic summary of the findings in the four blocks examined from each animal exposed to light of the lower intensity. A black square indicates that the event listed occurred within that block.

INNER RETINA												
REDUCED CELL NO. DAMAGED NORMAL												
MÜLLER CELLS												
DAMAGED PHAGOSOMES PRESENT NUCLEUS MIGRATION ENLARGED NORMAL												
RECEPTOR CELLS												
ABSENT REDUCED CELL NO. DAMAGED NORMAL												
PIGMENT EPITHELIUM												
ABSENT REDUCED CELL NO. PHAGOSOMES PRESENT IN UNUSUAL NOS. DAMAGED NORMAL												
MACROPHAGES												
PRESENT IN RETINA ABSENT IN RETINA												
CHORIOCAPILLARIS												
ABSENT PRESENT												
CHOROID												
RED CELL IMPACTION MONOCYTE / MACROPHAGE INVASION CELL DAMAGE NORMAL												

Figure 5.102

Diagrammatic summary of the findings in the four blocks examined from each animal exposed to light of the higher intensity. A black square indicates that the event listed occurred within that block.

COMPARISON OF LEVELS OF RETINAL ILLUMINATION

INDIRECT OPHTHALMOSCOPE ¹	68.6 mWcm ⁻²
SLIT-LAMP ¹	217 mWcm ⁻²
SURGICAL MICROSCOPES ²	460 mWcm ⁻² —970 mWcm ⁻²

1 Calkins, J.L. and Hochheimer, B.F. (1980)

2 Hochheimer, B.F., D'Anna, S.A. and Calkins, J.L. (1979).

Figure 5.103

Table showing retinal illumination levels associated with various light sources.

CHAPTER 6

FINAL DISCUSSION

The aims of this project were:

- 1) To investigate the fine structural changes in the rabbit retinae resulting from moderate intensity, moderate duration (1 hour), exposures to white light.
- 2) To determine the threshold for light damage.
- 3) To investigate qualitatively and quantitatively damage to individual retinal components resulting from various degrees of super threshold light exposure.
- 4) To investigate any possible effect of light on the structure of the choroid, and to assess the role of choroidal damage in producing secondary retinal changes.
- 5) To study the repair processes following light damage.

These aims shall be discussed in the order given above.

1) the light levels employed in this investigation were chosen, at first subjectively, to be comparable with the light levels used in such procedures as indirect ophthalmoscopy. The levels of retinal illumination were later calculated (as suitable equipment became available). A good agreement was found between the light levels employed in this investigation and the levels of illumination experience by human retina during indirect ophthalmoscopy. The levels of retinal illumination in this study were between 20mWcm^{-2} and 84mWcm^{-2} . Indirect ophthalmoscopy has been shown (Calkins and Hochheimer, 1980) to result in retinal illumination levels of about 69mWcm^{-2} .

The appearance of the light damaged retinal tissues was similar to previously published descriptions apart from the variation in damage seen within individual eyes. This variation has already been discussed. In the non-survival experiments, where

the animals were killed immediately after the experimental light exposure, ultrastructural abnormalities were first encountered in group 4. The pigment epithelial cells in the animals in this group occasionally had rounded nuclei, swollen mitochondria, and distended smooth endoplasmic reticulum. Both the rod and cone cells showed abnormalities of their inner and outer segments: the cone cells exhibiting a slightly greater degree of damage. As all these indications of damage appeared simultaneously in group 4, the primary site of light damage remains obscure. The unexpected sensitivity of the cone cells to damage does lead one to suspect that the cone receptor cells were the primary site of ultrastructural damage. However, it does not follow that they were the primary site of functional impairment. The histochemical studies of Hannson (1970b), and the report of Ham, Mueller and Sliney (1976) indicating increased retinal sensitivity to damage at short wavelengths, tend to suggest that impairment of some enzymic function of the retinal pigment epithelium may be the initial site of damage. Ultrastructural changes in the photoreceptor may be the first indications of damage, but this is not surprising due to the intimate metabolic relation between the pigment epithelium and the receptor cells.

As the intensity of illumination was increased (groups 3, 2 and 1) damage to the outer retina became more severe. At the two highest intensities employed, severe damage to the outer retina was associated with appreciable damage to the inner retina, particularly the horizontal, bipolar and amacrine cells. At the highest intensity employed varying degrees of damage were seen in all the cells of the retina. It seemed probable that the increased severity of damage to the inner retina, at the higher intensities, may be due to impairment of the transport systems

of the pigment epithelium. This would deprive the retina of essential metabolites, and probably produce an ischaemia-like pattern of damage. In some instances, especially in the higher intensity groups, occlusion of the choriocapillaris by platelets and impacted red cells was probably responsible for the damage to the inner retina.

2) The first definite structural changes were observed in group 4. This group was exposed to an estimated retinal illumination of 29mWcm^{-2} for one hour. The total energy delivered to the retina was therefore about 104Jcm^{-2} . From the American National Standard for the safe use of lasers (ANSI Z-136-1-1976 as quoted by Calkins and Hochheimer, 1980), the maximum permissible exposure (MPE) for a retinal illumination level of 29mWcm^{-2} is 101 seconds. However, the MPE is calculated to lie two orders of magnitude below the level of illumination which would result in a 50% probability of producing an ophthalmoscopically visible lesions of monkey retinae. Therefore, exposure times, at this level of illumination, would have to be in the order of 168 minutes ($\frac{101\text{sec.} \times 100}{60}$) to produce an ophthalmoscopically visible lesion.

The MPE and the MPE x 100 for the light intensities used in this investigation have been calculated (Figure 6.1).

The MPE x 100 gives the level of illumination at which lesions of the retina would be expected to become visible. In this study, lesions of the retina were seen in groups 1 and 2. The estimated retinal illumination in these groups was 0.084Wcm^{-2} and 0.038Wcm^{-2} . The MPE x 100 for 0.08mWcm^{-2} and 0.038mWcm^{-2} are 56 minutes and 126 minutes respectively. Therefore, as the exposures were of 60 minutes, the predicted appearance of visible lesions agrees well with their actual appearance.

3) The qualitative results of the immediate effects study were shown in Figure 4.40. However, these observations can be shown graphically (Fig. 6.2). It is apparent that the cone cells are the retinal cell type most sensitive to damage, followed by the rod cells and pigment epithelial cells. The cells of the inner nuclear layer appeared to be slightly less sensitive to damage than either the pigment epithelium or receptor cells, but more sensitive than either the Müller cells or the ganglion cells. The Müller cells and the ganglion cells were of similar sensitivity to damage at the higher light intensities, but the Müller cells appear to be slightly more sensitive at the lower intensities.

The quantitative results of this study were disappointing, as correlations between light intensity and counts for various cell components within the outer nuclear layer were poor. Reasons for this poor correlation have already been discussed in Chapter 4. The method of quantification did appear to be sensitive to changes in the morphology of the outer nuclear layer. Unfortunately the variation within and between animals was so large as to mask any positive results. The variation within the experimental tissues is probably related to the length of the exposure period (1 hour). This long exposure period would allow regions of severe damage to develop. Possible reasons for this have already been discussed in Chapters 4 and 5, focal occlusions of the choriocapillaris being the main candidate for the production of the variation seen in retinal damage.

A series of experiments investigating the combined effects of various periods of acute pressure induced ischaemia coupled with exposure to light have been conducted. These experiments will be reported elsewhere (McKechnie, Johnson and Foulds).

The light intensity employed in that investigation was similar to that to which group 5 was exposed. That was 23mWcm^{-2} for one hour. In addition one eye of each experimental animal was made ischaemic for one of the following periods, 15, 30, 45 or 60 minutes. The retinal damage produced by this procedure was more severe than that produced by light, or by ischaemia, in isolation. The retinal damage seen in the combined light and ischaemia experiments was very similar to that seen in this study where the choriocapillaris had been occluded by inflammatory cells, platelets or impacted red cells. In the combined light and ischaemia experiments the morphology of the damaged tissues varied little with location. This was further evidence that focal occlusion of the choriocapillaris was responsible for the variation seen in the purely light damage experiments.

4) Choroidal damage was only observed in the groups exposed to the highest light intensity (Group 1). The damaged choroidal cells being fibroblasts and endothelial cells. These damaged cells were only found on the retinal aspect of the choroid. Focal occlusions of the choriocapillaris were seen in the groups exposed to lower light intensities. The consequences of these occlusions of the choriocapillaris have already been discussed.

5) The two highest light intensities employed in the investigations described in Chapter 4 were chosen for further investigation into the recovery processes. They were chosen because they were already known to cause damage to the photoreceptors and the pigment epithelium, with the accumulation of cellular debris in the subretinal space. The aim of this part of the study was to investigate the appearance of the retina and choroid at various times after the photic insult to determine the fate of the cellular debris produced by the initial insult.

The findings of this part of the study were described in Chapter 5. Diagrammatic representations of the results are shown in Figures 5.101 and 5.102.

In the group exposed to the lower intensity the findings of note were:-

a) The association between severe retinal damage and occlusion of the choriocapillaris.

b) The appearance of cellular damage within retina one to four weeks after the exposure to light. The cause of this delayed retinal damage remains obscure but secondary retinal damage due to delayed appearance of capillary damage within the choroid seems a possibility.

In the group exposed to the higher intensity the findings of note were:

a) The good association between regions of severe retinal damage and occlusion of the choroidal vessels or choriocapillaris.

b) The phagocytosis of receptor cell debris by Muller cells.

c) The expansion of Müller cells' cytoplasm to replace lost elements of the outer nuclear layer, and the accompanying migration of the cells' nuclei.

d) The invasion of the light damaged retina by inflammatory cells of vascular origin, and the relation between inflammatory cell invasion and patency of the choroidal circulation.

e) The migration of monocytes through Bruch's membrane. Macrophages derived from these cells were, in the main, responsible for the removal of cellular debris.

f) The association of pigmentary disturbances, e.g. hyperplasia and budding of the pigment epithelium with the longer recovery periods.

g) The regenerative capabilities of the photoreceptors in the presence of pigment epithelium.

h) The high survival of cone cells following light damage, even though their outer segments appear to be very susceptible to damage.

6.2 Possible Modifications of Experimental Design

One of the main causes of concern and difficulty in these experiments was the system used to illuminate the experimental eyes. In any future experiments it would be preferable to use a modified fundus camera, or at least an optical system similar to that used in the fundus camera. With this type of optical arrangement it would be possible to observe the fundus of the experimental eye during the course of the light exposure. This would allow observations to be made on the formation of lesions, such as were seen in the non-survival experiments, and the resolution of lesions, such as were seen in the survival experiments. The rate of formation, the time of appearance, and the rate of resolution, of these lesions is not known from the present investigation.

Given direct visualisation of the rabbit's fundus during the experimental exposure it would be possible to make more exact measurements of the area of retinal illumination.

In the experimental design, the possibility of continuously measuring the output of the light sources using a radiometer was considered. Unfortunately, the cost of such equipment was prohibitive. The absence of such measuring equipment was recognised as a flaw in the experimental design but little could be done to rectify the problem.

In relation to the experiments of Ham, Mueller and Sliney (1976), it would have been advantageous to have been able to alter the wavelength distribution of the light reaching the retina. This could be achieved by the use of interference filters, either narrow band pass filters or by use of combinations of long and short wavelength pass filters. With combinations of these filters it would be possible to achieve bandpasses from about 10nm to 100nm in width. One unfortunate consequence of such filtering systems is the need for a powerful light source of relatively even output across the wavelengths considered for investigation. In this respect xenon arc lamps are probably ideal.

6.3 Other Possible Experimental Techniques

In the non-survival experiments, one of the major difficulties was the lack of localisation of the sites of retinal damage. It is probable that fluorescein angiography would show where there were defects in the pigment epithelium. This would allow more accurate localisation of lesions of the retina. It would also be of interest to follow the pattern of recovery by repeated fluorescein angiography.

The possibility of using ERG's to study the initial degree of damage, and the progress of recovery was considered. However, due to the system of illumination, the retina is only partly illuminated. This coupled with the irregular nature of the lesions greatly reduces the validity of the ERG in assessing the degree of retinal damage. Some studies were conducted into the use of ERGs but these were not successful. After exposure to damaging levels of illumination ERGs were not recordable. At lower levels of illumination the recovery of the ERG was very similar to the normal dark adaption curve obtained by measuring ERG wave

form amplitudes at various times after the cessation of illumination.

6.4 Future Lines of Investigation

The future lines of investigation fall into two categories:

- 1) Additional techniques.
- 2) New experimental models.

Additional techniques include the cyto-chemical demonstration of acid phosphatase (Gomori, 1952) and aryl sulphatase (Goldfischer, 1965) in the phagocytic cells present within the retina, and choroid, after damaging exposures. This may be useful in the determination of the origins of these phagocytic cells. These techniques were used successfully by Essner and Gorrin (1979) to demonstrate the presence of actively phagocytic cells in the retinae of rats with inherited retinal dystrophy.

Hanson (1970b), by light microscopy and histochemistry, successfully demonstrated a reduction in the activities of the following enzymes in the light damaged rat retina: a) Cytochrome oxidase, b) Nicotinamide adenine dinucleotide diaphorase. c) Succinate dehydrogenase. d) Lactate dehydrogenase.

It would be of interest to repeat this type of experiment but using the higher resolution afforded by EM cytochemistry. Seligman, Karnovsky, Wasserkrug and Henker (1968) have devised a technique suitable for the electron microscopic localisation of cytochrome oxidase activity. It is probably possible to stain for nicotinamide adenine dinucleotide diaphorase activity and succinate dehydrogenase activity by the use of ferricyanide or nitro-substituted tetrazolium salts. Similarly, lactate dehydrogenase activity can be demonstrated by the appropriate use of tetrazolium salts (Lewis and Knight, 1977). With these techniques it may be possible to localise the metabolic origin of light damage hypothesised by Ham, Mueller and Sliney (1976).

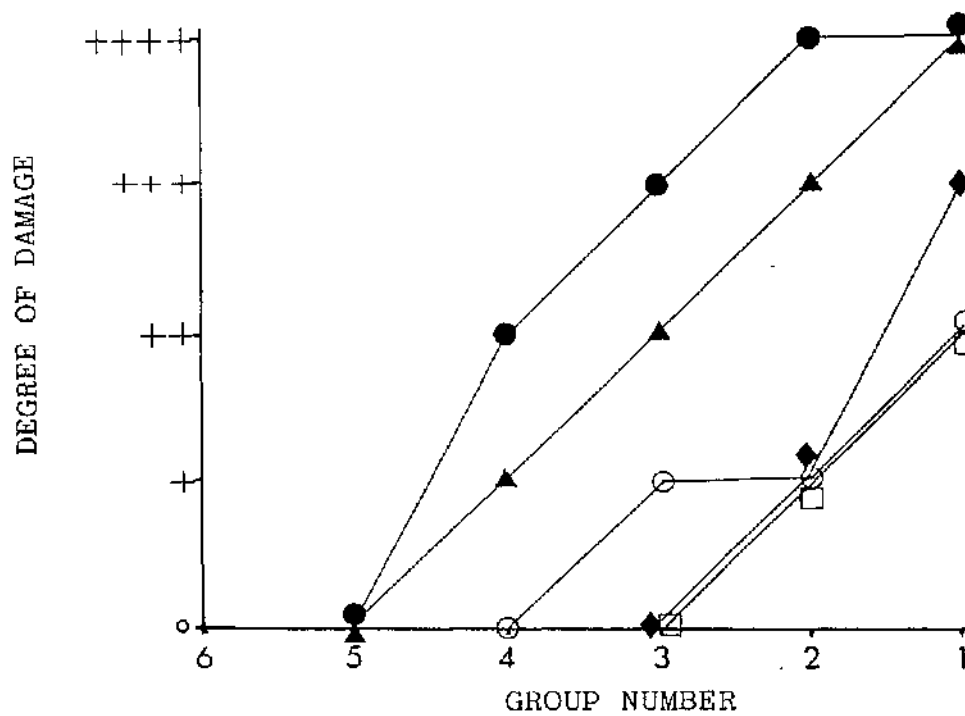
If light damage results from some metabolic disturbance of the cell it is possible that photosensitising agents such as the phenothiazines, the psoralens, and the tetracyclines may enhance, or produce light damage at unusually low levels of illumination. Phenothiazine has been shown to induce atrophy of the photoreceptors and proliferation of the pigment epithelium (Cerletti and Meier-Ruge, 1967). Studies utilising EM cytochemistry in combination with various photosensitising agents may be useful in elucidating the metabolic origin of light damage.

New experimental models to study the effects of light on tissues could include the use of tissue culture systems. It seems probable that light of short wavelengths, around 400nm, may damage cells by the photochemical production of highly reactive radicles, or ions, which cause chemical modification of other nearby molecules of the cell. If this is the case, then it should be possible to produce "light damage" in cells other than those of the retina. The ability to conduct studies on simple systems, such as cultured fibroblasts or pigment epithelium, may greatly simplify cytochemical and biochemical studies of light damage.

LIGHT INTENSITY (Wcm^{-2})	MPE (seconds)	MPEx100 (minutes)
0.084	34	56
0.038	76	126
0.032	91	151
0.029	101	168
0.023	126	210
0.020	146	243

Figure 6.1

Table giving the light intensities used in this investigation and the maximum permissible exposure (MPE) calculated from the recommendations of American National Standard for the Safe Use of Lasers (ANSI Z-136. 1-1976). The MPEx100 gives the exposure time at which there would be a 50% probability of producing an ophthalmoscopically visible lesion.



- Receptor Cells
- ▲ Pigment Epithelium
- ◆ Horizontal Bipolar
and Amacrine Cells
- Müller Cells
- Ganglion Cells

Figure 6.2

Graphic representation of the qualitative results given in Figure 4.40.

APPENDIX 1

ANIMALS

LIGHT DAMAGE IMMEDIATE EFFECTS SERIES

<u>GROUP AND INTENSITY</u>	<u>DESIGNATION</u>	<u>WEIGHT</u>	<u>SEX</u>	<u>COLOUR</u>	<u>ANAESTHETIC</u>	<u>DATE</u>
1	LD1.1	1.8kg	♂	B	9ML	7.10.77
	LD1.2	1.8kg	"	Br	8ML	30. 8.77
	LD1.3	1.5kg	"	B & W	8ML	30. 8.77
	LD1.4	1.8kg	"	B & W	9ML	30. 8.79
2	LD2.1	2.1kg	"	FA & W	10.5ML	7.11.77
	LD2.2	1.9kg	"	B & W	8ML	31.10.77
	LD2.3	1.9kg	"	B & W	9ML	19.11.78
	LD2.4	1.7kg	"	B & W	8ML	19.11.78
3	LD3.1	1.3kg	"	Br	7ML	21.10.77
	LD3.2	2.3kg	"	Br	10ML	21.10.77
	LD3.3	1.8kg	"	Dg & W	9ML	3. 9.79
	LD3.4	2.1kg	"	Dg & W	10ML	3. 9.79
4	LD4.1	2.0kg	"	B & W	9.5ML	10.11.77
	LD4.2	2.0kg	"	B & W	9.5ML	10.11.77
	LD4.3	1.5kg	"	Dg & W	8ML	17.11.78
	LD4.4	1.5kg	"	Dg & W	8ML	17.11.78
5	LD5.1	1.3kg	"	G & W	6ML	23.11.77
	LD5.2	1.5kg	"	G & W	7.5ML	23.11.77
6	LD6.1	2.4kg	"	Db	10ML	20.10.77

ANAESTHETIC I.V. 40% URETHANE

COLOUR CODE:

B	BLACK	Db & W	DARK BROWN AND WHITE
B & W	BLACK AND WHITE	Dg	DARK GREY
Br	BROWN	Dg & W	DARK GREY AND WHITE
Br & W	BROWN AND WHITE	FA & W	FAWN AND WHITE
Db	DARK BROWN	G & W	GREY AND WHITE

Figure A1-1

Table giving the details of the animals used in the "Light Damage Immediate Effects" experiments.

LIGHT DAMAGE RECOVERY SERIES

	<u>DESIGNATION</u>	<u>REC. PERIOD</u>	<u>WEIGHT</u>	<u>SEX</u>	<u>COLOUR</u>	<u>ANAESTHETIC</u>	<u>DATE</u>	<u>TIME KILLED</u>
HIGHER INTENSITY	LDR1/6 /1	6 HOURS	1.8 KG	♂	G & W	6ML	5.2.79	12.30
	LDR1/6 /2	6 HOURS	1.7 KG	"	B & W	8ML	15.5.79	14.45
	LDR1/24/1	24 HOURS	1.8 KG	"	B & W	7ML	29.1.79	12.15
	LDR1/24/2	24 HOURS	1.8 KG	"	B & W	6ML	29.1.79	15.15
	LDR1/48/1	48 HOURS	1.7 KG	"	G & W	6.5ML	30.1.79	12.15
	LDR1/48/2	48 HOURS	2.2 KG	"	BR	8ML	9.5.79	14.40
	LDR1/40/1	4 DAYS	1.4 KG	"	DG & W	6ML	5.2.79	14.40
	LDR1/40/2	4 DAYS	1.6 KG	"	G & W	8ML	4.5.79	11.50
	LDR1/1W/1	1 WEEK	1.8 KG	"	G & W	8.5ML	30.1.78	10.50
	LDR1/1W/2	1 WEEK	2.1 KG	"	B & W	8ML	5.5.79	14.30
	LDR1/2W/1	2 WEEKS	1.8 KG	"	G & W	7ML	12.1.79	10.45
	LDR1/2W/2	2 WEEKS	2.0 KG	"	G & W	8ML	12.1.79	12.40
	LDR1/4W/1	4 WEEKS	1.7 KG	"	G & W	7ML	15.1.79	11.30
	LDR1/4W/2	4 WEEKS	2.3 KG	"	BR & W	9ML	15.1.79	14.45

ANAESTHETIC 3ML SAGATAL + 1ML HEPARIN (5000 I.U. 5ML) + 6ML SALINE

LIGHT DAMAGE RECOVERY SERIES

	<u>DESIGNATION</u>	<u>REC. PERIOD</u>	<u>WEIGHT</u>	<u>SEX</u>	<u>COLOUR</u>	<u>ANAESTHETIC</u>	<u>DATE</u>	<u>TIME KILLED</u>
LOWER INTENSITY	LDR2/6 /1	6 HOURS	2.3 KG	♂	B & W	7ML	30.10.78	-
	LDR2/6 /2	6 HOURS	1.7 KG	"	B & W	8ML	31.10.78	-
	LDR2/24/1	24 HOURS	2.0 KG	"	B & W	8ML	2.11.78	-
	LDR2/24/2	24 HOURS	1.6 KG	"	B & W	8ML	13.11.78	11.45
	LDR2/48/1	48 HOURS	1.9 KG	"	B & W	9ML	11.12.78	14.00
	LDR2/48/2	48 HOURS	1.9 KG	"	B & W	9ML	11.12.78	15.30
	LDR2/40/1	4 DAYS	1.8 KG	"	B & W	8ML	30.11.78	12.30
	LDR2/40/2	4 DAYS	1.7 KG	"	B & W	8ML	30.11.78	15.10
	LDR2/1W/1	1 WEEK	1.8 KG	"	B & W	8ML	22.11.78	10.50
	LDR2/1W/2	1 WEEK	1.9 KG	"	B & W	8ML	22.11.78	14.00
	LDR2/2W/1	2 WEEKS	1.7 KG	"	B & W	6ML	7.11.78	11.45
	LDR2/2W/2	2 WEEKS	2.0 KG	"	G & W	9ML	7.11.78	14.30
	LDR2/4W/1	4 WEEKS	2.3 KG	"	B & W	10ML	6.11.78	15.00
	LDR2/4W/2	4 WEEKS	1.1 KG	"	DG & W	7ML	6.11.78	16.40

ANAESTHETIC 2ML SAGATAL + 1ML HEPARIN (5000 I.U. 5ML) + 7ML SALINE

Figure A1-2

Table giving the details of the animals used in the "Light Damage Recovery" experiments.

APPENDIX 2

MEASUREMENT OF LIGHT INTENSITIES AND ASSOCIATED
PARAMETERS

LIGHT INTENSITY MEASUREMENTS

The light intensity measurements were made using a Rank Hilager FT32 thermopile. All measurements were made at 50cm. from the end of the light guide. For each light source the four possible combinations of light input and output were measured. The ends of the light guide was manipulated to obtain the maximum output from the thermopile.

LIGHT SOURCE 1	LIGHT SOURCE 2	
0.62 mWcm ⁻²	0.42 mWcm ⁻²	
0.40 "	0.44 "	
0.40 "	0.40 "	
0.55 "	0.40 "	
<hr/>		
0.49.25 mWcm ⁻²	0.41.5 mWcm ⁻²	AVERAGE
<hr/>		
Combined average 0.91mWcm ⁻²		

The maximum light intensity used in this investigation was 0.91mWcm⁻² measured at 50cm. from the end of the light guide. Intensities at other distances from the end of the light guide were calculated by applying the law of inverse squares (Fig. A2-2).

BEAM ENERGY DISTRIBUTION AND TOTAL BEAM ENERGY

The radial energy distribution within the beam was measured 15cm. from the end of the fibre optic light guide. The photodiode circuit shown in Figure A2.1 was used. The distribution obtained is shown in Figure A2.5.

From measurements of the light intensity within the beam it was known that the maximum energy within the beam at 15cm. from the end of the light guide was 10.08mWcm^{-2} .

$$\text{We know } 10.08\text{mWcm}^{-2} \quad \equiv \quad 5.7 \text{ arbitrary units cm}^{-2} \text{ (Fig.A2.5)}$$

$$\therefore \quad 1 \text{ arbitrary unit} \quad = \quad \frac{10.08\text{mW}}{5.7}$$

$$= \quad 1.76\text{mW}$$

To find the total energy within the beam

$$\begin{aligned} E_{\text{TOT}} &= \text{Integral over the whole beam of the radial} \\ &\quad \text{energy distribution (i.e. Fig. A2.5)} \\ &\quad \times \text{scaling factor (i.e. } 1.76\text{mW}(\text{arb. units})^{-1}) \\ &= \quad 660\text{mW} \end{aligned}$$

AREA AND INTENSITY OF RETINAL ILLUMINATION

Hughes (1972) gives a schematic eye for the rabbit. This model is used to help evaluate the illumination falling on the rabbit's retina from a fibre optic light guide placed adjacent to the corneal vertex.

The ray diagram, utilising Hughes parameters, is shown in Figure A2.6.

From the diagram, by similar triangles the following are obtained:

$$\frac{y_2 - y_1}{s} = \frac{y_2}{f} \quad - \quad (1)$$

and $\frac{y_2 - y_1}{s'} = \frac{y_2}{s' + f'} \quad - \quad (2)$

Sizes from Hughes
s = distance to cornea + 4.0mm
s' = distance to cornea + 4.7mm
f' = 13.3mm
f = 9.9mm

From (1) $f(y_2 - y_1) = sy_2$

i.e. $y_2(f - s) = fy_1$

i.e. $y_2 = y_1 \frac{f}{(f - s)} \quad - \quad (3) \quad \left(\begin{array}{l} f - s \neq 0. \text{ if } f - s = 0 \text{ no real} \\ \text{or virtual image is formed} \end{array} \right)$

From (3) $y_2 - y_1 = y_1 \frac{f}{(f - s)} - y_1$

$$= y_1 \left[\frac{f - (f - s)}{f - s} \right]$$

$$= y_1 \cdot \frac{s}{(f - s)}$$

Now substitute into (2) for $y_2 = y_1$ and y_2

$$\left[y_2 \cdot \frac{s}{(f - s)} \right] \cdot \frac{1}{s'} = \left[y_1 \cdot \frac{f}{(f - s)} \right] \cdot \frac{1}{(s' + f')}$$

$$\text{i.e.} \quad \frac{s}{s'} = \frac{f}{(s' + f')}$$

$$\text{i.e.} \quad s(s' + f') = s'f$$

$$\text{i.e.} \quad s'(f - s) = f's$$

$$\text{i.e.} \quad \boxed{s' = s \cdot \frac{f'}{(f - s)}} \quad - (4)$$

Thus equations (3) and (4) may be used to derive values for y_2 and s' from the position and size of the source and the parameters given by Hughes.

For a 5mm. diameter fibre optic placed 2mm from the cornea.

$$\begin{aligned} y_2 &= \text{radius of effective source} \\ &= 2.5 \cdot \frac{9.9}{9.9 - (2.0\text{mm} + 4.0\text{mm})} \end{aligned}$$

$$\text{i.e. radius of effective source} = 6.35\text{mm.}$$

Equation (4) gives:

$$\begin{aligned} s' &= \text{position of effective source from plane } H' \\ &= \frac{(2.0 + 4.0)\text{mm} \cdot 13.3\text{mm}}{(9.9\text{mm} - (2.0\text{mm} + 4.0\text{mm}))} \\ &= 20.46\text{mm} \quad (= \text{distance to cornea} + 4.7\text{mm} = 15.76\text{mm to cornea}) \end{aligned}$$

Hughes described the retina as being positioned at a radius of 9.6mm with a centre of curvature of 8.3mm to the posterior of the cornea.

Thus the distance from the effective source to the retina is

$$(20.46\text{mm} - 4.7\text{mm}) + (9.6\text{mm} + 8.3\text{mm}) \\ = 33.66$$

i.e. say 33.7mm.

The source used and the optics of the rabbit eye may be replaced by an effective source of diameter 12.7mm. positioned 33.7mm. in front of the retina.

These data and the measured intensity distribution in the beam (Fig. A2.5) were used to construct an approximate intensity distribution in the plane of the back of the eye (Fig. A2.7).

The data on the absorption in the ocular media (Fig. A2.3 and A2.4) indicate that only 56% of light entering the eye will reach the retina. Observations during the experiments revealed that, because the pupils were maximally dilated, the iris did not restrict the entry into the eye of the light beam from the fibre optic so that only transmission losses need be considered. The total energy reaching the retina is then:-

$$0.56 \times 660\text{mW} = 370\text{mW}.$$

A scale factor for the abscissa of Figure A2.6b is readily deduced; integration of this distribution over the whole beam gives a total energy of 42.4 arbitrary units, which must equal 370mW.

Thus for Figure A2.7b

$$1 \text{ arb. unit} = 8.7\text{mW}.$$

Fig. A2.7b then reveals the highest intensity at the retina is 84.4mWcm^{-2} . (This figure is an average of the intensities out to a radius of 0.6cm). This figure of 84mWcm^{-2} represents the highest retinal illumination used in these studies. All the other intensity levels shown in Figure A2.8 were derived from this figure.

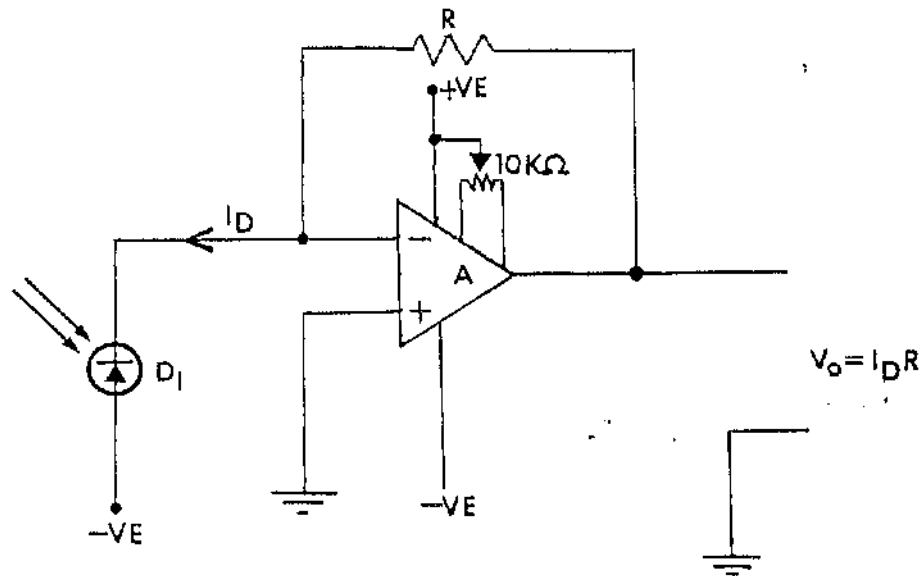


Figure A2.1

This figure shows the circuit diagram of the light meter used in the calibration of source 2 to give the required percentage output. This was achieved by measuring the light output while adjusting the iris diaphragm within the light source.

A. fet op amp. uAF355 TC

Diode. silicon photodiode (peak response 800nm).

The diode current I_D varies with light level from 1nA to 1mA. The resistor R (typically 1M) is chosen to give the required output. The output voltage was displayed on an oscilloscope (Tecktrinx 5103N).

GROUP	SOURCES		INTENSITY AT VARIOUS DISTANCES ¹		
	1	2	50cm	15cm	2.5cm
1	ON	100% ON	0.91mWcm ⁻²	10.08mWcm ⁻²	363mWcm ⁻²
2	OFF	100% ON	0.41mWcm ⁻²	4.61mWcm ⁻²	166mWcm ⁻²
3	OFF	85% ON	0.34mWcm ⁻²	3.92mWcm ⁻²	140mWcm ⁻²
4	OFF	75% ON	0.31mWcm ⁻²	3.46mWcm ⁻²	116mWcm ⁻²
5	OFF	60% ON	0.25mWcm ⁻²	2.77mWcm ⁻²	100mWcm ⁻²
6	OFF	53% ON	0.22mWcm ⁻²	2.44mWcm ⁻²	80mWcm ⁻²

1) ASSUMING INVERSE SQUARE LAW APPLIES

Figure A2.2

This table gives the maximum intensities within the beam from the fibre optic light guide at various distances from the end of the light guide.

TRANSMISSION OF LIGHT GUIDE AND OCULAR MEDIA

WAVELENGTH (NM)	SOURCE ^{*1}	LIGHT GUIDE		OCULAR MEDIA	
	% EMERGENCE (RELATIVE)	% TRANSMISSION ^{*2}	% EMERGENCE ^A	% TRANSMISSION ^{*3}	INCIDENT ON RETINA ^B
400	12.0	35	4.2	40	1.7
450	22.6	45	10.2	82	8.4
500	35.5	52	18.5	90	16.6
550	50.3	53	26.7	92	24.6
600	66.5	52	34.6	93	32.2
650	80.5	52	41.9	94	39.4
700	88.4	51	45.1	94	42.4
750	93.5	51	45.1	94	42.4
800	98.0	52	47.7	92	43.9
850	99.0	53	52.5	92	48.3
900	100.0	53	53.0	88	46.6
950	99.7	52	51.8	86	44.5
1000	97.4	52	50.6	56	28.3
1050	96.7	52	50.3	65	32.7
1100	93.5	52	48.6	82	39.2
1150	90.9	52	47.3	76	35.9
1200	87.7	52	45.6	22	10.0
1250	85.2	52	44.3	17	7.5
1300	81.3	52	42.3	23	9.7
1350	74.8	50	37.4	15	5.6
1400	69.6	46	32.0	5	1.5

* 1 MAKES DATA

* 2 MAKERS DATA

* 3 GEERAETS AND BERRY 1966.

INTEGRAL OF A = 50286.66

INTEGRAL OF B = 28328.33

TRANSMISSION FACTOR = $\frac{28328.33}{50286.66} = 0.56$

Figure A2.3

This table gives the transmission of the fibre optic light guide and the ocular media of the rabbit. Combining these parameters with the output of the source gives the wavelengths, and their relative energies, incident upon the retina. The integral of the percentage wavelength emergence of the fibre optic system divided by the integral of the percentage wavelength incident upon the retina gives the transmission factor for the rabbit ocular media over the wavelength employed in these experiments. This transmission factor of 0.56 is used in the calculation of the retinal illumination.

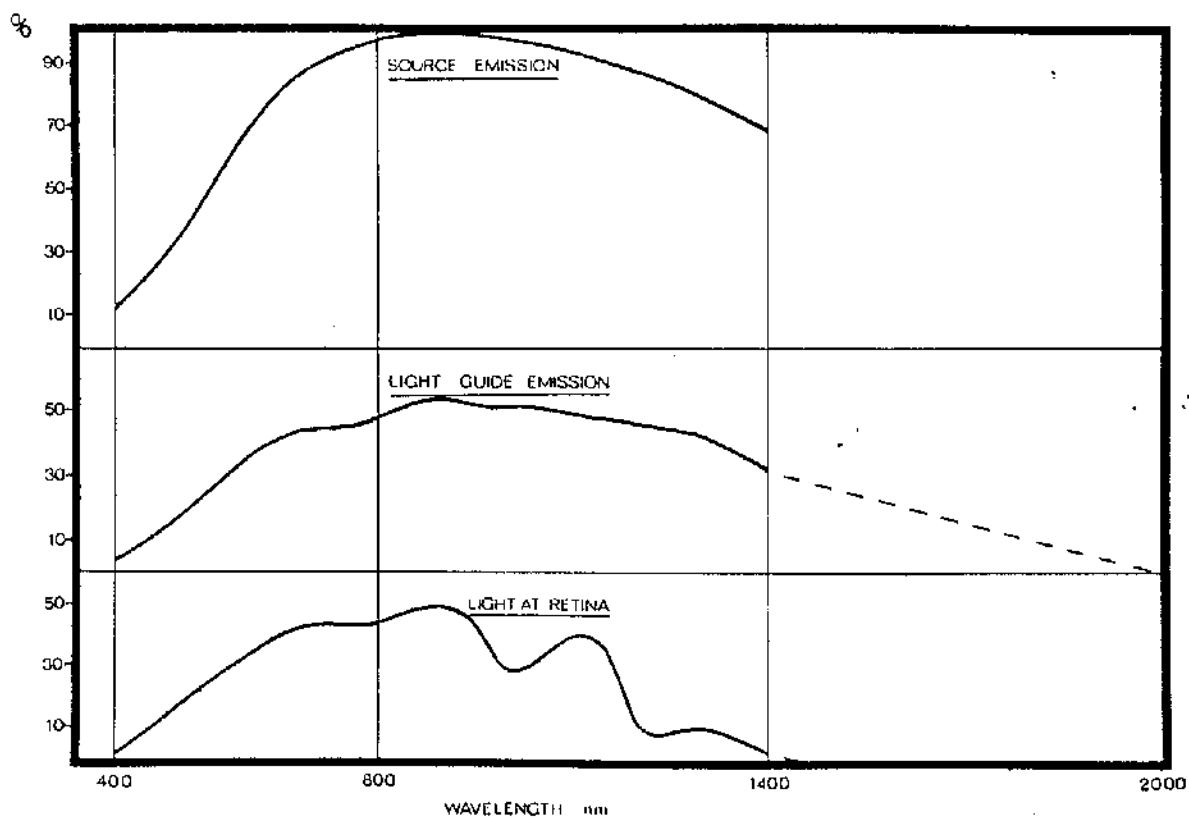


Figure A2.4

This figure shows the wavelength distribution of the sources, the light guide emission (extrapolated to 2,000nm), and the wavelengths incident upon the retina.

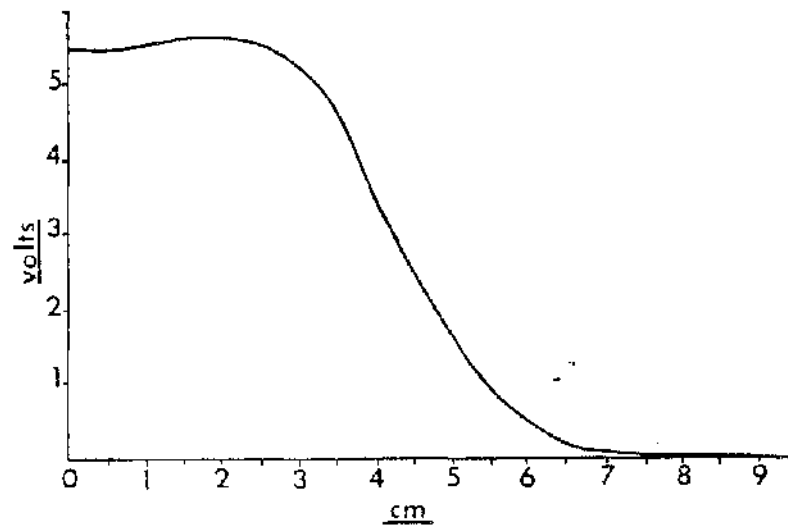


Figure A2.5

This figure gives the "radial" energy distribution within the beam of light emanating from the fibre optic light guide at 15cm. from the end of the light guide. The light is measured in terms of volts output of the photodiode light meter shown in Figure A2.1.

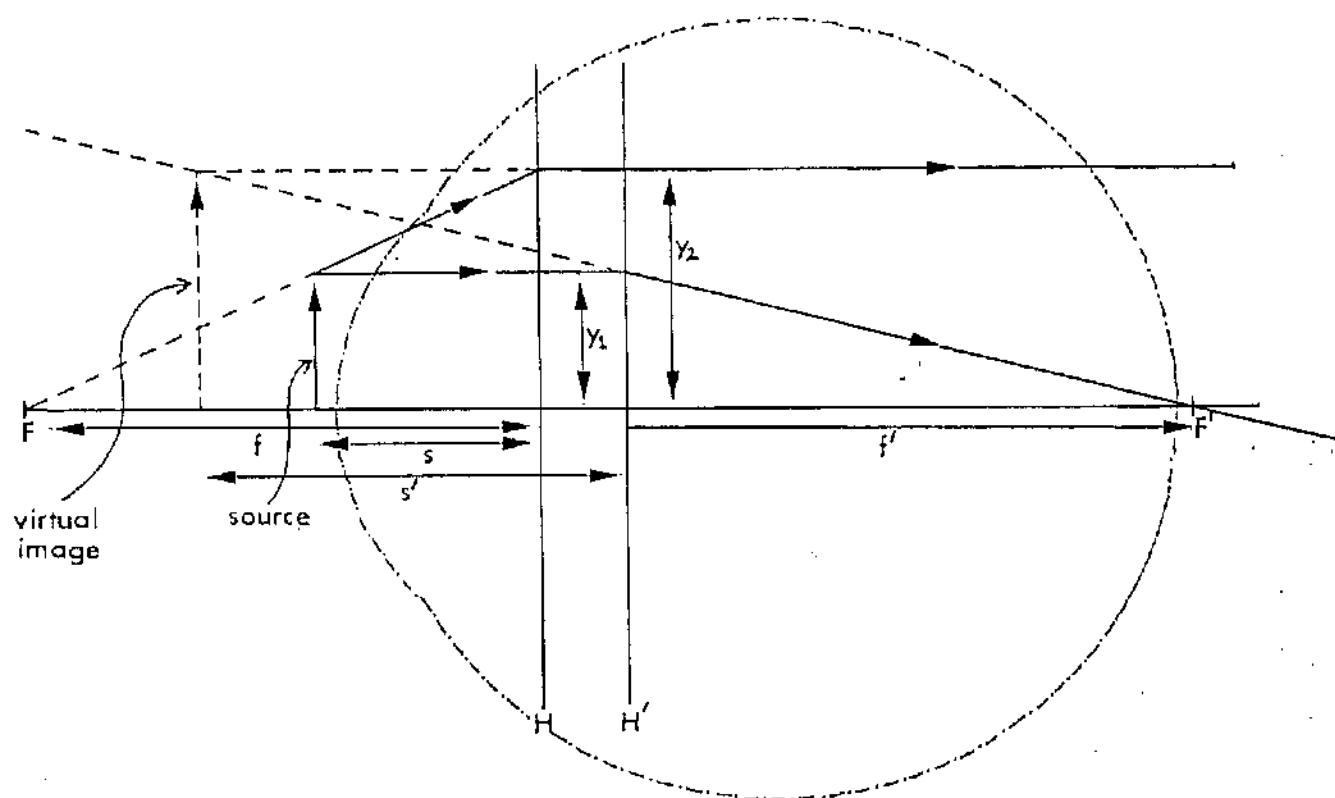


Figure A2.6

This figure shows the ray diagram, utilising the parameters of Hughes (1971), which was constructed to evaluate the area of illumination on the retina produced by a 5mm. diameter fibre optic placed 2mm. above the corneal vertex.

Figure A2.7

Derivation of approximate radial energy distribution in a plane at the back of the rabbit eye.

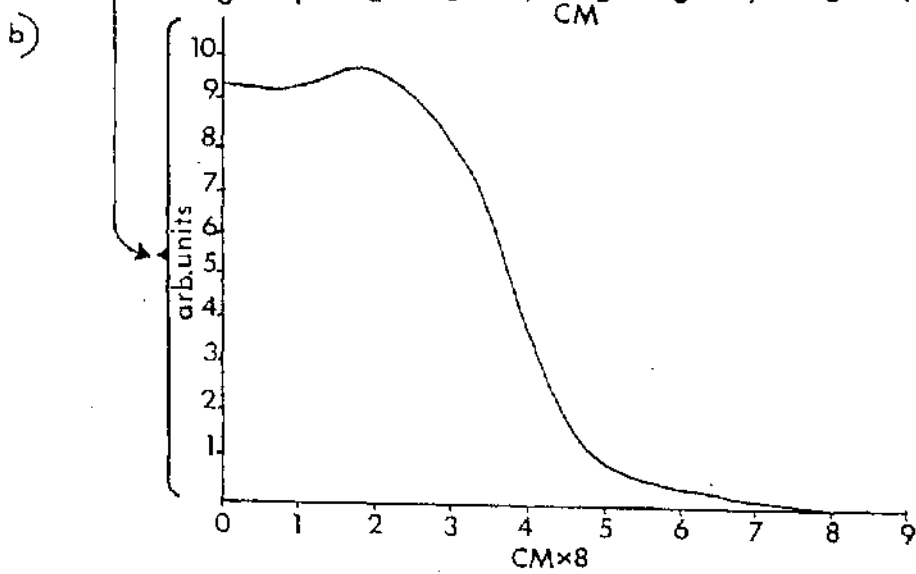
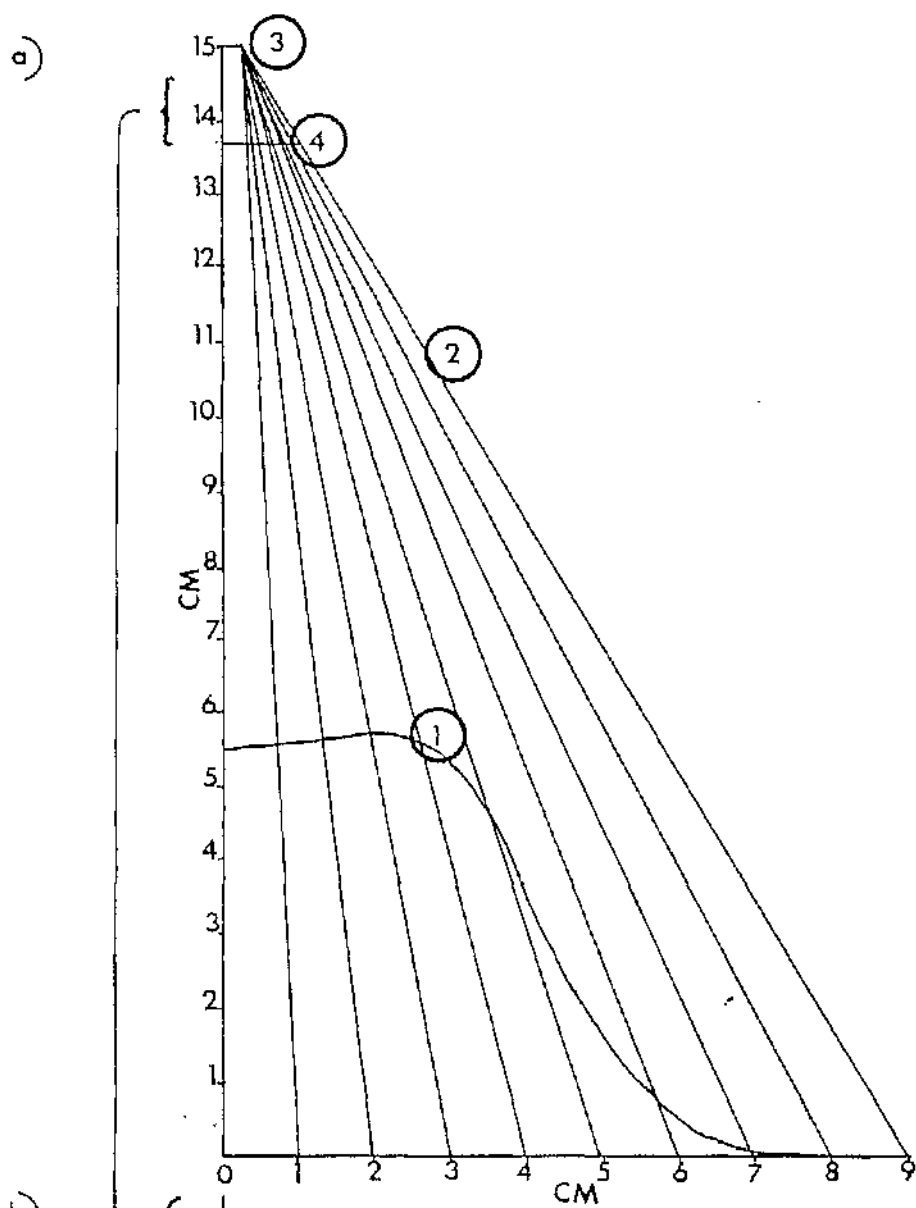
a) Diagrammatic basis of method. The curve (1) is the measured intensity distribution of Fig. A2.5. The ray lines (2) indicate the approximate spread of the fractional intensity contours along the beam. The diagram is scaled for the actual fibre optic (3) diameter of 5mm.

b) Derived approximate radial energy distribution in the plane of the back of the rabbit eye. This is deduced from Fig. A2.7(a) by:-

1) Selecting a plane at the distance of the retina from the effective source (i.e. 33.7mm) \times scaling factor of the ratio real/effective source diameters (i.e. $5/12.7$) from the source (3) in a). This position is thus 13.3mm from (3), indicated by the line (4) in a).

2) Reading off the radial positions of the fractional intensity contours on line (4) and scaling by $12.7/5 (= 2.54)$ to give true values.

3) Plotting fractional intensities against their corresponding radii to produce Fig. A2.7b.



LIGHT INTENSITIES

GROUP	SOURCES		INTENSITY AT VARIOUS DISTANCES ¹			ESTIMATED RETINAL ILLUMINATION	
	1	2	50cm	15cm	2.5cm	A*	B*
1	ON	100% ON	0.91mWcm ⁻²	10.08mWcm ⁻²	363mWcm ⁻²	84.4mWcm ⁻²	168.4mWcm ⁻²
2	OFF	100% ON	0.41mWcm ⁻²	4.61mWcm ⁻²	166mWcm ⁻²	38.6mWcm ⁻²	77.2mWcm ⁻²
3	OFF	85% ON	0.34mWcm ⁻²	3.92mWcm ⁻²	140mWcm ⁻²	32.8mWcm ⁻²	65.6mWcm ⁻²
4	OFF	75% ON	0.31mWcm ⁻²	3.46mWcm ⁻²	116mWcm ⁻²	28.9mWcm ⁻²	57.9mWcm ⁻²
5	OFF	60% ON	0.25mWcm ⁻²	2.77mWcm ⁻²	100mWcm ⁻²	23.2mWcm ⁻²	46.3mWcm ⁻²
6	OFF	53% ON	0.22mWcm ⁻²	2.44mWcm ⁻²	80mWcm ⁻²	20.4mWcm ⁻²	40.9mWcm ⁻²

1) ASSUMING INVERSE SQUARE LAW APPLIES

A* ASSUMING AREA OF RETINAL ILLUMINATION
TO BE AS ESTIMATED

B* ASSUMING AREA OF RETINAL ILLUMINATION
TO BE 1/2 OF THAT ESTIMATED

Figure A2.8

This table shows the relation between animal group numbers and the level of illumination to which they were exposed. The light intensities are given for a variety of distances from the end of the fibre optic light guide. Estimates of retinal illumination levels are also shown.

APPENDIX 3

QUANTIFICATION : NUMERICAL DATA

Figures A3.1 to 10

These figures give the complete numerical data from the quantification experiments. \bar{X} : mean; SD: standard deviation; P: the probability value of the results when t tested against the pooled control results.

ANIMAL L.D. 1.1.										
BLOCK RESULTS					ANIMAL RESULT					
		PYK RCN	RCN	RC CYTO	MC CYTO		PYK RCN	RCN	RC CYTO	MC CYTO
Block A1	\bar{x}	-	43.0	34.5	22.0	\bar{x}	1.1	44.6	35.6	18.6
	SD	-	6.3	2.0	3.9	SD	2.1	12.8	11.4	4.8
	P	-	0.02	NS	NS	P	-	0.005	0.02	NS
Block B4	\bar{x}	-	54.0	26.0	20.0					
	SD	-	7.0	2.6	5.0					
	P	-	NS	NS	NS					
Block C2	\bar{x}	4.5	27.0	52.0	17.0					
	SD	1.0	7.4	7.8	4.0					
	P	-	0.001	0.001	NS					
Block D1	\bar{x}	-	54.0	30.0	15.0					
	SD	-	9.0	8.0	3.3					
	P	-	NS	NS	NS					
CONTROL BLOCK										
	\bar{x}	-	45.0	30.0	24.0					
	SD	-	2.5	1.3	3.0					

Figure A3.1

Numerical data for animal LD1.1.

ANIMAL L.D. 1.2.

		BLOCK RESULTS				ANIMAL RESULT			
		PYK RCN	RCN	RC CYTO	MC CYTO	PYK RCN	RCN	RC CYTO	MC CYTO
Block A2	\bar{x}	-	50.0	27.8	22.8	\bar{x}	0.4	55.4	28.3
	SD	-	14.3	5.9	9.1	SD	1.5	7.7	6.0
	P	-	NS	NS	NS	P	-	0.01	NS
Block A4	\bar{x}	-	56.3	28.5	15.3				
	SD	-	2.4	4.5	4.4				
	P	-	NS	NS	NS				
Block B1	\bar{x}	-	61.3	25.0	14.0				
	SD	-	3.8	3.7	2.2				
	P	-	0.005	0.05	NS				
Block B3	\bar{x}	1.5	54.3	32.0	12.25				
	SD	3.0	2.9	8.8	8.1				
	P	-	NS	NS	NS				
		CONTROL BLOCK							
		\bar{x}	-	53.3	26.0				
		SD	-	5.3	6.1				

ANIMAL L.D. 1.3.

		BLOCK RESULTS				ANIMAL RESULT			
		PYK RCN	RCN	RC CYTO	MC CYTO	PYK RCN	RCN	RC CYTO	MC CYTO
Block A3	\bar{x}	10.5	38.8	37.0	13.5	\bar{x}	3.4	48.1	32.3
	SD	5.7	13.1	7.6	6.2	SD	4.9	9.7	7.0
	P	-	0.001	0.005	NS	P	-	NS	NS
Block B4	\bar{x}	0.3	48.3	34.5	17.0				
	SD	0.5	6.6	6.8	2.9				
	P	-	NS	NS	NS				
Block C2	\bar{x}	-	52.5	29.0	18.8				
	SD	-	5.3	7.8	5.9				
	P	-	NS	NS	NS				
Block D1	\bar{x}	2.8	53.0	28.5	15.8				
	SD	3.7	7.3	3.1	2.8				
	P	-	NS	NS	NS				
		CONTROL BLOCK							
		\bar{x}	-	49.5	31.8				
		SD	-	7.0	5.1				

Figure A3.2

Numerical data for animals LD1.2 and LD1.3.

ANIMAL L.D. 1.4.

		BLOCK RESULTS						ANIMAL RESULT			
		PYK RCN	RCN	RC CYTO	MC CYTO			PYK RCN	RCN	RC CYTO	MC CYTO
Block A4	\bar{x}	-	52.5	32.0	14.5	\bar{x}	-	47.7	38.1	15.9	
	SD	-	6.8	10.0	4.9	SD	-	7.0	7.9	4.8	
	P	-	NS	NS	NS	P	-	NS	0.005	NS	
Block B2	\bar{x}	-	46.2	41.5	12.0						
	SD	-	11.4	9.7	2.7						
	P	-	NS	0.001	0.05						
Block C3	\bar{x}	-	45.0	38.5	19.3						
	SD	-	5.0	5.9	3.8						
	P	-	NS	NS	NS						
Block D2	\bar{x}	-	47.0	35.5	17.7						
	SD	-	0.8	4.0	5.0						
	P	-	NS	NS	NS						
		CONTROL BLOCK									
	\bar{x}	-	50.3	32.0	18.3						
	SD	-	8.4	8.8	4.5						

ANIMAL L.D. 2.1.

		BLOCK RESULTS						ANIMAL RESULT			
		PYK RCN	RCN	RC CYTO	MC CYTO			PYK RCN	RCN	RC CYTO	MC CYTO
Block A3	\bar{x}	4.0	35.0	40.0	20.0	\bar{x}	1.7	44.9	34.4	18.8	
	SD	5.0	9.0	5.0	10.0	SD	2.4	7.8	4.7	6.3	
	P	-	0.001	0.005	NS	P	-	0.001	0.025	NS	
Block B2	\bar{x}	2.0	48.0	34.0	15.0						
	SD	2.3	4.9	2.2	6.0						
	P	-	NS	NS	NS						
Block C4	\bar{x}	-	20.0	30.5	19.0						
	SD	-	5.7	1.7	5.6						
	P	-	NS	NS	NS						
Block D2	\bar{x}	-	46.0	32.5	20.0						
	SD	-	2.0	5.0	4.4						
	P	-	NS	NS	NS						
		CONTROL BLOCK									
	\bar{x}	-	49.5	30.0	20.0						
	SD	-	2.9	1.3	1.3						

Figure A3.3

Numerical data for animals LD1.4 and LD2.1.

ANIMAL L.D. 2.2.

BLOCK RESULTS						ANIMAL RESULT				
		PYK		RC	MC	PYK		RC	MC	
		RCN	RCN	CYTO	CYTO	RCN	RCN	CYTO	CYTO	
Block A1	\bar{x}	-	56.0	29.0	20.0	\bar{x}	0.1	48.9	30.8	21.0
	SD	-	12.0	2.5	4.2	SD	0.3	8.4	6.7	4.8
	P	-	NS	NS	NS	P	-	NS	NS	0.05
Block A2	\bar{x}	0.3	50.0	31.0	18.0					
	SD	0.5	5.5	10.0	6.0					
	P	-	NS	NS	NS					
Block B1	\bar{x}	0.3	47.0	30.5	22.0					
	SD	0.5	7.0	10.5	4.0					
	P	-	NS	NS	NS					
Block B3	\bar{x}	-	43.0	32.0	23.5					
	SD	-	6.0	4.5	3.7					
	P	-	0.02	NS	0.05					
CONTROL BLOCK										
	\bar{x}	-	49.0	33.5	18.0					
	SD	-	5.0	2.6	5.0					

ANIMAL L.D. 2.3.

BLOCK RESULTS						ANIMAL RESULT							
			PYK RCN	RCN	RC CYTO	MC CYTO				PYK RCN	RCN	RC CYTO	MC CYTO
Block A1	\bar{x}	-	51.8	26.5	21.8	\bar{x}	0.4	50.8	31.6	17.3			
	SD	-	5.2	2.6	2.5	SD	1.1	4.1	4.8	5.8			
	P	-	NS	NS	NS	P	-	NS	NS	NS			
Block B2	\bar{x}	1.3	52.0	35.5	11.0								
	SD	1.5	5.2	6.0	4.2								
	P	-	NS	NS	0.025								
Block C3	\bar{x}	-	50.8	33.0	16.3								
	SD	-	5.4	2.2	4.8								
	P	-	NS	NS	NS								
Block D4	\bar{x}	-	48.0	31.5	20.3								
	SD	-	2.8	3.4	5.3								
	P	-	NS	NS	NS								
CONTROL BLOCK													
	\bar{x}	-	53.5	38.0	8.5								
	SD	-	4.1	2.4	3.1								

Figure A3.4

Numerical data for animals LD2.2 and LD2.3.

ANIMAL L.D. 2.4.

		BLOCK RESULTS				ANIMAL RESULT			
		PYK RCN	RCN	RC CYTO	MC CYTO	PYK RCN	RCN	RC CYTO	MC CYTO
Block A2	\bar{x}	1.3	50.3	30.3	18.3	\bar{x}	9.8	42.2	28.8
	SD	4.6	6.8	4.6	5.3	SD	12.3	13.6	8.1
	P	-	NS	NS	NS	P	-	0.001	NS
Block B3	\bar{x}	25.0	25.0	23.8	26.0				
	SD	5.6	4.8	8.9	11.4				
	P	-	0.001	0.02	0.01				
Block C3	\bar{x}	1.0	53.0	27.3	17.8				
	SD	1.2	8.5	9.1	1.5				
	P	-	NS	NS	NS				
Block D2	\bar{x}	11.0	40.5	33.8	15.5				
	SD	15.2	11.8	8.6	4.3				
	P	-	0.005	NS	NS				
		CONTROL BLOCK							
		\bar{x}	-	53.0	28.3				
		SD	-	7.0	7.2				

ANIMAL L.D. 3.1.

		BLOCK RESULTS				ANIMAL RESULT			
		PYK RCN	RCN	RC CYTO	MC CYTO	PYK RCN	RCN	RC CYTO	MC CYTO
Block A3	\bar{x}	-	47.0	32.0	20.0	\bar{x}	-	48.3	31.4
	SD	-	6.6	4.0	2.0	SD	-	6.3	7.2
	P	-	NS	NS	NS	P	-	NS	NS
Block B2	\bar{x}	-	48.0	34.0	21.0				
	SD	-	10.0	7.8	13.0				
	P	-	NS	NS	NS				
Block C4	\bar{x}	-	50.0	28.5	17.0				
	SD	-	4.4	8.8	3.3				
	P	-	NS	NS	NS				
Block D2	\bar{x}	-	47.0	30.0	22.0				
	SD	-	6.1	9.0	4.4				
	P	-	NS	NS	NS				
		CONTROL BLOCK							
		\bar{x}	-	53.0	30.0				
		SD	-	6.9	2.0				

Figure A3.5

Numerical data for animals LD2.4 and LD3.1.

ANIMAL L.D. 3.2.

BLOCK RESULTS						ANIMAL RESULT							
			PYK RCN	RCN	RC CYTO	MC CYTO				PYK RCN	RCN	RC CYTO	MC CYTO
Block A1	\bar{x}	-	39.0	39.0	22.0	\bar{x}	2.6	47.4	30.9	18.7			
	SD	-	6.8	6.2	1.0	SD	4.4	9.5	7.4	4.0			
	P	-	0.001	0.01	NS	P	-	NS	NS	NS			
Block B3	\bar{x}	4.0	47.0	29.5	19.0								
	SD	3.3	5.8	7.7	2.1								
	P	-	NS	NS	NS								
Block C2	\bar{x}	6.5	49.0	25.0	20.0								
	SD	6.6	7.0	4.6	3.8								
	P	-	NS	0.05	NS								
Block D3	\bar{x}	-	56.5	29.8	14.0								
	SD	-	5.0	4.5	3.9								
	P	-	NS	NS	NS								
			CONTROL BLOCK										
	\bar{x}	-	49.0	28.0	23.0								
	SD	-	7.3	2.2	7.4								

ANIMAL L.D. 3.3.

BLOCK RESULTS						ANIMAL RESULT							
			PYK RCN	RCN	RC CYTO	MC CYTO				PYK RCN	RCN	RC CYTO	MC CYTO
Block A2	\bar{x}	-	57.0	29.0	14.0	\bar{x}	0.3	53.8	28.1	17.7			
	SD	-	8.0	7.4	3.0	SD	1.0	7.5	5.7	8.1			
	P	-	NS	NS	NS	P	-	NS	NS	NS			
Block B3	\bar{x}	1.0	58.5	28.5	9.3								
	SD	2.0	6.2	1.7	6.7								
	P	-	0.05	NS	0.005								
Block C4	\bar{x}	-	49.5	27.3	23.5								
	SD	-	9.3	8.0	10.0								
	P	-	NS	NS	NS								
Block D2	\bar{x}	-	50.5	27.8	21.5								
	SD	-	5.0	6.0	7.1								
	P	-	NS	NS	NS								
CONTROL BLOCK													
	\bar{x}	-	50.5	33.0	16.0								
	SD	-	3.0	2.6	3.7								

Figure A3.6

Numerical data for animals LD3.2 and LD3.3.

ANIMAL L.D. 3.4.

BLOCK RESULTS						ANIMAL RESULT				
		PYK RCN	RCN	RC CYTO	MC CYTO		PYK RCN	RCN	RC CYTO	MC CYTO
Block A1	\bar{x}	-	54.0	30.3	16.0	\bar{x}	2.2	47.9	31.6	18.4
	SD	-	7.0	7.8	1.6	SD	3.9	8.3	5.5	6.0
	P	-	NS	NS	NS	P	-	NS	NS	NS
Block B2	\bar{x}	-	52.0	34.0	13.8					
	SD	-	3.5	4.2	2.3					
	P	-	NS	NS	NS					
Block C2	\bar{x}	6.8	40.8	33.3	20.0					
	SD	4.3	5.6	5.2	2.9					
	P	-	0.005	NS	NS					
Block D2	\bar{x}	2.0	44.8	29.0	24.0					
	SD	4.0	9.8	4.8	8.8					
	P	-	NS	NS	0.05					
CONTROL BLOCK										
	\bar{x}	-	61.0	26.3	13.0					
	SD	-	8.1	4.3	4.7					

ANIMAL L.D. 4.1.

BLOCK RESULTS						ANIMAL RESULT				
		PYK RCN	RCN	RC CYTO	MC CYTO		PYK RCN	RCN	RC CYTO	MC CYTO
Block A2	\bar{x}	-	50.5	24.0	25.3	\bar{x}	-	47.9	27.9	24.3
	SD	-	9.3	5.7	4.9	SD	-	6.5	6.1	4.6
	P	-	NS	0.02	0.01	P	-	NS	0.05	0.001
Block B3	\bar{x}	-	47.0	28.0	24.5					
	SD	-	8.0	8.0	1.0					
	P	-	NS	NS	0.02					
Block C2	\bar{x}	-	44.7	31.0	24.7					
	SD	-	7.6	5.5	7.8					
	P	-	NS	NS	0.02					
Block D3	\bar{x}	-	49.0	28.2	22.7					
	SD	-	2.9	5.2	3.7					
	P	-	NS	NS	NS					
CONTACT BLOCK										
	\bar{x}	-	51.0	31.7	16.7					
	SD	-	7.0	8.3	1.7					

Figure A3.7

Numerical data for animals LD3.4 and LD4.1.

ANIMAL L.D. 4.2.

		BLOCK RESULTS						ANIMAL RESULT			
		PYK RCN	RCN	RC CYTO	MC CYTO			PYK RCN	RCN	RC CYTO	MC CYTO
Block A3	\bar{x}	-	45.8	30.0	15.8	\bar{x}	0.1	50.8	30.8	20.0	
	SD	-	2.6	4.8	7.2	SD	0.3	6.8	5.6	6.2	
	P	-	NS	NS	NS	P	-	NS	NS	NS	
Block B2	\bar{x}	0.3	55.8	28.8	27.0						
	SD	0.5	10.3	3.8	7.3						
	P	0.3	NS	NS	NS						
Block C4	\bar{x}	-	49.3	36.3	13.0						
	SD	-	2.5	6.6	7.3						
	P	-	NS	NS	NS						
Block D2	\bar{x}	-	52.5	28.3	24.5						
	SD	-	5.9	5.2	9.9						
	P	-	NS	NS	NS						
CONTROL BLOCK											
	\bar{x}	-	47.8	33.5	14.3						
	SD	-	3.0	2.6	5.3						

ANIMAL L.D. 4.3.

		BLOCK RESULTS						ANIMAL RESULT			
		PYK RCN	RCN	RC CYTO	MC CYTO			PYK RCN	RCN	RC CYTO	MC CYTO
Block A2	\bar{x}	-	47.3	31.0	19.0	\bar{x}	-	49.7	31.6	17.9	
	SD	-	3.9	8.2	2.8	SD	-	6.8	6.1	4.7	
	P	-	NS	NS	NS	P	-	NS	NS	NS	
Block B2	\bar{x}	-	46.5	35.3	19.8						
	SD	-	3.7	5.7	5.2						
	P	-	NS	NS	NS						
Block C3	\bar{x}	-	55.3	29.0	15.5						
	SD	-	10.0	5.0	5.8						
	P	-	NS	NS	NS						
Block D4	\bar{x}	-	50.8	31.3	17.5						
	SD	-	5.0	5.9	5.0						
	P	-	NS	NS	NS						
CONTROL BLOCK											
	\bar{x}	-	50.3	28.5	21.0						
	SD	-	5.0	6.2	4.0						

Figure A3.8

Numerical data for animals LD4.2 and LD4.3

ANIMAL L.D. 4.4.

		BLOCK RESULTS				ANIMAL RESULT			
		PYK RCN	RCN	RC CYTO	MC CYTO	PYK RCN	RCN	RC CYTO	MC CYTO
Block A2	\bar{x}	-	51.0	37.5	11.5	\bar{x}	4.8	46.6	30.5
	SD	-	2.7	7.9	6.0	SD	11.9	9.7	6.0
	P	-	NS	0.05	0.05	P	-	0.025	NS
Block B4	\bar{x}	-	46.3	31.3	22.8				
	SD	-	6.0	4.6	3.6				
	P	-	NS	NS	NS				
Block C1	\bar{x}	18.3	37.0	25.0	20.0				
	SD	19.6	16.4	5.2	2.8				
	P	-	0.001	0.05	NS				
Block D3	\bar{x}	0.8	51.8	28.3	19.3				
	SD	1.5	2.9	4.4	5.9				
	P	-	NS	NS	NS				
		CONTROL BLOCK							
		\bar{x}	-	55.3	28.3				
		SD	-	6.1	5.1				

ANIMAL L.D. 5.1.

		BLOCK RESULTS				ANIMAL RESULT			
		PYK RCN	RCN	RC CYTO	MC CYTO	PYK RCN	RCN	RC CYTO	MC CYTO
Block A2	\bar{x}	-	52.3	28.5	19.0	\bar{x}	0.4	52.2	27.1
	SD	-	4.8	1.0	4.2	SD	1.1	6.2	4.8
	P	-	NS	NS	NS	P	-	NS	0.05
Block B2	\bar{x}	-	50.5	29.3	20.5				
	SD	-	7.0	6.7	2.4				
	P	-	NS	NS	NS				
Block C4	\bar{x}	0.8	51.8	25.5	22.0				
	SD	1.5	5.7	3.0	2.9				
	P	-	NS	NS	NS				
Block D1	\bar{x}	1.0	53.5	25.3	21.2				
	SD	1.2	9.1	6.7	3.3				
	P	-	NS	0.05	NS				
		CONTROL BLOCK							
		\bar{x}	-	54.3	27.8				
		SD	-	2.6	2.1				

Figure A3.9

Numerical data for animals LD4.4 and LD5.1.

ANIMAL L.D. 5.2.

BLOCK RESULTS						ANIMAL RESULT						
		PYK RCN	RCN	RC CYTO	MC CYTO			PYK RCN	RCN	RC CYTO	MC CYTO	
Block A1	\bar{x}	0.8	51.8	29.8	19.3			\bar{x}	0.2	54.3	30.4	15.8
	SD	1.5	3.9	5.2	4.3			SD	0.8	6.7	7.1	3.7
	P	-	NS	NS	NS			P	-	NS	NS	NS
Block B3	\bar{x}	-	58.5	28.0	13.3							
	SD	-	3.9	2.8	1.9							
	P	-	0.05	NS	NS							
Block C2	\bar{x}	-	55.8	33.5	13.5							
	SD	-	9.4	13.4	1.3							
	P	-	NS	NS	NS							
Block D3	\bar{x}	-	51.3	30.3	18.5							
	SD	-	7.6	3.9	4.2							
	P	-	NS	NS	NS							
		CONTROL BLOCK										
		\bar{x}	-	45.5	38.0							
		SD	-	8.3	2.9							

ANIMAL L.D. 6.1.

BLOCK RESULTS						ANIMAL RESULT							
			PYK RCN	RCN	RC CYTO	MC CYTO				PYK RCN	RCN	RC CYTO	MC CYTO
Block A3	\bar{x}	-	57.8	30.0	12.3		\bar{x}	-	51.7	33.2	14.9		
	SD	-	13.0	10.2	3.4		SD	-	7.7	5.7	3.3		
	P	-	NS	NS	NS		P	-	NS	NS	NS		
Block B1	\bar{x}	-	50.0	32.3	17.5								
	SD	-	3.7	2.4	4.1								
	P	-	NS	NS	NS								
Block C3	\bar{x}	-	48.8	35.8	15.3								
	SD	-	6.2	4.2	1.7								
	P	-	NS	NS	NS								
Block D4	\bar{x}	-	50.3	34.8	14.8								
	SD	-	3.7	3.0	1.9								
	P	-	NS	NS	NS								
CONTROL BLOCK													
	\bar{x}	-	51.3	36.5	16.5								
	SD	-	7.5	2.6	1.0								

Figure A3.10

Numerical data for animals LD5.2 and LD6.1.

These figures show the raw data for the block results as histograms. The histograms give the percentage of points, within the outer nuclear layer, falling on each feature of interest. The group number is given at the top of each figure. The animal number is given at the side of each figure. RCN: receptor cell nuclei; RCC: receptor cell cytoplasm; MCC: Müller cell cytoplasm.

EXPERIMENTAL GROUP 1

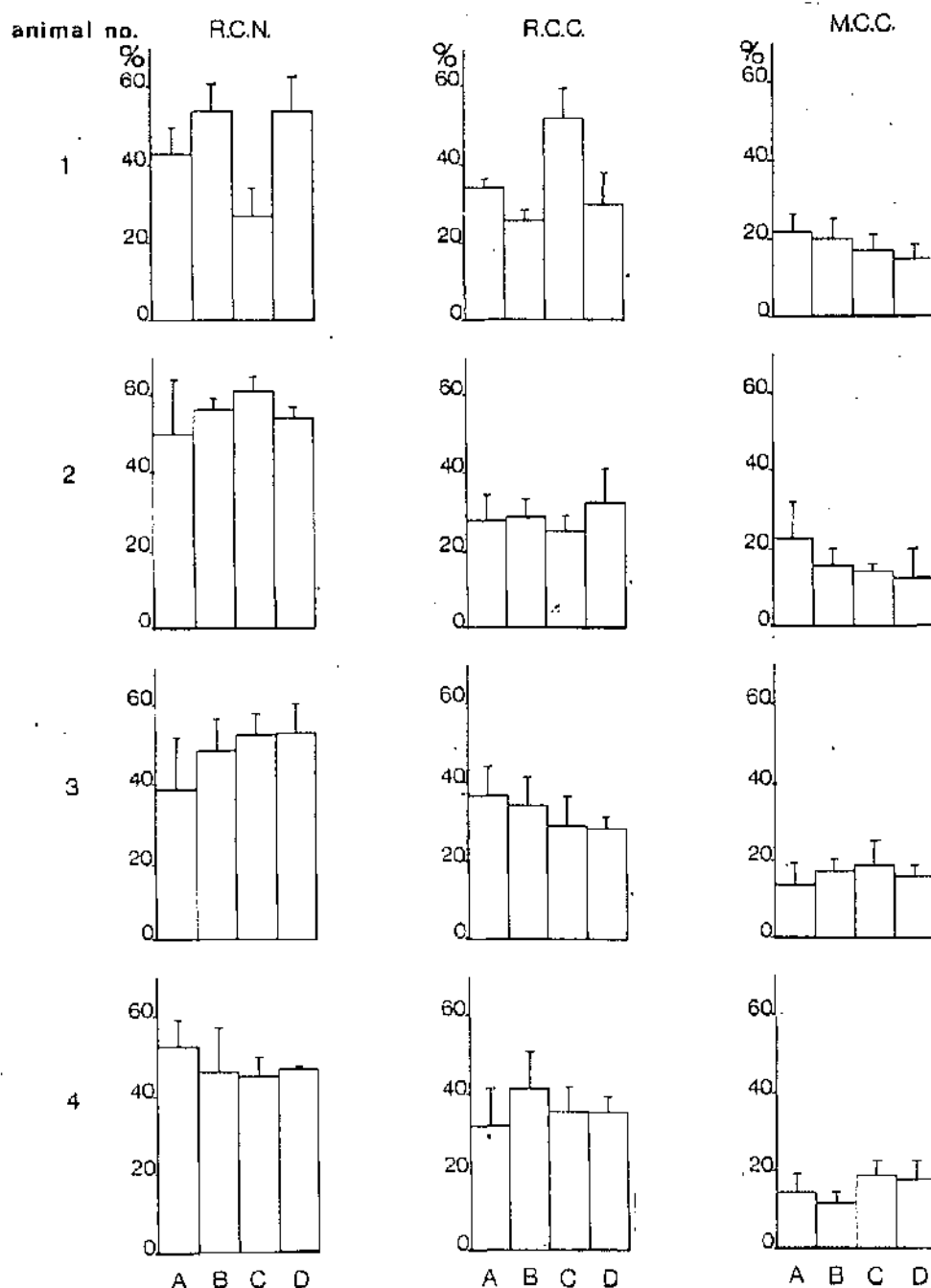


Figure A3.11

Histograms of the individual block results from the four animals in group 1.

EXPERIMENTAL GROUP 2

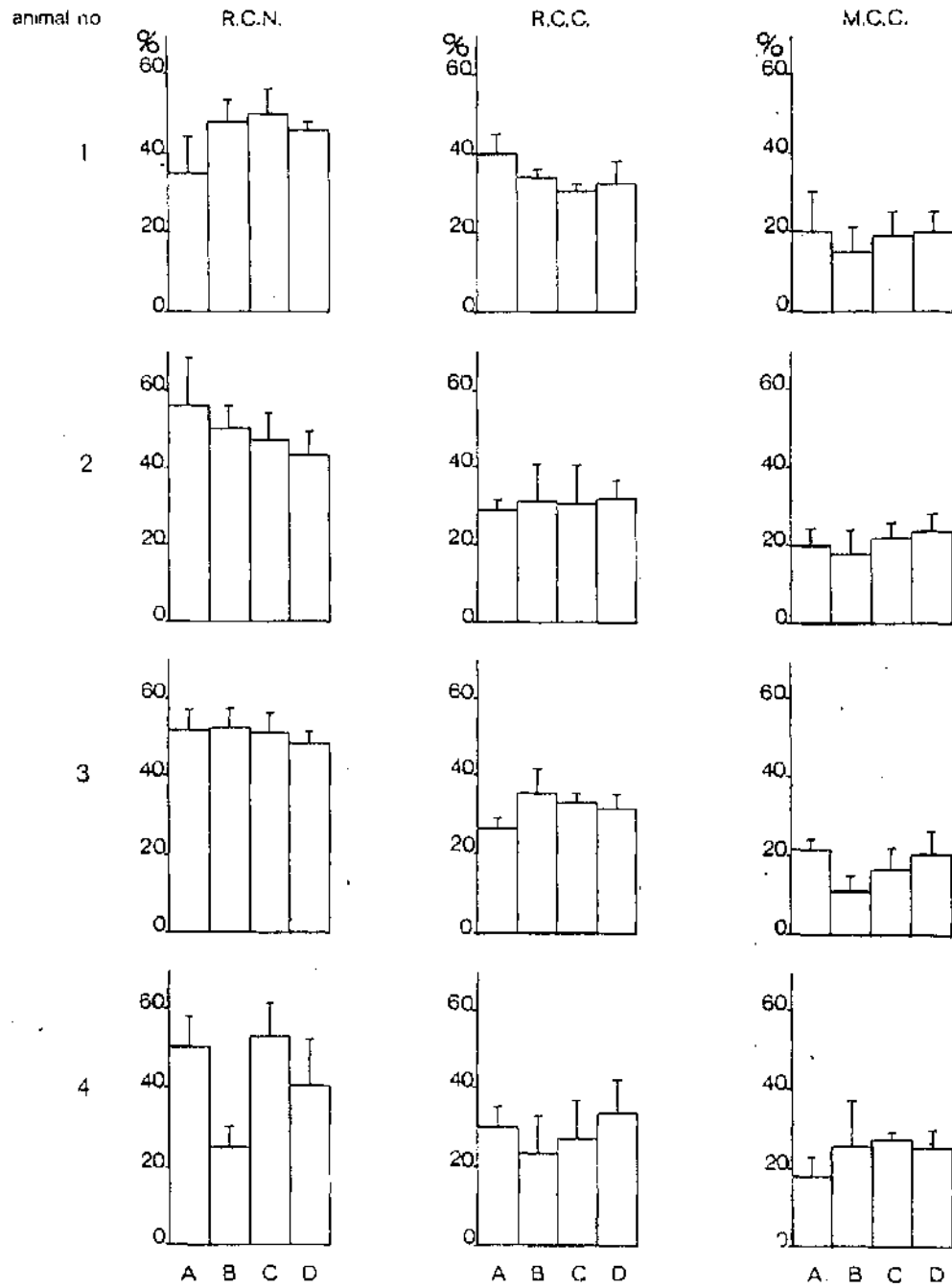


Figure A3.12

Histograms of the individual block results from the four animals in group 2.

EXPERIMENTAL GROUP 3

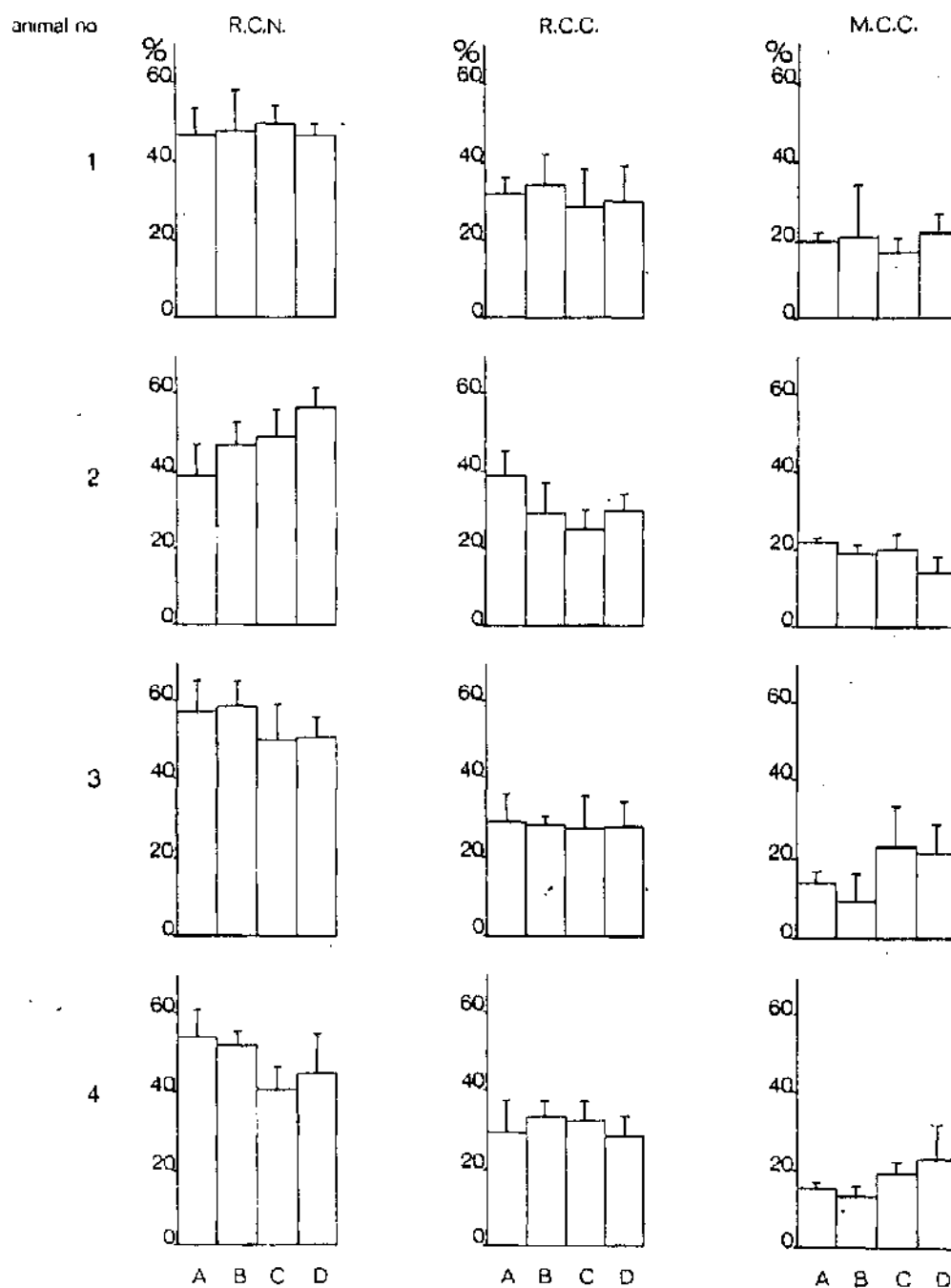


Figure A3.13

Histograms of the individual block results from the four animals in group 3.

EXPERIMENTAL GROUP 4

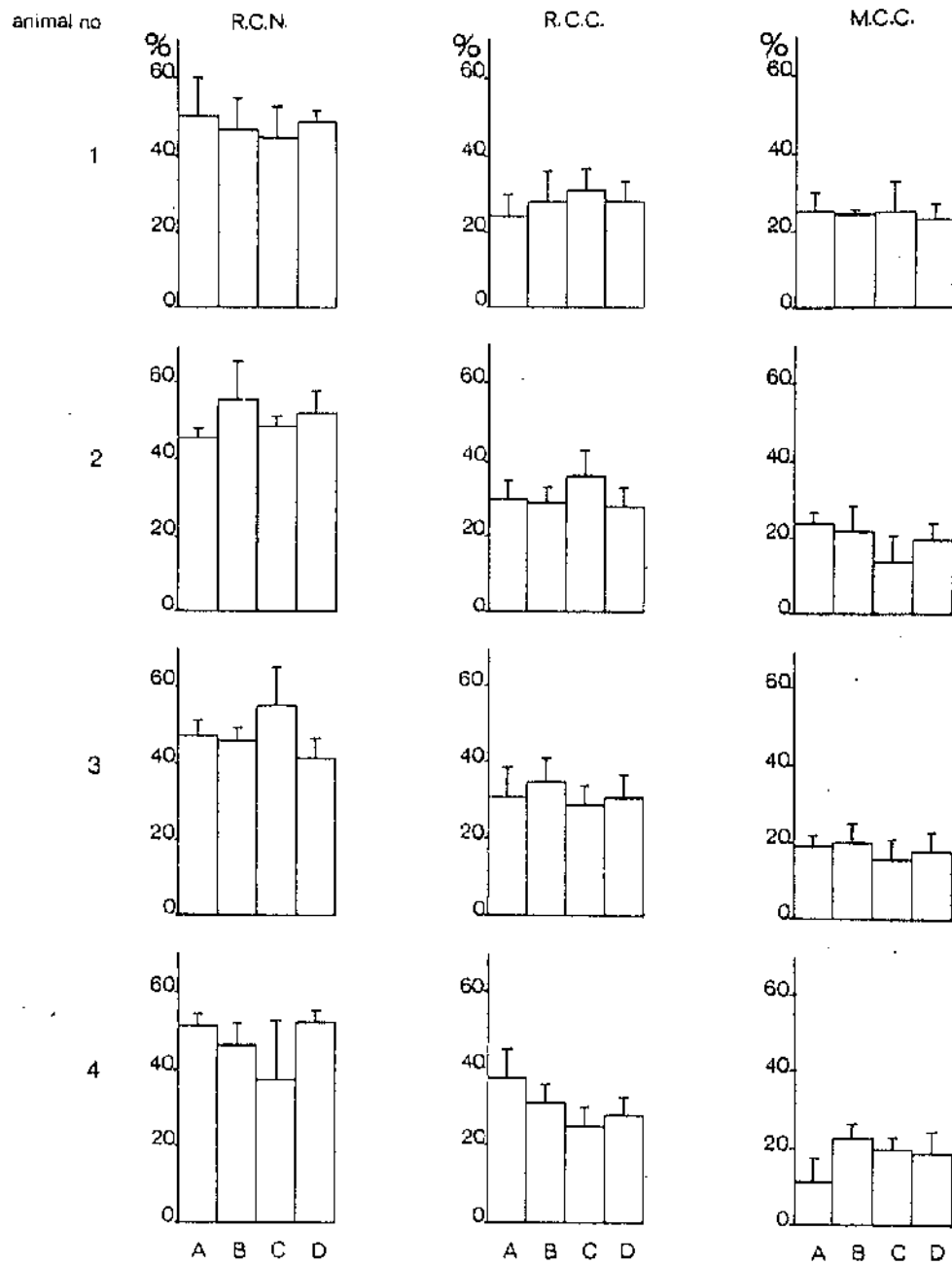
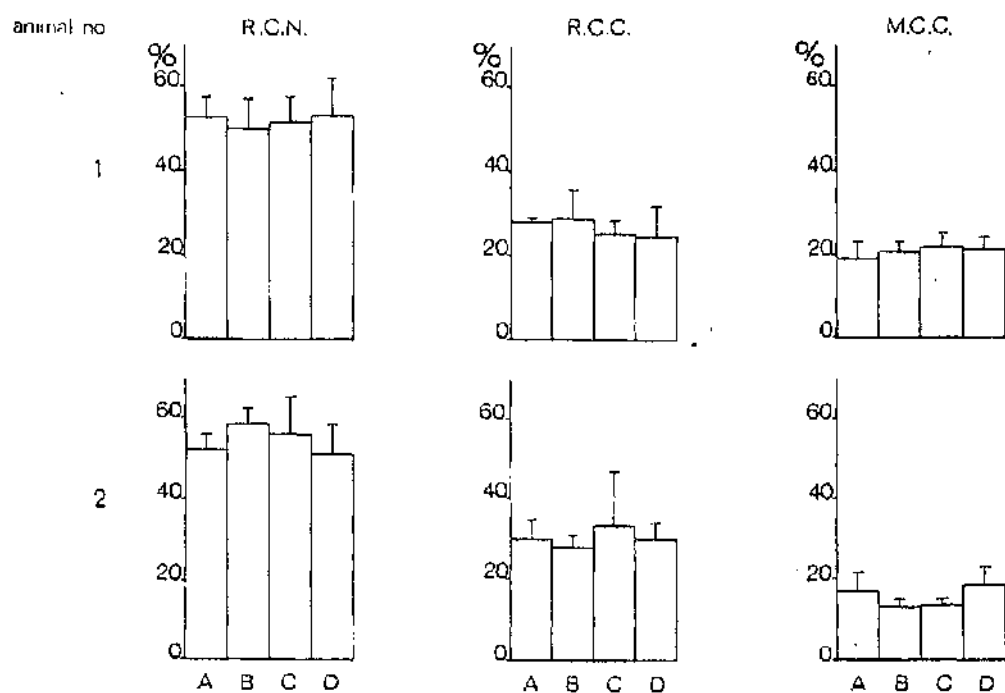


Figure A3.14

Histogrammes of the individual block results from the four animals in group 4.

EXPERIMENTAL GROUP 5



EXPERIMENTAL GROUP 6

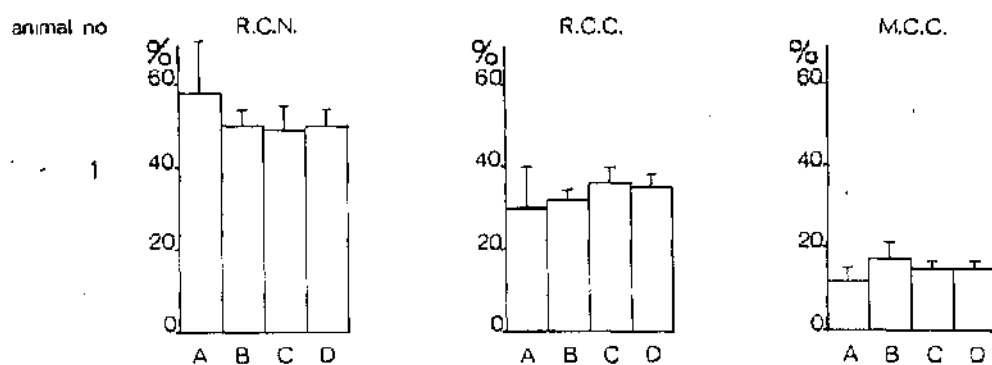


Figure A3.15

Histograms of the individual block results from the two animals in group 5 and the one animal in group 6.

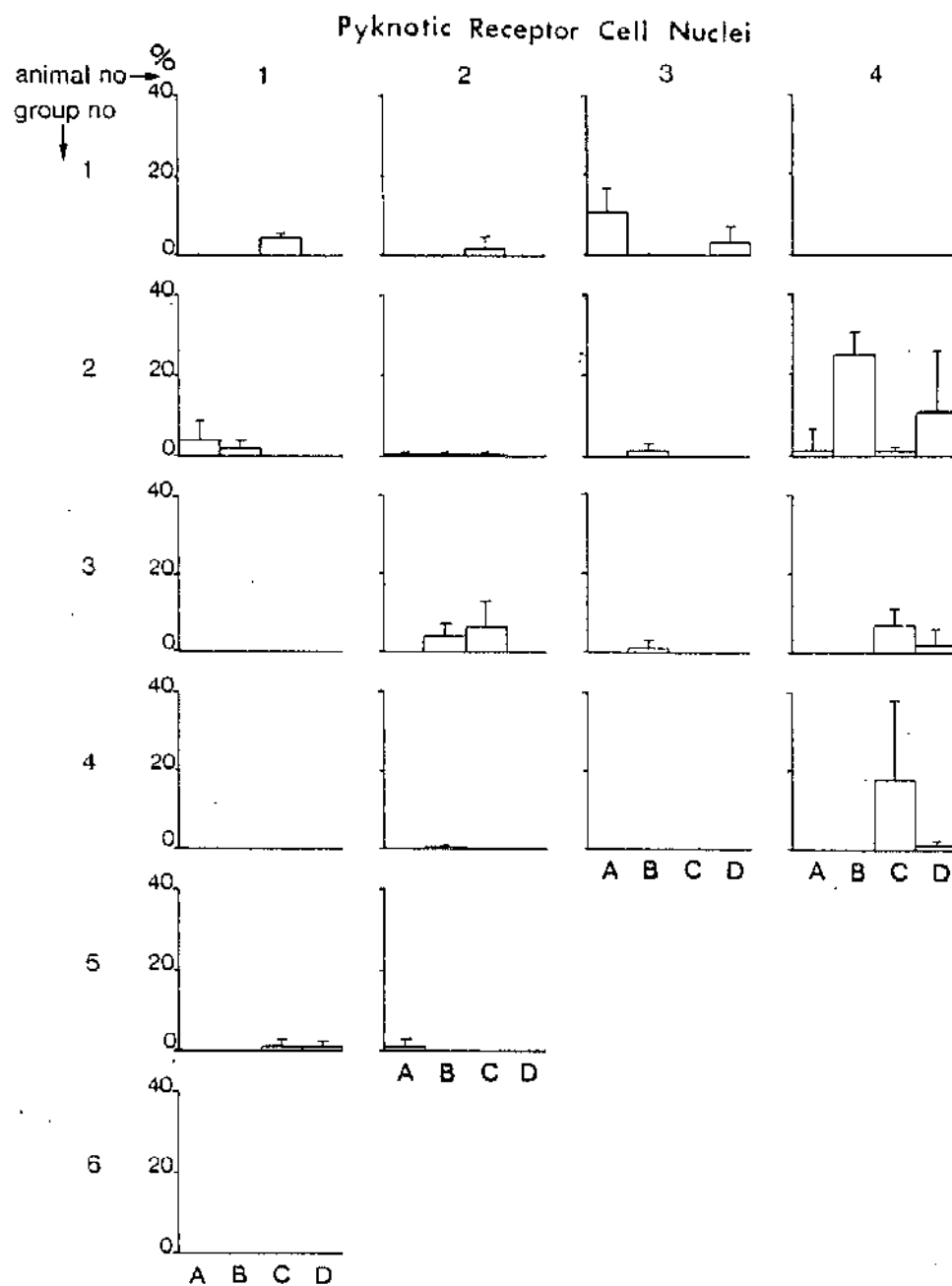


Figure A3.16

This figure gives the counts obtained for pyknotic receptor cell nuclei as histograms. The histograms show the percentage of points, within the outer nuclear layer, which fell on pyknotic receptor cell nuclei.

APPENDIX 4

RETINAL TEMPERATURE MEASUREMENTS

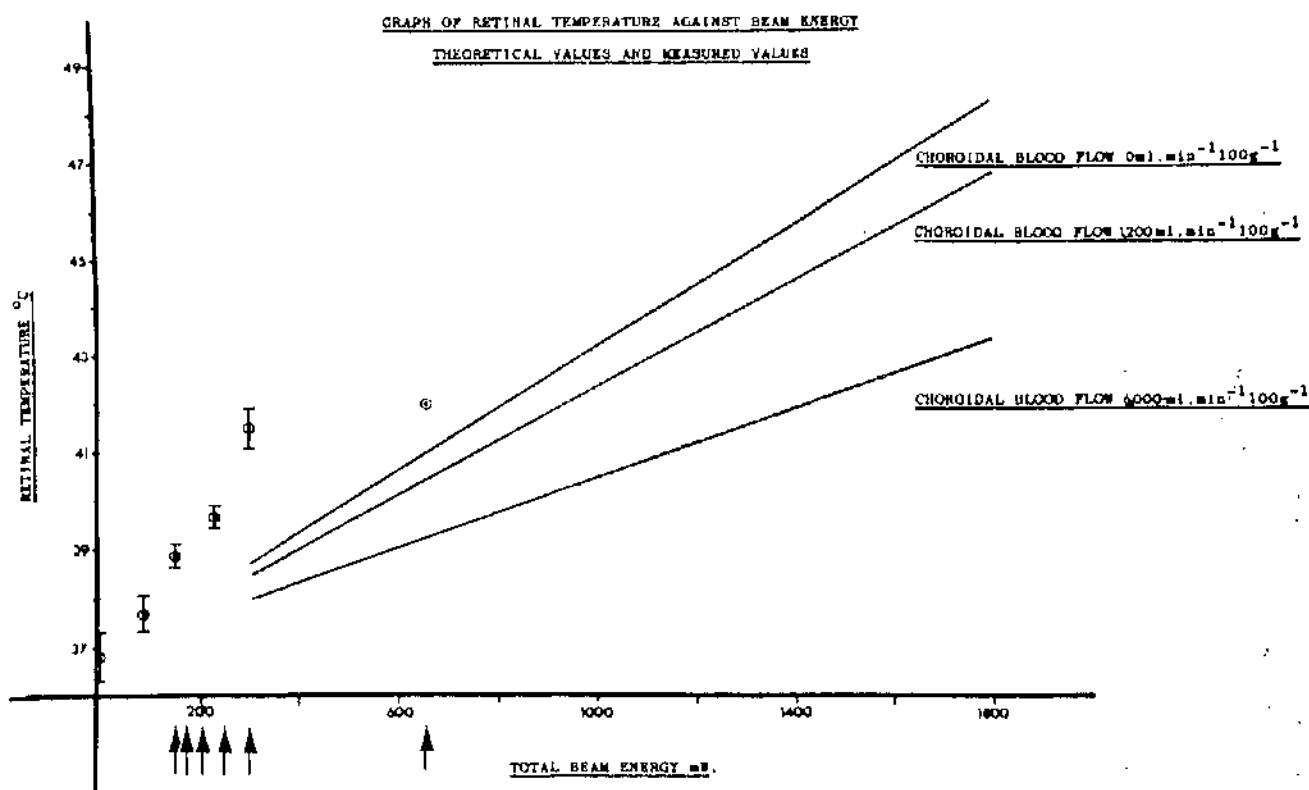


Figure A4.1

This figure shows both the predicted retinal temperature, assuming various levels of choroidal blood flow, and the measured retinal temperature, at various levels of total beam power. The lines represent the results predicted by Moseley and Strang, 1981. The encircled points are direct measurements of retinal temperature, using a needle mounted thermocouple, at various levels of illumination. The results showing error bars are the mean results, and standard deviations, of four observations. The small arrows on the axis show the light intensities employed in these investigations.

REFERENCES

REFERENCES

- Adams, D.O., Beatrice, E.S. and Bedell, R.B. (1972)
Retina: ultrastructural alterations produced by extremely low levels of coherent radiation. *Science*: 177; 58-60.
- Anderson, K.V., Coyle, F.P., and O'Steen, W.K. (1972)
Retinal degeneration produced by low intensity coloured light. *Exp. Neurol*: 35, 233-238.
- Anderson, K.V., and O'Steen, W.K. (1972)
Black-White and pattern discrimination in rats without photoreceptors. *Exp. Neurol*: 34, 446-454.
- Anderson, D.H., Fisher, S.K., and Steinberg, R.H. (1978).
Mammalian cones: disc shedding, phagocytosis, and renewal. *Invest Ophthalm*: 17, 117-133.
- Apple, D.J., Goldberg, M.F. and Wyhinng, G. (1973)
Histopathology and ultrastructure of the argon laser lesion in human retinal and choroidal vasculatures. *Am. J. Ophthalm*: 75, 595-609.
- Bairati, A., and Orzalesi, N. (1963)
The ultrastructure of the pigment epithelium and of the photo-receptor - pigment epithelial junction in the human retina. *J. Ultrastruc. Res*: 9, 484-496.
- Basinger, S., Hoffman, R., and Matthes, M. (1976)
Photoreceptor shedding is initiated by light in the frog retina. *Science*: 194, 1074-1076.
- Bassi, M., Bernelli-Zazzera, A., and Cassi, E. (1960)
Electron microscopy of rat liver cells in hypoxia. *J. Path. Bact*: 79, 179-183.
- Bassi, M., and Bernelli-Zazzera, A. (1964).
Ultrastructural cytoplasmic changes of liver cells after reversible and irreversible ischaemia. *Exp. Mol. Path*: 3, 332-350.
- Bernstain, M.H. Functional architecture of the retinal pigment epithelium. In: Smelser, G. ed. *The structure of the eye*. London and New York: Academic Press 1961.
- Bernstein, M.H. and Hollenberg, M.F. Movement of electron opaque markers through capillaries of the retina. In: Rohen, E.W. ed. *The structure of the eye*. Stuttgart: Schauttaue-Verlag, 1965.
- Beshause, J.C., Hollfield, J.G., and Rayborn, M.E. (1977)
Turnover of rod photoreceptor outersegments: membrane addition and loss in relationship to light. *J. Cell. Biol*: 75; 507-527.
- Bok, D., and Hall, M.O. (1971)
The role of the pigment epithelium in the etiology of inherited retinal dystrophy in the rat. *J. Cell Biol*: 49, 664-682.
- Bresnick, G.H., Frisch, D.G., Powell, J.O. (1970)
Ocular effects of argon lasers radiation. 1. Retinal damage threshold effects. *Invest. Ophthalm*: 9, 901-910.

- Brown, K.T. (1968). The electroretinogram: Its components and their origins. *Vision Research*: 8, 633-677.
- Buettner, K. and Rose, H.W. (1953). Eye hazards from an atomic bomb. *Sight Saving Rev*: 23, 1.
- Bunt, A.H. (1978). Fine structure and radioautography of rabbit photoreceptor cells. *Invest Ophthal*: 17; 90-104.
- Byrnes, V.A., Brown, D.V.L., Rose, H.W. and Cibis, P.A. (1955) Choriorretinal burns produced by atomic flash. *Arch. Ophthal*: 53, 351-364.
- Byrnes, V.A., Brown, D.V.L., Rose, H.W.L. and Cibis, P.A. (1956) Choriorretinal lesions due to thermal radiation from the atomic bomb. *Arch. Ophthal*: 55, 904-914.
- Calkins, J.L. and Hochheimer, B.F. (1980) Retinal light exposure from ophthalmoscopes, slit lamps and overhead surgical lamps. An analysis of potential hazards. *Invest Ophthal*: 19, 1009-1015.
- Campbell, C.J., Rittler, M.C., Noyori, K.S., Swope, C.H., and Joester, C.J. (1966). The threshold of the retina to damage by laser energy. *Arch. Ophthal*: 76, 437-442.
- Cavonius, C.R., Elgin, S., and Robbins, D.O. (1974). Thresholds for damage to the human retina by white light. *Exp. Eye Res*: 19, 543-548.
- Cerletti, A., and Meier-Ruge, W. (1967) Toxicological studies on phenothiazine induced retinopathy. In: *Toxicity and Side Effects of Psychotropic Drugs*. *Proc. Eur. Soc. Drug Toxicity*: 9, 197-198.
- Cicerone, C.M. (1976). Cones survive rods in the light-damaged eye of the albino rat. *Science*: 194, 1183-1185.
- Cogan, D.G. (1968) Lighting and health hazards. *Arch. Ophthal*: 79, 2.
- Cohen, A.I. (1965) A possible cytological basis for the 'R' membrane in the vertebrate eye. *Nature*: 205, 1222.
- Cohen, A.I. (1968) New evidence supporting the linkage to intracellular space of outer segment of frog cone but not rod. *J. Cell. Biol*: 37, 424-444.
- Cohen, A.I. (1971) Electron microscopic observations on form changes in photoreceptor outer segments and their saccules in response to osmotic stress. *J. Cell. Biol*: 48, 547-565.

- Denton, E.J. (1959)
The contributions of the oriented photosensitive and other molecules to the absorption of the whole retina.
Proc. R. Soc. B: 150, 78-94.
- Dingle, J.T., and Lucy, J.A. (1965)
Vitamina A carotenoids and cell function. Biol. Rev: 40, 422-461.
- Dingle, J.T., Sharman, I.M. and Moore, T. (1966)
Nutritional and lysosomal activity: The influence of the vitamin A status on the proteolytic activity of extracts from the livers and kidneys of rats. J. Biochem: 98, 476-484.
- Dobson, V., Cowett, R.M., and Riggs, L.A. (1975)
Long-term effect of phototherapy on visual function.
J. Pediatr: 86, 555-559.
- Dobson, V. (1976).
Editorial: Phototherapy and retinal damage. Invest Ophthalm: 15, 595-598
- Dowling, J.E. and Gibbons, I.R. (1962).
The fine structure of the pigment epithelium in the albino rat.
J. Cell Biol: 14, 459-474.
- Dowling, J.E. and Boycott, B.B. (1966).
Organisation of the primate retina: electron microscopy.
Proc. R. Soc. B: 166, 80-111.
- Dowling, J.E. (1970).
Organization of vertebrate retinas.
Invest. Ophthalm: 9, 665-680.
- Einthoven and Jolly, W.A. (1908).
The form and magnitude of the electrical response of the eye to stimulation by light at various intensities.
Quart. J. Exper. physiol: 1, 343-416.
- Essner, E., and Gorrin, G. (1979).
An electron microscopic study of macrophages in rats with inherited retinal dystrophy. Invest. Ophthalm: 18, 11-25.
- Farquhar, M.G. and Palade, G.E. (1963).
Junctional complexes in various epithelia.
J. Cell Biol: 17, 345-412.
- Fifkova, E. (1972).
Effect of light and visual deprivation on the retina.
Exp. Neurol: 35, 450-457.
- Fifkova, E. (1973).
Effect of light on the synaptic organisation of the inner plexiform layer of the retina in albino rats.
Experimentia: 29, 851-854.
- Firsh, G.D., Beatrice, E.S., and Holsen, R.C. (1971).
Comparative study of argon and ruby laser retinal damage thresholds.
Invest. Ophthalm: 10, 911-919.

- Flynn, P.J. (1942).
Photoretinitis in anti-aircraft lookouts.
Med. J. Aust: 2, 400-401.
- Friedman, E., and Kuwabara, T. (1968).
The retinal pigment epithelium. IV. The damaging effects of radiant energy. Arch. Ophthal: 8, 265-269.
- Fuller, D., Machemer, R., and Knighton, R.W. (1978).
Retinal damage produced by intraocular fibre optic light.
Am. J. Ophthalmol: 85, 519-537.
- Geeraets, W.J., Williams, R.C., Chan, G., Ham, W.T., Guerry, D. and Schmidt, F.H. (1962).
The relative absorption of thermal energy in the retina and choroid.
Invest Ophthal: 1, 340-347.
- Geeraets, W.J. and Ridgeway, D. (1963).
Retinal damage from high intensity light.
Acta Ophthal: 76 suppl. 109-112.
- Gibbons, W.D. and Allen, R.G. (1977)
Retinal damage from long-term exposure to laser radiation.
Invest. Ophthal: 16, 521-529.
- Gloor, B.P. (1969).
Phagocytotische Aktivitat des Pigmentepithels nach Lichtcoagulation.
Zur Frage der Herkunft von Makrophagen in der Retina.
Albrecht v. Graefes Arch. klin. exp. Ophthal: 179, 105-117.
- Goldman, A.I., Ham, W.T. and Mueller, H.A. (1975).
Mechanisms of retinal damage resulting from the exposure of rhesus monkeys to ultra short laser pulses.
Exp. Eye Res: 21, 457-469.
- Goldfischer, S. (1965).
The cytochemical demonstration of aryl sulphatase activity by light and electron microscopy.
J. Histochem. Cytochem: 13, 520
- Gomori, G.
Microscopic Histochemistry: Principles and Practice. Chicago: University of Chicago Press, 1952.
- Gorn, R.A. and Kuwabara, T. (1967).
Retinal damage by visible light: A physiologic study.
Invest Ophthal: 77, 115-118.
- Granit, R.
Sensory mechanisms of the retina. London: Oxford University Press. 1947.
- Granit, R.
The visual pathway. In: Davson ed. The eye. Volume II - The visual process. New York and London: Academic Press 1962.

- Grignolo, A., Orzalesi, N. and Calabria, G.A. (1966).
Studies of the fine structure and rhodopsin cycle of the rabbit retina in experimental degeneration induced by sodium iodate.
Exp. Eye Res. 5, 86-97.
- Grignolo, A. Orzalesi, N., Castellazzo, R., and Vittone, P. (1969).
Retinal damage by visible light in albino rats: An electron microscopic study.
Ophthalmologica: 157, 43-59.
- Hager, H., Hirschberger, W., and Scholz, W, (1960).
Electron microscopic changes in brain tissue of Syrian hamsters following acute anoxia.
Aerospace Med: 31, 379-387.
- Ham, W.T., Wiesinger, H., Schmidt, F.H., Williams, R.C., Ruffin, R.S., Shaffer, M. and Guerry, D. (1958).
Flash burns on the rabbit retina.
Am. J. Ophthal. 46, 700-723.
- Ham, W.T., Williams, R.C., Mueller, H.A., Guerry, D., Clarke, A.M. and Geeraets, W.J. (1966).
Effects of laser radiation on the mammalian eye.
Trans. N.Y. Acad. Sci. 28, 517-529.
- Ham, W.T., Geeraets, W.J., Mueller, H.A., Williams, R. C., Clarke, A.M., and Cleary, S.F. (1970).
Retinal burn thresholds for the helium-neon laser in the rhesus monkey.
Arch. Ophthal. 84, 797-809.
- Ham, W.T., Mueller, H.A., Newman, B.E., Holland, L.M., and Kuwabara, T. (1974).
Ocular hazard from pico second pulses of Nd Yag laser radiation.
Science, 185, 362-363.
- Ham, W.T., Mueller, H.A., Sliney, D.H. (1976).
Retinal sensitivity to damage from short wavelengths of light.
Nature, 260, 153-155.
- Ham, W.T., Ruffolo, J.J., Mueller, A., Clarke, A.M. and Moon, M.E. (1978)
Histologic analysis of photochemical lesions produced in rhesus retina by short-wave-length light.
Invest ophthal. 17, 1029-1035.
- Hansson, H.A. (1970a).
Ultrastructural studies on rat retina damaged by visible light.
Virchows Arch. Cell. Pathol. 6, 247-262.
- Hansson, H.A. (1970b)
A histochemical study of oxidative enzymes in rat retina damaged by visible light.
Exp. Eye Res. 9, 285-296.
- Hansson, H.A. and Sourander, P. (1970).
A lipid histochemical study of the rat retina damaged by visible light. Exp. Eye Res. 10, 64-70.

- Harworth, R.S. and Sperling, H.G. (1971).
Prolonged colour blindness induced by intense spectral lights in rhesus monkeys.
Science, 174, 520-523.
- Hayes, K.C. (1974).
Retinal degeneration in monkeys induced by deficiencies of vitamin E or A.
Invest Ophthalmol: 13, 499-510.
- Hockheimer, B.F., D'Anna, S.A. and Calkins, J.L. (1979).
Retinal damage from light. *Am. J. Ophthalmol.* 88, 1039-1044.
- Hogan, M.J., Alvarado, J.A. and Weddel, J.E.
Histology of the human eye. Philadelphia and London: W.B. Saunders Co. 1971.
- Hogan, M.J., Wood, I., and Steinberg, R.H. (1974).
Cones of human retina: phagocytosis by pigment epithelium.
Nature, 252, 303.
- Hollyfield, J.G., Besharse, J.C., and Rayborn, M.E. (1976).
The effect of light on the quantity of phagosomes in the pigment epithelium.
Exp. Eye Res. 23, 623-635.
- Holmgren, F. (1865).
Method att objectivera effecten au ljusinttryck pa retina.
Upsala Lakaref Forh, 177-191.
- Hudspeth, A.J. and Yee, A.G. (1973).
The intercellular junctional complexes of retinal pigment epithelia.
Invest Ophthalmol. 12, 354-365.
- Hughes, A. (1971).
Topographical relationships between anatomy and physiology of the rabbit visual system.
Doc. Ophthalmol. 30, 33-159,
- Hughes, A. (1972).
A schematic eye for the rabbit.
Vision Res. 12, 123-138.
- Ishikawa, Y., Uga, S. and Ikai, H. (1973).
The cell division of the pigment epithelium in the repairing retina after photocoagulation.
J. Electron Microscopy, 22, 273-275.
- Ishikawa, Y., and Ikai, H. (1974).
Electron microscopic studies on the retinal repair in the monkey after Xenon photocoagulation I. Cellular responses in the early stages of repair. *Jap. J. Ophthalmol.* 18, 334-349.
- Johnson, N.F. (1974).
Effects of acute ischaemia on the structure of the rabbit retina. Preliminary observations.
Trans. Ophthalmol. Soc. U.K., 94, 394-405.

- Johnson, N.F. (1977).
Retinal glycogen content during ischaemia.
Albrecht v. Graefes Arch. klin. exp. Ophthalm. 203, 271-282.
- Johnson, N.F., and Foulds, W.S. (1977).
Observations on the retinal pigment epithelium and retinal macrophages in experimental retinal detachment.
B.J. Ophthalm. 61, 564-572.
- Johnson, N.F. and Foulds, W.S. (1978).
The effects of total acute ischaemia on the structure of the rabbit retina.
Exp. Eye Res. 27, 45-59.
- Kalina, R.E. and Forrest, G.L. (1971).
Ocular hazards of phototherapy for hyperbilirubinemia.
J. Pediat. Ophthalm. 8, 116-118.
- Kolb, H. (1970).
Organization of the outer plexiform layer of the primate retina. Electron microscopy of Golgi-impregnated cells.
Phil. Trans. B. 258, 261-283.
- Konigsmark, B.W., and Sidman, R.L. (1963).
Origin of brain macrophages in the mouse.
J. Neuropath exp. Neurol. 22, 643-676.
- Kroll, A.J. and Machemer, B.
Experimental retinal detachment in owl monkey. III. electron microscopy of retina and pigment epithelium.
Exp. Eye Res. 66, 410-427.
- Kuwabara, T., and Cogan, D.G. (1961).
Retinal glycogen.
Arch. Ophthalm. 66, 96-104.
- Kuwabara, T. and Gorn, R.A. (1968).
Retinal damage by visible light. An electron microscopic study.
Arch. ophthalm. 79, 69-78.
- Kuwabara, T., and Okisaka, S. (1976).
Effect of electronic strobe flashlight on the monkey retina.
Jap. J. Ophthalm. 20, 9-18.
- Lappin, P. W. and Coogan, P.S. (1970).
Histologic evaluation of ophthalmoscopically subvisible laser exposures.
Invest Ophthalm. 9, 537-542.
- Laties, A.M., Bok, D. and Liebman, P. (1976).
Procion yellow: A Marker Dye for Outer Segment Disc Patency and for Rod Renewal.
Exp. Eye Res. 23, 139-148.
- La Vail, M.M., Sidman, R.L., and O'Neil, D. (1972).
Photoreceptor - pigment epithelial cell relations in rats with inherited retinal degeneration, radioautographic and electron microscopic evidence for a dual source of extra lamellar material.
J. Cell Biol. 53, 185-209.

- La Vail, M.M. (1976a).
Survival of some photoreceptor cells in albino rats following long-term exposure to continuous light.
Invest. Ophthalm., 15, 64-70.
- La Vail, M.M. (1976b).
Rod outersegment disc shedding in relation to cyclic lighting.
Exp. Eye Res. 23, 277-280.
- Lawwill, T. (1973).
Effects of prolonged exposure of rabbit retina to low intensity light
Invest Ophthalm. 12, 45-51.
- Lawwill, T., Crocketts, S., and Currier, G. (1977a).
Functional and histological measures of retinal damage in chronic light exposure.
Doc. Ophthalm. Proc. Series: 15, 285-295.
- Lawwill, T. Crockett, S. and Currier, G. (1977b).
Retinal damage secondary to chronic light exposure, thresholds and mechanisms.
Doc. Ophthalm. 44, 370-402.
- Lee, W.R. and Grierson, I. (1977).
Macrophage infiltration in the human retina.
Albrecht v. Graefes arch. klin. exp. Ophthalm. 203, 293-309.
- Leibovitz, H.M., Peacock, G.R. and Friedman, E. (1969).
The retinal pigment epithelium: Radiation thresholds associated with the Q switched ruby laser.
Arch. Ophthalm. 82, 332-338.
- Lerche, W., Beeger, R.L., and Russow, B. (1978).
Electron microscopic observations on the effect of laser beams on the retina of the rabbit.
Albrecht Von Graefes Arch. Klin. Ophthalm., 205, 81-99.
- L'Esperance, F.A. and Kelly, G.R. (1969).
The threshold of the retina to damage by argon laser radiation.
Acta Ophthalm., 81, 583-588.
- Lewis, P.R., and Knight, D.P.
Staining methods for sectioned material.
Amsterdam. New York. Oxford: North Holland Publishing Co. 1977
- Machmer, R. (1968).
Experimental retinal detachment in the owl monkey. II. Histology of the retina and pigment epithelium.
Exp. Eye Res. 66, 396-410.
- Machemer, R., and Laqua, H. (1975).
Pigment epithelial proliferation in retinal detachment (Massive peri-retinal proliferation).
Am. J. Ophthalm., 80, 1-23.
- Magalhaes, M.M. and Coimbra, A. (1972).
The rabbit retina Müller cell. A fine structural and cytochemical study.
J. Ultrastruc. Res. 39, 310,326.

- Maiman, T.H. (1960).
Stimulated optical radiation in ruby.
Nature, 187, 493-494.
- Mainster, M.A., White, T.J., and Allen, R.G. (1970).
Spectral dependence of retinal damage produced by intense light sources
J. Opt. Soc. Amer. 60, 848-855.
- Makous, W.L., Gould, J.D. (1968).
Effects of lasers on the human eye.
I.B.M. Journal, May, 257-271.
- Mandelcom, M.S., Machemer, R., Fineberg, E. and Hersch, S.B. (1975)
Proliferation and metastasia of intravitreal retinal pigment
epithelium cell autotransplants.
Am.J.Ophthal. 80, 227-237.
- Marshall, J. and Mellerio, J. (1968).
Histology of Retinal Lesions Produced with Q-switched lasers.
Exp. Eye Res. 7, 225-230.
- Marshall, J. (1970).
Thermal and mechanical mechanisms in laser damage to the retina.
Flying Personnel Research Committee, FPRC/1305 October.
- Marshall, J. and Mellerio, J. (1970).
Laser irradiation of retinal tissue.
Brit. Med. Bull. 26, 156-160.
- Marshall, J., Fankhauser, F., Lotmar, W., and Roulier, A. (1971).
Pathology of short pulse retinal photocoagulators using Goldman
contact lens.
Albrecht von Graefes Arch. Klin. ophthal. 182, 154-169.
- Marshall J., Mellerio, J. and Palmer, D.A. (1972).
Damage to pigeon retinae by moderate illumination from fluorescent
lamps.
Exp. Eye Res., 14, 164-169.
- Marshall, J., Hamilton, A.M., and Bird, A.C. (1975).
Histopathology of ruby and argon laser lesions in monkey and human
retina. A comparative study.
Br.J.Ophthal., 59, 610-630.
- Mayer-Schwickerath, G.
Light Coagulation. St. Louis Missouri : C.V. Mosby Company.
1969.
- Meier-Ruge, W. (1969).
The pathophysiological morphology of the pigment epithelium and its
importance for retinal structures and functions.
Med. Probl. Ophthal., 8, 32-48.
- Mellerio, J. (1967).
Laser light and its effects on the retina.
Trans Ophthal. Soc. UK., 87, 335-343.

- Moseley, H., and Strang, R. (1981).
Prediction of the effect of the choroidal circulation on the retinal temperature during illumination.
Bull Math. Biol., 43, 233-238.
- Mueller Jensen, K., Machemer, R. and Azarnia, R. (1975).
Autotransplantation of retinal pigment epithelium in intravitreal diffusion chambers.
Am.J.Ophthalm., 80, 530-542.
- Nakaizumi, Y. (1964).
The ultrastructure of Bruch's membrane. I. Human, monkey, rabbit, guinea pig and rat eyes.
Arch.Ophthalm., 72, 380-387.
- Noel, W.K. (1963).
Cellular physiology of the retina.
J.Opt.Soc.Am., 53, 36-48.
- Noel, W.K. . . .
Aspects of experimental and hereditary retinal degeneration.
In: Graymore C.N. ed. Biochemistry of the retina. New York Academic Press. 1965.
- Noel, W.K., Walker, V.S., Kang, B.S., and Berman, S. (1966).
Retinal damage by light in rats.
Invest ophthalm., 5, 450-473.
- Noel, W.K., Albrecht, R. (1971).
Irreversible effects of visible light on the retina: Role of vitamin A.
Science, 172, 76-80.
- Orzalesi, N., Gignolo, A., and Calabria, G.A. (1967).
Experimental degeneration of the rabbit retina induced by sodium fluoride.
Exp.Eye Res., 6, 165-170.
- Orzalesi, N., Gignolo, A., Calabria, G.A., and Castellazzo (1967).
A study on the fine structure and the rhodopsin cycle of the rabbit retina in experimental degeneration induced by diaminodiphenoxypentane.
Exp.Eye Res. 6, 376-382.
- Orzalesi, N., Calabria, G.A.L., and Grignolo, A. (1970).
Experimental degeneration of the rabbit retina induced by Iodoacetic Acid. A study of the ultrastructure, the rhodopsin cycle and the uptake of C-labelled Iodoacetic Acid.
Exp. Eye Res. 9, 246-253.
- O'Steen, W.K., Shear, C.R. and Anderson, K.V. (1972).
Retinal damage after prolonged exposure to visible light: A light and electron microscope study.
Am.J.Anat., 134, 5-22.
- O'Steen, W.K., and Lytle, R.B. (1971).
Early cellular disruption and phagocytosis in photically induced retinal degeneration.
Am.J.Anat., 130, 227-234.

- O'Steen, W.K., and Karcioglu, Z.A. (1974).
Phagocytosis in the light-damaged albino rat eye: light and electron microscopic study.
Am.J.Anat., 139, 503-517.
- Oudea, P.R. (1963).
Anoxic changes of liver cells.
Lab.Invest., 12, 386-394.
- Parval, J.M., Machemer, R., and Aumagr, W. (1974).
A new concept for vitreous surgery. 4. Improvements in instrumentation and illumination.
Am.J.Ophthalm., 77, 6-12.
- Pease, D.C. (1956).
Infolded basal plasma membranes found in epithelia noted for their water transport.
J.Biophys.Biochem.Cytol.Suppl., 2, 203-208.
- Peyman, A.G., Spitznas, M.L., and Straatsma, B.R. (1971a).
Peroxidase diffusion in the normal and photocoagulated retina.
Invest Ophthalm., 10, 181-189.
- Peyman, G.A., Spitznas, M., and Straatsma, B.R. (1971b).
Chorioretinal diffusion of peroxidase before and after photocoagulation.
Invest Ophthalm., 10, 489-495.
- Peyman, G.A., and Bok, D. (1972).
Peroxidase diffusion in the normal and laser-coagulated primate retina.
Invest Ophthalm., 11, 35-45.
- Polhamus, G.D., and Welch, A.J. (1975).
Effect of pre-exposure fundus temperature on threshold lesion temperatures in the laser-irradiated rabbit retina.
Invest Ophthalm., 14, 562-565.
- Polyak, S.L. (1941).
The retina. Chicago: University of Chicago press. 1941.
- Pomerantzeff, O., Govignon, J., and Schepens, C.L. (1969).
Indirect ophthalmoscopy: is the illuminative level dangerous.
Tran Amer. Acad. ophth. and Otol., 73, 246-251.
- Powel, J.O., Bresnick, G.H., Yanoff, M., Firsch, G.D., and Chester, J.E. (1971).
Ocular effects of argon laser radiation. II. Histopathology of chorio-retinal lesions.
Am.J. Ophthalm., 71, 1267-1276.
- Radnot, M., Jabbagy, P., Heszeiger, I., and Lovas, B. (1969).
Les donnees a l'ultrastructure de la retine humaine sous l'effect de la lumiere.
Ophthalmologica, 159, 460-471.
- Raviola, G., and Raviola, E. (1967).
Light and electron microscopic observations on the inner plexiform layer of the rabbit retina.
Amer.J.Anat., 120, 403-425.

- Raviola, G. (1977).
The structural basis of the blood ocular barriers.
Exp. Eye Res., 25, 27-63.
- Reynolds, E.S. (1963).
The use of lead citrate at high pH as an electron-opaque stain in electron microscopy.
J. Cell. Biol., 17, 208-212.
- Revel, J.P., Yee, A.G., and Hudspeth, A.J. (1971).
Gap junctions between electronically coupled cells in tissue culture and brown fat.
Proc. Nat. Acad. Sci., 68, 2924-2931.
- Rosan, R.C., Flocks, M., Vassiliadis, A., Rose, H.W., Peabody, R.R., and Hammond, A. (1969).
Pathology of monkey retina following irradiation with an argon laser.
Arch. Ophthalmol., 81, 84-88.
- Rose, H.W., Brown, D.V.L., Byrnes, V.A., and Cibis, P.A. (1956).
Human chorioretinal burns from atomic fireballs.
Arch. ophthalmol., 55, 205-210.
- Schulz, M. (1866).
Zur anatomie and physiologie der retina.
Arch. microsk. Anat. Entw. Mech., 2, 175-286.
- Seligman, A.M., Karnovsky, M.T., Wasserkrug and Hanker. (1968).
Non-droplet ultrastructural demonstration of cytochrome oxidase activity with a polymerising osmiophilic reagent, diaminobenzidine (DAB).
J. Cell Biol. 38, 1-14.
- Shiose, Y. (1970).
Electronmicroscopic studies on blood-retinal, blood aqueous barriers.
Jap. J. Ophthalmol., 14, 73-87.
- Sisson, T.R.C., Glauser, S.C., Glauser, E.M., Tasman, W. and Kuwabara, T. (1970).
Retinal changes produced by phototherapy.
J. Pediatr., 77, 221-227.
- Sjostrand, F.S., and Nilsson, S.E.
In: Prince J.H. ed. The rabbit in eye research. Illinois: Thomas Springfield, 1964.
- Sliney, D.H., and Freasier, B.C. (1973).
Evaluation of Optical Radiation Hazards.
Applied Optics, 12, 1-23.
- Sperling, H.G., and Johnson, C. (1974).
Histological findings in the receptor layer of primate retina associated with light induced dichromacy.
Mod. Prob. Ophthalmol., 13, 291-298.
- Spitznas, M. and Hogan, M.J. (1970).
Outersegments of photoreceptors and the retinal pigment epithelium.
Arch. Ophthalmol., 84, 810-819.
- Spurr, A.R. (1969).
A low viscosity epoxy resin embedding medium for electron microscopy. J. Ultrastruct. Res., 26, 31-43.

- Stell, W.K. (1965).
Correlation of retinal cytoarchitecture and ultrastructure in Golgi preparations.
Anat. Rec., 163, 389-398.
- Stell, W.K. (1967).
The structure and relationship of horizontal cells and photoreceptor-bipolar synaptic complexes in goldfish retina.
Amer. J. Anat., 121, 401-424.
- Straatsma, B.K., Hall, M.O., Allen, R.A., and Cresatelli, F. .
The Retina. Los Angeles, University of California Press. (1969)
- Sulkin, N.M.L., and Sulkin, D.F. (1965).
An electron microscopic study of the effects of chronic hypoxia on cardiac muscle, hepatic and autonomic ganglion cells.
Lab. Invest. 8, 1523-1546.
- Tripathi, B., and Ashton, N. (1971).
Vaso glial connections in the rabbit retina.
Brit. J. Ophthalm., 55, 1-11.
- Tso, M.O.M., and Friedman, E. (1967).
The retinal pigment epithelium. I. Comparative histology.
Arch. Ophthalm., 78, 641-649.
- Tso, M.O.M., Fine, B.S., and Zimmerman, L.E. (1972).
Photoc maculopathy produced by the indirect ophthalmoscope.
I. clinical and histopathic study.
Am. J. Ophthalmol., 73, 686-699.
- Tso, M.O.M., Wallow, I.H.L., Powell, J.O., and Zimmerman, L.E. (1972).
Recovery of the rod and cone cells after photic injury.
Trans.Am.Acad.Ophthalmol.Otolaryngol., 76, 1247-1262.
- Tso, M.O.M. (1973).
Photoc maculopathy in rhesus monkey: A light and electron microscopic study.
Invest Ophthalm. 12, 17-34.
- Tso, M.O.M., Wallow, I.H.L., and Powell, J.O. (1973).
Differential susceptibility of rods and cone cells to argon laser.
Arch. Ophthalm., 89, 228-234.
- Van Pelt, W.F., Payne, W.R., and Peterson, R.W. (1973).
A review of selected bioeffects thresholds for various spectral ranges of light.
U.S. Department of Health, Education and Welfare.
DHEW Publication (FDA 74-8010).
- Verhoeff, F.H., and Bell, I. (1916).
The pathological effects of radiant energy on the eye.
Proc.Am.Acad.Arts and Sci., 51, 630-759.
- Wald, G., Brown, P.K., and Gibbons. (1962).
Visual excitation: a chemo-anatomical study.
Symph. Soc. exp. Biol., 16, 32-57.

- Walker, A.M. (1916).
The pathological effects of radiant energy on the eye: a
systematic review of the literature.
Proc.Am.Acad.Art and Sci., 51, 760-817.
- Wallow, I.H.L., Tso, M.O.M., Fine, B.S. (1973).
Retinal repair after experimental xenon arc photocoagulation.
I. a comparison between rhesus monkey and rabbit.
Am.J.Ophthalm., 75, 32-52.
- Ward, B., and Bruce, W.R. (1971a).
Role of body temperature in the definition of retinal burn threshold.
Invest Ophthalm., 10, 955-958.
- Ward, B., and Bruce, W.R. (1971b).
Chorioretinal burn: body temperature dependence.
Ann. Ophthalm., 3, 898-899.
- Webster, H. and Ames, A. (1965).
Reversible and irreversible changes in the fine structure of nervous
tissue during oxygen and glucose deprivation.
J. Cell Biol., 26, 885-908.
- Weisse, I. and Stotzer, H. (1974).
Age and light-dependent changes in the rat eye.
Virchows Arch. Path. Anat. Histol., 362, 145-156.
- Wyse, J.P.H. (1980).
Renewal of rod outer segments following light-induced damage of the
retina.
Can.J.Ophthalm., 15, 15-19.
- Young, R.W. (1965).
Renewal of photoreceptor outer segments.
Anat.Rec., 151, 484.
- Young, R.W. (1967).
The renewal of photoreceptor cell outer segments.
J.Cell Biol., 33, 61-72.
- Young, R.W. (1969).
A difference between rods and cones in the renewal of outer segment
protein.
Invest. Ophthalm., 8, 222-231.
- Young, R.W., and Bok, D. (1969).
Participation of the retinal pigment epithelium in the rod outer
segment renewal process.
J.Cell Biol., 42, 392-403.
- Young, R.W., and Droz, B. (1969).
The renewal of protein in the retinal rods and cones.
J. Cell Biol., 39, 169-184.
- Young, R.W. and Bok, D. (1970).
Autoradiographic studies on the metabolism of the retinal pigment
epithelium.
Invest Ophthalm., 9, 524-536.

Young, R.W. (1971).
Shedding of discs from rod outer segments in the rhesus monkey.
J. Ultrastruct Res., 34, 190-203.

Young, R.W. (1976).
Visual cells and the concept of renewal.
Invest. Ophth., 15, 700-725.

Young, R.W. (1978).
The daily rhythm of shedding and degradation of rod and cone outer
segment membranes in the chick retina.
Invest Ophthal., 17, 105-116.

